Characterization and Toxicity of SMOKE

Harry K. Hasegawa
EDITOR

ASTM
STP 1082

Copyright by ASTM Int'l (all rights reserved) Wed Feb 07 10:53:32 UTC 2024
Downloaded/printed by
The University of Delaware pursuant to License Agreement. No further reproductions authorized.

STP 1082

Characterization and Toxicity of Smoke

Harry K. Hasegawa, editor

ASTM
1916 Race St.
Philadelphia, PA 19103

Copyright by ASTM Int'l (all rights reserved) Wed Feb 07 10:53:32 UTC 2024
Downloaded/printed by
The University of Delaware pursuant to License Agreement. No further reproductions authorized.

Library of Congress Cataloging-in-Publication Data

Characterization and toxicity of smoke/Harry K. Hasegawa, editor.
(STP; 1082)
Contains papers presented at a symposium held in Phoenix, Ariz. on Dec. 5, 1988 and sponsored by ASTM Committee E-5 on Fire Standards.
"ASTM publication code number (PCN) 04-010820-31"--T.p. verso.
Includes bibliographical references.
ISBN 0-8031-1386-2
1. Combustion gases—Toxicology—Congresses,. 2. Smoke—Toxicology—Congresses. I. Hasegawa, Harry K., 1947- .
II. ASTM Committee E-5 on Fire Standards. III. Series: ASTM special technical publication; 1082.
RA1247.C65C49 1990
615.9'1—dc20

Copyright © by AMERICAN SOCIETY FOR TESTING AND MATERIALS 1990

NOTE

The Society is not responsible, as a body,
for the statements and opinions
advanced in this publication.

Peer Review Policy

Each paper published in this volume was evaluated by three peer reviewers. The authors addressed all of the reviewers' comments to the satisfaction of both the technical editor(s) and the ASTM Committee on Publications.

The quality of the papers in this publication reflects not only the obvious efforts of the authors and the technical editor(s), but also the work of these peer reviewers. The ASTM Committee on Publications acknowledges with appreciation their dedication and contribution of time and effort on behalf of ASTM.

Printed in Baltimore, MD
May 1990

Copyright by ASTM Int'l (all rights reserved) Wed Feb 07 10:53:32 UTC 2024
Downloaded/printed by
The University of Delaware pursuant to License Agreement. No further reproductions authorized.

Foreword

This publication, *Characterization and Toxicity of Smoke,* contains papers presented at the symposium of the same name held in Phoenix, Arizona on 5 Dec. 1988. The symposium was sponsored by ASTM Committee E-5 on Fire Standards. Harry K. Hasegawa, Lawrence Livermore National Laboratory, presided as symposium chairman and was editor of this publication.

Copyright by ASTM Int'l (all rights reserved) Wed Feb 07 10:53:32 UTC 2024
Downloaded/printed by
The University of Delaware pursuant to License Agreement. No further reproductions authorized.

Contents

Copyright by ASTM Int'l (all rights reserved) Wed Feb 07 10:53:32 UTC 2024
Downloaded/printed by
The University of Delaware pursuant to License Agreement. No further reproductions authorized.

Copyright by ASTM Int'l (all rights reserved) Wed Feb 07 10:53:32 UTC 2024
Downloaded/printed by
The University of Delaware pursuant to License Agreement. No further reproductions authorized.

Overview

Statistics[1] have consistently shown that a large proportion of fatalities from fires are caused by the inhalation of smoke[2] rather than exposure to the thermal effects of fire. Similarly, extensive damage to property can be attributed to the physical and chemical properties of smoke even when the actual fire has been relatively small. Although, historically, much of the blame has been placed on man-made synthetic polymers, all burning organic materials will generate smoke with the potential to threaten life and property. In terms of life safety, physical properties of smoke such as particulate concentration hamper or prevent the safe exiting of buildings. Toxic effects in the form of asphyxiation and irritation incapacitate and kill in fire situations. The severity of damage to property is dependent on the chemical composition of the smoke and/or the physical properties. Corrosive effects on building structures and contents have become an area of great concern and have prompted a number of regulating bodies to restrict or prohibit the use of materials identified as generating corrosive smokes, e.g., halogenated cable and wire insulations. These regulations raise many questions as to the appropriateness of certain tests in what they measure and how the results are obtained. Until recently, the major thrust of fire research, fire modelling, and standard fire tests dealt with the thermal aspects of fire with smoke as a secondary component. A significant reason for this emphasis was the extreme complexity and magnitude of the many aspects of smoke. However, the following collection of papers will demonstrate that there is a great deal of leading edge research underway in the characterization and toxicity of smoke.

This special technical publication (STP) has been published as a result of the 1988 symposium on Characterization and Toxicity of Smoke held in Phoenix, Arizona in an effort to provide regulators, producers, users, and researchers with an overview of the most current studies in the many facets of smoke. The symposium was conceived within ASTM Subcommittee E 5.32 on Research. The intent was to solicit papers dealing with as many different aspects of smoke as possible. The reader will find a variety of studies which address topics such as smoke hazard assessment, smoke spread modeling, appropriateness of toxicity tests, appropriateness of animal species as human substitutes, effect of materials on "nuclear winter," etc.

A collection of twelve papers published in this volume has been separated into three broad categories. These categories are smoke toxicity, smoke chemistry, and smoke characterization.

Smoke Toxicity

The papers in this section are divided between quantitative research on smoke toxicity and methodologies to use test results as part of an overall methodology to assess the toxic hazard

[1] *Fire and Smoke: Understanding the Hazards.* Committee on Fire Toxicology, Board of Environmental Studies and Toxicology Commission on Life Sciences, National Research Council, National Academy Press, Washington, DC, 1986.

[2] Smoke is defined by ASTM E 176 as "the airborne solid and liquid particulates and gases evolved when a material undergoes pyrolysis or combustion."

Copyright by ASTM Int'l (all rights reserved) Wed Feb 07 10:53:32 UTC 2024
Downloaded/printed by
The University of Delaware pursuant to License Agreement. No further reproductions authorized.

of materials. *Hinderer* and *Hirschler* present an extensive work which presents an update of information regarding the toxicity of polyvinyl chloride (PVC) smoke and of hydrogen chloride (HCL). Because animals are being used as models for humans in toxicity tests, special attention is given to the sensitivity and appropriateness of certain animal species for specific small-scale tests. The paper also discusses the fate of HCL in realistic fire atmospheres. The authors provide a nice overview on the toxicity of PVC smoke, studies on HCL toxicity, and test methods to measure the toxic potency of smoke produced from burning materials. Some of their conclusions include:

1. There is no single toxicity for the products in PVC smoke; it can vary widely.
2. The toxic potency of the smoke from most PVC products is similar to that of most ordinary products in use in society.
3. HCL decays rapidly in a fire atmosphere while CO does not.
4. Toxicity tests based solely on LC_{50}s cannot predict toxic hazard, and the UPITT test is less satisfactory than other tests.

Tewarson presents data to analyze the relationship between the combustion behavior of materials and the toxicity of the resultant environment. The author uses a toxicity relationship suggested by researchers at the National Institute of Standards Technology on the synergism between CO and CO_2 and data measured in the Factory Mutual Small-Scale Flammability Apparatus. He uses the relationship to examine the effects of chemical structure, fire ventilation, and dilution of fire products on the toxicity, created by CO and CO_2, of the environment. In closing, Tewarson applies his findings to small-scale toxicity tests.

The paper by *P. J. Briggs* presents a potential methodology for smoke hazard assessment that considers fire test, product design, and room scenarios in a way that would reflect the dangers of a product in a realistic fire situation. This proposed methodology would prevent misinterpretation of test data which can occur when smoke test data is compared in isolation without reference to other fire parameters. The author reviews and evaluates the current status of selected small-scale smoke tests as well as large-scale room tests. A standard protocol for smoke hazard analysis is presented with the following components:

1. Fire scenario definition and probability of occurrence.
2. Consideration of ignitability.
3. Consideration of fire growth.
4. Consideration of smoke test data.
5. Consideration of rate of smoke hazard development.

Clarke, van Kuijk, and *Steele* also present a global toxic hazard assessment tool which is specifically oriented to burning electrical cables. This tool for fire hazard assessment utilizes small-scale fire property tests, computer modeling, and full-scale tests to estimate cable smoke hazard in a fire environment. The paper provides an update on predicting cable toxic hazard using a modified Harvard V mathematical model and how laboratory-based hazard prediction methods, i.e., toxic potency and the newly established NIBS test, compare with toxic hazard assessment in their ability to distinguish between the performance of several different kinds of cable. Material input data for the model were obtained from lab scale tests such as the Cone Calorimeter and Lateral Ignition and Flammability Tester (LIFT). Model-based predictions were compared to two-full-scale fire test series of various cable insulating materials. One of the authors' conclusions is that no laboratory test by itself can make allowances for the conditions of use in more than one fire scenario. Therefore, hazard assessment, whether by mathematical modelling and small-scale testing or by full-scale fire test, will remain the most reliable method of determining relative cable performance.

Copyright by ASTM Int'l (all rights reserved) Wed Feb 07 10:53:32 UTC 2024
Downloaded/printed by
The University of Delaware pursuant to License Agreement. No further reproductions authorized.

Norris presents an investigation of dual LC_{50} values for red oak from combustion toxicity testing using the University of Pittsburgh Combustion Toxicity (UPITT) apparatus. No report of any material displaying a dual LC_{50} value had been made to this point in time. Since red oak was the first reported to have this dual value, white oak, southern pine, and Douglas fir were also selected for testing. The study also attempts to correlate the maximum concentrations and concentration × time (*Ct*) products of carbon monoxide (CO), the ratio of carbon dioxide (CO_2) to carbon monoxide, and Maximum ∂ Temperature Area with LC_{50} values. As a result of the study, three LC_{50} values were found for red oak and southern pine, while one was found for white oak and Douglas fir. Maximum CO concentrations offered no correlation with the LC_{50} values. The *Ct* products of CO did not clearly correlate with the LC_{50} values. The Maximum ∂ Temperature Area indicated there was a continuous change in burning characteristics as the specimen weight increased, but it did not correlate with the LC_{50} values.

Smoke Chemistry

Two of the papers in this section address corrosive aspects of smoke while the third relates to animal toxicity studies. *Ryan, Babrauskas, O'Neill,* and *Hirschler* propose a series of criteria and a specific test method to measure the corrosive effects of combustion products. The paper addresses the emergence of the corrosion issue and attempts to formulate an appropriate response to it. One of the authors' contentions is that laboratory tests proposed to date to measure the corrosive effects of combustion products all have significant deficiencies; some methods are not performance-based at all and are merely tests for pH. In others, unrealistic specimen heating or unrealistic exposure targets are used. These shortcomings are addressed by sections on fire hazard assessment, damage from corrosion-related effects, and test development. Ten criteria for an acceptable test for corrosion and related damage listed by the ASTM E5.21 TG70 Task Group are used to evaluate a number of laboratory tests. The authors' conclusions call for a systematic and rational means for assessing actual corrosivity performance of materials and to develop an acceptable test.

The paper by *Grand* describes a laboratory method for the combustion of PVC and other polymeric materials in such a manner as to produce a constantly flowing, steady-state atmosphere for animal toxicity studies. Although the method is based on the principles of the German Standard DIN 53 436, the method described has a much larger combustion tube and specimen, greater versatility in specimen size and air dilution rates, utilizes radiant heating, and has achieved continuous flaming as well as nonflaming. Because hydrogen chloride gas has a tendency to "decay" from smoke atmospheres, this flow-through combustion system was developed to provide a constant level of HCL in PVC smoke for between 15 and 30 min. Other materials (besides PVC) used to evaluate this methodology included: Douglas fir, flexible polyurethane foam, and two rigid polyurethane/polyisocyanurate foams. Primary conclusions from this study were:

1. The apparatus performed very well for its intended design—combustion of PVC. Steady-state combustion of PVC was maintained for 20 to 25 min flaming, and for approximately 60 min nonflaming.
2. From the three other materials tested, it appears from the experiments conducted so far that the device is more suited to materials that burn relatively slowly.

Another paper dealing with the smoke generated from burning electrical cables is presented by *Tewarson* and *Khan*. Their study describes results for the generation of smoke in terms of smoke yield, mass optical density, and specific corrosion constant for electrical cables during fire propagation. The authors use the results of this study to classify cables into

Copyright by ASTM Int'l (all rights reserved) Wed Feb 07 10:53:32 UTC 2024
Downloaded/printed by
The University of Delaware pursuant to License Agreement. No further reproductions authorized.

three groups based on the Fire Propagation Index. Small-scale cable fire propagation experiments were performed in the Factory Mutual Small- (50 kW-) and Intermediate- (500 kW-) Scale Flammability Apparatuses. Large-scale cable fire propagation experiments were performed in the Factory Mutual Large- (5000 kW-) Scale Flammability Apparatus. Preliminary conclusions from the study suggest that nonthermal fire damage is not expected if the following conditions are satisfied: (1) fire propagation index is less than 10; (2) yield of smoke is less than 0.03 g/g; (3) mass optical density is less than 0.11 m^2/g; and (4) the specific corrosion constant of the cable is less than 0.92×10^{-6} μm/h ppm.

Smoke Characterization

The final section on smoke characterization contains four papers that deal with the physical properties of smoke, from micro to macroscales. *Newman* presents a study on smoke transport and characterization in large enclosure fires to complement detailed laboratory results for smoke particulate properties (e.g., volume fraction, mass concentration, generation efficiency, particulate size, and particulate yield). Fire experiments of fire sources, including heptane, methanol, propylene, PMMA, and various electrical cable types with variable forced ventilation conditions, were performed in a large heavily instrumented enclosure. Results of this study discuss heat release rates, fire product transit times, temperature distributions, distribution of carbon dioxide concentration, distribution of smoke particulate concentration, and ventilation effects.

In contrast, *Tran* reports on a comparative study of smoke generation from red oak and Douglas fir plywood using the National Bureau of Standards (NBS) smoke density chamber and the Ohio State University (OSU) heat release rate calorimeter. In the NBS smoke chamber, three nonpiloted heating fluxes of 2.0, 2.5, and 3.0 W/cm^2 were used for each material. A total of 90 tests were conducted (two materials, three flux levels, five durations, and three replicates). Comparative data were obtained of smoke release rates (SRR) from red oak and Douglas fir plywood at a nonpiloted heat flux of 2.5 W/cm^2 in the OSU apparatus. The conditions were analogous to those in the NBS unit at the same heating flux, except that in the OSU apparatus, the smoke was swept out continuously. The unit of particulate mass produced per unit area was found to be an appropriate basis to compare the data from the two apparatuses. Although the reduced data from the two methods were of the same order of magnitude, the data could not be reconciled exactly.

Fleischmann et al. present a study which has global implications as input into predictions for "nuclear winter." The concept of "nuclear winter" has been postulated with a number of assumptions regarding the smoke produced by postnuclear exchange fires. The general premise is that following the use of nuclear weapons, sufficient smoke would be generated from fires and deposited in the atmosphere to cause a decrease in the incident solar energy reaching the earth's surface. The paper describes results from a series of "medium-scale" (200 to 1000-kW) smoke experiments of representative urban fuels such as wood, plywood, asphalt roofing, and liquid hydrocarbons burned in the open with no ventilation restrictions. In addition, some of the fuels were burned in a test room under limited ventilation conditions. Smoke was characterized by the mass of airborne particulates, the size and distribution of the particulates, i.e., "graphitic" or "black" carbon and organic carbon. Mass loss and heat release rate were recorded during each experiment to characterize combustion. Results of the 16 experiments demonstrated the considerable influence of the compartment on smoke production. The smoke emission factors measured for wood cribs burning in the compartment were more than an order of magnitude higher than those burning in the open. Conversely, the fuel oil burned in the compartment produced significantly less smoke than being burned in the open. Results for asphalt shingles demonstrated the significant impact a

Copyright by ASTM Int'l (all rights reserved) Wed Feb 07 10:53:32 UTC 2024
Downloaded/printed by
The University of Delaware pursuant to License Agreement. No further reproductions authorized.

single material might have on the urban smoke production in a post nuclear war environment. The smoke emission factors found for asphalt roofing shingles, averaged for two experiments, was over 12% with more than 60% being black carbon.

The final article by *Tamura* and *Klote* presents a study to develop a fire-safe elevator for evacuating handicapped people and for aiding firefighters. The paper describes methods for calculating pressure differences caused by wind and stack action and the results of tests conducted in the ten-story experimental fire tower of the National Research Council of Canada National Fire Laboratory. The researchers' conclusions included the following:

1. Good agreement was found between experimental results and stack effect theory over a wide range of leakage conditions representative of many commercial buildings.
2. For the conditions of these experiments, the adverse pressure differences of stack action and fire can be added to provide a good approximation of the pressure difference resulting from the two acting in combination and, hence, the amount of pressurization required to prevent smoke migration into elevator lobbies under these conditions. A broken window can result in a jump in pressure differential, which is an important design consideration.
3. Mechanical pressurization of the elevator shaft or lobbies greatly reduces the possibility of smoke contamination of these spaces due to stack action.
4. Although further studies of wind effects are needed, mechanical pressurization of the elevator shaft greatly reduces the possibility of smoke contamination of elevator shafts and lobbies due to wind action.

The papers summarized above should provide the reader with an overview of state-of-the-art information pertaining to the very broad and complicated field of smoke research. One conclusion common to all studies is that further work is needed in the understanding and characterization of smoke. The selection of papers reflects the efforts of the symposium committee to provide a program that touched on as many areas of ongoing research in smoke as possible. The symposium committee gratefully acknowledges the efforts of the authors and ASTM personnel who have made this publication possible.

Harry K. Hasegawa
Lawrence Livermore National Laboratory, Livermore, CA 94550; symposium chairman and editor

Copyright by ASTM Int'l (all rights reserved) Wed Feb 07 10:53:32 UTC 2024
Downloaded/printed by
The University of Delaware pursuant to License Agreement. No further reproductions authorized.

Smoke Toxicity

Copyright by ASTM Int'l (all rights reserved) Wed Feb 07 10:53:32 UTC 2024
Downloaded/printed by
The University of Delaware pursuant to License Agreement. No further reproductions authorized.

Robert K. Hinderer[1] *and Marcelo M. Hirschler*[2]

The Toxicity of Hydrogen Chloride and of the Smoke Generated by Poly (Vinyl Chloride), Including Effects on Various Animal Species, and the Implications for Fire Safety

REFERENCE: Hinderer, R. K. and Hirschler, M. M., **"The Toxicity of Hydrogen Chloride and of the Smoke Generated by Poly (Vinyl Chloride), Including Effects on Various Animal Species, and the Implications for Fire Safety,"** *Characterization and Toxicity of Smoke, ASTM STP 1082,* H. K. Hasegawa, Ed., American Society for Testing and Materials, Philadelphia, 1990, pp. 1–22.

ABSTRACT: Toxicity of smoke is only one of many factors determining the hazard or the risk resulting if a product were involved in a fire in a specific scenario. Other factors include: amount of smoke (i.e., concentration of combustion products in the atmosphere), rate and quantity of heat release, mass loss rate, and flame spread rate, as well as such "environmental" factors as ignition source characteristics, fire detection and suppression devices, building occupancy, and code enforcement. A factor almost specific to the smoke generated from burning poly (vinyl chloride) (PVC) is the decay of hydrogen chloride (HCl) by reaction with building surfaces. The values of smoke toxic potency measured will also be affected by a number of parameters, including combustion mode, exposure mode, toxicological end point, and statistical analysis of results.

A crucial factor, often overlooked, is the choice of an animal model appropriate as a surrogate for man, and its validation. Test animals are frequently chosen on the basis of convenience, cost, or other characteristics (e.g., sensitivity) rather than because of their similarity to man. This is particularly important in combustion toxicology, where one test species may not be a good model for all the major combustion products generated. Thus, comparisons of materials producing different major combustion products must be approached with caution to ensure that any apparent differences encountered in tests are not simply an artifact of test species.

Over recent years, increasing evidence has surfaced that some rodent species are poor models for the toxic response of man to irritant gases or to smoke-containing irritants. Studies on HCl (as a pure gas) and on the smoke generated from the burning of PVC have indicated that mice are much more sensitive than rats. More importantly, they are much more sensitive than primates. It has also been established that rats are a good model for primates in terms of the lethal effects of irritant products. Although primates have survived 15-min exposures to 10 000 ppm of HCl, 2500 ppm is lethal to mice. Moreover, under the same exposure conditions, mice will die at PVC smoke levels four to seven times lower and HCl levels seven to ten times lower than those at which rats will. In contrast, lethal doses of asphyxiants such as carbon monoxide (CO) are similar in rats and mice.

These results indicate that the response of the mouse significantly overestimates the toxic potency of HCl and of PVC smoke to man.

KEY WORDS: PVC, HCl, poly (vinyl chloride), hydrogen chloride, smoke toxicity, fire hazard, animal models, toxic potency, smoke, fire

[1] Manager of Toxicology, BF Goodrich Corporate Environmental Health Department, Bath, OH 44313.

[2] R&D Manager, Fire Sciences, BF Goodrich Geon Vinyl Division, Technical Center, Avon Lake, OH 44012.

Copyright by ASTM Int'l (all rights reserved) Wed Feb 07 10:53:32 UTC 2024
Copyright © 1990 by ASTM International www.astm.org
Downloaded/printed by
The University of Delaware pursuant to License Agreement. No further reproductions authorized.

Preface

This paper will deal with several aspects associated with fire safety. It is of interest, therefore, to present definitions of some terms used in order to avoid confusion.

Fire hazard can be defined as the potential for harm associated with fire, addressing threats to people, property, or operations, resulting from a particular fire scenario. *Fire risk* is a combination of (*a*) the fire hazard, (*b*) the probability of occurrence of a fire in that scenario, and (*c*) the probability of the material or product being present in the fire scenario. *Toxic potency* (of smoke) is a quantitative expression relating concentration and exposure time to a certain adverse effect on exposure of a test animal, usually death. It should be stressed that the toxic potency of smoke is also heavily dependent on the conditions under which the smoke was generated. Finally, *smoke* is here used as the sum total of the gaseous, liquid, and solid airborne products of combustion. *Exposure dose* represents an integration of the toxic insult, as calculated from the smoke concentration versus time curve. If the insult results from an individual toxicant and its concentration is constant, the exposure dose is the product of concentration and time. Time of exposure and time to a toxic effect are very different: the action of many toxicants may take effect at considerable time postexposure.

Toxicity information is, unfortunately, expressed in a variety of common units. Toxic potency of smoke is usually expressed in mg/L (although the results of some tests, e.g., the UPITT test [*3*], tend to be reported in terms of the mass loaded, in g, based on a fixed size exposure chamber), while that of individual toxicants (commonly gases) is normally expressed in ppm. Exposure doses are thus presented in ppm min or mg/L min.

Introduction

During the 1970s and early 1980s a number of test methods were developed to measure the toxic potency of the smoke produced from burning materials (e.g., Refs *1–4*). These methods differ in a variety of respects: in particular in the relative rankings they generate for the toxic potency of the different materials they test. A case in point was made in a study of the toxic potency of 14 materials by two methods [*5*]. It showed (Table 1) that the material deemed most toxic by one of the protocols appeared to be the least toxic by the other method! The test methods used in the latter paper [*5*] were different from the major ones in

TABLE 1—*Comparative mortality data of combustion products of polymers.*

LC_{50}, g	Static Chamber, Sample	Toxicity Ranking (Toxicity Increases Upwards)	Dynamic Chamber, Sample	LC_{50}, g
9	Red Oak	1	Wool	0.4
10	Cotton	2	Polypropylene	0.9
21	ABS (FR)	3	Polypropylene (FR)	1.2
23	SAN	4	Polyurethane foam (FR)	1.3
25	Polypropylene (FR)	5	Poly (vinyl chloride)	1.4
28	Polypropylene	6	Polyurethane foam	1.7
31	Polystyrene	7	SAN	2.0
33	ABS	8	ABS	2.2
37	Nylon 6,6	9	ABS (FR)	2.3
37	Nylon 6,6 (FR)	10	Nylon 6,6	2.7
47	Polyurethane foam (FR)	11	Cotton	2.7
50	Polyurethane foam	12	Nylon 6,6 (FR)	3.2
50	Poly (vinyl chloride)	13	Red Oak	3.6
60	Wool	14	Polystyrene	6.0

Copyright by ASTM Int'l (all rights reserved) Wed Feb 07 10:53:32 UTC 2024
Downloaded/printed by
The University of Delaware pursuant to License Agreement. No further reproductions authorized.

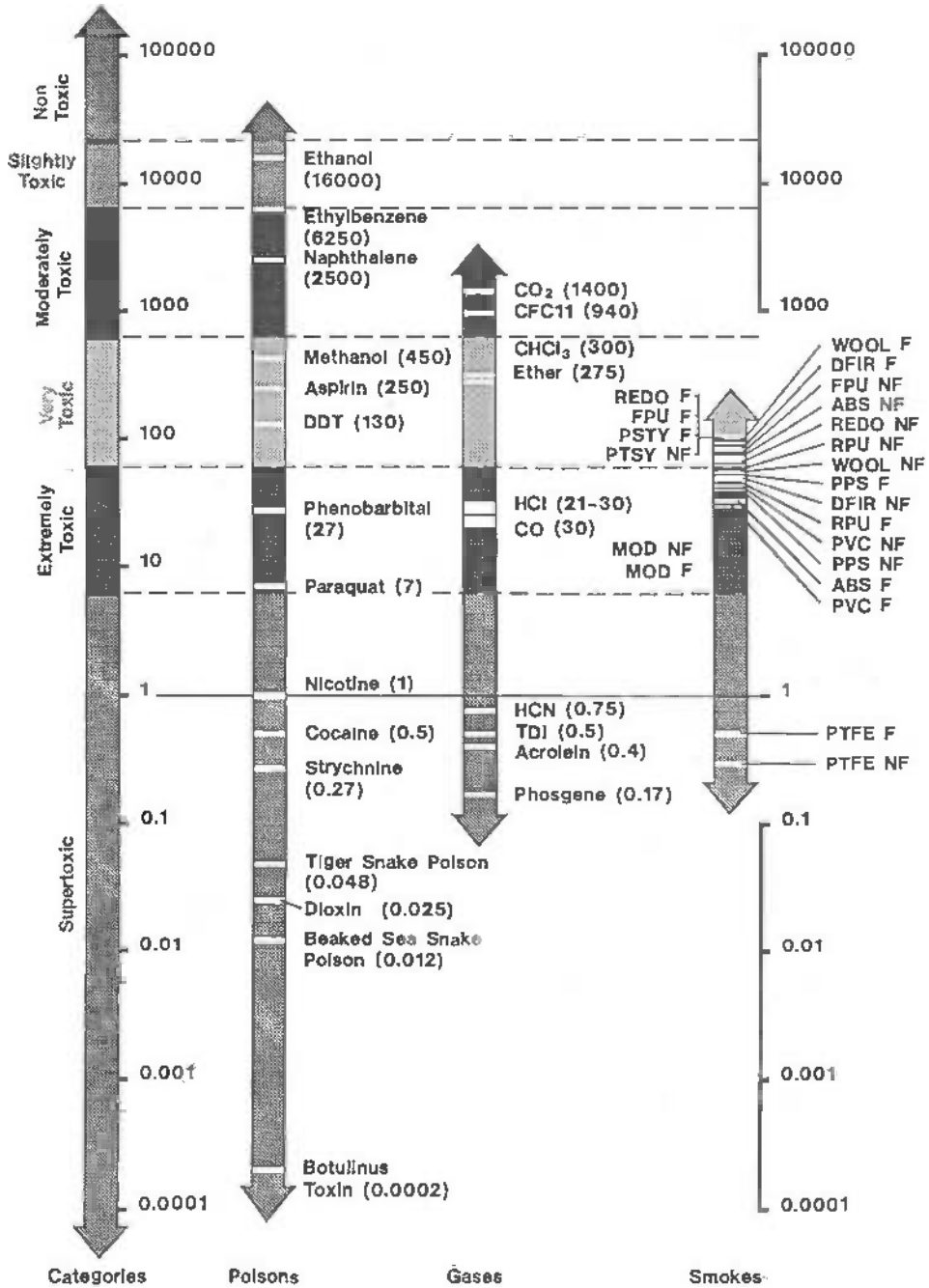

FIG. 1—*Toxic potency (expressed as the lethal dose required to kill half the exposed animals, LD_{50}, in mg/kg) of substances and of smoke. The smoke toxic potency was measured using the cup furnace (NBS) protocol. The animal models used were rats or primates.*

Copyright by ASTM Int'l (all rights reserved) Wed Feb 07 10:53:32 UTC 2024
Downloaded/printed by
The University of Delaware pursuant to License Agreement. No further reproductions authorized.

use today [*1–4*]. However, the work illustrates one of the dangers of relying on toxic potency test methods: different combustion atmospheres are generated in each toxic potency protocol, and these result in crossovers in toxic potency results. This is due to the similarity in toxic potency of most materials in common use.

It has now become clear that the toxic potency of most materials is really very similar, with very few exceptions, a point clearly illustrated in Fig. 1 [*6*]. The figure presents some results on toxic potency of smoke from a variety of common materials, as measured by the NBS cup furnace toxic potency test [*1*]. These toxic potency values are compared with the intrinsic toxic potency of other poisons and of toxic gases, as well as with textbook toxicity categories [*7*].

The reason for this similarity of toxic potencies is that the most important toxic product in any fire is carbon monoxide (CO), produced when all organic materials burn. Furthermore, there is wide agreement today that small-scale smoke toxicity tests show only broad toxicity categories and do not really distinguish among most materials.

This indicates that the toxicity of the smoke of most materials can be approximated by the product of a median toxic potency and the amount of smoke produced from the material per unit time, in other words, the material's mass loss rate. The only materials that do not follow this rule are those very few that have an exceptionally high toxic potency. PVC is not among these materials. That is why a low mass loss rate will generally mean a low toxic fire hazard, almost irrespective of the toxic potency of the smoke itself.

Most of the primary toxicants in a fire atmosphere can be classified in one of two categories according to their mechanism of action: asphyxiants [e.g., CO, hydrogen, cyanide (HCN), low oxygen] and irritants [e.g., hydrogen chloride (HCl), acrolein, hydrogen fluoride (HF), nitrogen oxides].

There has been, in recent years, a great deal of controversy regarding the smoke toxicity of poly (vinyl chloride) (PVC), much of it based on the lack of a proper understanding of the facts. The issue is of importance inasmuch as smoke toxicity is occasionally, albeit incorrectly, directly correlated with fire hazard or fire risk.

The majority of combustion products of PVC are the same as those given off by virtually all organic materials, both natural and synthetic: viz. carbon oxides, hydrocarbons, and water [*8,9*]. However, PVC releases an important combustion product not generated by natural materials: HCl.

This paper will present an update of available information regarding the toxicity of PVC smoke and that of HCl. It places special attention on the sensitivity of different animal species to them. This is important because animals are being used as models for humans in toxicity tests, and some are more appropriate than others. The paper will also, briefly, deal with HCl decay in a fire atmosphere. The toxicity of PVC smoke decreases rapidly because of HCl decay. In contrast, the toxicity of the smoke of most other polymers remains the same since the other main smoke toxicants do not decay.

It has already been stated that toxic fire hazard is associated mainly with the amount of combustion products being generated per unit time, viz., the mass loss rate. Combustion mass loss rate is, in turn, a consequence of fire properties, which are determined in small-scale tests, large-scale tests, and can be predicted by fire models. The paper ends referring to the low tendency of PVC polymer to burn and, thus, to generate toxic products at all.

Background on Toxicity of PVC Smoke

A number of studies have evaluated the toxic potency of the smoke of groups of materials based on a particular protocol. Almost invariably they show that the toxic potencies of most common smokes differ little, virtually irrespective of the protocol used. The comparative

Copyright by ASTM Int'l (all rights reserved) Wed Feb 07 10:53:32 UTC 2024
Downloaded/printed by
The University of Delaware pursuant to License Agreement. No further reproductions authorized.

rankings of materials within a certain study can vary tremendously, however. Consequently, it has been suggested that if an exposure dose within the range of 300 to 3000 mg/L min leads to animal lethality, this represents average smoke toxicity [*10*]. Figure 1 illustrates this point by putting smoke toxic potencies in an overall toxicological perspective.

Reviews by Hinderer [*11*], Huggett and Levin [*12*], and Doe [*10*] have discussed some of the most important studies of PVC smoke toxicity. Separately, Huggett [*13*] has analyzed the reporting procedure with respect to PVC smoke (and its major toxic gases: CO and HCl) of several protocols.

There is general agreement, both in the specific studies on PVC smoke and in many general toxicity studies such as those mentioned earlier, that *the toxic potency of PVC is within the normal range* of common materials.

However, considerable misinformation on the toxicity of PVC smoke still remains in the public domain, causing apparent controversies. These are based on articles studying particular incidents, such as the 1975 fire at the New York telephone exchange [*14–16*]. It would appear as if some such articles were written with disregard for a scientific interpretation of the facts. Although the claims made in each of the specific articles has been rebutted and their flaws highlighted [*17–18*], apparent confusion persists.

One of the best-researched medical studies on human exposure to PVC smoke [*19*] showed that PVC decomposition products do indeed have short-term adverse effects on pulmonary function. These can be attributed to HCl since they mirror the results of animal studies, which will be discussed later in this paper. The minor pulmonary function abnormalities seen after three months could not be separated from those due to smoking.

The first aspect to be discussed in this paper is the toxicity of the principal unique toxicant contained in PVC smoke: hydrogen chloride.

Studies on HCl Toxicity

Very Early Studies

A number of very early studies were carried out on the inhalation toxicology of HCl in the late 19th and early 20th centuries using a variety of animal species [*20–24*]. These studies used cats, guinea pigs, rabbits, hares, doves, frogs, and humans. The exposure doses for the nonprimate mammals ranged from a few thousand ppm min to over a million ppm min. The results indicated that HCl, as expected, was an irritant which could cause lethality at very high exposures.

Interestingly, there was, for each animal species, a threshold below which lethality was never observed (lowest lethal concentration). These investigators found considerable variation in the biological handling (absorption) and toxic response of the different species to HCl, but no evidence of synergistic effects. For example, a cat survived an exposure dose of $>300\,000$ ppm min (3400 ppm for 1.5 h). Rabbits were very variable: one survived an exposure dose of 560 000 ppm min (1400 ppm for 6 h 40 min), but another died at just over 100 000 ppm min; levels above 150 000 ppm min seemed often to be lethal in one study, but levels of $>300\,000$ ppm min were not lethal in another. Lowest lethal exposure doses for guinea pigs were close to 200 000 ppm min, while rats survived exposure doses of almost 1 000 000 ppm min (2400 to 4500 ppm for almost 5 h). Multiple long-term exposures to low concentrations seemed to cause no serious effects in rabbits, guinea pigs, or doves.

The studies on humans involved only fairly low concentrations and exposures (<5000 ppm min) and were geared towards a search for safe work place concentrations. All of the effects experienced by the subjects were minor and disappeared soon after exposure.

An Appendix contains an edited translation of the major aspects of these early studies.

Copyright by ASTM Int'l (all rights reserved) Wed Feb 07 10:53:32 UTC 2024
Downloaded/printed by
The University of Delaware pursuant to License Agreement. No further reproductions authorized.

More Recent Studies

Recent studies of lethality concentrated primarily on three animal species: baboons, rats, and mice [*25–38*]. A comparative study of the effects of HCl exposure on a rodent (rat) and a nonhuman primate (baboon) [*28*] investigated the ability of these animals to escape from a hazardous fire environment. Some earlier investigators had speculated how HCl would reduce escape ability based on investigations of mouse sensory irritation. This study provided the first indication of how primates and rodents respond to similar levels of HCl exposure. The baboons were able to accomplish a complicated escape paradigm after 5-min exposure to very high HCl levels without being incapacitated. The rats did not suffer incapacitation due to HCl either.

The studies by Kaplan et al. [*28,30,31*] also indicated that primates are much more tolerant of HCl than was previously believed. All the baboons exposed to doses of up to 150 000 ppm min survived the normal 14-day postexposure period used for testing inhalation toxicity.

However, two of these animals later developed pulmonary infections and were not adequately treated. They died postexposure at 18 days (after 16 570 ppm HCl for 5 min) and at 76 days (after 17 290 ppm HCl for 5 min). Since these two baboons developed pulmonary infections, it is not possible to determine whether they would have survived in the absence of infection or if they had received the same level of treatment that would have been provided to a human being. It has been suggested that the exposure of the baboons to HCl might have increased their susceptibility to pulmonary infection. This is a reasonable hypothesis, which cannot easily be confirmed either way. However, infection-free baboons have survived exposures of 150 000 ppm min (30 000 ppm for 5 min, 15 000 ppm for 10 min, or 10 000 ppm for 15 min). Furthermore, three baboons have later been exposed to levels of 10 000 ppm for 15 min (i.e., 150 000 ppm min) without observing any mortality. Exposures of baboons to doses of over 150 000 ppm min were not carried out, and this level is, therefore, conservatively, estimated to be close to a lethality threshold.

The lethality response to HCl of the rat and the primate thus appears to be very similar. The lowest lethal dose for a 5-min exposure (including postexposure) is virtually identical for rats and baboons. At longer exposures the primate appears to be somewhat less sensitive than the rat for a 30-min HCl exposure [28,30,31].

It is of interest, for comparison purposes, to mention the long-term exposure of rats and primates to another irritant, chlorine [*39,40*]: it gave similar results. Chlorine produces both upper and lower respiratory tract effects in rats, but only upper respiratory tract irritation in primates.

It was suggested [*41*] that rodents are less sensitive to HCl because rodents differ from primates by breathing through their noses only. Thus, it was further speculated, rodent nose ciliae will "scrub" out the water-soluble gases. In an effort to demonstrate this effect [*42*], mice were cannulated to bypass their noses and exposed to HCl: HCl LC_{50} was reported to decrease considerably. The author speculated that results with mice needed "correction" by this same factor to be an appropriate model for humans. However, tracheal cannulation bypasses the pharynx, the larynx, and a portion of the trachea, all of which are of major importance in scrubbing out water-soluble gases in man. For this reason, this approach exaggerates, unrealistically, the effects of HCl by sending it deep into the respiratory system. Such a procedure makes the mouse, an already sensitive animal, even more sensitive. An example of this excess sensitivity is the fact that mice often die of stress in the toxic potency test restrainers prior to smoke exposure.

There is abundant evidence that, when exposed to HCl, mice are much more sensitive than rats or primates and by implication humans. This excess mouse sensitivity ranges from four times, based on the LC_{50} [*26*], to 8 to 10 times, based on the lowest lethal dose for a 5-

Copyright by ASTM Int'l (all rights reserved) Wed Feb 07 10:53:32 UTC 2024
Downloaded/printed by
The University of Delaware pursuant to License Agreement. No further reproductions authorized.

min exposure, both within exposure [*38*] and including postexposure [*27*]. This suggests that, while the mouse is not a good model for humans in terms of lethality following HCl inhalation, the rat appears to approximate primate response well.

It has been suggested that this excess sensitivity of mice over rats may be due to the difference in body weight (rats being ca. ten times heavier than mice). This is based on the assumption that the mouse is roughly ten times more sensitive than the rat to all toxicants. However, studies with carbon monoxide suggest that both animal species have similar lethal sensitivities to asphyxiants: for a 30-min exposure, the LC_{50} for rats is 4600 ppm [*43*] and the LC_{50} for mice is 3000 ppm [*44*].

Exposure of rats and baboons to carbon monoxide has also suggested that both animal species are very similar in sensitivity to this asphyxiant gas in terms of both incapacitation and lethality [*28*].

Pulmonary Function Studies: Comparison of Primates with Rodents

It is critical to consider species differences when making qualitative and quantitative predictions of human response to pure gaseous HCl and to PVC smoke. Therefore, the Vinyl Institute sponsored a number of comparative studies of the response of primates and rodents. A fundamental objective of this investigation was to evaluate the validity of the various rodent species as models for man. The specific focus of the work was to gain information on HCl penetration damage into the respiratory tract. In particular, it was important to investigate whether the effects of HCl on pulmonary function reported by Burleigh-Flazer et al. [*45*] for the guinea pig also occur in other species, and, more importantly, in man. The primate chosen as surrogate for man was the baboon because its respiratory response to irritants, its upper airways, and its general physiology are all very similar to those of humans, in particular young children [*46*].

Experimental Details

Groups of three anesthetized baboons were exposed (head only) to air and to HCl at nominal concentrations of 500, 5000, and 10 000 ppm for 15 min. One of two continuous HCl measurement methods [*47,48*] was used to maintain constant concentration by flow rate adjustments. Actual measurements were made with titration of soda lime tubes [*49*]. The average HCl concentrations measured during all the exposures were 562, 4145, and 10 170 ppm. Room air was maintained at ca. 23°C and 50% relative humidity. The exposure chamber was a ca. 200-L poly (methyl methacrylate) (PMMA) box (Fig. 2).

Respiratory rate (f), tidal volume (V_T), and minute volume (MV) were measured continuously with an inductive plethysmograph, starting prior to the test and ending 15 min after exposure. Pulmonary function was measured before exposure and at three days and three, six, and twelve months by three methods: two direct ones [*50,51*] and an indirect one (CO_2 challenge: 5-min ramping up to 10% CO_2 and 5 min at this final value). Arterial blood samples were analyzed also for pH and partial pressures of oxygen (PaO_2) and of carbon dioxide ($PaCO_2$) before, during, and immediately after exposure until the animal's appearance was normal. Anteroposterior and lateral chest X-rays were taken within 1 h after all exposures to the highest HCl concentration (10 000 ppm).

Further details of these experiments are published elsewhere [*36*].

Results

The response of the baboons exposed to the lower HCl concentration (500 ppm) was not statistically distinguishable from that of those exposed to air for all parameters measured.

Copyright by ASTM Int'l (all rights reserved) Wed Feb 07 10:53:32 UTC 2024
Downloaded/printed by
The University of Delaware pursuant to License Agreement. No further reproductions authorized.

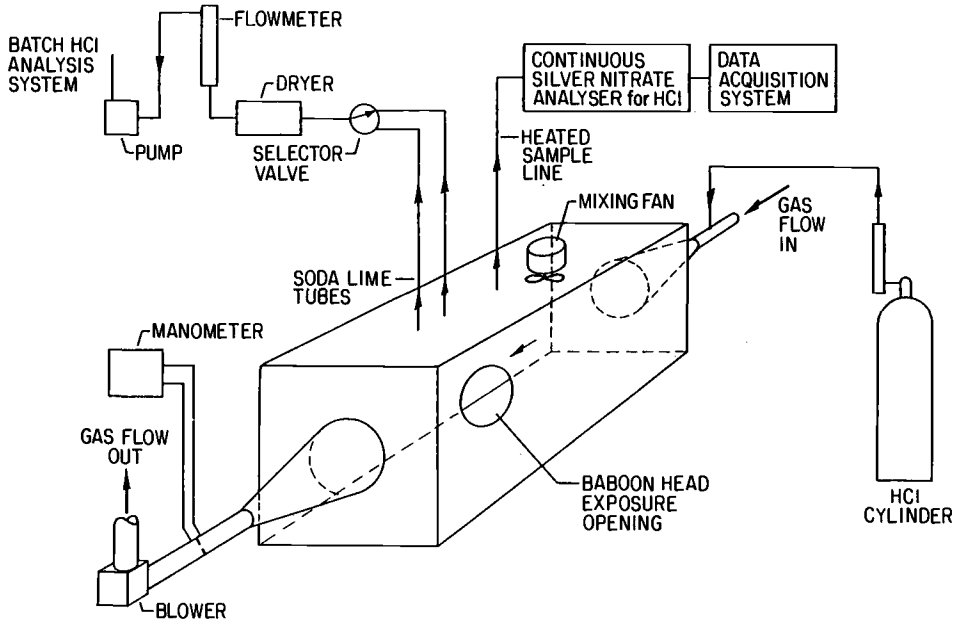

FIG. 2—*Baboon exposure system.*

For the baboons exposed to 5000 and 10 000 ppm HCl, their respiratory frequency increased during exposure after they had held their breaths for 10 to 20 s. This is consistent with previous findings [*52,53*] of responses of human and nonhuman primates to irritants. On the other hand, rodents respond to irritants by decreasing their respiratory frequency. The tidal volume of all baboons remained unchanged. In other words, the baboons exposed to high HCl concentrations breathed more frequently, but took in the same amount of air in each breath. However, their arterial oxygen pressure decreased rapidly throughout exposure and up to 10 min postexposure. These decreased PaO_2 values reverted to normal within 10 min and remained normal throughout at least three months postexposure.

The arterial blood pH and CO_2 pressure did not change for the baboons at any dose level. This contrasts with reports on rodent (rabbit) exposures to PVC combustion products (including HCl) wherein decreased blood pH was measured [*54*]. This may be due to baboons being better able than rabbits to compensate for pH changes or to a lack of proper statistical analysis of the rodent data. It is also possible, albeit unlikely, that a species other than HCl is responsible for the increased blood acidity.

The noninvasive pulmonary function tests showed no significant differences between the control and the exposed groups throughout at least three months postexposure.

The carbon dioxide challenge tests showed considerable variability among the animals in each group, making the results difficult to interpret. The tidal volume response was not changed. The respiratory frequency of the baboons appeared to increase at three months (although not at six months) for the baboons at the highest exposure levels. This is likely to be a measurement artifact, since an impairment in lung function due to HCl producing any obstructive lung disease would result in a decrease in ventilatory response.

Guinea pigs have been shown to develop decreased respiratory response to CO_2 challenge up to ten days after exposure to HCl levels as low as 1040 ppm for 30 min (31 200 ppm min) [*45*]. For the primates tested in this study no evidence of changes in pulmonary function

Copyright by ASTM Int'l (all rights reserved) Wed Feb 07 10:53:32 UTC 2024
Downloaded/printed by
The University of Delaware pursuant to License Agreement. No further reproductions authorized.

were observed after exposures to levels of HCl as high as 10 000 ppm for 15 min (i.e., 150 000 ppm min) following three months of postexposure observations.

The X-rays and the clinical observations show that these baboons, exposed to high levels of HCl (75 000 to 150 000 ppm min), suffered no pulmonary edema, but only some hypoxia via small airway constriction. This is in contrast to reports of pulmonary edema in guinea pigs, although those rodents were exposed to much lower HCl doses [*45*]. It is interesting that in a recent study on guinea pigs these animals were shown to be both much more sensitive to HCl than rats (guinea pig HCl LC_{50} values of 1350 ppm for 15 min and 2900 ppm for 30 min [*55*]), and much less sensitive to CO.

Primates can tolerate 150 000 ppm min HCl without lethality occurring, while death was observed at exposures as low as 16 000 ppm min for mice [*28*] and 30 000 ppm min for guinea pigs [*45*].

Summary of Effects of HCl

HCl is an irritant, the effect of which often occurs long after exposure. It has now been established that HCl will not cause lethality until exposures to very high concentrations are maintained for long periods. The combination of HCl with other toxicants, in particular the asphyxiants CO and HCN, appears to cause additive, but not synergistic, toxic effects [*37, 55*]. This is similar to the combined effects of CO and HCN [*43,45*], even though the mechanisms of action of the various toxicants are very different.

However, HCl has a very disagreeable odor, noticeable at an extremely low concentration: less than 1 ppm [*56*]. Moreover, low concentrations of HCl can cause unpleasant irritating effects which make its presence noticeable very early on in a fire. The appearance of such an odor at a concentration much lower than one which will cause health effects may serve, of course, as a warning of the need to leave the room or building, although it produces the erroneous impression that HCl is causing severe harm.

Overall: HCl toxicity on animal species can be summarized as follows:

Baboons

1. *Incapacitation:* baboons will not be incapacitated by exposure to up to 30 000 ppm HCl in 5 min or to other exposure doses of 150 000 ppm min.
2. *Lethality:* baboons have survived, without adverse long-term effects, exposures of up to 30 000 ppm HCl for 5 min (although one baboon died 18 days after an exposure to 16 570 ppm) and other exposures to ca. 150 000 ppm min. The lethal exposure dose threshold is, however, unlikely to be much higher than 150 000 ppm min.
3. *Pulmonary function:* baboons have not developed long-term physiological or pulmonary function effects after exposures to nominal concentrations of 5000 or 10 000 ppm HCl for 15 min.
4. *Model for humans:* baboons have an anatomical and physiological system very similar to that of a young child.

Rats

1. *Incapacitation:* rats will not be incapacitated by up to 76 730 ppm HCl in 5 min, although they will die postexposure at concentrations higher than 20 000 ppm.
2. *Lethality:* rats do not die from exposures of 5000 ppm for 15 min.
3. *Lethality:* rats have a lowest lethal concentration at 5 min within exposure of 87 660 ppm, and at seven days' postexposure of 32 255 ppm.

Copyright by ASTM Int'l (all rights reserved) Wed Feb 07 10:53:32 UTC 2024
Downloaded/printed by
The University of Delaware pursuant to License Agreement. No further reproductions authorized.

4. *Lethality:* rats have a lethal exposure dose ranging between 112 000 and 169 000 ppm min, depending on time of exposure.

5. *Model for humans:* while rats are not similar to primates either in lung anatomy or in respiratory response (i.e., they are obligate nose breathers and respond by respiratory depression), their lethality response to HCl appears to model that of baboons very well.

Mice

1. *Incapacitation:* mice will be incapacitated and die at an exposure of 2550 ppm for 15 min.

2. *Lethality:* mice have a lowest lethal concentration of 11 482 ppm at 5 min within exposure, and of 3200 ppm after seven days' postexposure, i.e., one eighth to one tenth of rat levels.

3. *Lethality:* the LC_{50} for mice is three to eight times lower than the one for rats when exposed to smoke containing irritants in similar scenarios.

4. *Lethality:* mice and rats are of similar sensitivity towards asphyxiants.

5. *Model for humans:* mice have a much higher sensitivity to HCl in particular and to irritants in general than rats or primates.

Studies on PVC Smoke Toxicity

Influence of Toxicity Protocol and Animal Species

A number of screening tests are being used to evaluate the toxicity of smoke from burning materials. Some even form the basis of regulation or specifications. Three tests methods were, therefore, chosen in order to investigate how they would affect a number of flexible PVC compounds [*38*]. The test methods chosen were the NBS cup furnace protocol, in the flaming and nonflaming modes [*1*], the radiant furnace (RF) test (in the flaming mode at 5 W/cm^2) [*4*], and the UPITT test [*3*]. The PVC compounds chosen were two standard commercial compounds [a standard jacket (SJ) and a standard insulation (SI)] as well as two experimental wire coating materials. Results on a nylon compound (NR) and on wood (Douglas fir) were also used for some comparisons.

The concentration of the major toxicants in PVC smoke, viz., HCl (by a combination of a continuous method [*48*] and soda lime tubes [*49*]) and CO, as well as carbon dioxide and oxygen, were measured for all protocols and materials. The mechanisms by which lethality occurs in each case were inferred from toxicological interpretation of the analytical results.

The experimental compounds were developed in order to decrease HCl emission. According to a laboratory procedure [*57*], they generate only 38.1% (EXP B) and 19.3% (EXP C) of their available chlorine as HCl. This is much less than the percentage of available chlorine generated by most standard commercial compounds; the ones investigated here released 87.7% (SI) and 95.3% (SJ) of available chlorine. Interestingly, the experimental compounds also generate much less HCl per unit mass burnt than the standard materials in all the test protocols (Table 2 shows results based on total gas measurements). Furthermore, the experimental compounds also generate much less CO than the standard materials (Table 2). It is not surprising, therefore, that the associated toxic potencies of the experimental materials (measured in terms of the LC_{50}, according to the published protocols) are also much lower (Table 3).

This is an important result in itself because it indicates that the toxic potency of a PVC compound is not a fixed value. Comparisons between the various test protocols give some further insight into the extent of the protocols' utilities. Table 3 also shows the extent to which results can be differentiated: results are designated with letters indicating those which are significantly different at $p = 0.05$ level (i.e., with statistical validity).

Copyright by ASTM Int'l (all rights reserved) Wed Feb 07 10:53:32 UTC 2024
Downloaded/printed by
The University of Delaware pursuant to License Agreement. No further reproductions authorized.

TABLE 2—*Relative generation of major toxicants in test protocol atmospheres.*

	NBS NF	NBS F	RF	UPITT
		HCl		
SI	100	100	100	100
SJ	62	91	66	197
EXP B	21	11	8	45
EXP C	4	0.2	0	17
		CO		
SI	100	100	100	100
SJ	66	82	63	125
EXP B	30	48	38	63
EXP C	25	23	23	36

TABLE 3—*Lethal potencies (LC_{50} values) of PVC compounds determined by three test methods.*[a,b]

NBS Nonflaming, mg/L			NBS Flaming, mg/L		
A	SI	25.0 (20.0–32.4)	A	SJ	29.6 (22.7–37.4)
A	SJ	31.6 (27.8–36.1)	A	SI	35.0 (31.3–39.2)
B	EXP B	55.7 (44.5–66.0)	B	EXP B	60.8 (53.0–70.0)
B	EXP C	59.9 (52.5–64.9)	C	EXP C	159.0 (127.0–199.0)
Radiant Heater, mg/L			**UPITT, g**		
A	SI	33.4 (29.5–56.1)[c]	A	SJ	5.5 (4.2–7.1)
B	SJ	53.1 (49.6–55.9)	A	SI	5.6 (3.9–8.2)
C	EXP B	86.2 (79.0–93.5)	BA	EXP B	10.0 (5.1–19.4)
D	EXP C	149.0 (122.0–184.0)	B	EXP C	21.6 (11.1–42.0)

[a] Values are LC_{50} values and 95% confidence limits calculated from initial sample weights. UPITT values were determined using a standard 2.3-L exposure chamber.

[b] Values with a different letter are significantly different at $p = 0.05$ level. For NBS and radiant heater materials, comparisons were done by potency ratio analysis. UPITT statistical comparisons were by S. Debanne of Case Western Reserve University.

[c] Calculated from three experiments: 25 mg/L: 0/6; 30 mg/L: 1/6; and 35 mg/l: 4/6.

In the NBS protocol, nonflaming mode, the LC_{50}'s of the four compounds can be statistically differentiated into two groups: standard compounds and experimental compounds. Moving on to NBS, flaming, differentiation becomes even clearer: while the LC_{50}'s of the standard compounds are similar, the LC_{50} of EXP B is statistically different and higher and the LC_{50} of EXP C even higher. In the radiant furnace protocol, the LC_{50}'s of all four compounds are statistically differentiable. In fact, in the NBS flaming and in the radiant heater protocols, there is a five-fold difference between the LC_{50} of standard insulation and that of EXP C! However, in the UPITT protocol, only the LC_{50} of EXP C can be statistically differentiated from that of the other compounds.

This suggests that there may be some specific problems with the UPITT test protocol. A deeper study of this protocol identified some of the problems [*58*]. The analytical data showed that the experimental materials generated atmospheres of very low lethal potential. Furthermore, the analytical ranking of toxic potential was the following, similar to that of the NBS and radiant furnace protocols:

$$\text{SJ} > \text{SI} \gg \text{EXP B} > \text{EXP C}$$

Copyright by ASTM Int'l (all rights reserved) Wed Feb 07 10:53:32 UTC 2024
Downloaded/printed by
The University of Delaware pursuant to License Agreement. No further reproductions authorized.

There are two main reasons for the discrepancies: (1) the extreme sensitivity of the mouse as an animal model for inhalation of irritants, and of HCl in particular (which has already been discussed); and (2) the short burst of extremely high toxic gas concentrations during the test.

The mouse is much more sensitive than the rat (or, for that matter, the primate) to HCl. Moreover, while HCl decreases the sensitivity of rats to CO [*38*], it increases the sensitivity of mice to CO.

The LC_{50}'s of four materials were also tested, using identical tests but varying the animals. Table 4 shows that mice are 2.4 to 7.5 times more sensitive than rats to smoke-containing irritants [*38*], a result similar to that found for pure gases.

The UPITT method generates the toxic gases over a very short period: for many materials the entire mass loss process takes place over a 3 to 7 min period. This type of exposure is generally much more toxicologically severe than exposure to the same dose, but involving lower concentrations and a longer exposure period.

The type of exposure simulated in this test would correspond to a very intense fire in the proximity of the victim. Fire exposures in the room of origin are only of real-life relevance if they are limited to preflashover conditions. After flashover the smoke and toxic gases will be transported to other rooms, and the exposures will no longer be so short and intense.

Other serious technical problems have been identified for the UPITT test protocol: design features leading to leakages [*59*] and safety concerns and unrealistic representations of any stage of a real fire [*60*], as well as a poor statistical method of calculation of results [*61*]. Recent results suggest that multiple LC_{50} values can also be obtained for a single material [*62*].

The specific problems with the UPITT protocol should not overshadow the fact that the measurement of LC_{50}'s is a very poor means of quantifying toxic hazard. Several better ways have been identified recently. Two intermediate procedures are a test for potential toxic hazard being developed by the National Institute for Building Sciences (NIBS) for application to end-use products and a quick measure of toxic hazard, based on the combination of toxic potency, mass loss rate, and time to igniton [*6*]. Both of these methods recognize that the comparison of product toxicity should take into account their propensities to resist burning. Ultimately, toxic hazard is but one element in an overall fire hazard assessment.

Summary of Effects of PVC Smoke

Overall results of recent studies on PVC smoke toxicity can be summarized as follows:

1. The toxic potency of PVC smoke is within the normal range found for those of all common products.

TABLE 4—*Lethal potencies (LC_{50} values) of SJ, EX C, NR, and Douglas fir determined by NBS test method with rats and mice.*

	NBS-NF,[a] Rats	NBS-NF,[a] Mice	NBS-F,[b] Rats	NBS-F,[b] Mice
SJ	31.6 (27.8–36.1)	4.2 (2.5–6.7)		
EX C	59.9 (52.5–64.9)	13.9 (7.7–20.8)		
NR			49.0 (42.2–57.0)	20.2 (14.3–30.4)
DF[c]	32.8 (29.3–36.7)	8.9 (6.5–11.8)	37.6 (33.2–44.6)	

NOTE: Values are sample charges in mg/L units.
[a] NBS nonflaming mode.
[b] NBS flaming mode.
[c] DF = Douglas fir.

Copyright by ASTM Int'l (all rights reserved) Wed Feb 07 10:53:32 UTC 2024
Downloaded/printed by
The University of Delaware pursuant to License Agreement. No further reproductions authorized.

2. Different PVC products can have a very wide range of toxic potencies within that overall range.
3. Lower toxic potency is, as stated before, only a minor aspect of fire safety.
4. Toxic potency test protocols, measuring LC_{50}'s, are a poor way of measuring potential toxic hazard.
5. The UPITT test is the least satisfactory protocol in U.S. use.

Decay of HCl

A series of studies was also done to investigate the lifetime of HCl in a fire atmosphere [*49,63–64*]. These studies showed that HCl reacts very rapidly with most common construction surfaces (cement block, ceiling tile, gypsum board, etc.). Therefore, the peak HCl concentration found in a fire is much lower than would have been predicted from the chlorine content of the burning material. Moreover, this peak concentration soon decreases, and HCl disappears completely from the air. The peak HCl concentration found in a full-scale plenum was only up to 35% of the theoretical concentration [*50*]. In a simulated smaller-scale plenum this decreased even further: 10% of theory [*63*]. These and other studies were used as the basis for developing a mathematical model for HCl generation, transport, and decay [*64*]. This model was also applied successfully to PVC burning and HCl emission in experiments involving a full-scale room-corridor-room design [*65*].

One of the consequences of these studies is that toxicity tests carried out in glass or plastic exposure chambers may exaggerate PVC smoke toxicity. On such surfaces HCl does not decay as fast as on realistic surfaces, so that toxic gases remain present longer than in real fires.

Carbon monoxide gas phase concentration does not decay in a fire atmosphere [*49*]. Carbon monoxide causes physiological harm by reacting with hemoglobin in blood and forming carboxyhemoglobin (COHb). Interestingly, high blood COHb levels have been found to correlate well with fire fatalities [*6*]. Furthermore, actual HCl concentrations found in real fires are much lower than those of CO [*6*]. This means that the toxic hazard associated with HCl in a fire is likely to be relatively small compared with that of the main fire toxicant: CO.

Fire Properties of PVC

There are a great variety of PVC products, with tremendous differences in fire performance. However, there is one common thread: PVC contains chlorine in its structure. This decreases the tendency to ignite or burn because it is one of the very few chemical elements conferring fire retardancy when introduced at the appropriate level and form [*9*].

In general, unplasticized (rigid) PVC products will not sustain combustion or spread flame in the absence of a continuous applied heat source. Most small-scale test results show PVC products (particularly rigids) to be among those with better fire properties. Such results are further confirmed by large-scale tests [*66*] and by model calculations [*67*].

Conclusions

1. There is no single toxicity for the products in PVC smoke: it can vary widely.
2. The toxic potency of the smoke from most PVC products is similar to that of most ordinary products in use in society.
3. PVC is unusual because it liberates HCl when it burns.
4. HCl is of similar toxicity to the principal fire toxicant: CO.
5. HCl decays rapidly in a fire atmosphere, while CO does not.
6. Rats are reasonable models of lethality for humans, but mice are excessively sensitive.

Copyright by ASTM Int'l (all rights reserved) Wed Feb 07 10:53:32 UTC 2024
Downloaded/printed by
The University of Delaware pursuant to License Agreement. No further reproductions authorized.

7. Toxicity tests based solely on LC_{50}'s cannot predict toxic hazard, and the UPITT test is less satisfactory than other tests.

8. Better predictions can be made from measurements combining toxicity, mass loss rate, and ignition resistance, leading ultimately to fire hazard assessment.

APPENDIX

Details of Very Early HCl Experiments

Reference 20
HCl Experiments on Animals

I. 7 Dec. 1885. 1 cat: 6 h; 0.1 0/00 HCl: secretion after 50 min, no eye irritation, no dyspnea, very few pain symptoms.

II. 30 Nov. 1885. 1 rabbit, 1 guinea pig, 3 frogs; 3 h 10 min; 0.14 0/00 HCl: Rabbits and guinea pigs show mild signs of irritation, slight conjunctivitis, no secretion. Frogs all died after 90 min.

III. 24 Nov. 1885. 1 rabbit, 2 guinea pigs; 6 h; 0.3 0/00 HCl. Rabbits: few signs of irritation during test, some catarrh, cornea somewhat deepened, crust formation around nose, back to normal after 3 days. Guinea pigs: deepened respiration, some reaction of their cornea to acid gases, all effects clear by 11 days.

IV. 27 March 1886. 1 very large, very old cat: 6 h; 0.9 0/00 HCl. Respiration rate decreases after only 20 min, tears and salivation after 80 min, lack of reaction for the rest of exposure, except for heavy snoring, destroyed 20 min after exposure, pulmonary hemorrhage found on autopsy, no stomach hemorrhage.

V. 11 Dec. 1885. 1 cat, 1 rabbit and 1 guinea pig; 6 h: overall average 1 0/00 HCl, but 1 h at 0.47 0/00 HCl and 5 h at 0.103 0/00 HCl. Cat: abundant secretion very soon, some tears at 20 min, low respiration rate after 85 min, low level of activity for the rest of the exposure and recovered after a few days. Rabbit: no symptoms for 2 h, corneal damage at 140 min, very low activity for remainder of exposure, lesions develop after exposure on outside of nasal cavities and death occurs after 5 weeks, although no pathological explanation was found. Guinea pig: dyspnea after 15 min, ocular secretion after 90 min, worsening and death after 230 min. Pathology suggests it died of asphyxiation due to tracheal blockage.

VI. 2 Dec. 1885. 1 rabbit, 1 guinea pig, 4 frogs; 2 h at 1.06 0/00 HCl and 2 h 15 min at 1.00 0/00 HCl. 3 frogs died by 50 min; 1 was taken out at 25 min with some effects of acid attack; all suffered respiratory abnormalities very early on. Rabbit had some secretion at 20 min; some light corneal damage after experiment; no respiratory damage; recovered well. Guinea pig suffered severe respiratory damage; corneal opacity; dyspnea; died after 3 days.

VII. 27 Oct. 1885. 1 not quite adult hare, 1 guinea pig, 1 rat; 1 h 15 min; 1.35 0/00 HCl. Hare died at 23 days, with dyspnea, very strong respiratory damage, some lung hemorrhage, emphysema, no corneal damage. Guinea pig had some secretion at 15 min, some corneal damage, recovered well, and was reused for exposure. Rat suffered only decreased respiration and recovered by 48 h.

VIII. 20 Nov. 1885. 2 rabbits, 1 guinea pig. 100 min; 1.29 0/00 HCl. No serious ill effects except for some corneal opacity; slight lung hemorrhages in rabbits and some tracheal damage. All animals recovered well.

IX. 19 March 1886. 2 almost adult guinea pigs, 1 adult rabbit. 1.54 0/00 HCl; 6 h 40 min. Guinea pigs died at 2 h 10 min with pulmonary edema and corneal opacity. Rabbit suffers decreased respiration, secretion after 20 min, escapes from captivity at 17 days.

X. 8 Dec. 1885. 1 2–3 month old cat; 1 big adult rabbit; 1 guinea pig. 3.4 0/00 HCl; 1 h 30 min. Cat suffers severe pain and secretion, corneal damage; sacrificed after exposure show-

Copyright by ASTM Int'l (all rights reserved) Wed Feb 07 10:53:32 UTC 2024
Downloaded/printed by
The University of Delaware pursuant to License Agreement. No further reproductions authorized.

TABLE 5—*Animal exposures to HCl by Lehmann (Ref 20).*

No.	HCl, (0/00)	Time, h	Symptoms	Fate
			CAT	
I	0.10	6	Light nasal secretion	Fine
IV	0.90	6	Secretion, dyspnea, lung damage	Sacrif. immedat.
V	0.47/1.0	6	Similar symptoms to IV	Recovers
X	3.4	1.5	Pain, Secretion, Emphys., Edema, corneal damage	Sacrif. immedat.
XIII	5.0	0.2	No secretion, deeply narcotized before exposure	Dead
			RABBIT	
II	0.14	3.17	Light effects	Fine
III	0.3	6	Corneal damage, slight respir. irritation	Recovers at 3 days
V	0.47/1.0	6.33	Slight damage, catarrh	Dead 6 wks
VI	1.1	4.33	Similar to V	Recovers
VII	1.35	1.25	Dyspnea, corneal damage, lung hemorrhages	Recovers + dead 23 d
VIII	1.35	1.17	Slight respiratory dam.	Fine
VIII	1.35	1.67	Idem	Fine
IX	1.40	6.67	Slight respir. dam, wt loss, slight corneal dam	Escapes at 17 days
X	3.4	1.5	Dyspnea, conjunct, lung damage	Dead at 5.5 days
XI	2.43–4.45	4.67	Lung hemorrhage, tracheal damage, dyspnea	Dead 24 h
XIII	5.6	3.75	Dyspnea, laryngeal hemorr.	Dead 5 d
			GUINEA PIG	
III	0.3	6	Respir. trouble, corneal damage	Recovers at 11 d
III	0.3	6	Idem	Recov. 6 d
V	1.03	3.73	Dyspnea, lung hemorrh.	Dead in exp
VI	1.1	4.33	Idem	Dead 3 d
VII	1.35	1.25	Irritation, corneal dam.	Recov. 16 d
VIII	1.35	1.67	Dyspnea, lung hemorrhage	Sacrif.
IX	1.54	2.17	Idem	Dead in exp
IX	1.54	2.17	Idem	Dead in exp
XI	2.43	0.85	Dyspnea, convulsion, lung and stomach hemorrhage	Dead in exp
X	3.4	1.55	Dyspnea, lung hemorrhage	Dead 48 h
XIII	5.6	0.58	Idem	Dead soon
			RAT	
VII	1.35	1.25	Decreased respiration	Recov. 48 h
XI	2.43–4.45	4.67	Dyspnea, secretion, resp.	Sacrif.
XI	2.43–4.45	4.67	Dyspnea, no secretion	Dead at 2 d

ing lung emphysema and tracheal damage. Rabbit dies at 5½ days, with lung emphysema. Guinea pig dies at 48 h, with lung hemorrhages.

XI. 20 March 1886. 1 not fully grown rabbit, 1 guinea pig, 2 rats. 1 h at 2.67 0/00 HCl, 2.5 h at 3.49 0/00 HCl, and 1 h at 4.9 0/00 HCl. Rabbit dies 24 h after exposure; guinea pig dies at 51 min within exposure. 1 rat is sacrificed 1 day after exposure and the other one dies 3 days after exposure.

Copyright by ASTM Int'l (all rights reserved) Wed Feb 07 10:53:32 UTC 2024
Downloaded/printed by
The University of Delaware pursuant to License Agreement. No further reproductions authorized.

XII. 30 March 1886. 1 big adult cat. 5.0 0/00 HCl; 12 min. Cat was exposed under chloroform anesthetic because of its hyperactivity and died at 12 min.

XIII. 30 March 1886. 1 big rabbit; 1 guinea pig. 1 h at 5.88 0/00 HCl and 2 h 45 min at 5.4 0/00 HCl. Guinea pig was taken out at 35 min and died soon after exposure. Rabbit died 6 days after exposure.

Details of all these experiments are shown in Tables 5 and 6.

Experiment on a man (30 yr old)

The subject wore a type of gas mask by means of which he could breathe through his mouth if the HCl became intolerable.

12 min; 0.05 0/00 HCl; found working in the room absolutely impossible and requested to terminate the experiment after 12 min, part of which was spent outside. He had some

TABLE 6—*Animal HCl exposure doses (Lehmann exposures; Ref* 20).

No.	HCl, (0/00)	Time, h	Exposure dose, ppm min	Lethality
		CAT		
I	0.10	6	36 000	No
IV	0.90	6	324 000	No
V	0.47/1.0	6	336 300	No
X	3.4	1.5	306 000	No
XIII	5.0	0.2	60 000	Yes
		RABBIT		
II	0.14	3.17	26 600	No
III	0.3	6	108 000	No
V	0.47/1.0	6.33	356 900	At 6 wks
VI	1.1	4.33	286 000	No
VII	1.35	1.25	101 250	At 23 days
VIII	1.35	1.17	94 500	No
VIII	1.35	1.67	135 000	No
IX	1.40	6.67	560 000	No
X	3.4	1.5	306 000	At 5.5 days
XI	2.43–4.45	4.67	977 700	At 24 h
XIII	5.6	3.75	1,260 000	At 5 days
		GUINEA PIG		
III	0.3	6	108 000	No
III	0.3	6	108 000	No
V	1.03	3.73	236 900	Yes
VI	1.1	4.33	286 000	At 3 days
VII	1.35	1.25	101 250	No
VIII	1.35	1.67	135 000	No
IX	1.54	2.17	200 200	Yes
IX	1.54	2.17	200 200	Yes
XI	2.43	0.85	123 930	Yes
X	3.4	1.55	316 200	At 48 h
XIII	5.6	0.58	196 000	Yes
		RAT		
VII	1.35	1.25	101 250	No
XI	2.43–4.45	4.67	977 700	No
XI	2.43–4.45	4.67	977 700	At 2 days
		MAN		
	0.05	0.2	600	No lasting effect

Copyright by ASTM Int'l (all rights reserved) Wed Feb 07 10:53:32 UTC 2024
Downloaded/printed by
The University of Delaware pursuant to License Agreement. No further reproductions authorized.

irritation of respiratory system (nose, larynx), irregular respiration solely through nose, chest pains (needle-like sensation), shortness of breath, no eye irritation, no acid taste.

Reference 21
3 HCl Experiments on Humans

1. 13 Dec. 1888. 3 men; 0.01 0/00 HCl; 10 min.
Exposure Dose: 100 ppm min

Cold and acid sensation in nose, mouth, and throat, no effect on eyes, slight discomfort in larynx, trachea, and lung. Some secretion and coughing. One subject had slight head and chest pains. Recovery immediate on leaving HCl atmosphere.

2. 18 Dec. 1888. 1 man; 0.07 0/00 HCl; 15 min.
Exposure Dose: 1,050 ppm min

Little eye irritation, some irritation on breathing through mouth, respiration somewhat superficial, irritation in nose, throat, larynx, trachea, and sternum, including "scratching" feelings, coughing. Room had to be exited because of chest pains. Slight headache on termination of experiment, which disappeared very rapidly.

3. 13 Dec. 1888. 1 man; 0.1 0/00 HCl; 15 min.
Exposure Dose: 1,500 ppm min

Slight irritation in eyes, abundant tear secretion, strong feeling of coldness and irritation in nose, mouth, throat, larynx, and trachea. Respiration enhanced and salivation increased. Strong coughing and sensation of heat in head, forcing room exit. On reentry, abundant coughing and catarrh. After experiment, slight headache and catarrh, soon disappearing.

Matt's Recommendation of Human Work-Place Limits for HCl:

Work Unhindered	Work Possible but Uncomfortable	Work Impossible
0.01 0/00 HCl 10 ppm	0.01–0.05 0/00 HCl 10–50 ppm	0.05–0.1 0/00 HCl 50–100 ppm

This work was destined to address safe work-place concentrations of HCl and did not involve any studies at concentrations which were incapacitating or lethal.

Reference 22
HCl Experiments on Humans and Animals

3 Human Experiments: a man (Dr. Yamada) breathes from a ca. 5-L bottle containing 60 cm^3, 80 cm^3, and 70 cm^3 of concentrated HCl, for 20, 20, and 5 min, respectively, and exhales into another ca. 5-L bottle. There is no mention whatever of any ill effects on the subject, who is one of the paper's authors. The total HCl present in the experiment is: (1) 22.8 g; (2) 30.4 g; and (3) 26.6 g. The inhaled doses were: (1) 4021 ppm min; (2) 4107 ppm min; and (3) 5170 ppm min.

Narcotized cannulated rabbits were also exposed at doses ranging from 3800 ppm min to 680 900 ppm min and their HCl uptake determined. Almost all the HCl contained in the atmosphere was absorbed by the human body (over 95%), a slightly higher uptake (referred in the paper as absorption) than that of the narcotized, cannulated rabbits (60 to 75%). It is worth mentioning, however, that the rabbits were exposed to much higher doses of HCl, not

Copyright by ASTM Int'l (all rights reserved) Wed Feb 07 10:53:32 UTC 2024
Downloaded/printed by
The University of Delaware pursuant to License Agreement. No further reproductions authorized.

TABLE 7—*Uptake of HCl in humans and rabbits (Lehmann et al. tests; Ref. 22).*

Test	Time, min	Initial HCl		Final HCl		Inhaled Dose		Absorption, %
		mg	mg/L	mg	mg/L	ppm	ppm min	
				HUMANS				
I	20	1.4	0.292	0.05	0.0106	201	4,021	96.4
II	20	1.4	0.298	0.06	0.0125	205	4,107	95.8
III	5	1.8	0.375	1.8	0.0170	258	5,170	95.5
				RABBITS				
XI	60		0.34	9	0.13	228	13 700	61
X	15		0.38		0.10	255	3 800	73
I	60		1.44		0.47	966	58 000	68
VIII	15		2.0		0.7	1 342	20 100	65
III	35		2.57		1.1	1 725	60 400	63
II	60		3.0		1.22	2 013	120 800	59
V	60		3.3		1.36	2 215	132 900	59
IV	60		3.1		1.1	2 081	124 800	64
IV	60		11.6		2.85	7 785	467 100	75
VII	57		17.0		5.5	11 946	680 900	69

NOTE: There are typographical errors in the paper for Exp. III.

only higher concentrations (0.34 to 17.8 mg/L) but also longer times (15 to 60 min). Only one rabbit died at the highest exposure dose, that of 680 900 ppm min.

Details of these results are shown in Table 7.

Reference 23
Long-Term Exposures of Animals to HCl

Exposures to 0.1 0/00 HCl, 6 h/day for 50 days.

Exposure doses: 36 000 ppm min per day times 50 days: 1 800 000 ppm min total. For: 15 rabbits, 20 guinea pigs, and 3 doves.

During inhalations, the animals were restless, had light tear secretion, and some mucus secretion on the first day. Some lost weight, between 10 and 60 g, while others gained weight, between 10 and 50 g, without a discernible pattern.

The conclusion was that these inhalations had no noticeable postexposure effects on the animals except for a very minor decrease in blood hemoglobin. There was no effect, either, on production of antibodies for a variety of illnesses.

Reference 24
Exposures of Rabbits to HCl

Rabbits underwent tracheotomies and were exposed to flows of atmospheres containing HCl. The exposure doses ranged from 66 400 ppm min to 566 400 ppm min. They were monitored every few minutes, and it was found that they absorb between 58 and 80% of the HCl they inhale, with 63% being the most frequent result. Some animals died during the experiments, but this was not directly related to dose since the rabbit exposed to the highest dose survived the experiment.

Details of these results are shown in Table 8.

Footnote: It is interesting to find out that neither the concentration of HCl to which a subject is being exposed nor the exposure dose, in concentration × time units, are sufficient on their own to determine lethal levels. There was a threshold HCl concentration below which lethality was never observed for each animal species. However, in some cases, lethality was not observed at higher concentrations when the exposures were shorter.

Copyright by ASTM Int'l (all rights reserved) Wed Feb 07 10:53:32 UTC 2024
Downloaded/printed by
The University of Delaware pursuant to License Agreement. No further reproductions authorized.

TABLE 8—*Exposures of tracheotomised rabbits by Lehmann and Burck (Ref 24).*

Test	Time, min	Exposure, ppm	Survivor	Dose, ppm min
I	60	5400–6000	Yes	346 600
II: Same animal as I				
II	20	11 400	No	228 000
III	90	3000–3800	Yes	310 300
IV	120	560–1600	Yes	99 800
V	60	1250	No	75 200
VII	120	800–1210	No	114 200
VIII	60	940–1270	No	66 400
IX	100	1560–1970	No	186 300
X	120	4070–5380	Yes	567 400
XI	30	2020	No	355 500
XII	120	2280–2550	No	295 000
XIII	45	3550	No	160 000
XIV	75	4020–4290	No	310 700

NOTE: 1 L HCl is equivalent to: 1.49 g HCl; 1000 ppm HCl in 1-L air is equivalent to: 1.49 mg HCl.

References

[*1*] Levin, B. C., Fowell, A. J., Birky, M. M., Paabo, M., Stolte, A., and Malek, D., "Further Development of a Test Method for the Assessment of the Acute Inhalation Toxicity of Combustion Products," NBSIR 82-2532, National Bureau of Standards, Gaithersburg, MD, 1982.

[*2*] Kimmerle, G., "Aspects and Methodology for the Evaluation of Toxicological Parameters during Fire Exposure," *Journal of Combustion Toxicology,* Vol. 1, 1974, p. 4.

[*3*] Alarie, Y. C. and Anderson, R. C., "Toxicologic and Acute Lethal Hazard Evaluation of Thermal Decomposition Products of Synthetic and Natural Polymers," *Toxicology and Applied Pharmacology,* Vol. 51, 1979, p. 341.

[*4*] Alexeeff, G. V. and Packham, S. C., "Use of a Radiant Furnace Fire Model to Evaluate Acute Toxicity of Smoke," *Journal of Fire Sciences,* Vol. 2, 1984, p. 306.

[*5*] Cornish, H. H., Hahn, K. J., and Barth, M. L., "Experimental Toxicology of Pyrolysis and Combustion Hazards," *Environmental Health Perspectives,* Vol. 11, 1975, pp. 191–96.

[*6*] Hirschler, M. M., "Fire Hazard and Toxic Potency of the Smoke from Burning Materials," *Journal of Fire Sciences,* Vol. 5, 1987, pp. 289–307.

[*7*] Casarett, L. J., in *Toxicology—The Basic Science of Poisons,* L. J. Casarett and J. Doull, Eds., New York, Macmillan, 1975, p. 24.

[*8*] Hilado, C. J., *Flammability Handbook of Plastics,* 3rd Ed., Technomic, Lancaster, PA, 1982.

[*9*] Cullis, C. F. and Hirschler, M. M., "The Combustion of Organic Polymers," Oxford University Press, Oxford, 1981.

[*10*] Doe, J., "The Combustion Toxicology of Polyvinylchloride Revisited," *Journal of Fire Sciences,* Vol. 5, 1987, pp. 228–47.

[*11*] Hinderer, R. K., "A Comparative Review of the Combustion Toxicity of Polyvinyl Chloride," *Journal of Fire Sciences,* Vol. 2, 1984, pp. 82–97.

[*12*] Huggett, C. and Levin, B., "Toxicity of Pyrolysis and Combustion Products of Poly (Vinyl Chloride): A literature Assessment," NBSIR 85-3286, National Bureau of Standards, Gaithersburg, MD, 1985.

[*13*] Huggett, C., "Reporting Combustion Product Toxicity Test Results," *Journal of Fire Sciences,* Vol. 2, 1984, pp. 79–82.

[*14*] Dyer, R. F. and Esch, V. H., "Polyvinyl Chloride Toxicity in Fires," *Journal of the American Medical Association,* Vol. 235, 1976, pp. 393–397.

[*15*] Wallace, D. N., "Dangers of Polyvinyl Chloride Wire Insulation Decomposition. I. Long Term Health Impairments: Studies of Fire Fighters of the 1975 New York Telephone Fire and Survivors of the 1977 Beverly Hills Supper Club Fire," *Journal of Combustion Toxicology,* Vol. 8, 1981, pp. 205–26.

[*16*] Wallace, D. N., Nelson, N., and Gates, T., "Polyvinyl Chloride Wire Insulation Decomposition.

Copyright by ASTM Int'l (all rights reserved) Wed Feb 07 10:53:32 UTC 2024
Downloaded/printed by
The University of Delaware pursuant to License Agreement. No further reproductions authorized.

II. Consideration of the Long Term Health Effects from Chlorinated Hydrocarbons," *Journal of Combustion Toxicology,* Vol. 9, 1982, pp. 105–12.

[*17*] Sorenson, W. R., "Polyvinyl Chloride in Fires," *Journal of the American Medical Association,* Vol. 236, 1976, pp. 1449.

[*18*] Cleveland, F. P., "A Critique of Two Papers on 'Dangers of Polyvinyl Chloride Wire Insulation Decomposition'," *Journal of Combustion Toxicology,* Vol. 9, 1982, pp. 115–20.

[*19*] Colardyn, F., van der Straeten, M., Lamont, H., and van Peteghem, T., "Acute Inhalation-Intoxication by Combustion of Polyvinylchloride," *International Archive of Occupational and Environmental Health,* Vol. 38, 1976, pp. 121–127.

[*20*] Lehmann, K. B., (University of Wurzburg), "Experimental Studies on the Influence of Technical and Hygienically Important Gases and Vapours on the Organism, Parts I and II: Ammonia and Hydrogen Chloride Gas," *Archiv fur Hygiene,* Vol. 5, 1886, pp. 1–125.

[*21*] Matt, L., "Experimental Studies to Understand the Influence of Poisonous Gases on Humans," medical doctoral dissertation, Faculty of Medicine, King Julius-Maximilian University of Wurzburg, Ludwigshafen-am-Rhein, Germany, 1889.

[*22*] Lehmann, K. B., (University of Wurzburg), Wilke, J., Yamada, J., and Wiener, J., "New Investigations on the Quantitative Absorption of Some Poisonous Gases by Animals and Humans via the Respiratory Tract and its Parts: Ammonia, Hydrochloric Acid, Sulphurous Acid, Acetic Acid and Carbon Disulphide," *Archiv fur Hygiene,* Vol. 67, 1908, pp. 57–100.

[*23*] Ronzani, E. (University of Padua, Italy), "Regarding the Influence of Inhalation of Irritating Industrial Gases on the Defensive Mechanisms of the Organism with Regards to Infectious Diseases, Part II: Hydrogen Fluoride Gas, Ammonia and Hydrogen Chloride Gas.," *Archiv fur Hygiene,* Vol. 70, 1909, pp. 217–269.

[*24*] Lehmann, K. B. and Burck, A. (University of Wurzburg), "On the Absorption of Hydrogen Chloride Vapours by Animals in Long Term Exposures," *Archiv fur Hygiene,* Vol. 72, 1910, pp. 343–357.

[*25*] DiPasquale, L. C. and Davis, H. V., "The Acute Toxicity of Brief Exposures to Hydrogen Fluoride, Hydrogen Chloride, Nitrogen Dioxide and Hydrogen Cyanide Singly and in Combination with Carbon Monoxide," Report AD-751, 442, U.S. Dept. Commerce, 1971.

[*26*] Higgins, E. A., Fiorca, V., Thomas, A. A., and Davis, H. V., "Acute Toxicity of Brief Exposures to HF, HCl, NO_2 and HCN with and without CO," *Fire Technology,* Vol. 8, 1972, pp. 120–30.

[*27*] Darmer, K. I., Kinkead, E. R., and DiPasquale, L. C., "Acute Toxicity in Rats and Mice Exposed to Hydrogen Chloride Gas and Aerosols," *Journal of American Industrial Hygienists Association,* Vol. 35, 1974, pp. 623–31.

[*28*] Kaplan, H. L., Grand, A. F., Rogers, W. R., Switzer, W. G., and Hartzell, G. E., "A Research Study of the Assessment of Escape Impairment by Irritant Combustion Gases in Postcrash Aircraft Fires," DOT/FAA/CT-84/16, U.S. Dept. Transportation, FAA, September 1984.

[*29*] Hartzell, G. E., Grand, A. F., Kaplan, H. L., Priest, D. N., Stacy, H. W., Switzer, W. G., and Packham, S. C., "Analysis of Hazards to Life Safety in Fires: a Comprehensive Multi-Dimensional Research Program—Year 1," NBS Contract NB83NADA4015, Southwest Research Institute, May 1985.

[*30*] Hartzell, G. E., Packham, S. C., Grand, A. F., and Switzer, W. G., "Modeling of Toxicological Effects of Fire Gases: III. Quantification of Post-Exposure Lethality of Rats from Exposure to HCl Atmospheres," *Journal of Fire Sciences,* Vol. 3, 1985, pp. 195–207.

[*31*] Kaplan, H. L., Grand, A. F., Switzer, W. G., Mitchell, D. S., Rogers, W. R., and Hartzell, G. E., "Effects of Combustion Gases on Escape Performance of the Baboon and the Rat," *Journal of Fire Sciences,* Vol. 3, 1985, pp. 228–44.

[*32*] Hartzell, G. E., Stacy, H. W., Switzer, W. G., Priest, D. N., and Packham, S. C., "Modeling of Toxicological Effects of Fire Gases: IV. Intoxication of Rats by Carbon Monoxide in the Presence of a Toxicant," *Journal of Fire Sciences,* Vol. 3, 1985, pp. 263–79.

[*33*] Kaplan, H. L., Anzueto, A., Switzer, W. G., and Hinderer, R. K., "Respiratory Effects of Hydrogen Chloride in the Baboon," *25th Annual Meeting of the Society of Toxicologists,* 1986.

[*34*] Anzueto, A., Switzer, W. G., Kaplan, H. L., and Hinderer, R. K., "Long-Term Effects of Hydrogen Chloride on Pulmonary Function and Morphology in NonHuman Primates," *26th. Annual Meeting of the Society of Toxicologists,* 1987.

[*35*] Kaplan, H. L., Hinderer, R. K., and Anzueto, A., "Extrapolation of Mice Lethality Data to Humans," *Journal of Fire Sciences,* Vol. 5, 1987, pp. 149–51.

[*36*] Kaplan, H. L., Anzueto, A., Switzer, W. G., and Hinderer, R. K., "Effects of Hydrogen Chloride on Respiratory Response and Pulmonary Function of the Baboon," *Journal of Toxicological and Environmental Health,* Vol. 23, 1988, pp. 473–93.

Copyright by ASTM Int'l (all rights reserved) Wed Feb 07 10:53:32 UTC 2024
Downloaded/printed by
The University of Delaware pursuant to License Agreement. No further reproductions authorized.

[37] Hartzell, G. E., Grand, A. F., and Switzer, W. G., "Modeling of Toxicological Effects of Fire Gases: VI. Further Studies on the Toxicity of Smoke Containing Hydrogen Chloride," *Journal of Fire Sciences,* Vol. 5, 1987, pp. 368–91.

[38] Kaplan, H. L., Hirschler, M. M., Switzer, W. G., and Coaker, A. W., "A Comparative Study of Test Methods Used to Determine the Toxic Potency of Smoke," *Proceedings,* 13th International Conference on Fire Safety, San Francisco, CA, C. J. Hilado, Ed., Product Safety Corp., San Francisco, CA, 1988, pp. 279–301.

[39] Klonne, D. R., Ulrich, C. E., Riley, M. G., Barrow, C. S., Hamm, Jr., T. E., and Morgan, K. T., "Chlorine: Chronic Inhalation Toxicity Studies in Rhesus Monkeys," *The Toxicologist,* Vol. 5, No. 1, 1984, p. 28.

[40] Barrow, C. S., Kociba, R. J., Rampy, L. W., Keyes, D. G., and Albee, R. R., "An Inhalation Toxicity Study of Chlorine in Fischer 344 Rats Following 30 Days of Exposure," *Toxicology and Applied Pharmacology,* Vol. 49, 1979, pp. 77–88.

[41] Alarie, Y. C., "The Toxicity of Smoke from Polymeric Materials During Thermal Decomposition," *Annual Review of Pharmacology and Toxicology,* Vol. 25, 1985, pp. 325–47.

[42] Alarie, Y. C., "Toxicological Evaluation of Airborne Chemical Irritants and Allergens Using Respiratory Reflex Reactions," in *Inhalation Toxicology and Technology,* B. K. J. Leong, Ed., Ann Arbor Science, Ann Arbor, 1981, pp. 207–32.

[43] Babrauskas, V., Levin, B. C., and Gann, R. G., "A New Approach to Fire Toxicity Data for Hazard Evaluation," *Fire Journal,* Vol. 81, No. 2, 1987, pp. 22–28, pp. 70–71.

[44] Esposito, F. M. and Alarie, Y. C., "Inhalation Toxicity of Carbon Monoxide and Hydrogen Cyanide Released During the Thermal Decomposition of Polymers," *Journal of Fire Sciences,* Vol. 6, 1988, pp. 195–239.

[45] Burleigh-Flazer, H., Wong, K. L., and Alarie, Y. C., "Evaluation of the Pulmonary Effects of HCl Using CO_2 Challenges in Guinea Pigs," *Fundamentals of Applied Toxicology,* Vol. 5, 1985, pp. 978–85.

[46] Patra, A. L., Gooya, A., and Menache, M. G., "A Morphometric Comparison of the Nasopharyngeal Airway of Laboratory Animals and Humans," *Anatomical Record,* Vol. 215, 1986, pp. 42–50.

[47] Herrington, R. M. and Story, B. A., "The Release Rate of Heat, Smoke, and Primary Toxicants from Burning Materials," *Journal of Fire Flammability,* Vol. 9, 1978, pp. 284–307.

[48] Grand, A. F., "Continuous Monitoring of Hydrogen Chloride in Combustion Atmospheres and in Air," *Journal of Fire Sciences,* Vol. 6, 1988, pp. 61–79.

[49] Beitel, J. J., Bertelo, C. A., Carroll, Jr., W. F., Gardner, R. O., Grand, A. F., Hirschler, M. M., and Smith, G. F., "Hydrogen Chloride Transport and Decay in a Large Apparatus, I. Decomposition of Poly (Vinyl Chloride) Wire Insulation in a Plenum by Current Overload," *Journal of Fire Sciences,* Vol. 4, 1986, pp. 15–41.

[50] Sackner, M. A., Greeneltch, M. S., Heiman, S., et al., "Diffusing Capacity, Membrane Diffusing Capacity, Capillary Blood Volume, Pulmonary Tissue Volume, and Cardiac Output Measured by a Rebreathing Technique," *American Review of Respiratory Disease,* Vol. 111, 1975, pp. 157–65.

[51] Pengelly, L. C., "Curve-fitting Analysis of Pressure Volume Characteristics of the Lung," *Journal of Applied Physiology,* Vol. 42, 1977, pp. 111–6.

[52] Amdur, M. O., Silverman, L., and Drinker, P., "Inhalation of Sulfuric Acid Mist by Human Subjects," *Industrial Hygiene and Occupational Medicine,* Vol. 6, 1952, pp. 305–13.

[53] Purser, D. A. and Woolley, W. D., "Biological Studies of Combustion Atmospheres," *Journal of Fire Sciences,* Vol. 1, 1983, pp. 118–44.

[54] Boudene, C., Jounaz, J. M., and Truhaut, R., "Protective Effects of Water Against Toxicity of Pyrolysis and Combustion Products of Wood and Poly (Vinyl Chloride)," *Journal of Macromolecular Science (Chemistry),* Vol. *A11*(8), 1977, pp. 1529–45.

[55] Hartzell, G. E., Grand, A. F., and Switzer, W. G., "Studies on Toxicity of Smoke Containing HCl," *Fire And Polymers,* Macromolecular Secretariat American Chemical Society Symposium, 10–13 April, 1989, Dallas, TX.

[56] Amoore, J. E. and Hautala, E., "Odor as an Aid to Chemical Safety: Odor Thresholds Compared with Threshold Limit Values and Volatilities for 214 Industrial Chemicals in Air and Water Dilution," *Journal of Applied Toxicology,* Vol. 3, No. 6, 1983, pp. 272–90.

[57] Smith, G. F., "A Quick Method for Determining the Acid Gas Evolution from PVC Formulations," *Journal of Vinyl Technology,* Vol. 9, No. 1, 1987, pp. 18–21.

[58] Kaplan, H. L., Hirschler, M. M., Switzer, W. G., and Coaker, A. W., "Limitations of the UPITT Method for the Screening of Materials for the Toxic Potency of Smoke," *1988 Annual Meeting Society of Toxicology,* Houston, paper No. 574, February, 1988.

Copyright by ASTM Int'l (all rights reserved) Wed Feb 07 10:53:32 UTC 2024
Downloaded/printed by
The University of Delaware pursuant to License Agreement. No further reproductions authorized.

[59] Grand, A. F., "Effect of Experimental Conditions on the Evolution of Combustion Products Using a Modified University of Pittsburgh Toxicity Test Apparatus," *Journal of Fire Sciences,* Vol. 3, 1985, pp. 280–304.

[60] Fardell, P. J. and Rogowski, Z. W., "Report of the Performance of the Pittsburgh/Alarie Combustion Model," Fire Research Station, Building Research Establishment CR21/85, September 1985, Borehamwood, U.K.

[61] Debanne, S. M., Haller, H. S., and Rowland, D. Y., "A Statistical Comparison of Test Protocols Used in The Assessment of Combustion Product Toxicity," *Journal of Fire Sciences,* Vol. 5, 1987, pp. 416–34.

[62] Norris, J. C., "Investigation of the Dual LC_{50} values in Woods Using the University of Pittsburgh Combustion Toxicity Apparatus," this publication.

[63] Beitel, J. J., Bertelo, C. A., Carroll, Jr., W. F., Grand, A. F., Hirschler, M. M., and Smith, G. F., "Hydrogen Chloride Transport and Decay in a Large Apparatus: II. Variables Affecting Hydrogen Chloride Decay," *Journal of Fire Sciences,* Vol. 5, 1987, pp. 105–45.

[64] Galloway, F. M. and Hirschler, M. M., "Model for the Mass Transfer and Decay of Hydrogen Chloride in a Fire Scenario," in *Mass Modeling of Fire, ASTM STP 983,* J. R. Mehaffey, Ed., ASTM, Philadelphia, 1987, pp. 35–57.

[65] Galloway, F. M. and Hirschler, M. M., "Application of a Model for Transport and Decay of Hydrogen Chloride from Burning Poly (Vinyl Chloride) to Room-Corridor-Room Experiments," *Proceedings,* 14th International Conference on Fire Safety, San Francisco, C. J. Hilado, Ed., Product Safety Corp., San Francisco, 1989, pp. 287–303.

[66] Smith, G. F. and Dickens, E. D., "New Low Smoke Thermoplastics to Meet New Needs in the Marketplace," *Proceedings,* 8th. International Conference on Fire Safety, Product Safety Corp., San Francisco, C. J. Hilado, Ed., Product Safety, 1983, pp. 227–42.

[67] Hirschler, M. M., "First Order Evaluation of Fire Hazard in a Room Due to the Burning of Poly (Vinyl Chloride) Products in a Plenum: Estimation of the Time Required to Establish an Untenable Atmosphere," *Journal of Fire Sciences,* Vol. 6, 1988, pp. 100–120.

Copyright by ASTM Int'l (all rights reserved) Wed Feb 07 10:53:32 UTC 2024
Downloaded/printed by
The University of Delaware pursuant to License Agreement. No further reproductions authorized.

Archibald Tewarson [1]

Relationship Between Generation of CO and CO_2 and Toxicity of the Environments Created by Materials in Flaming and Nonflaming Fires and Effect of Fire Ventilation

REFERENCE: Tewarson, A., **"Relationship Between Generation of CO and CO_2 and Toxicity of the Environments Created by Materials in Flaming and Nonflaming Fires and Effect of Fire Ventilation,"** *Characterization and Toxicity of Smoke, ASTM STP 1082,* H. K. Hasegawa, Ed., American Society for Testing and Materials, Philadelphia, 1990, pp. 23–33.

ABSTRACT: In fires, combustion behavior of materials, generation rates, and concentrations of fire products depend on many factors, such as the chemical structures of materials (aliphatic to aromatic to highly halogenated), fire ventilation, airflow and mixing, shape, size and arrangement of the materials, heat flux received by the materials, etc. Thus, toxicity of the environment is expected to depend on these factors.

This paper examines the relationship between the combustion behavior of materials and the toxicity of the environment. In this analysis, only CO and CO_2 are used, using the toxicity relationship suggested by Levin et al. [*3*] on the synergism between CO and CO_2 and data measured in the Factory Mutual Research Corp. (FMRC) small-scale flammability apparatus.

KEY WORDS: toxicity, fire properties, fire ventilation, combustion efficiency

All organic materials are combustible and contain carbon which is converted to carbon dioxide (CO_2), carbon monoxide (CO), particulates, hydrocarbons, and other carbon-containing products. The efficiency of combustion in fires depends on the conversion of carbon atoms to CO_2 and hydrogen atoms to water; the higher the amount of CO_2 generated in a fire, the higher the combustion efficiency. The higher the amounts of CO, particulates, hydrocarbons, and other carbon-containing products, the lower the combustion efficiency. In practice, the mixture of CO_2, CO, particulates, hydrocarbons, hydrogen chloride (HCl), hydrogen cyanide (HCN), and other fire products are called "smoke." The products present in smoke, individually or in combination, are considered to be responsible for not only immediate or delayed deaths (70 to 80% of fire deaths are caused by smoke inhalation [*1*]), but smoke is also responsible for impeding escape and causing injuries.

The amounts and nature of the products present in smoke depend on the chemical structure of the materials and fire ventilation. The concentrations of the products depend on the generation rates of the products and on the mixing and dilution of the products with air. It is thus expected that toxicity of smoke will depend not only on the material, but also on fire ventilation, fire size, and the mixing of fire products and air.

In most fires, CO, CO_2, and particulates are the dominant products present in smoke. CO is considered to be the cause or a contributing cause in 80% of fire deaths based on the data

[1] Manager, Flammability Section, Factory Mutual Research Corp., Norwood, MA 02062.

Copyright by ASTM Int'l (all rights reserved) Wed Feb 07 10:53:32 UTC 2024
Copyright © 1990 by ASTM International www.astm.org
Downloaded/printed by
The University of Delaware pursuant to License Agreement. No further reproductions authorized.

collected in Maryland [*1*]. CO binds the red blood cells and forms carboxyhemoglobin (COHb), which interferes with oxygen transport in the body. COHb concentrations of 50 to 60% are generally accepted as fatal [*1*]. CO_2, on the other hand, is not toxic up to 5%; it, however, stimulates breathing (at 3% CO_2, the volume of air breathed per minute is approximately doubled and at 5% CO_2, it is tripled) [*2*].

Levin et al. [*3*] have examined the CO and CO_2 synergism and suggest the following conditions for creating environments expected to be toxic

$$M\,\mathbf{C}_{CO}/[\mathbf{C}_{CO_2} - B] \geq 1.0 \tag{1}$$

where

M and B = constants,
and $\mathbf{C}_{CO}$ and $\mathbf{C}_{CO_2}$ = concentrations of CO and CO_2 in ppm, respectively.

For $\mathbf{C}_{CO_2} \leq 50\,000$ ppm, $M = -28$ and $B = 117\,000$ ppm; and for $\mathbf{C}_{CO_2} > 50\,000$ ppm, $M = 150$ and $B = -313\,000$ ppm.

In this paper an attempt has been made to use Eq 1 to examine the effects of chemical structures, fire ventilation, and dilution of the fire products on the toxicity of the environment created by CO and CO_2.

Concentration and Toxicity

The concentration of a compound can be expressed as

$$\mathbf{C}_j = [A(\dot{G}''_j/\rho_j)/\dot{V}_T] \times 10^6 \tag{2}$$

where

C_j = the concentration of compound j in ppm,
$\dot{G}''_j$ = the generation rate of the compound, g/m^{2}s,
ρ_j = the density of the compound (g/m^3),
$\dot{V}_T$ = the total volumetric flow rate of the fire product, m^3/s, and
A = the total surface area of the material involved in fire, m^2.

The generation rate of the compound is directly proportional to the generation rate of the material vapors where the proportionality constant is defined as the yield of the product [*4*].

$$\dot{G}''_j = Y_j\,\dot{G}''_f \tag{3}$$

where

$\dot{G}''_j$ = the generation rate of material vapors, g/m^{2}s, and
Y_j = the yield of compound j (g/g).

From Eqs 1 through 3

$$\frac{M\,(Y_{CO}/\rho_{CO})(A\dot{G}''_f/\dot{V}_T) \times 10^6}{[(Y_{CO_2}/\rho_{CO_2})(A\dot{G}''_f/\dot{V}_T) \times 10^6] - B} \geq 1.0 \tag{4}$$

The left side of Eq 4 is defined as the toxicity parameter in this paper.

Copyright by ASTM Int'l (all rights reserved) Wed Feb 07 10:53:32 UTC 2024
Downloaded/printed by
The University of Delaware pursuant to License Agreement. No further reproductions authorized.

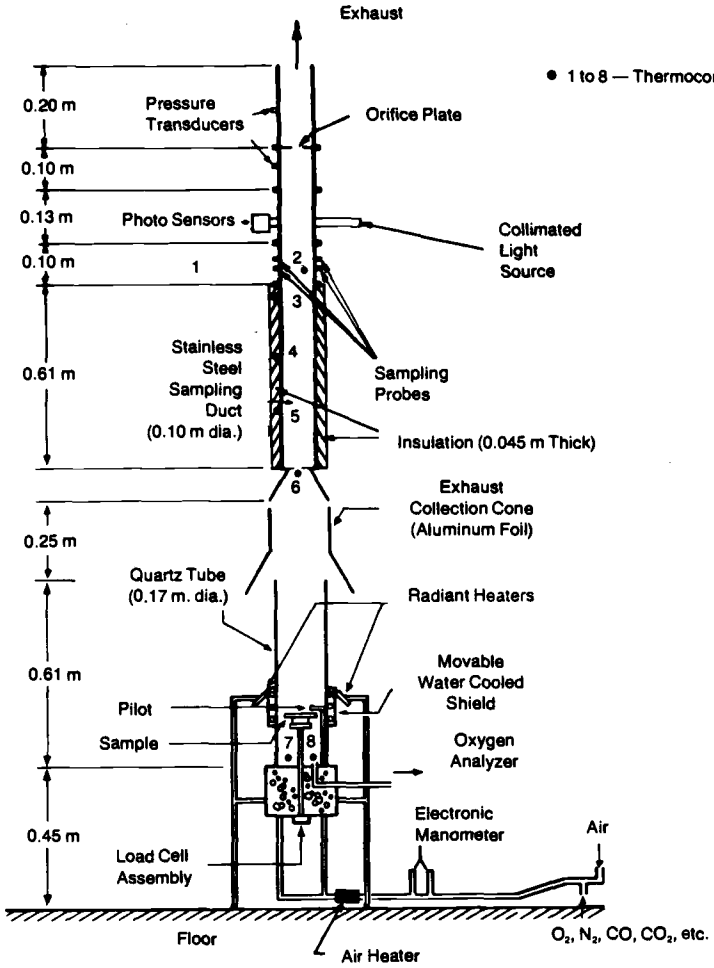

FIG. 1—*Factory mutual small-scale (10-kW scale) flammability apparatus.*

Dependency of Y_{CO} and Y_{CO_2} on Chemical Structure and Combustion Conditions

Y_{CO} and Y_{CO_2} depend on the chemical structure of the material and fire ventilation, but do not depend on fire size, if flames are turbulent [*4–6*]. Extensive data have been reported for various materials under varying ventilation conditions, where measurements were made in the FMRC small-scale flammability apparatus shown in Fig. 1 [*4–6*]. Table 1 lists some selected data for the yield of CO, where it can be noted that Y_{CO} increases with decrease in fire ventilation and as the chemical structure changes from saturated aliphatic, oxygenated to unsaturated aliphatic to aromatic to halogenated structures. The yield of CO_2 decreases as Y_{CO} increases, as shown in Figs. 2 and 3. Thus, the effect of chemical structure and ventilation on the toxicity parameter is expected to have a double-fold effect, i.e., increase in the numerator due to increase in Y_{CO} and a simultaneous decrease in the denominator due to increase in Y_{CO_2} as ventilation is decreased or as chemical structure changes from saturated to unsat-

Copyright by ASTM Int'l (all rights reserved) Wed Feb 07 10:53:32 UTC 2024
Downloaded/printed by
The University of Delaware pursuant to License Agreement. No further reproductions authorized.

TABLE 1—*Yield of CO for well-ventilated and underventilated fires of materials.*

Material	Well-Ventilated Fires[a]	Under-Ventilated Fires[b]
Methane (gas)	NR	0.175
Propane (gas)	0.005	0.229
Propylene (gas)	0.020	0.200
Hexane (liquid)	0.011	0.195
Toluene (liquid)	0.066	0.107
Methanol (liquid)	0.001	0.236
Ethanol (liquid)	0.002	0.219
Isopropanol (liquid)	0.002	0.168
Acetone (liquid)	0.003	0.304
Pine (solid)	0.004	0.138
Polymethylmethacrylate (granular)	0.010	0.189
Silicone (solid)	0.021	NR
Polyethylene foams	0.023	NR
Polyethylene (granular)	0.024	0.180
Polypropylene (granular)	0.024	NR
Nylon (granular)	0.038	NR
Flexible polyurethane foams	0.010 to 0.042	NR
Rigid polyurethane foams	0.025 to 0.051	NR
Polystyrene foams	0.060	NR
Polystyrene (granular)	0.060	NR
Polyvinyl chloride (granular)	0.063	NR
Fluoropolymers (granular)	0.120	NR

[a] Data taken from Reference *6*.
[b] Data taken from Reference *7*.
NR = Not reported.

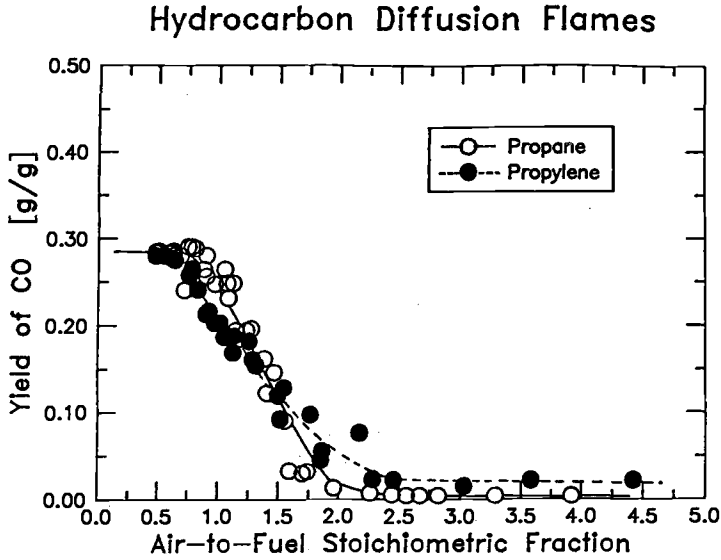

FIG. 2—*Yield of CO as function of air-to-fuel stoichiometric fraction for diffusion flames of propane and propylene. Data taken from Ref 6 were measured in the Factory Mutual small-scale flammability apparatus.*

Copyright by ASTM Int'l (all rights reserved) Wed Feb 07 10:53:32 UTC 2024
Downloaded/printed by
The University of Delaware pursuant to License Agreement. No further reproductions authorized.

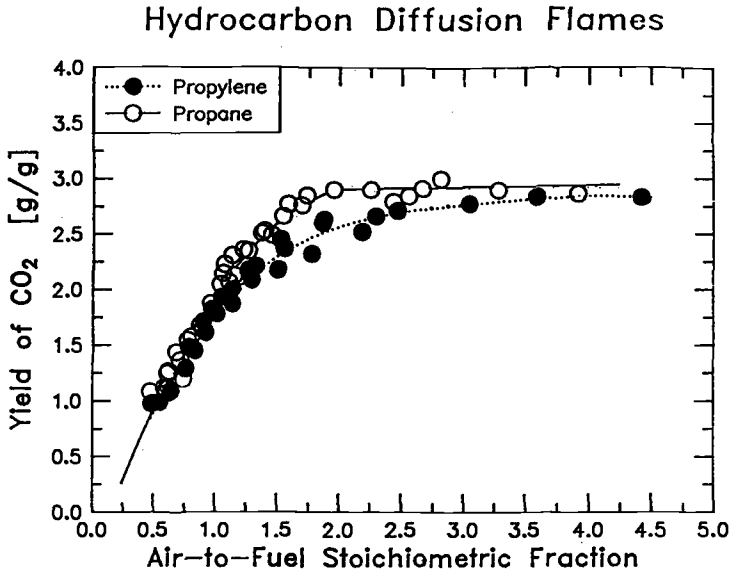

FIG. 3—*Yield of CO_2 as a function of air-to-fuel stoichiometric fraction for propane and propylene diffusion flames. Data taken from Ref* 6 *were measured in the Factory Mutual small-scale flammability apparatus.*

urated aliphatic to aromatic to halogenated, assuming all the other parameters are very similar.

The effect of fire ventilation on combustion behavior is generally expressed in terms of the ratio Y_{CO}/Y_{CO_2}. The increase in the ratio is indicative of the increase in the incompleteness of combustion accompanied by higher amounts of CO and other products resulting possibly

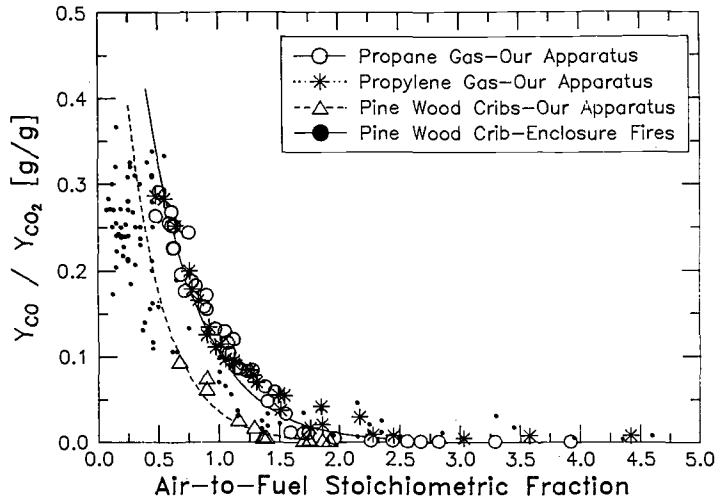

FIG. 4—*Ratio of the yields of CO to CO_2 as a function of the air-to-fuel stoichiometric fraction for the diffusion flames of propane, propylene, and wood cribs. Data taken from Ref* 6 *were measured in the Factory Mutual small-scale flammability apparatus.*

Copyright by ASTM Int'l (all rights reserved) Wed Feb 07 10:53:32 UTC 2024
Downloaded/printed by
The University of Delaware pursuant to License Agreement. No further reproductions authorized.

in increase in the toxicity of the environment. Figure 4 shows data for some selected materials taken from Reference *6*, where Y_{CO}/Y_{CO_2} increases with decrease in the air-to-fuel stoichiometric fraction.

The air-to-fuel stoichiometric fraction, ϕ, is defined as

$$\phi = x\dot{V}_T\rho_a / A\dot{G}''_f k_a \tag{5}$$

where

k_a = the mass air-to-fuel stoichiometric ratio and is a constant for each material
$x\dot{V}_T$ = the flow rate of air entering the combustion zone of the fire, m^3/s, and
ρ_a = the density of air, g/m^3.

For $\phi = 1$ the airflow is equal to the flow required for stoichiometric (complete) combustion for premixed material vapor air mixture. When $\phi \geq 1.0$, fire is defined as a well-ventilated fire, and when $\phi < 1.0$, fire is defined as an underventilated fire [*8*].

Combustion Conditions and Toxicity Chambers

In toxicity testing, various types of apparatuses and procedures are used—extensive data are available in the literature [*1,2,9–11*]. For illustration purposes, we have selected data for polyethylene-based products from Potts et al. [*12*]. Polyethylene products contain carbon and hydrogen atoms, and thus toxicity is expected to be due to CO, CO_2, and other carbon-containing products. The apparatus and test procedures used by Potts et al. [*12*] were similar to those used in the National Bureau of Standards toxicity test method [*10*]. The test chamber is a sealed 200 L volume chamber. The sample is heated in a cup furnace located under the floor at one end. The animals (rats) are exposed nose only. The sample weight is varied in each test and the results are expressed as concentration (sample weight/chamber volume). From the test data, LC_{50} value is determined, which is a concentration at which 50% of the animals die during exposure or within 14 days after exposure.

Figure 5 shows the data for Y_{CO}/Y_{CO_2} as a function of sample weight in the cup furnace in

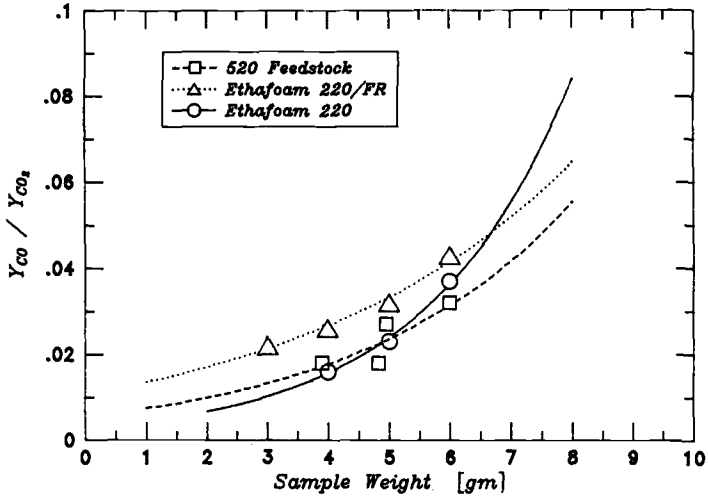

FIG. 5—*Ratio of the yields of CO to CO_2 as a function of the sample weight used in toxicity chamber for the flaming fires. Data used in the calculations are taken from Ref* 12.

Copyright by ASTM Int'l (all rights reserved) Wed Feb 07 10:53:32 UTC 2024
Downloaded/printed by
The University of Delaware pursuant to License Agreement. No further reproductions authorized.

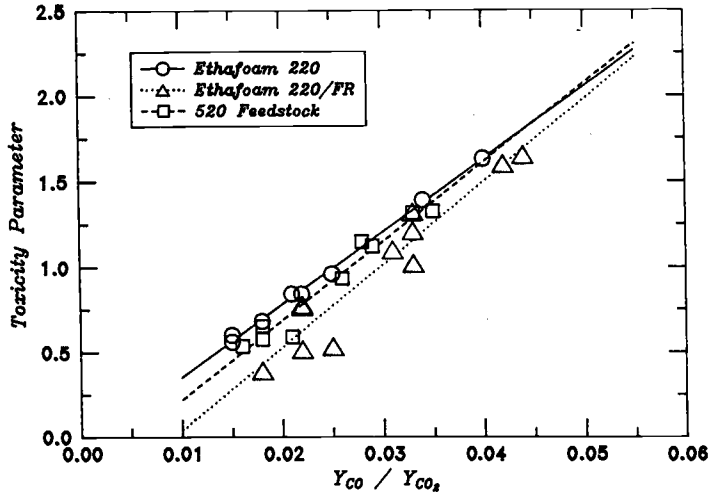

FIG. 6—*Relationship between toxicity parameter and ratio of yields of CO and CO_2 in flaming fires. Data used in the calculations are taken from Ref* 12.

the toxicity test chamber used by Potts et al. [*12*]. As can be noted, Y_{CO}/Y_{CO_2} increases with increase in the sample weight, i.e., fire becomes underventilated, a behavior similar to the behavior shown in Fig. 4. The fire-retardant treatment increases the value of Y_{CO}/Y_{CO_2}. An increase in Y_{CO}/Y_{CO_2} possibly indicates an increase in toxicity, as suggested by the data in Fig. 6 for flaming fires and in Fig. 7 for nonflaming fires. A linear relationship is indicated between the toxicity parameter and Y_{CO}/Y_{CO_2}. The data for flaming fires suggest that for $Y_{CO}/Y_{CO_2} \geqslant 0.025$, the toxicity parameter exceeds a value of 1 or the environment becomes toxic. The data for nonflaming fires show that the toxicity parameter does not exceed a value beyond 0.35 up to Y_{CO}/Y_{CO_2} value of 0.25, although animal deaths were observed.

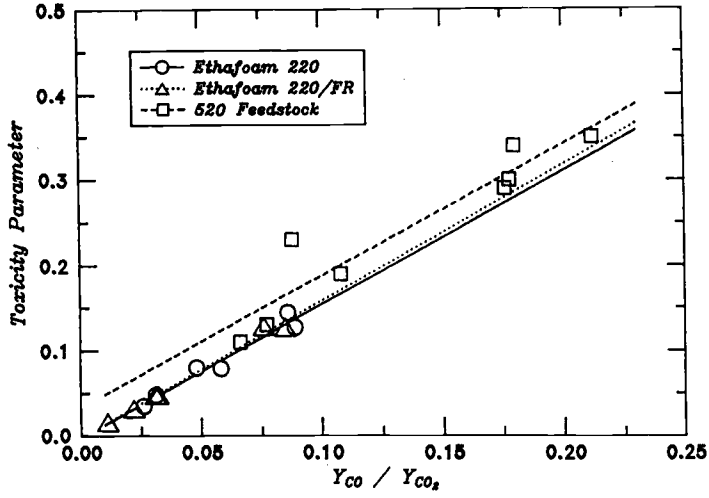

FIG. 7—*Relationship between toxicity parameter and ratio of yields of CO and CO_2 in nonflaming fires. Data used in the calculations are taken from Ref* 12.

Copyright by ASTM Int'l (all rights reserved) Wed Feb 07 10:53:32 UTC 2024
Downloaded/printed by
The University of Delaware pursuant to License Agreement. No further reproductions authorized.

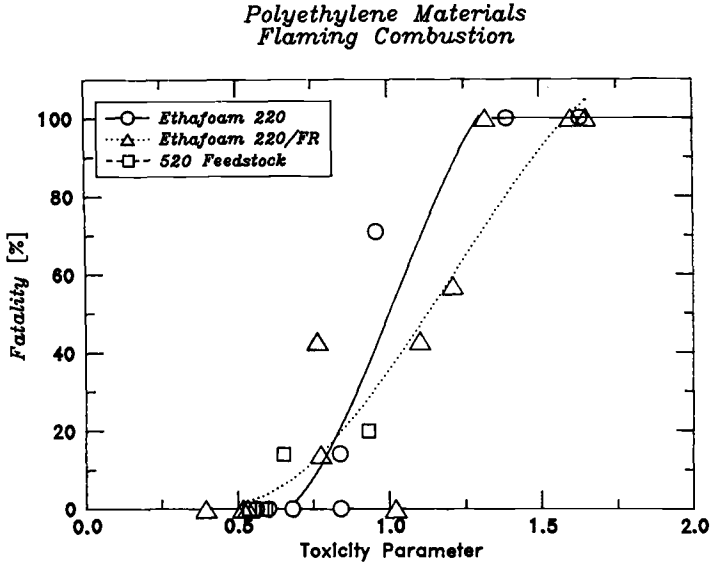

FIG. 8—*Relationship between fatality of rats and the toxicity parameter based on CO and CO_2 in flaming fires. Data used in the calculations are taken from Ref* 12.

Relationships between fatality to rats and the toxicity parameter for flaming and nonflaming fires of polyethylenes are shown in Figs. 8 and 9, respectively. The conditions for toxicity parameters equal to or greater than 1.0 for toxic environments (fatalities 50% or larger) suggested in Eq *1* are satisfied in flaming fires (Fig. 8), but not in nonflaming fires (Fig. 9). The data in Fig. 9 show that fatalities (50% or larger) are observed for toxicity parameters as low

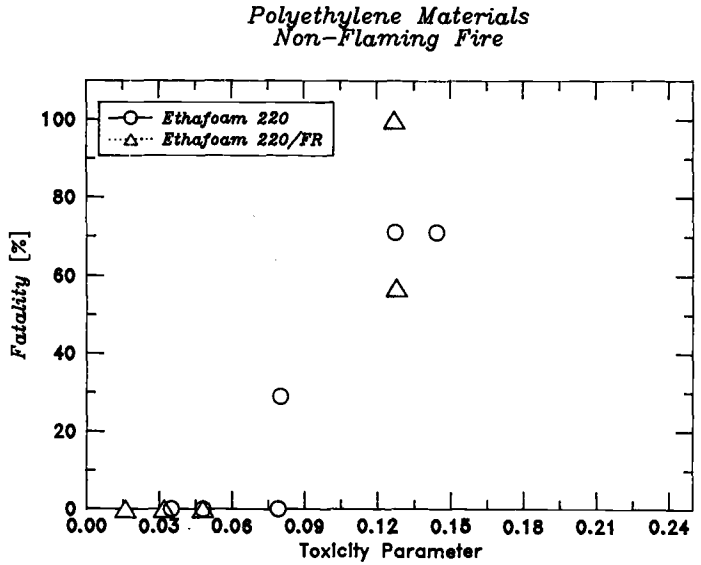

FIG. 9—*Relationship between fatality of rats and toxicity parameter based on CO and CO_2 in nonflaming fires. Data used in the calculations are taken from Ref* 12.

Copyright by ASTM Int'l (all rights reserved) Wed Feb 07 10:53:32 UTC 2024
Downloaded/printed by
The University of Delaware pursuant to License Agreement. No further reproductions authorized.

as about 0.12 in the nonflaming fires of polyethylenes. In nonflaming fires, carbon atoms in polyethylenes are expected to be converted to products of incomplete combustion in addition to CO and CO_2. Thus, the fatalities in nonflaming fires of polyethylenes are expected to be associated with these products in addition to CO and CO_2. Potts et al. [*12*] have identified one of the products to be acrolein.

Toxicity Parameter and Fire Ventilation

The toxicity parameter based on CO and CO_2 depends on the chemical structure and fire ventilation. The higher the yield of CO, the higher is the toxicity parameter for a specified value of fire ventilation. The data in Table 1 show that in well-ventilated fires Y_{CO} varies by a factor of 60 as the chemical structure of the materials changes from saturated and oxygenated aliphatic to unsaturated aliphatic to aromatic to highly halogenated.

The toxicity parameter is also expected to vary with fire ventilation. As fires change from well-ventilated to underventilated fires, Y_{CO} can increase by factors as large as 236, as indicated by the data in Table 1. The degree of variation of the toxicity parameter with ventilation is expected to depend on the material as shown in Fig. 10 for propane, propylene, and wood crib as examples. For wood crib and propane and propylene, the toxic environments are created (toxicity parameter ≥ 1.0) when the air-to-fuel stoichiometric fraction is ≤ 1.0 and 1.7, respectively. For other materials with higher Y_{CO} values, the toxic environments would be created at higher values of the stoichiometric fraction.

An environment which is toxic at a specified fire ventilation (toxicity parameter ≥ 1.0), however, could be shifted to a nontoxic environment (toxicity parameter ≤ 1.0) by dilution of the fire products. The higher the air-to-fuel stoichiometric fraction where the toxicity parameter ≥ 1.0, the higher the dilution of the product required to change the conditions where toxicity parameter < 1.0. Thus, according to data in Fig. 10, propane and propylene would require higher dilution than wood crib to satisfy the conditions where toxicity param-

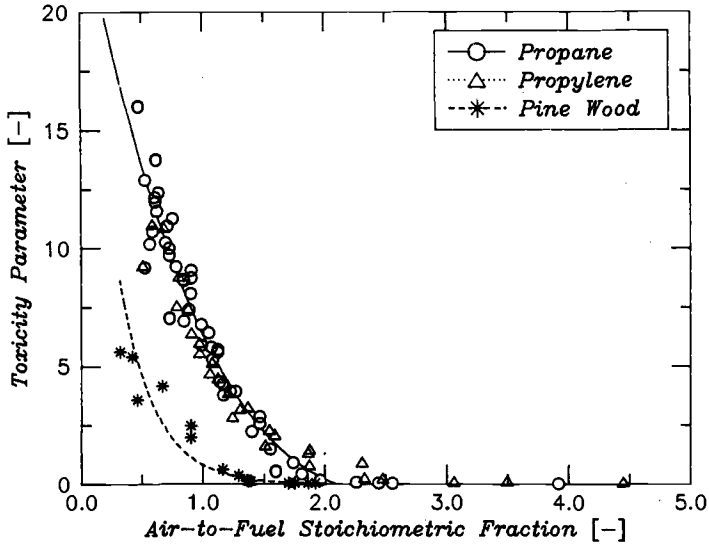

FIG. 10—*Toxicity parameter based on CO and CO_2 as a function of air-to-fuel stoichiometric fraction in diffusion flames. No downstream dilution of fire products.*

Copyright by ASTM Int'l (all rights reserved) Wed Feb 07 10:53:32 UTC 2024
Downloaded/printed by
The University of Delaware pursuant to License Agreement. No further reproductions authorized.

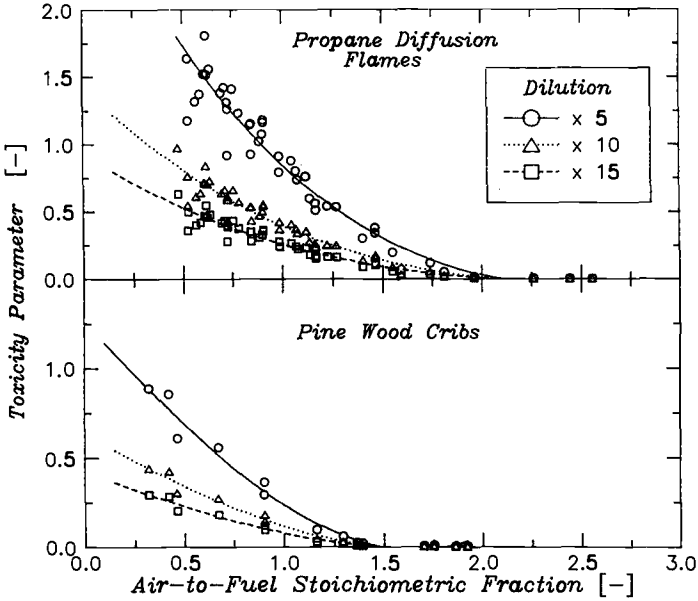

FIG. 11—*Variations in the toxicity parameter based on CO and CO_2 with the downstream dilution of fire products. The dilution is 5, 10, and 15 times the stoichiometric air flow rate requirement.*

eter < 1.0. The calculated data for propane and wood crib are shown in Fig. 11. The data suggest that in flaming fires, if fire products are diluted ten times the stoichiometric air requirements or higher, then the conditions whose toxicity parameter > 1.0 are not achieved for wood crib, and for propane they are not achieved until the air-to-fuel stoichiometric fraction reaches a value of about 0.30 (at or below which flames cannot be sustained and fire is extinguished).

It is interesting to note that at the mean flame height, the flow of air in the plume is some twelve times the stoichiometric requirements [*13*], and thus downstream of the well-ventilated fires the airflow would always be greater than twelve times the stoichiometric requirements. It thus appears that in well-ventilated fires of carbon and hydrogen atom-containing materials for which Y_{CO} are low and are comparable with propane and wood (see Table 1), the hazard may be due primarily to heat rather than toxic compounds.

Although the analysis presented here is not a generalized analysis, it appears that for carbon and hydrogen-containing materials which produce higher amounts of CO than wood and propane, higher dilution would be required, and thus the area of contamination probably would be larger than with materials for which amounts of CO are comparable with wood and propane. For such materials, not only would the thermal hazard (heat) be important to consider, but the nonthermal hazard (toxic) as well.

Conclusions

1. For the assessment of toxic hazards of fire environments, chemical structures of materials and additives, fire ventilation, dilution and mixing of fire products with air are important. These factors are important in the design and performance of small-scale toxicity tests.
2. The relationship developed by Levin et al. [*3*] appears to be useful in establishing rela-

Copyright by ASTM Int'l (all rights reserved) Wed Feb 07 10:53:32 UTC 2024
Downloaded/printed by
The University of Delaware pursuant to License Agreement. No further reproductions authorized.

tionships between fire properties of materials and effects of ventilation and toxicity of the environment based on CO and CO_2.

References

[1] *Fire and Smoke: Understanding the Hazards,* Committee on Fire Toxicology, Board on Environmental Studies and Toxicology Commission on Life Sciences, National Research Council, National Academy Press, Washington, DC, 1986.

[2] Purser, D. A., "Toxicity Assessment of Combustion Products," Chapt. 14, Sect. 1, *The SFPE Handbook of Fire Protection Engineering,* P. J. Dinenno, Ed., National Fire Protection Association, Quincy, MA, 1988, p. I-200.

[3] Levin, B. C., Paabo, M., Gurman, J. L., Harris, S. E., and Braun, E., "Evidence of Toxicological Synergism Between Carbon Monoxide and Carbon Dioxide," *Toxicology,* (to be published).

[4] Tewarson, A., "Experimental Evaluation of Flammability Parameters of Polymeric Materials," Chapt. 3, *Flame Retardant Polymeric Materials,* Vol. 3, M. Lewin, S. M. Atlas, and E. M. Pearce, Eds., Plenum Press, New York, 1982, p. 97.

[5] Tewarson, A. and Newman, J. S., "Scale Effects on Fire Properties of Materials," *Fire Safety Science—Proceedings of the First International Symposium,* Hemisphere Publishing Corp., New York, NY, 1986, p. 451.

[6] Tewarson, A., "Generation of Heat and Chemical Compounds in Fires," Chapt. 13, Sect. 1, *The SFPE Handbook of Fire Protection Engineering,* P. J. Dinenno, Ed., National Fire Protection Association, Quincy, MA, 1988, p. I–179.

[7] Beyler, C. L., "Major Species Production by Solid Fuels in a Two-Layer Compartment Fire Environment," *Fire Safety Science—Proceedings of the First International Symposium,* Hemisphere Publishing Corp., New York, NY, 1986, p. 431.

[8] Tewarson, A. and Steciak, J. S., "Fire Ventilation," *Combustion and Flame,* Vol. 52, 1983, p. 123.

[9] Kaplan, H. L., Grand, A. F., and Hartzell, G. E., "A Critical Review of the State-of-the-Art of Combustion Toxicology," Final Report SWRI Project No. 01-6862, Southwest Research Institute, San Antonio, TX, June 1982.

[10] Levin, B. C., Paabo, M., and Birby, M. M., "An Interlaboratory Evaluation of the 1980 Version of the National Bureau of Standards Test Method for Assessing the Acute Inhalation Toxicity of Combustion Products," Technical Report NBS1R83-2678, National Bureau of Standards, Gaithersburg, MD, April 1983.

[11] Anderson, R. C., Croce, P. A., Feeley, F. G., and Sakura, J. D., "Study to Assess the Feasibility of Incorporating Combustion Toxicity Requirements into Building Material and Furnishing Codes of New York State," Vols. 1, 2, and 3, Technical Reports Reference 88712, Arthur D. Little, Inc., Cambridge, MA, May 1983.

[12] Potts, W. J., Lederer, T. S., and Quast, J. F., "A Study of the Inhalation Toxicity of Smoke Product Upon Pyrolysis and Combustion of Polyethylene Foams, Part I, Laboratory Studies," *Journal of Combustion Toxicology,* Vol. 5, 1978, p. 408.

[13] Heskestad, G., "Fire Plume Air Entrainment According to Two Competing Assumptions," *Twenty First Symposium (International) on Combustion,* The Combustion Institute, Pittsburgh, PA, 1986, p. 111.

Copyright by ASTM Int'l (all rights reserved) Wed Feb 07 10:53:32 UTC 2024
Downloaded/printed by
The University of Delaware pursuant to License Agreement. No further reproductions authorized.

Peter J. Briggs[1]

Developments in International Smoke Obscuration Tests and British Assessment Procedures for Smoke Hazards in Fire Scenarios Containing Plastics

REFERENCE: Briggs, P. J., **"Developments in International Smoke Obscuration Tests and British Assessment Procedures for Smoke Hazards in Fire Scenarios Containing Plastics,"** *Characterization and Toxicity of Smoke, ASTM STP 1082,* H. K. Hasegawa, Ed., American Society for Testing and Materials, Philadelphia, 1990, pp. 34–45.

ABSTRACT: Assessment of the smoke hazard caused by materials and products has normally been solely from the results of small-scale or full-scale test methods. Recent British proposals suggest that the results of smoke tests should be used as part of a total method of smoke hazard assessment which would consider fire test data, product design, and room scenario in a way which would reflect the dangers of a product in a real fire situation. This proposed assessment procedure would prevent the misinterpretation of test data which can occur when smoke test data are compared in isolation without reference to other fire parameters.

Developments in static and dynamic procedures show that there are still significant differences in the fire models used in internationally recognized smoke obscuration tests. Results for small-scale tests (e.g., ISO single and dual chamber tests, NIST cone calorimeter) and large-scale tests (e.g., IEC 3m cube, room/duct, and room/corridor tests) are described. These results emphasize the need for a standardized analytical approach to smoke hazard assessment.

KEY WORDS: fire scenarios, smoke hazard assessment, chamber tests, cone calorimeter, room tests, plastics

Important decisions about the smoke emission properties of materials have often been based solely on the results of small-scale chamber methods; rarely have regulators specified the use of large-scale tests. There have been few cases where an overall smoke hazard assessment has been required, so the contribution of a material to fire growth and the relationship to the rate of smoke generation has not always been understood. Overreliance on single small-scale tests has led to misinterpretation of the performance of some products (especially composites). This paper reviews the present status of smoke tests with particular emphasis on their use in evaluating products containing plastics.

Single-Chamber Tests

One of the most widely used fire tests in the world is the ASTM Test Method for Specific Optical Density of Smoke Generated by Solid Materials (E 662) smoke chamber, which has also been adopted by many other national standards and regulatory authorities. This pro-

[1] Head, Corporate Fire Laboratory, Imperial Chemical Industries PLC, Fine Chemicals Research Centre, Manchester, United Kingdom.

Copyright by ASTM Int'l (all rights reserved) Wed Feb 07 10:53:32 UTC 2024
Copyright © 1990 by ASTM International www.astm.org
Downloaded/printed by
The University of Delaware pursuant to License Agreement. No further reproductions authorized.

TABLE 1—*ASTM E 662 smoke density results for 1-mm-thick cable materials.*

Material	Max Specific Optical Density	
	Nonflaming	Flaming
Conventional PVC[i]	354	261
FR, LA[a]-PVC	318	521
FR, RS[b]-PVC	242	252
CSP[c]	162	190
PTFE[h]	4	74
EPR[d]/ATH[e]	175	48
EVA[f]/ATH	184	75
PEEK[g]	2	19

[a] Fire retardant, low acid.
[b] Fire retardant, reduced smoke.
[c] Chlorosulphonated polyethylene.
[d] Ethylene propylene rubber.
[e] Alumina trihydrate.
[f] Ethylene vinyl acetate copolymer.
[g] Polyetheretherketone.
[h] Polytetrafluoroethylene.
[i] Polyvinylchloride.

cedure is useful for material development and quality assurance; typical results for plastic cable materials are shown in Table 1. Several deficiencies have been identified [*1*] in this single-chamber test, particularly the fire model, which only requires specimens to be irradiated at 25 kW/m^2 in the vertical position. Recognizing the large number of these smoke chambers throughout the world, the International Standards Organisation (ISO) Technical Committee TC92 (Fire Tests for Building Materials) initiated development of an improved procedure using a 450 W radiant cone yielding an irradiance range of 10 to 50 kW/m^2 and a specimen assembly which allows either horizontal or vertical orientation. This development is now being continued in ISO/TC61/SC4 (Fire Tests for Plastics). The modified procedure has already been shown to be valuable in evaluating the smoke emission characteristics of thermoplastics, which were often underestimated when testing only in a vertical orientation due to melting. Results of ISO experiments with thermoplastics at the same irradiance used in the ASTM E 662 smoke chamber are shown in Table 2 [*2*]. All except one

TABLE 2—*ISO/DP5659 smoke density results for thermoplastics in horizontal and vertical orientations using irradiance of 25 kW/m^2* [2].

Material	Thickness, mm	Max Specific Optical Density	
		Horizontal	Vertical
Radiant cone only			
Polyethylene	3	567	224[a]
Polypropylene	3	824[a]	650[a]
Expanded Polystyrene, 20 kg/m^3	20	209[a]	49[a]
Radiant Cone + pilot flame			
Polyethylene	3	424	78
Polypropylene	3	449	73
Expanded Polystyrene, 20 kg/m3	20	314	119

[a] Not ignited.

Copyright by ASTM Int'l (all rights reserved) Wed Feb 07 10:53:32 UTC 2024
Downloaded/printed by
The University of Delaware pursuant to License Agreement. No further reproductions authorized.

TABLE 3—*ISO/DP5659 smoke density results for plastics in the horizontal orientation irradiated with radiant cone only.*

Material	Thickness, mm	Max Specific Optical Density		
		20 kW/m^2	30 kW/m^2	50 kW/m^2
FR, LA[b]-PVC	1	388[a]	640[a]	476
PMMA[c]	3	207[a]	401	437
Expanded polystyrene, 14 kg/m^3	24	48[a]	313[a]	201

[a] Not ignited.
[b] Fire retarded, low acid.
[c] Polymethylmethacrylate.

of the specimens exposed to the radiant cone only did not ignite, while all the specimens exposed to the radiant cone and pilot flame ignited.

It is well-known that the opacity and volume of smoke generated by materials is significantly affected by their burning mode, especially nonflaming combustion compared to flaming combustion as shown in Table 2. Additional results for thermoplastics using the ISO/DP5659 procedure at various irradiances are shown in Table 3. The results in Tables 2 and 3 illustrate the extent of the differences in smoke levels between nonflaming and flaming burning for some plastics. A single propane burner was used in these tests with horizontally mounted specimens to give a 25-mm-long pilot flame in a position 10 mm above the center of the specimen. Further results [*2*] for thermoplastics over a range of irradiances are given in Table 4; these results also show how the maximum rate of smoke formation (R_m) varies. R_m is calculated according to ASTM E 662 to give an indication of how fast smoke is generated; however, since the data do not show at what time the rate of smoke formation reaches a maximum, the test report for ISO/DP5659 should also give the time to reach R_m.

Since the test results of specific optical density measurements in the ASTM E 662 smoke chamber only relate to the thickness of the specimen tested, the ISO single chamber equipment is being modified further so that the specimen holder is mounted on a load cell. The mass optical density can then be found by measuring the weight loss of the specimen during the test. The mass optical density is given as MOD by the relation

$$\text{MOD} = \frac{V}{L\,\Delta m}\left(\log_{10}\frac{100}{T}\right) \tag{1}$$

TABLE 4—*ISO/DP5659 smoke density results for plastics in the horizontal orientation irradiated with radiant cone and pilot flame* [2].

Material	Thickness, mm	20 kW/m^2		30 kW/m^2		40 kW/m^2	
		D_m	R_m[c]	D_m	R_m[c]	D_m	R_m[c]
Polyethylene	3	458	135	332	119	545	245
Polypropylene	3	339	98	414	166	433	183
PMMA[b]	2.5	234	99	156	77	141	68
Expanded polystyrene, 20 kg/m^3	20	157[a]	15[a]	320	158	346	166

[a] Not ignited.
[b] Polymethylmethacrylate.
[c] Maximum rate of increase in specific optical density per minute, measured over any 2-min period; units are min^{-1}

Copyright by ASTM Int'l (all rights reserved) Wed Feb 07 10:53:32 UTC 2024
Downloaded/printed by
The University of Delaware pursuant to License Agreement. No further reproductions authorized.

where

V = the volume of the chamber,
L = the length of the light path through the smoke,
T = the percent light transmittance, and
Δm = the weight loss of the specimen.

Development of the ISO single-chamber static test is being continued, and an interlaboratory trial is currently taking place.

Dual Chamber Tests

ISO/TC92 have developed a dual chamber test DIS5924 for measuring the smoke generated by building products. The test is used for specimens of essentially flat materials, composites, or assemblies not exceeding 70 mm thickness when in a horizontal orientation and exposed to irradiance in the range 0 to 50 kW/m^2. Smoke is generated in one compartment of a box (the decomposition chamber) using a modified ISO5657 ignitability test apparatus with the pilot flame attachment removed. The smoke then passes using a fan into a second (measuring) chamber where its optical density is measured.

For each different exposed surface, at least seven specimens are tested. Specimens are tested at 50, 40, 30, and 20 kW/m^2; then repeat tests are carried out at the level of irradiance, which caused the highest maximum optical density D_h during the pretests. For this set of repeat tests, the mean value D_{hm} (highest smoke density) is calculated as well as the mean time t_{hm} to the highest smoke density and the mass loss W_m.

Current work in ISO/TC92/SC1 is directed at modifications to the fan, to assessing the effect of a pilot flame in the decomposition chamber, and to evaluating composites (especially rigid foams with inorganic facings). The results [*3*] shown in Table 5 indicate that D_{hm} is not significantly affected by the presence of an ignitor, although there is evidence that D_{hm} occurs at the lower irradiance and earlier in the test when an ignitor is used.

Dynamic Tests

A limitation of chamber methods is that only thin specimens may be reliably evaluated since the oxygen level will decrease as the specimen burns; with thicker specimens, the oxy-

TABLE 5—*ISO/DIS5924 smoke density results for plastics* [3].

Material	Thickness, mm	Radiant Cone Only			Radiant Cone + Ignitor		
		D_{hm}	Irradiance at D_{hm}, kW/m^2	Time to D_{hm}, min	D_{hm}	Irradiance at D_{hm}, kW/m^2	Time to D_{hm}, min
Pilot flame							
PIR[a] foam, 31 kg/m^3	30	1.15	30	4.3	0.80	50	1.9
EPS[b], 30 kg/m^3	30	1.70	50	1.8	1.40	40	1.5
Spiral heating filament							
EPS[b], 15 kg/m^3	30	2.65	30	9.5	2.11	30	6.4
TP[c] sheet	3	3.97	35	16.9	3.84	30	13.1

[a] Polyisocyanurate.
[b] Expanded polystyrene.
[c] Thermoplastic.

Copyright by ASTM Int'l (all rights reserved) Wed Feb 07 10:53:32 UTC 2024
Downloaded/printed by
The University of Delaware pursuant to License Agreement. No further reproductions authorized.

TABLE 6—*Heat release and smoke results for plastics from NIST cone calorimeter using irradiance of 30 kW/m².*

Material	Max Rate of Heat Release, kW/m²	Specific Smoke Extinction Area, m²/kg
Conventional PVC	189	1073
FR, LA[a]-PVC	139	566
FR, RS[b]-PVC	28	17
Polyethylene	869	525
EVA[c] + ATH[d] filler	160	184
PPO[e] (styrene-modified)	738	1129

[a] Fire retardant, low acid.
[b] Fire retardant, reduced smoke.
[c] Ethylene vinylacetate copolymer.
[d] Alumina trihydrate.
[e] Polyphenylene oxide.

gen content of the chamber may drop to 14% when extinguishment of the flames may occur. Dynamic, flow-through methods such as the NIST cone calorimeter [*4*] overcome this problem. In addition to the heat release measurements which form the basis of ISO/DIS5660, smoke obscuration may be determined in the exhaust duct using a helium-neon laser and silicon photodiodes as detectors. Results of specific smoke extinction areas for plastics under an irradiance of 30 kW/m² are given in Table 6. In this procedure for measuring heat release and smoke obscuration, electric spark ignition is used at 13 mm above the central point of the specimen in the horizontal orientation. When ignition has occurred, the sparking plug is withdrawn.

The cone calorimeter allows smoke volumes and rates of mass loss to be determined. For hazard assessment purposes a limitation of the procedure (as with chamber methods such as ISO/DIS5924 and ISO/DP5659) is that the area of the specimen exposed to radiation from the cone is fixed and no contribution due to spread of flame can be evaluated. In order to introduce a contribution for fire growth, Babrauskas [*5*] has combined two of the most important characteristics of fire hazards (i.e., rate of heat release and smoke obscuration) into a single smoke parameter, which is defined by the relationship

$$\text{Smoke Parameter} = \sigma_m \times (\text{RHR})/10^5 \tag{2}$$

where σ_m is the specific extinction area, normally taken as the average specific extinction area during the period from ignition to ignition time plus 5 min. Smoke parameters for three plastics over the irradiance range 20 to 50 kW/m² are shown in Table 7. While it is valuable to combine data from the same test procedure into this smoke parameter, it would be even more useful for smoke hazard analysis if a modified smoke parameter could be developed which would combine rate of heat release and smoke obscuration (from cone calorimeter) with spread of flame characteristics (derived from another test).

Room Tests

Full-scale room tests are essential to provide validation of small-scale smoke tests. They can provide vital supporting data on fire effects which cannot be obtained from the small-scale tests. Important evaluations can be made on composite structures (since most small

Copyright by ASTM Int'l (all rights reserved) Wed Feb 07 10:53:32 UTC 2024
Downloaded/printed by
The University of Delaware pursuant to License Agreement. No further reproductions authorized.

TABLE 7—*Smoke parameters for NIST cone calorimeter over a range of irradiances.*

Material	Smoke Parameters, kW/kg			
	20 kW/m^2	30 kW/m^2	40 kW/m^2	50 kW/m^2
EVA[a] + ATH[b] filler	0.14	0.21	0.45	0.46
FR, LA[c]-PVC	0.48	0.79	0.99	1.06
PPO[d] (styrene-modified)	4.36	8.33	6.70	7.33

[a] Ethylene vinylacetate copolymer.
[b] Alumina trihydrate.
[c] Fire retardant, low acid.
[d] Polyphenylene oxide.

tests only examine flat specimens) as well as spread of flame characteristics away from the initially exposed part of the specimen (since in the small smoke tests previously described, the specimen area is completely irradiated). For realistic smoke hazard assessment of full-scale fire scenarios, it is often not accurate to extrapolate from small-scale smoke tests, particularly when the materials being assessed are fire-retardant or char-forming polymers.

The 3m cube room test has been standardized in the U.K. for measuring the smoke density of some specialist electric cables, i.e., BS 6724 Armoured Cables for Electricity Supply and BS 6853 Code of Practice for Railway Passenger Rolling Stock. This procedure has been adopted as the International Union of Public Transport (UITP) E4 test and is now being developed by the International Electrotechnical Commission (IEC) Technical Committee 20 (Electric Cables). The test is most appropriately used for assessing low smoke-emitting materials for potential use in high-risk applications (e.g., underground trains, warships, cables for nuclear power plants). The fire source used for testing cables consists of 1 L of 94% industrial methylated spirit contained in a steel tray with base dimensions 210 by 110 mm. This source is positioned 175 mm below the 1-m-long test array of horizontally oriented cables. Observations of absorbance with the cube are made by plotting smoke emission with time. The first phase (ON) applies when the alcohol source is burning. The second phase (OFF) applies after the source has been extinguished and the material or product is smoldering or still burning. Results of smoke absorbance for wires insulated with various plastics are shown in Table 8.

Room tests which allow dynamic flow-through measurements of smoke volume and obscuration are particularly useful to specifiers and architects since they provide extra data for smoke hazard control, especially concerning effects of ventilation. Two types of dynamic room tests have been used.

1. *Room with hood and duct.* This procedure is being developed by ASTM, the Scandinavian standards organization (Nordtest), and ISO/TC92. Since the measurements are similar to those in the cone calorimeter, there is interest in correlating the results of the small-scale cone calorimeter equipment with this room test [*6*].
2. *Room with corridor.* This procedure has been used in the U.K. to devise experimental conditions similar to real fires. The room may be operated either closed or with an inflow of air. Smoke measurements are usually taken at the end of the corridor with vertical light beams.

These dynamic room tests are valuable for smoke hazard assessment since they allow full-scale effects to be determined. The room may be used as proposed by ASTM for tests on wall linings; alternatively, the walls and ceiling may be covered with a noncombustible mate-

Copyright by ASTM Int'l (all rights reserved) Wed Feb 07 10:53:32 UTC 2024
Downloaded/printed by
The University of Delaware pursuant to License Agreement. No further reproductions authorized.

TABLE 8—*Smoke absorbance results for plastic cable materials*[a] *in the 3-m cube test.*

Material	A_o [ON] max, m^2/metre bunch	A_o [OFF] max, m^2/metre bunch
Conventional PVC	1.39	1.69
FR, LA[b]-PVC	1.44	1.70
CSP[c]	0.48	1.20
FEP[d]	0.20	0.45
Polyethylene	0.33	0.54
EVA[e]/ATH[f]	0.21	0.52
EVA/ATH (silane cross-linked)	0.13	0.35
PPO[g] (styrene-modified)	1.94	2.27

NOTE: A_o = absorbance.
[a] 30 wires, each 1 m long, were combined by twisting together to form a bunch. Each wire had a copper conductor of 1.5 mm^2 cross-section and insulation of 0.75 mm radial thickness.
[b] Fire retardant, low acid.
[c] Chlorosulphonated polyethylene.
[d] Fluoroethylene copolymer.
[e] Ethylene vinylacetate copolymer.
[f] Alumina trihydrate.
[g] Polyphenylene oxide.

rial so that tests on furnishings or parts of full-scale structures (e.g., corner/wall assemblies) may be performed inside the room. Calibration of different rooms can be made by burning a specified quantity of liquid fuel in a pool fire. Results of room/corridor tests comparing toluene pool fires with a small-scale corner test are shown in Table 9 for different ventilation conditions.

Smoke Hazard Analysis

Recognizing the significant differences in the test conditions used for measuring smoke, proposals have been made for developing a standard protocol for smoke hazard analysis. A

TABLE 9—*Measurements of smoke generated by fires in ventilated 84-m^3 room and corridor.*

Material	Airflow, m/s	Fire Model	Max Smoke Density, OD/m	Time to Max Smoke Density, min	Total Vol of Smoke (m^3) of OD/m = 1
Toluene, 250 mL	0.3	Pool	0.64	2.00	45
Toluene, 250 mL	0.65	Pool	0.86	2.00	87
Toluene (1000 mL), isopropanol (1500 mL)	0.65	Pool	1.6	7.00	343
PIR[a] foam/Al[b]-foil faced (33 kg/m^3; 50 mm thick)	0.3	ISO/DP8337 corner	1.08	5.00	160
Glassfibre-reinforced PIR[a] foam/Al-foil faced (34 kg/m^3; 50 mm thick)	0.3	ISO/DP8337 corner	0.52	4.20	56

NOTE: OD = optical density.
[a] Polyisocyanurate.
[b] Aluminum.

Copyright by ASTM Int'l (all rights reserved) Wed Feb 07 10:53:32 UTC 2024
Downloaded/printed by
The University of Delaware pursuant to License Agreement. No further reproductions authorized.

BSI Draft for Development on the Assessment of Toxic Hazards in Fires in Buildings and in Transport is to be published in 1989; this code of practice uses defined steps which require assessors to consider all the relevant parameters controlling growth of a fire. A similar approach has been taken by the British Plastics Federation in their Code of Practice (1989) to assess the smoke hazards of plastics products in fires.

Step 1: Definition of the Fire Scenario and Assessment of the Probability That This Fire Scenario Will Occur (Fig. 1)

Step 2: Consideration of Ignitability (Fig. 2)

Materials are evaluated with a variety of relevant ignition sources and test conditions. Classification of performance can then be recorded based upon a simple points system, which is decided by the assessor, e.g., nonignitable—0 points, difficult to ignite—1 point, and easy to ignite—2 points.

The ignitability hazard factor h_I may then be estimated as Σi_n, where i_n is the score obtained from as many ignitability tests as possible.

After considering all factors associated with the product design and fire scenario which would influence ignition in addition to the estimated value of h_I, a decision is made about the ignition risk. If satisfactory, Step 3 should be assessed; otherwise all the inputs to Step 2 must be reconsidered including a redesign of the product.

i) Define fire scenario

ii) Assess probability of its occurrence.

iii) Draw diagrams of fire scenario and anticipated movement of smoke

FIG. 1—*Smoke hazard analysis: Step 1.*

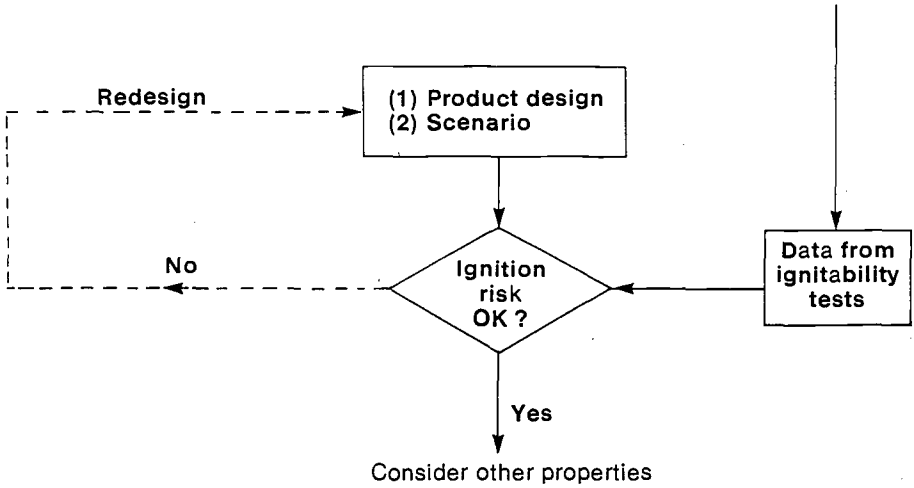

FIG. 2—*Smoke hazard analysis: Step 2.*

Copyright by ASTM Int'l (all rights reserved) Wed Feb 07 10:53:32 UTC 2024
Downloaded/printed by
The University of Delaware pursuant to License Agreement. No further reproductions authorized.

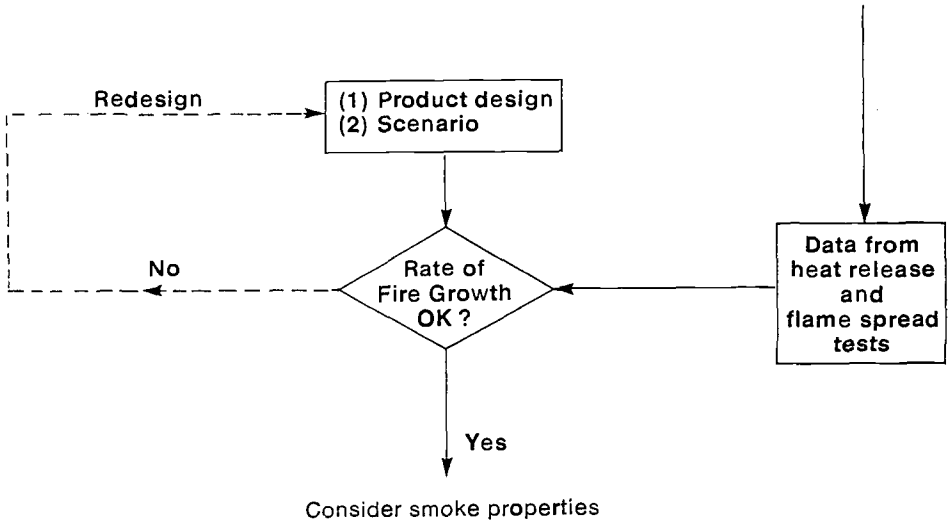

FIG. 3—*Smoke hazard analysis: Step 3.*

Step 3: Consideration of Fire Growth (Fig. 3)

Hazard factors for flame spread (h_F) and heat release (h_H) may be estimated in a similar manner to ignitability; i.e., a points system is derived so that three categories for both flame spread and heat release are defined. For each test condition, the points allocated will be higher for poorer performance; e.g., for both flame spread and heat release tests, little reaction attracts 0 points, medium reaction 1 point, and large reaction 2 points. The weightings and number of tests will be determined by the assessor so that h_F and h_H are summations of points allocated for as many tests as possible. If test data are limited, only the results of tests relevant to the application should be considered. Again, it is necessary to examine the effects of product design and the fire scenario before making a decision about the rate of fire growth. If satisfactory, Step 4 should be assessed; otherwise all the inputs to Step 3 must be reconsidered including a redesign of the product.

Step 4: Consideration of Smoke Test Data (Fig. 4)

All relevant data should be recorded specifying whether this applies to materials or products. These data should include smoke obscuration, rate of generation, rate of mass loss, and total smoke volume (m^3) of optical density per metre equal to one. The results of ad hoc tests should also be included. A smoke hazard factor (h_s) may be derived from the available test data by a similar points and summation system as used in Steps 2 and 3. Thus, the assessor can decide to allocate points for performance to whatever test conditions (e.g., static or dynamic, flaming or nonflaming) are perceived to be most relevant to the real fire scenario, e.g., low smoke—0 points, medium smoke—1 point, high smoke—2 points. A decision is then made about the acceptability of the experimental data. If satisfactory, Step 5 should be assessed; otherwise all the tests should be reconsidered.

Step 5: Consideration of Rate of Smoke Hazard Development (Fig. 5)

Smoke hazards should be considered for the scenario in terms of escape times (i.e., perceived reduction in visibility and obscuration of exits). Factors for assessment include the

Copyright by ASTM Int'l (all rights reserved) Wed Feb 07 10:53:32 UTC 2024
Downloaded/printed by
The University of Delaware pursuant to License Agreement. No further reproductions authorized.

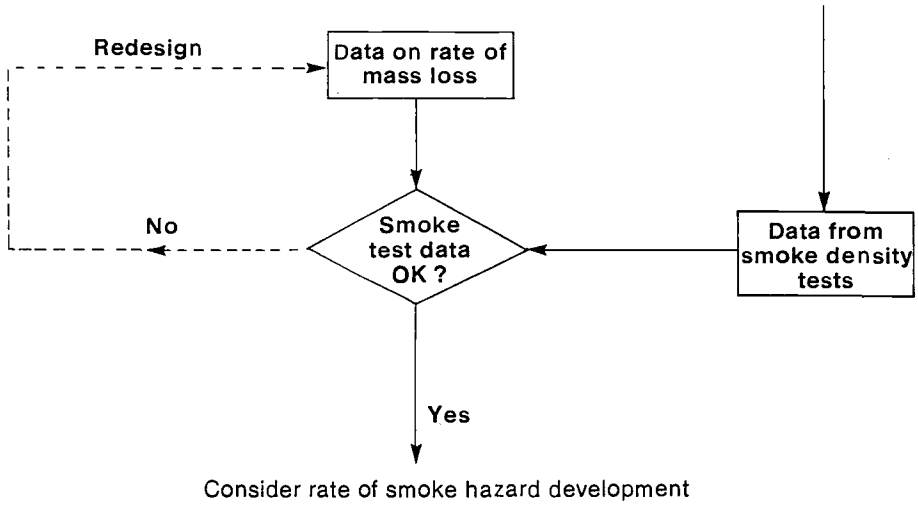

FIG. 4—*Smoke hazard analysis: Step 4.*

ventilation conditions and smoke spread control facilities as well as the behavioural response of occupants of the builting.

Assuming satisfactory conditions are likely, a decision to accept the product for the proposed use can be taken. Alternatively, it may be necessary to reconsider some aspects of the proposed use depending on whether the application is a high or low risk one.

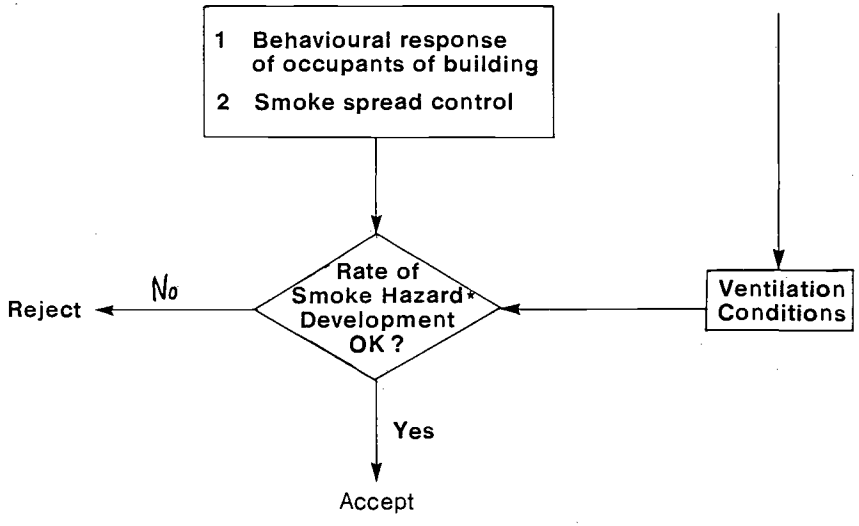

FIG. 5—*Smoke hazard analysis: Step 5.*

Copyright by ASTM Int'l (all rights reserved) Wed Feb 07 10:53:32 UTC 2024
Downloaded/printed by
The University of Delaware pursuant to License Agreement. No further reproductions authorized.

Conclusions

Small-scale smoke obscuration tests will continue to provide valuable data for research, development, and quality assurance purposes. Since there are significant differences in the fire models and conditions used in these tests, there will be an additional need to perform full-scale tests, especially for reliable regulatory purposes.

The control of smoke hazards by material tests alone has been questioned [*7*], and wider use of smoke management systems is believed to be a more effective way to prevent smoke spread within buildings. Material suppliers and specifiers should be able to assess smoke hazards more accurately by adoption of a code of practice which requires all the fire parameters to be considered as well as factors associated with the product design and the fire scenario.

Acknowledgments

I wish to thank colleagues on the British Plastics Federation (BPF) and ISO fire committees for their support and contributions to this paper.

References

[*1*] Hirschler, M. M., "The Measurement of Smoke in Rate of Heat Release Equipment in a Manner Related to Fire Hazard," international conference on "Fire: Control the heat . . . . Reduce the hazard," QMC Fire and Materials Centre, London, 1988, pp. 9.1 to 9.17.
[*2*] Hovde, P. J., "NBS Smoke Density Chamber. Testing of Materials in the Horizontal Position by Use of a Conical Shaped Radiation Furnace," SINTEF (Norway) Report STF 25 A81002, 1981.
[*3*] Prager, F. H. and Muller, B., "ISO/DIS5924 Development," ISO/TC92/SC1/WG4 N95, 1988.
[*4*] Babrauskas, V., *Fire and Materials,* Vol. 8, No. 2, 1984, pp. 81–95.
[*5*] Babrauskas, V., *Journal of Fire and Flammability,* Vol. 12, January 1981, pp. 51–64.
[*6*] Wickstrom, U., "Cone Calorimeter and Room/Corner Tests for Reaction-to-Fire Classification of Building Products," ISO/TC92/SC1/WG7 N63, 1988.
[*7*] Benjamin, I. A., *Fire Safety Journal,* Vol. 7, 1984, pp. 3–9.

DISCUSSION

Vytenis Babrauskas[1] *(written discussion)*—In searching for a parameter to better characterize smoke production from a product, it should be possible to follow procedures very similar to those for toxic gas production. The yield of smoke (m^2 of smoke/kg of specimen mass loss) should be multiplied by the specimen mass loss rate (kg/m^2-s). The mass loss rate needs to be defined over some finite period; a good choice is from 10% of specimen mass loss to 90%. Finally, the area actively involved in flames (m^2) in the full scale needs to be factored in. In some cases, this may simply be the total exposed area of the specimen. In other cases, actual flame spread may need to be taken into account. In those cases, a method was recently evolved, based on some empirical correlations [Babrauskas, V., A Simplified Method for Approximating Toxic Fire Hazard, pp. 16.1 to 16.10 in **Fire: Control the Heat . . . Reduce the Hazard,** QMC Fire & Materials Centre, London (1988)]. According to that procedure, the area of flame involvement can be set as $\propto 1/t_{ig}$, where t_{ig} is the bench-scale ignition time in the cone calorimeter.

Peter Briggs (author's closure)—The principle of relating toxic gas production to smoke production is accepted, and it is desirable to introduce mass loss rate into the data presentation. Gas analysis with combustion toxicity experiments has shown that the composition

[1] NIST, Bldg. 224, A363, Gaithersburg, MD 20899.

Copyright by ASTM Int'l (all rights reserved) Wed Feb 07 10:53:32 UTC 2024
Downloaded/printed by
The University of Delaware pursuant to License Agreement. No further reproductions authorized.

of the effluent varies with the mode of burning (i.e., flaming versus nonflaming or smoldering) in the same way as smoke obscuration tests give different results depending on the burning mode. Because of this effect, it is vital to ensure that smoke obscuration measurements are carried out in *both* modes since both types of burning occur in real fires.

It is also desirable to introduce a factor for the area of the specimen burning. The proposal to use $1/t_{ig}$ to estimate the flame spread characteristics needs further validation under a wider set of experimental conditions. It may be preferable to combine data derived from a separate flame spread test (e.g., ISO/DP5658) with heat release and smoke density results obtained from a dynamic test such as the cone calorimeter. This approach would allay concern that the ignition times determined in the cone calorimeter are apparatus-dependent and do not simulate many ignition situations in real fires. It should also be noted that some materials do not ignite under the irradiances of 25 or 35 kW/m^2; if a higher irradiance (e.g., 50 kW/m^2) is selected to ensure flaming combustion, this would introduce a limitation, and data could only then be used for fully-developed fires.

Copyright by ASTM Int'l (all rights reserved) Wed Feb 07 10:53:32 UTC 2024
Downloaded/printed by
The University of Delaware pursuant to License Agreement. No further reproductions authorized.

Frederick B. Clarke,[1] *Henri van Kuijk,*[1] *and Sharon Steele*[1]

Predicting the Toxic Hazard of Cable Fires

REFERENCE: Clarke, F. B., van Kuijk, H., and Steele, S., **"Predicting the Toxic Hazard of Cable Fires,"** *Characterization and Toxicity of Smoke, ASTM STP 1082,* H. K. Hasegaua, Ed., American Society for Testing and Materials, Philadelphia, 1990, pp. 46–56.

ABSTRACT: Despite a growing interest in cable fires, no systematic evaluation of the toxic threat from cables under actual fire conditions has been attempted. The present paper demonstrates the methodology used by Benjamin/Clarke Associates to estimate hazard of cable smoke. The method makes use of small-scale fire property tests and computer modeling. Certain of the predictions have been tested at full scale.

The small-scale tests provide data on the response of the cables to a radiative heat environment, predicted by the mathematical model. In this work, the NIST cone calorimeter provided mass loss data and the LIFT apparatus was used to measure flame spread parameters. All cable fire data were obtained over a range of imposed flux. Bench-scale measurement of toxic potency of cable smoke was obtained; in some cases, full-scale smoke potency data were obtained as well. The modeling was done by modifying a room fire code (Harvard V) to allow for cable fires. This involved specific calculation of the incident flux to substrates in the hot upper layer of a room fire. Once the flux to a cable bed could be predicted, it was possible to calculate the rate of smoke evolution from the cables, making use of the small-scale test data described above. In a full-scale test of the method, good agreement between predicted and observed mass loss was obtained.

The methodology was then extended to a series of four cables in two fire scenarios similar to burn studies carried out by the U.S. Navy. The predicted rankings of the cables in these two scenarios were compared with the rankings of the cables by: (1) a toxic potency test; (2) results of a toxic potency test adjusted by the amount of cable present in each case; and (3) a new smoke toxicity test, which makes some allowance for the fire properties of the material. It was found that the bench-scale toxic potency measurements were not good indicators of full-scale performance.

KEY WORDS: fire hazard assessment, fire modeling, cone calorimeter, flame spread, smoke toxicity

The past five years have seen greatly increased interest in the fire hazards posed by electrical cables. The decision of New York State to require listing of wire and cable products by smoke toxicity data, coupled with the development of new insulation and jacketing materials, have prompted the fire community to examine how modern tools of fire protection and hazard assessment can be applied specifically to cables. Recent applications have included an analysis of the threat posed by plenum cable [*1*], the behavior of cables in a developing room fire [*2*], and, in a slightly different vein, the hazard posed by nonmetallic tubing used as electrical conduit [*3*]. All of these analyses have, in one sense or another, employed modern fire science; two have used mathematical room fire models. This paper will provide an update on the capabilities of the model-based methods of predicting toxic fire hazard from cables.

[1] President, Benjamin/Clarke Associates, Inc., Kensington, MD 20879.

Copyright by ASTM Int'l (all rights reserved) Wed Feb 07 10:53:32 UTC 2024
Copyright © 1990 by ASTM International www.astm.org
Downloaded/printed by
The University of Delaware pursuant to License Agreement. No further reproductions authorized.

As the computational approach to fire hazard has advanced, so also has a laboratory test for smoke toxicity hazard. This test, which is being developed under the auspices of the National Institute of Building Sciences (NIBS), is conceived as a preferred alternative to the simple measure of smoke's toxic potency. It takes some account of a material's fire properties in the course of determining smoke's effect on test animals.

This paper has a twofold purpose: first, to provide an update on predicting cable toxic hazard using a numerical approach (laboratory test data in and in combination with mathematical fire models); and, second, to show how laboratory toxicity tests, i.e., toxic potency and the newly established NIBS test, compare with the numerical approach in their ability to identify the toxic hazard.

Toxic Hazard Assessment of Cables

General

The term "toxic hazard" is used in this paper to mean the threat posed by the potential lethal effects offered by smoke from a fire. Toxic hazard is only a part of fire hazard, where the threats from temperature, hindered escape, and the like are also considered. The usual approach to fire hazard assessment is to identify the threat, whether thermal or from smoke, which is first encountered. As a general rule, potential fire victims located close to the fire are threatened first by heat, in which case it matters little what the details of the smoke toxicity might be. When the potential victims are sufficiently far from the fire, however, the heat is dissipated and the main threat is the effect of the smoke. Generally, both kinds of hazard can be evaluated with numerical hazard assessment; the techniques which give rise to estimates of thermal hazard can be used to estimate toxic hazard as well, provided suitable smoke data are at hand.

Hazard assessment using an analytical approach consists of three separate steps:

1. *Evaluating how the product of interest behaves over a range of thermal environments.* The environment is usually described in terms of the total heat flux it imposes on the product. Recently, several instruments have been developed which measure material fire properties as a function of heat flux. At present, data from two instruments are required. Either the cone calorimeter [*4*], developed at the National Institute of Standard and Technology (NIST), or the factory mutual flammability apparatus [*5*] are used to provide mass loss rate, heat release rate, and smoke yield. The lateral ignition and flammability tester (LIFT) [*6*], also developed at NIST, is used to determine the minimum flux for flame spread, the flux interval over which flame spread occurs at a finite rate, and the dependence of spread rate on flux within that interval.

2. *A method is found to describe the flux the product will receive in an actual fire.* Where suitable full-scale data are available, they can be used. Computational approaches, such as room fire models, are, however, more common and have been developed to the point where the flux received by the wall surfaces, floors, and ceilings can be predicted in a variety of fires. When products under study are located in these locations, the flux they receive in the fire is thus estimated, so that the actual mass loss and heat release rate of the products can be predicted using the data obtained in the small-scale tests described above.

3. *For estimates of toxic hazard, the rate of mass loss from the product, calculated as part of Step 2, is combined with the toxic potency of the smoke, which is measured in a laboratory smoke toxicity test.* The result is used to estimate the buildup of a lethal (or incapacitating) dose of the smoke in someone exposed to the fire. This information can be used to describe toxic conditions in the developing fire and to choose products which offer the lowest toxic hazard.

Copyright by ASTM Int'l (all rights reserved) Wed Feb 07 10:53:32 UTC 2024
Downloaded/printed by
The University of Delaware pursuant to License Agreement. No further reproductions authorized.

Products are usually compared on the basis of the time required for conditions to reach a given level of thermal or toxic severity. The shorter the time required, the comparatively poorer the product's performance.

Full-Scale Confirmation

To date, only predictions of mass loss have been checked by full-scale experiments. Benjamin has predicted the decomposition of electrical nonmetallic tubing in room fires, and those predictions have beend found to be valid at full scale [*3*].

Recently, a series of full-scale fire studies on fluoropolymer-insulated cables have been concluded at the University of Ghent in Belgium [*7*]. As part of this work, sizable amounts of cable in a burn room were exposed to wood crib fires with peak energy release rates around 1 MW. From the heat release profile obtained from burning the crib alone, a modified Harvard V room fire code [*8–10*] can predict the corresponding profile of heat flux on a cable bed suspended in the hot layer. Making use of measured cable mass loss rate data obtained from the cone calorimeter, the weight loss of cable in the tray could be predicted and compared with experiment. The results of the comparison are shown in Fig. 1. Agreement between theory and experiment was found to be very good, as was the case in the work previously reported by Benjamin. The real utility of these results is that accurate prediction of mass loss rates paves the way for assessment of toxic hazard since the smoke production rate, in combination with the toxic potency, determines the effects on those exposed.

A more difficult class of problem is one in which the fire is spreading on the cables. In this case, the area burning is changing with time, so the cables' mass loss rate is affected not only by the heat flux which reaches them but also by the amount of cable burning. Van Kuijk [*10*] has modified the Harvard V fire code to accommodate a simple flame spread algorithm.

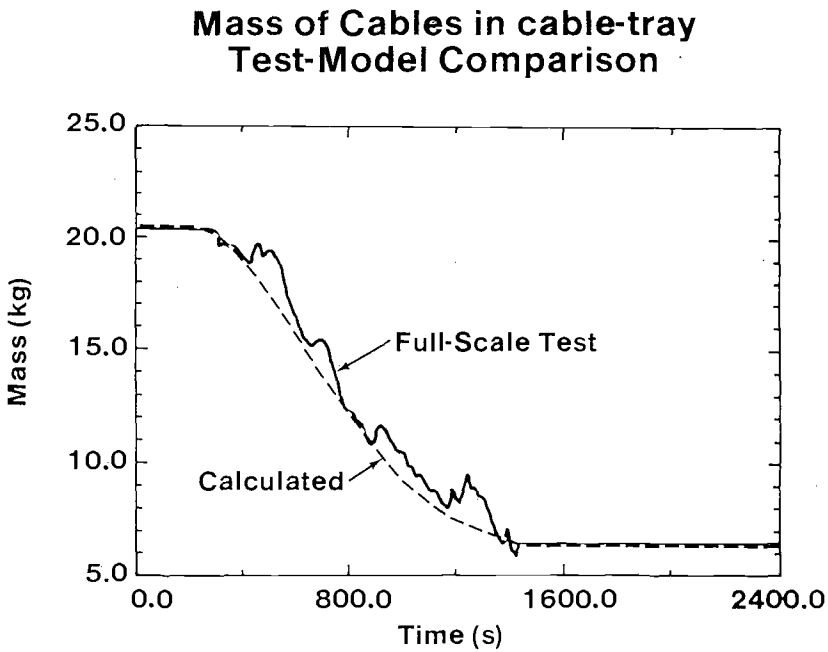

FIG. 1—*Weight loss of cables in full-scale room fire.*

Copyright by ASTM Int'l (all rights reserved) Wed Feb 07 10:53:32 UTC 2024
Downloaded/printed by
The University of Delaware pursuant to License Agreement. No further reproductions authorized.

Further refinements, based on the flame spread work of Quintiere and Harkleroad [*6*], have recently been incorporated. For predictions of flame spread, an apparatus like LIFT must be used to describe flame spread rate as a function of flux.

Shipboard Cable Toxic Hazard Assessment

Methodology

In 1987, the Naval Research Laboratory carried out a series of full-scale shipboard fire tests designed to evaluate the effect of new shipboard cable specifications [*11*]. The same shipboard environment was used as a setting to examine the fire hazard offered by a variety of shipboard cable designs. No full-scale experiments were done; rather an analytical hazard assessment of cables in the shipboard environment was conducted. A portion of the work is presented here as an illustration of the utility of the approach as a tool for evaluating cable performance in real fire situations and to provide a benchmark for comparison with other suggested methods of assessing toxic hazard.

The basic fire model used was the Harvard Fire Code (Version 5.2) designed for normal buildings. As originally designed, it failed to provide solutions for a shipboard compartment having steel walls: normal building walls conduct far less heat from the room. This problem was solved by using a more robust algorithm for solving the heat transfer equations in the model. Good agreement with experimental was found when the modified code results were used to reproduce the temperature profile for a blank test in which no cables were burned.

The test compartment, Fig. 2, was 5.2 by 2.8 by 2.4 m high; the walls were steel. The doorway opening was 1.4 by 1.83 m high with a sill of 0.18 m. The source fire was a 2 by 2-ft pan of ethanol. A cable tray suspended 0.2 m from the ceiling ran the length of the room. For purposes of assessing toxic hazard, it was assumed that the door opened to a corridor which led to a remote room (Fig. 3). The dimensions of the remote room were the same as the burn room.

Four different types of cable were evaluated in each of two scenarios. In Scenario 1, a 750-kW fire was located 1 m away from the cables; in Scenario 2, the fire was 1000 kW and 2 m away. The first 0.1 m (4 in.) of the cables were assumed to be ignited by the fire at the start of the burn. The modeled cable configuration was a tray containing 82 cables arranged two layers deep. Each of the four cable types was evaluated in both scenarios. The mass loss rates, flame progression on the cables, visibility, toxicity, and temperature in the room of origin and remote room were calculated for each cable in each scenario using its measured properties in conjunction with the modified model.

Properties of the four different experimental electrical cables evaluated in this assessment are listed in Table 1. The heat of gasification and the heat of combustion were measured on the NIST cone calorimeter over a range of external heat flux from 15 to 50 kW/m^2.

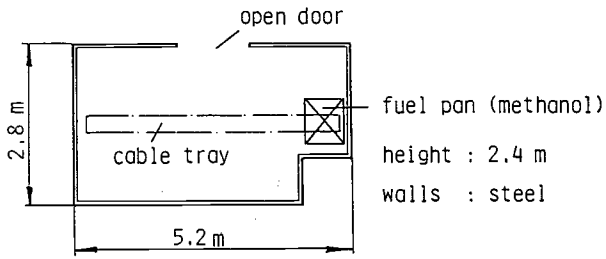

FIG. 2—*Burn room (plan view).*

Copyright by ASTM Int'l (all rights reserved) Wed Feb 07 10:53:32 UTC 2024
Downloaded/printed by
The University of Delaware pursuant to License Agreement. No further reproductions authorized.

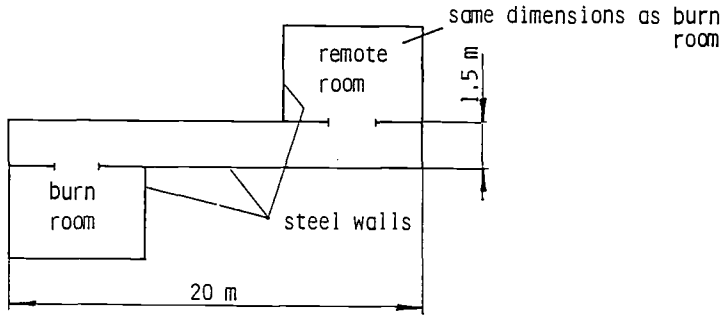

FIG. 3—*Remote room (plan view).*

The minimum flame spread flux, $\dot{q}''_{fs}$, was measured using the lateral ignition and flame travel (LIFT) apparatus. The minimum ignition flux $\dot{q}''_i$ was determined in the flame spread and ignition modes of the LIFT apparatus, and also using the cone calorimeter. The results of the three methods were averaged to yield the final value. For Cable D, the ignition flux value was obtained using only the LIFT apparatus in the flame spread mode. The combustible content of the cables was measured by irradiation to constant weight in the cone calorimeter at 50 kW/m^2.

Toxic potency of cable smoke was determined using the NIST toxicity test [*12*] modified to accept a radiant heat source as suggested by Packham [*13*]. LC_{50}s for each cable, determined at an imposed flux of 50 kW/m^2, are for a 30-min animal exposure followed by a 14-day postexposure observation period. The lethal dose, $L(Ct)_{50}$ (shown in Table 1), is taken to be the product of the measured LC_{50} and the 30-min exposure period.

In addition, the NIST test apparatus was operated in a mode analogous to that prescribed by the newly developed NIBS test [*14*]. In the NIBS procedure, the sample is irradiated with a fixed heat flux (here 50 kW/m^2), but instead of varying the amount of sample needed to produce a lethal atmosphere, the *time* necessary for a fixed sample area to generate a lethal atmosphere is measured and reported. This parameter, the irradiation time needed to produce enough smoke to cause death in 50% of the animals—the so-called IT_{50}—was recorded.

The most important assumptions in the assessment were the following:

1. Smoke movement occurred in only one direction, that is, from the burn room into the corridor and the remote room. No smoke flow from the corridor back into the burn room was permitted.
2. Mass loss was experienced only by the part of the cable which was burning. Mass loss of the cables began when $\dot{q}''_{fs}$ was reached, regardless of how long the cables had soaked in the hot layer.
3. Heat of gasification and heat of combustion of the cables were independent of imposed flux. This is probably the weakest assumption, since it is strictly true only when the chemistry of decomposition and combustion is invariant over the flux range studied.

Results

The buildup of cable smoke in the remote room for Scenarios 1 and 2 are shown in Figs. 4 and 5, respectively. The vertical axis is the fraction of "tolerable" smoke dose—"tolerable" being defined here as one quarter of the lethal dose. When the fraction of tolerable dose approaches unity, one may expect smoke toxicity to be important in inhibiting escape from

Copyright by ASTM Int'l (all rights reserved) Wed Feb 07 10:53:32 UTC 2024
Downloaded/printed by
The University of Delaware pursuant to License Agreement. No further reproductions authorized.

TABLE 1—*Cable data.*

	Description					Flame Spread Parameters			Pyrolysis/ Burning		Smoke Toxicity	
Label	kg/m	% Combustible	Diameter m	Combustible Amount per Cable, kg	Width of Cable Bed Exposed to Fire, m (82 Cables)	$\dot{q}''_{fs}$, kW/m^2	$\dot{q}''_i$, kW/m^2	a	ΔH_V, MJ/kg	ΔH_c MJ/kg	$L(Ct)_{50}$, g-min/m^3	IT_{50}, min
A	0.291	42.6	0.0137	0.645	0.79	10	15	1.19	5.2	16.5	36	2.1
B	0.248	30.1	0.0117	0.388	0.48	10	23	0.784	6.6	19.5	67	4.6
C	0.558	26.5	0.024	0.769	0.98	10	20	0.896	6.0	18.6	72	3.7
D	0.204	30.0	0.0102	0.318	0.42	10	38	0.440	3.2	7.2	29	4.0

NOTE:
1. Approximate value calculated by NBS software from LIFT flame spread data.
2. Where [flame spread rate (mm/s)]$^{-1/2} = a\,(\dot{q}''_i - \dot{q}'')$, $\dot{q}''_{fs} \leq \dot{q}'' \leq \dot{q}''_i$.
3. Average of values from cone, LIFT apparatus in ignition mode, and LIFT apparatus in flame spread mode.
4. Average of values obtained at two lowest flux exposures on cone calorimeter.

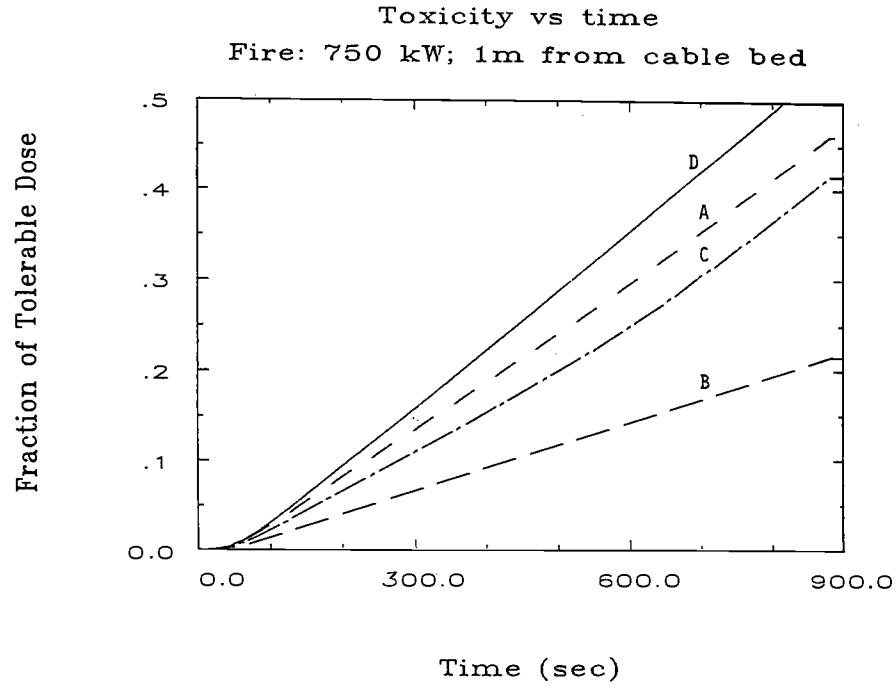

FIG. 4—*Buildup of smoke toxicity, Scenario 1.*

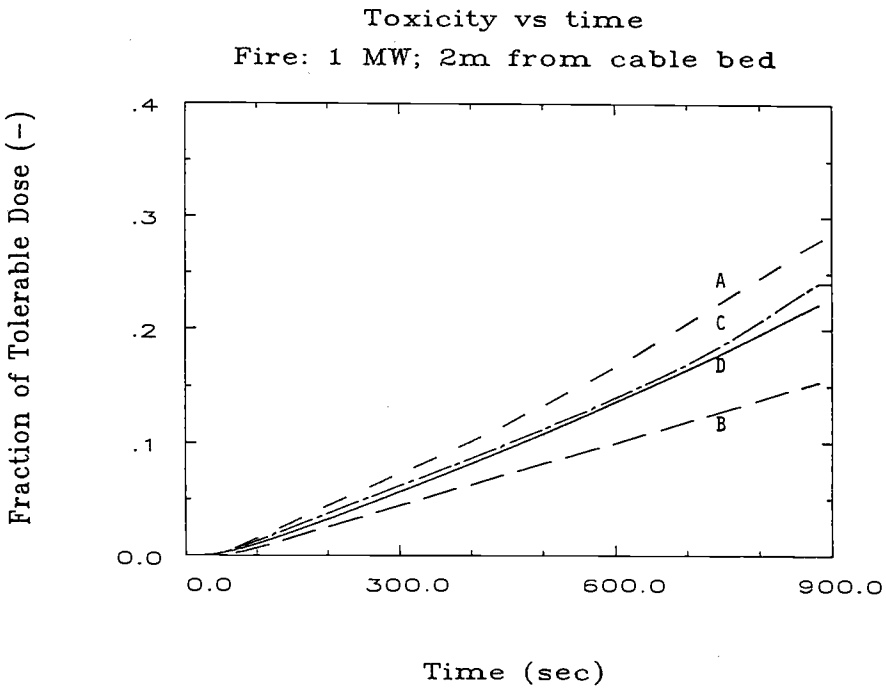

FIG. 5—*Buildup of smoke toxicity, Scenario 2.*

Copyright by ASTM Int'l (all rights reserved) Wed Feb 07 10:53:32 UTC 2024
Downloaded/printed by
The University of Delaware pursuant to License Agreement. No further reproductions authorized.

the smoke. (Not shown is the buildup of toxicity from the exposure fire alone, which, in these scenarios, was negligible.)

The threat from smoke toxicity was not found to be an important factor over the 15 min studied: the tolerable dose was not approached by any of the modeled cable fires. Cable B performed the best in both scenarios. This is due to the fact that its flame-spread and pyrolysis properties were quite good, so that while the fire was spreading the area aflame was less than some of the others. Even where the cable was fully aflame, its high heat of gasification (ΔH_v) meant that the mass loss rate was relatively low. Finally, the smoke, once produced, was, by the test used, somewhat less toxic.

The different fire conditions in the two scenarios changed the order of cable performance in the two scenarios. Cable D, which had the best flame-spread properties, burned comparatively less in Scenario 2 than the other cables, thus reducing the amount of smoke produced and improving its relative performance.

Comparison of Methods to Predict Toxic Hazard

Numerically based hazard assessment makes use of data from laboratory tests and mathematical room fire models to predict, in this case, the order of toxic hazard of a series of cables. However, in the course of this work, three less sophisticated predictors of cable performance have already been encountered:

Predictor 1—First among these is the toxic potency measurement which was used in part of the hazard assessment. Toxic potency data such as these are sometimes used by themselves in an attempt to estimate the relative toxic hazard of a set of materials.

Predictor 2—In the scenarios under discussion, the same number of cables were used in every case, but owing to differences in construction the weight of each cable in the room was different. Therefore one can construct an estimate of toxic hazard based on the amount of cable used divided by the toxic potency of the smoke from that cable. This would constitute a somewhat more sophisticated estimate of hazard than the use of simple toxic potency data alone.

Predictor 3—A third estimate of toxic hazard is afforded by the data using the modified NIBS approach to toxicity, the IT_{50} measurement. Because the radiation time needed to produce a toxic level of smoke implicitly reflects the ease with which the materials are ignited and the rate at which they produce smoke once ignited, the IT_{50} is a rudimentary attempt to incorporate some notion of a material's burning behavior into an estimate of its toxic hazard.

Finally, as a basis for comparison with these three methods, we have Predictor 4, which gives the results of the hazard assessment discussed in the previous section.

The results of the toxic potency measurements, the basis of Prediction 1, are shown in Table 2. Also shown is the range of toxic potency measurements found for each determi-

TABLE 2—*Prediction 1: Toxic hazard based on toxic potency.*

Cable	LC_{50}, mg/L[a]	Range
A	36	15–57
B	67	63–75
C	72	33–76
D	29	23–37

Result: C (= B) > D (= A) (> = better than).
[a]NBS Box—Packham heating system.

Copyright by ASTM Int'l (all rights reserved) Wed Feb 07 10:53:32 UTC 2024
Downloaded/printed by
The University of Delaware pursuant to License Agreement. No further reproductions authorized.

TABLE 3—*Prediction 2: Toxic hazard based on cable weight.*

Cable	LC_{50}	Total Length (m) of Cable in Room[a]	kg/m	Mass Used, kg	H[b]
A	36	426	0.291	124	3.4
B	67	426	0.248	106	1.6
C	72	426	0.558	238	3.3
D	29	426	0.204	87	3.0

Result: $B > D \overset{?}{>} A\ (=C)$.
[a] 82 pieces, each 5.2 m long.
[b] Hazard (H) = Cable mass used/LC_{50}.

nation. Cables B and C share essentially the same LC_{50}, as do Cables A and D. Thus, if one were basing a hazard prediction on the toxic potency, one would conclude that C and B are essentially equivalent and offer a better choice than do Cables D and A, which are also equivalent.

If the toxic potency numbers are weighted based on the amount of cable actually used in each case, the results constitute Prediction 2, shown in Table 3. The hazard parameter, H, is simply the quotient of the mass used in each case divided by the respective LC_{50}. On this basis, one would conclude that B is superior to the other three, which are nearly equivalent.

The effect of going from the simplest predictive method, i.e., toxic potency, to one which takes account of the amount of cable present would definitely influence what cable was chosen. Although the first method of prediction would show no difference between Cable B and C, taking account of cable weight would definitely distinguish between the two.

The prediction of a NIBS-type test parameter is shown in Table 4. Using this determinant, B offers the lowest toxic hazard (i.e., the longest IT_{50}) followed by Cables C and D, which are essentially equivalent based on the overlap of the ranges of the IT_{50}. Finally, Cable A is predicted to be the poorest of the four.

The results of the hazard assessment carried out on the previous section are presented as Prediction 4, Table 5. The order of performance varies somewhat between Scenario 1 and Scenario 2. In both cases, however, Cable B is shown to be superior. The same result was shown by Predictions 2 and 3, but was not disclosed by the toxic potency method alone.

Table 6 tabulates the predicted order of cable toxic hazard for each of the prediction techniques used. Predictions based on toxic potency (1 and 2) fail to predict the order of cable hazard performance in either of the two scenarios analyzed. The order of cable hazard performance in Scenario 2 is the same as predicted by the NIBS test.

Although toxic potency measurements have been embraced by some as an improvement in our ability to predict toxic hazard, the work presented here should show that such mea-

TABLE 4—*Prediction 3: Toxic hazard based on modified "NIBS" test.*

Cable	IT_{50}, min[a]	Range
A	2.1	0.9–2.9
B	4.6	4.0–5.6
C	3.7	3.4–4.1
D	4.0	3.0–4.6

Result: $B > D\ (= C) > A$.
[a] Equal lengths (0.09 m) of cable; the present NIBS test calls for a fixed area of exposed sample.

Copyright by ASTM Int'l (all rights reserved) Wed Feb 07 10:53:32 UTC 2024
Downloaded/printed by
The University of Delaware pursuant to License Agreement. No further reproductions authorized.

TABLE 5—*Prediction 4: Toxic hazard based on analytical assessment. (Fraction of Tolerance Dose Reached After 900 s.)*

Cable	Scenario 1	Scenario 2
A	0.30	0.18
B	0.15	0.10
C	0.26	0.14
D	0.35	0.14

Result: $B > C \overset{?}{>} A > D$ $B > C (= D) > A$.

TABLE 6—*Prediction of toxic hazard.*

	Tool	Predicted Order
Better Predictions ↓	1. Toxic potency	(C or B) > (A or D)
	2. Potency by weight	B > (D or A or C)
	3. "NIBS" test	B > (C or D) > A
	4. Analytical hazard assessment	Scenario 1: B > (A or C) > D Scenario 2: B > (C or D) > A

surements have definite limitations. Since the common toxicity tests (e.g., the NIST test [*12*] and the UPITT test [*15*]) decompose the sample with an external heat source, rather than allow it to burn on its own, one would expect such tests to predict hazard best for a severe fire, where any differences among products in ignitability and flame spread are overpowered by the intensity of the exposure fire. Put another way, if toxic potency is a valid measure of hazard, the numerical hazard assessment of the four cables in progressively larger fires would move the performance of Cables C and B closer together, as it would Cable A and Cable D.

One would not expect toxic potency alone to be the true indicator of hazard, however, simply because there are different amounts of each of the four cables in the room. This is addressed by Prediction 2, where toxic potency is corrected for the weight of the cables present. In sufficiently large fires, one would expect Prediction 2 to mirror the order of performance determined by hazard assessment.

Conversely, the IT_{50} measured by the NIBS test directly reflects the time required for ignition and smoke production. Even though the radiant exposure of the sample is relatively severe, it is not a factor until after the sample has been ignited. Hence, one would intuitively expect the NIBS test to be a better indicator of true performance under less severe fire conditions, and this perhaps is why it correctly predicts the order of performance in Scenario 2, which is a less severe fire exposure.

However well a single laboratory test by itself can foresee one set of fire conditions, it can *only* foresee that set. Hence, a hazard assessment, based on whatever fire conditions are envisioned for a particular use, remains the most reliable method of determining relative cable performance. This is true whether it be done by mathematical modelling and small-scale testing or by full-scale fire experiment. The other advantage of condition-based hazard assessment is that it provides an estimate of the *absolute* importance of a material's contribution to the overall fire. Here, for example, none of the cables showed smoke toxicity to be a significant contributor to immediate fire hazard in the scenarios examined, a fact which would not have been uncovered using any of the other techniques. This allows one to distinguish between scenarios where a detailed comparison of a product's smoke toxicity is useful and where such a comparison would have relatively little impact on product selection.

Copyright by ASTM Int'l (all rights reserved) Wed Feb 07 10:53:32 UTC 2024
Downloaded/printed by
The University of Delaware pursuant to License Agreement. No further reproductions authorized.

Acknowledgment

The cone calorimetry and LIFT measurements were done by the Fire Technology Center Polymer Products Department, E. I. du Pont de Nemours & Company, under the direction of Drs. Almut Breazeale and John Ryan. The smoke toxicity measurements were carried out at DuPont's Haskell Laboratory under the direction of Dr. Rudolph Valentine.

References

[*1*] Bukowski, R., "Toxic Hazard Evaluation of Plenum Cables," *Fire Technology,* Vol. 21, No. 4, 1986, p. 252.

[*2*] Clarke, F., Benjamin, I., and DiNenno, P., "Overall Fire Safety of Wire and Cable Materials," *Proceedings of the 32nd International Wire and Cable Symposium,* 1983, p. 390.

[*3*] Benjamin, I., "Toxic Hazard Analysis: Electrical Non-Metallic Tubing," *Journal Fire Science,* Vol. 5, No. 1, 1987, p. 25.

[*4*] Barauskas, V., "Development of the Cone Calorimeter—a Bench-scale Heat Release Apparatus Based on Oxygen Consumption," *Fire and Materials,* Vol. 8, 1984, p. 81.

[*5*] Tewarson, A., "Experimental Evaluation of Flammability Parameters of Polymeric Materials," Chap. 3, in *Flame Retardant Polymeric Materials,* Vol. 3, M. Lewin, S. M. Atlas, and E. M. Pearce, Eds., Plenum Press, New York, 1982, p. 97.

[*6*] Quintiere, J., "A Simplified Theory for Generalizing Results from a Radiant Panel Flame Spread Apparatus," *Fire and Materials,* Vol. 6, 1982, p. 52.

[*7*] Clarke, F. B., et al., "Full-Scale Fire Experiments on Cables with Fluoropolymer Insulation," abstract of presentation at NBS-CFR annual conference, preprint for combined meeting, *Combustion Institute/Eastern States Section, Chemical and Physical Processes in Combustion, 20th Fall Technical Meeting and NBS/Center for Fire Research,* annual conference on fire research, combined technical meeting, 2–5 Nov. 1987, Gaithersburg, MD.

[*8*] Emmons, H., "Prediction of Fire in Buildings," *17th Symposium on Combustion,* The Combustion Institute, Pittsburgh, PA, 1979, p. 1101.

[*9*] Mitler, H., "Documentation of CFC-V (The Harvard Fire Code)," NBS-GCR-87-344, National Bureau of Standards, Gaithersburg, MD, 1987.

[*10*] van Kuijk, H., "Modelling of Cable Fires," *Fire Safety Journal, in press.*

[*11*] "Full Scale Cable Fire Tests at U.S. Coast Guard Fire and Safety Detachment, Mobile, Alabama," 360/NRL Prob: 61-2296-0-5, Ser 6180-699, Naval Research Laboratory, Washington, DC, September 1985.

[*12*] Levin, B., et al., "Further Development of a Test Method for the Assessment of Acute Inhalation Toxicity of Combustion Products," NBSIR 87-2532, National Bureau of Standards, Gaithersburg, MD, June 1987.

[*13*] Packham, S. and Alexeeff, G., "Use of a Radiant Furnace to Evaluate Acute Toxicity of Smoke," *Journal Fire Science,* Vol. 2, 1984, p. 306.

[*14*] Roux, H., "The NIBS SMOTOX WG Program," *Proceedings of the 37th International Wire and Cable Symposium,* 1988, p. 543.

[*15*] Alarie, Y. and Anderson, R., "Toxicologic Classification of Thermal Decomposition Products of Synthetic and Natural Polymers," *Toxicology and Applied Pharmacology,* Vol. 57, 1981, p. 181.

Copyright by ASTM Int'l (all rights reserved) Wed Feb 07 10:53:32 UTC 2024
Downloaded/printed by
The University of Delaware pursuant to License Agreement. No further reproductions authorized.

James C. Norris[1]

Investigation of the Dual LC_{50} Values in Woods Using the University of Pittsburgh Combustion Toxicity Apparatus

REFERENCE: Norris, J. C., **"Investigation of the Dual LC_{50} Values in Woods Using the University of Pittsburgh Combustion Toxicity Apparatus,"** *Characterization and Toxicity of Smoke, ASTM STP 1082,* H. K. Hasegawa, Ed., American Society for Testing and Materials, Philadelphia, 1990, pp. 57–71.

ABSTRACT

Dual LC_{50} values for red oak (8 and 30 g) were observed in the combustion toxicity testing using the University of Pittsburgh combustion toxicity (UPITT) apparatus. No report of any material displaying a dual LC_{50} value had been made prior to now.

The National Forest Products Association became interested in knowing whether this was an anomaly of red oak or a property of other materials. A probative investigation was initiated to determine the existence and extensiveness of a dual LC_{50} value phenomenon using the UPITT apparatus. Since red oak was the first reported to have a dual LC_{50} value, other woods were selected for testing. White oak, southern pine, and Douglas fir were chosen.

Another objective of the investigation was to determine if there were analytical characteristics of thermal decomposition that would correlate with the LC_{50} values. Attempts to correlate the maximum concentrations and concentration x time (Ct) products of carbon monoxide, the ratio of carbon dioxide to carbon monoxide, and maximum ∂ temperature area with the LC_{50} values were made.

Three LC_{50} values were found for red oak (8.48, 15.0, 29.2 g) and southern pine (7.34, 12.39, 20.62 g), while one LC_{50} value was found for white oak (36.52 g) and Douglas fir (25.38 g). Maximum carbon monoxide concentrations reached a plateau and offered no correlation with the LC_{50} values. The Ct products of carbon monoxide did fluctuate but did not clearly correlate with the LC_{50} values. For red oak, ratios of carbon dioxide to carbon monoxide demonstrated a very good correlation with its LC_{50} values, but this was not so for the other woods. The maximum ∂ temperature area indicated that there was a continuous change in burning characteristics as the specimen weight increased, but it did not correlate with the LC_{50} values.

These data suggest that multiple LC_{50} values cannot be strictly related to nonflaming and flaming modes or char formation. Therefore, until an explanation for the multiple LC_{50} values is known, there remains the possibility that other products could also exhibit this phenomenon.

KEY WORDS: University of Pittsburgh toxicity test, dual LC_{50} values, multiple LC_{50} values, New York State toxicity legislation, red oak.

In 1986 the state of New York enacted legislation requiring the filing of LC_{50} values for building products sold in their state, and the LC_{50} values were to be obtained using the University of Pittsburgh combustion toxicity (UPITT) apparatus. During the extensive testing that ensued, it was discovered that red oak had the unusual property of two LC_{50} values, a property unreported for any other product previously tested. It was noted that the LC_{50} val-

[1] Toxicologist, Weyerhaeuser Co., Fire Technology Laboratory, P.O. Box 188, Technical Center, Lab B, Longview, WA 98632.

Copyright by ASTM Int'l (all rights reserved) Wed Feb 07 10:53:32 UTC 2024
Copyright © 1990 by ASTM International www.astm.org
Downloaded/printed by
The University of Delaware pursuant to License Agreement. No further reproductions authorized.

ues were contingent on the amount of red oak placed in the furnace; that is, masses of approximately 8 and 30 g each produced an LC_{50} value. This was assumed to be the result of different burning modes for the red oak in the furnace. The two suggested modes were nonflaming and flaming for 8 and 30 g, respectively.

The National Forest Products Association became interested in the anomaly as to whether it was, in fact, a unique property to red oak. Since the anomaly was first discovered in a wood product, it was a reasonable assumption that there should be an increased likelihood of discovering other wood products with dual LC_{50} values. Consequently, a study was initiated to investigate the existence of dual LC_{50} values in other woods. Woods selected for testing were red oak, white oak, Douglas fir, and southern pine. There were some dissimilarities in anatomical and biochemical components between red and white oak's composition, possibly affecting their burning characteristics, but the overwhelming composition of the two woods was the same. Consequently, white oak was tested to determine if the phenomenon could be related to these differences, such as permeability and extractives. Douglas fir was tested because of its previous involvement in combustion toxicity testing and its use as dimensional lumber. Southern pine was also tested because of its use as dimensional lumber.

Method

The UPITT apparatus consisted of a Lindberg furnace (Pittsburgh, Pennsylvania) connected to an animal exposure chamber. Within the furnace was a weight load cell upon which the specimen was placed. There was an airflow of 11 L/min proceeding from the furnace toward the animal exposure chamber. That airflow was mixed, cooled, and diluted with 9 L/min of cold air (~15°C) before being presented to the animals. The furnace temperature was ramped 20°C/min. The furnace, however, was not connected to the animals exposure chamber until the specimen had lost 1% of its weight as indicated by the weight load cell. The time at which this occurred was the beginning of the 30-min animal exposure. The animal exposure chamber simultaneously housed four male Swiss-Webster mice in a head-only exposure mode. The decomposition products passed to gas analyzers (carbon monoxide, carbon dioxide, and oxygen) after being presented to the animals. The apparatus and protocol were according to the methodology of Alarie [*1*].

Procedurally, a 10-g quantity of the material was placed in the furnace after which the ramping of the furnace started. At the 1% weight loss, the animal exposure chamber was connected to the furnace. After the 30-min exposure was completed, the animals were observed for an additional 10 min. Any deaths occurring during these 40 min were used in the determination of the LC_{50} value. If all the animals died with the 10 g, the next experiment would be with a lower weight. If no animals died, then a higher weight would be used in the next experiment.

That next weight would be determined by a geometric factor. The geometric factor was necessary because of the statistical procedure [*2*] used for determining the LC_{50} values. This factor (for example, 1.1) would be multiplied by the weight to determine the next higher weight, or the weight would be divided by the factor to determine the next lower weight. Using this statistical procedure, four consequent weights (spaced by the geometric factor along with the corresponding deaths as required by the tables supplied in the reference) were needed to determine an LC_{50} value.

A program was written for a Macintosh Plus computer in conjunction with a Fluke 2400A [analog/digital (A/D) and digital/analogue (D/A) measurement and control link] to specifically operate this apparatus. Ramping of the furnace was accomplished by the Macintosh monitoring the furnace temperature and varying the power supply to the furnace. The specimen weight, the percent of weight loss, concentrations of carbon monoxide (CO), carbon

Copyright by ASTM Int'l (all rights reserved) Wed Feb 07 10:53:32 UTC 2024
Downloaded/printed by
The University of Delaware pursuant to License Agreement. No further reproductions authorized.

dioxide (CO_2) and oxygen (O_2), time (from the initiation of ramping and from the 1% weight loss), temperatures of the furnace and chamber, and the difference between the actual and theoretical furnace temperatures were displayed on the computer monitor during the experiment as well as recorded on a diskette.

In order to confirm that there were no leaks in the system and that the pump, airflow, and flowmeters were operating properly, the flow rates of 9 and 20 L/min were tested prior to each test with a Mini-Buck calibrator (A.P. Buck, Inc., Orlando, Florida). This flow meter is traceable to the National Institute of Standards and Technology (formerly National Bureau of Standards).

The only modification to the procedure was that weights of the wood were tested above and below the initial 10-g quantity regardless of the results of that experiment. From a specimen weight of 5.79 g, the weight of the wood being tested was increased by the geometric factor of 1.1 up to 30 g.

Results

Values listed in Table 1 are some of those required in the report filed with New York State [*3*]. These values are from specimen weights which were $\pm 5\%$ of the LC_{50} value. The "% weight loss" was calculated from the difference in the initial weight and the weight measured at the end of the 30-min test period. CO and CO_2 values were the maximum concentrations (in ppm) recorded during the experiment, while the O_2 value was the minimum concentration (in percentage) noted.

From these data several observations were made. As the specimen weight increased there

TABLE 1—*LC_{50} values along with other values required by New York State legislation:*

Red Oak				
LC_{50} Value	%Wgt. Loss	Max. CO	Max. CO_2	Min. O_2
8.48	89.9	7041	5415	19.9
15.00	86.0	9112	36282	16.6
29.20	83.6	11339	58192	12.5

White Oak				
LC_{50} Value	%Wgt. Loss	Max. CO	Max. CO_2	Min. O_2
36.52	82.7	13158	76306	13.0

Douglas Fir				
LC_{50} Value	%Wgt. Loss	Max. CO	Max. CO_2	Min. O_2
25.38	87.2	11567	49500	20.9

Southern Pine				
LC_{50} Value	%Wgt. Loss	Max. CO	Max. CO_2	Min. O_2
7.34	89.9	5369	4527	19.9
12.39	88.6	11790	25364	16.9
20.62	84.6	11276	29662	16.1

Copyright by ASTM Int'l (all rights reserved) Wed Feb 07 10:53:32 UTC 2024
Downloaded/printed by
The University of Delaware pursuant to License Agreement. No further reproductions authorized.

TABLE 2—*LC_{50} values based on partial data along with other values required by New York State legislation:*

White Oak				
Est. LC_{50} Value	%Wgt. Loss	Max. CO	Max. CO_2	Min.O_2
9.00	82.0	9963	8588	19.2
15.00	87.9	12385	10548	18.8

Douglas Fir				
Est. LC_{50} Value	%Wgt. Loss	Max. CO	Max. CO_2	Min.O_2
7.00	80.3	6800	4951	19.9
15.00	84.6	9298	32797	16.2

was approximately 5% decrease in the total weight loss. The maximum CO concentrations were approximately the same for the second and third LC_{50} values. Consequently, additional CO concentrations should be acquired to understand this phenomenon. Also, the oxygen concentration decreased as the specimen weight increased, possibly affecting the response of the animals.

In Table 2 the LC_{50} values were estimates from specimen weights in which only partial data were obtained. By that I mean, at two consecutive specimen weights there were some deaths, but at the next specimen weights there were no deaths. In order to calculate an LC_{50} value there must be four consecutive specimen weights with the proper level of lethality. So these values were estimates based on the two or three specimen weights resulting in dead animals.

Figures 1 and 3 illustrate that as the specimen weight of red oak and southern pine were initially increased there was an elevation in the number of deaths, allowing an LC_{50} value determination. As the specimen weight continued to be increased, however, there was a reduction in animals deaths followed by an elevation in animal deaths. This sequence occurred again as the specimen weight was further increased. Consequently, three LC_{50} values for red oak and southern pine were determined.

In certain specimen weight ranges of Douglas fir and white oak, an interesting observation

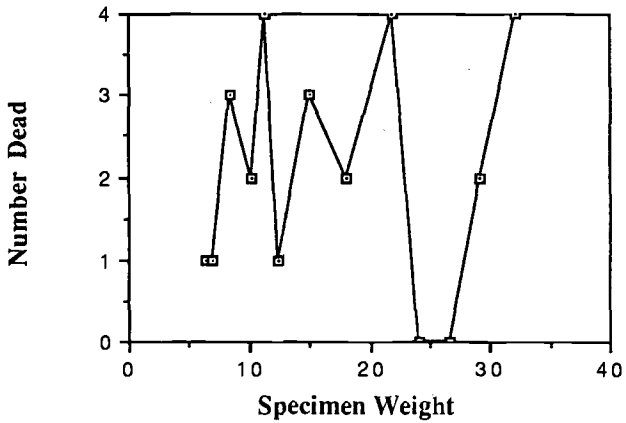

FIG. 1—*Red oak.*

Copyright by ASTM Int'l (all rights reserved) Wed Feb 07 10:53:32 UTC 2024
Downloaded/printed by
The University of Delaware pursuant to License Agreement. No further reproductions authorized.

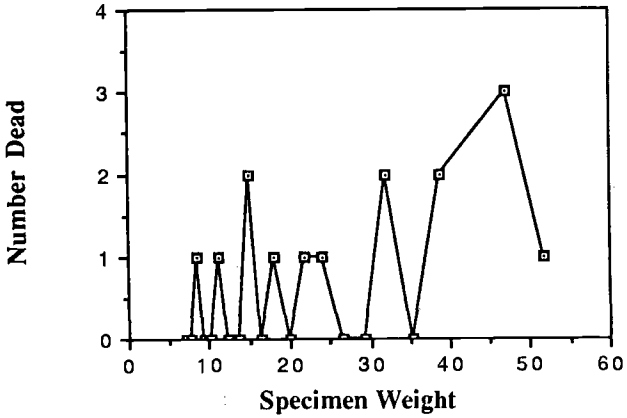

FIG. 2—*White oak.*

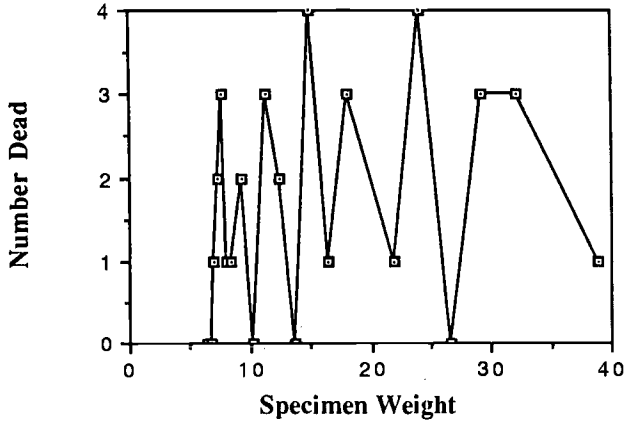

FIG. 3—*Southern pine.*

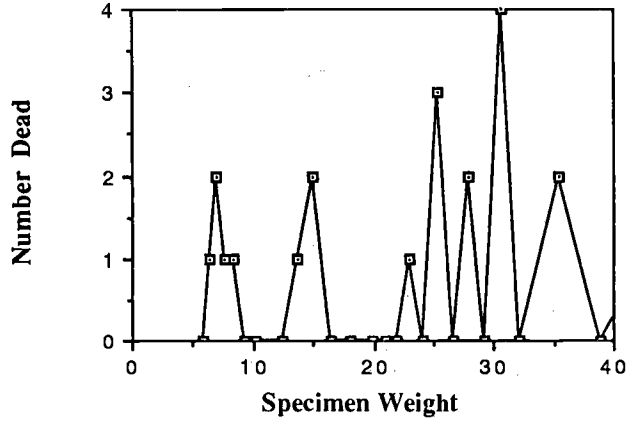

FIG. 4—*Douglas fir.*

Copyright by ASTM Int'l (all rights reserved) Wed Feb 07 10:53:32 UTC 2024
Downloaded/printed by
The University of Delaware pursuant to License Agreement. No further reproductions authorized.

was made (Figs. 2 and 4). There were specimen weights where one or two deaths were obtained, but at the next higher specimen weight no deaths were observed. This type of up/down phenomenon persisted for a given weight range, and then an LC_{50} value would be determined at the higher specimen weights. The weight range having the up/down phenomenon would not yield an LC_{50} value because the higher deaths were not obtained.

One explanation could be that the burning characteristics were changing as the weight increased. If these changes were such that there was less CO and more CO_2 released, the number of deaths would not increase. The specimen weight would have to be increased to compensate for the change in burning characteristics.

This could also explain why there was more than one LC_{50} value for red oak and southern pine. For those woods, however, the changes would not have occurred so rapidly, thus allowing the four consecutive specimen weights and corresponding deaths necessary for an LC_{50} value.

The next step was to examine the data for changes in the burning characteristics. Since the University of Pittsburgh protocol requires the reporting of the maximum CO concentra-

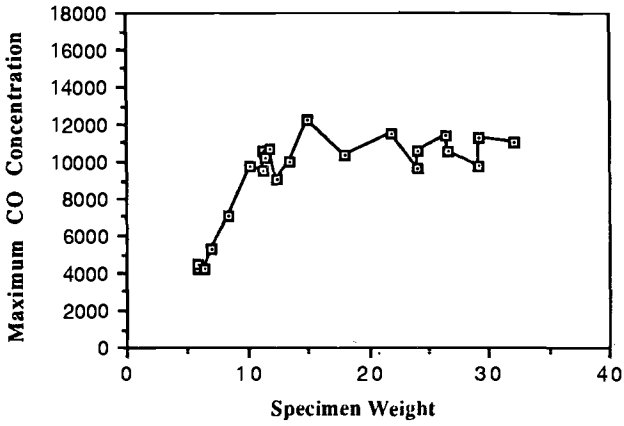

FIG. 5—*Red oak.*

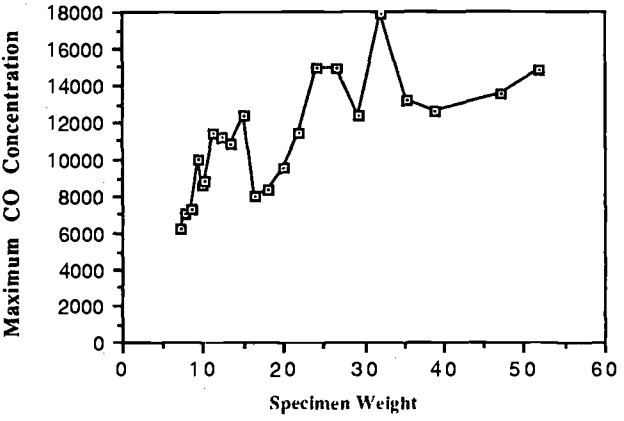

FIG. 6—*White oak.*

Copyright by ASTM Int'l (all rights reserved) Wed Feb 07 10:53:32 UTC 2024
Downloaded/printed by
The University of Delaware pursuant to License Agreement. No further reproductions authorized.

tion, that was the first consideration for review. The maximum CO concentration was plotted against the specimen weight (Figs. 5 to 8).

For red oak there was an increase in the maximum CO concentration, but after about 12 g it reached a plateau (Fig. 5). Consequently, the three LC_{50} values do not correspond with any peaks and valleys. There was some fluctuation in the values for southern pine's higher weight ranges; however, two LC_{50} values had already been found (Fig. 6). Therefore, there was no correlation with those values. White oak had apparently more fluctuation in the maximum CO concentration as the weight was increased (Fig. 7). But again, it was unrelated to the LC_{50} value. The values for Douglas fir also changed to some degree but not in accordance with the LC_{50} value (Fig. 8). Therefore, these results demonstrated there was no correlation between these concentrations and the LC_{50} values.

One aspect of comparing the maximum CO concentration with the specimen weights is that it does not account for the change in width of the peak. The peak width may change without necessarily altering the peak height. Consequently, the area under the curve (concentration multiplied by exposure time or Ct product) might be a better indicator of changes (Figs. 9 to 12).

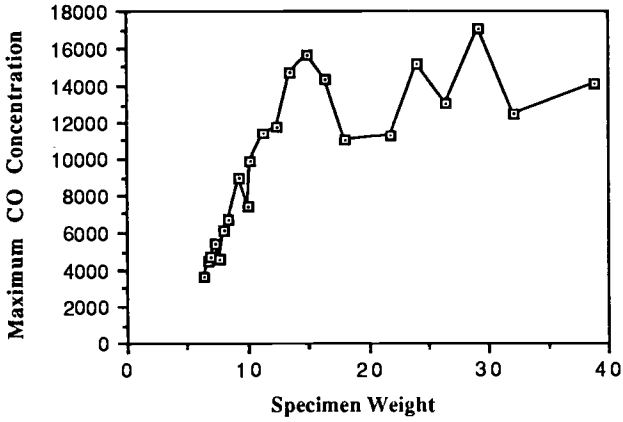

FIG. 7—*Southern pine.*

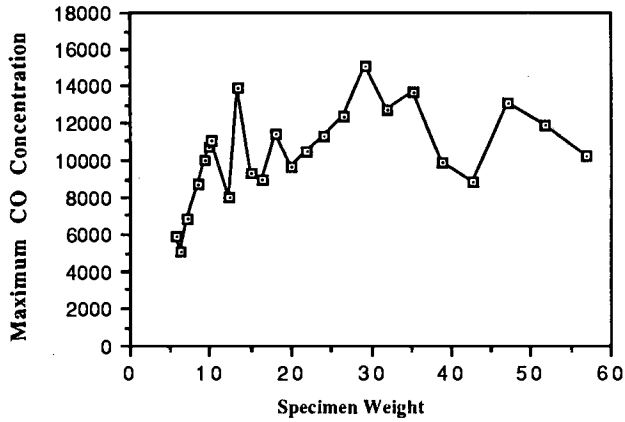

FIG. 8—*Douglas fir.*

Copyright by ASTM Int'l (all rights reserved) Wed Feb 07 10:53:32 UTC 2024
Downloaded/printed by
The University of Delaware pursuant to License Agreement. No further reproductions authorized.

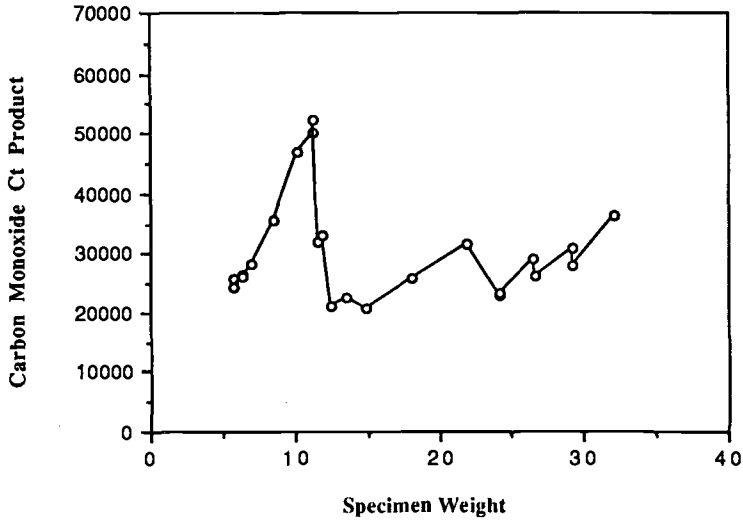

FIG. 9—*Red oak.*

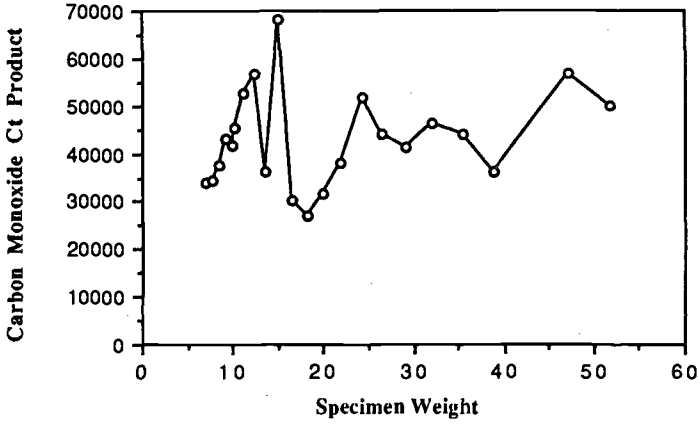

FIG. 10—*White oak.*

There was a fluctuation in the CO Ct products for red oak, but the three LC_{50} values do not correspond exactly with any peaks and valleys. Southern pine, white oak, and Douglas fir also displayed fluctuations in the values, but there were no correlations (Figs. 9 to 12).

The CO Ct products did have a greater degree of correlation than with maximum CO values, particularly with red oak; however, it does not clearly correlate with the LC_{50} values. These values appear to be more indicative of changes in the burning characteristics than the maximum CO concentration.

Another parameter which would demonstrate any changes in the burning characteristics is the CO_2/CO ratio. Since the Ct product, the area under the curve, was a more definitive value for the yield of the gases, the ratio was calculated from the Ct products of CO_2 and CO (Figs. 13 to 16).

Copyright by ASTM Int'l (all rights reserved) Wed Feb 07 10:53:32 UTC 2024
Downloaded/printed by
The University of Delaware pursuant to License Agreement. No further reproductions authorized.

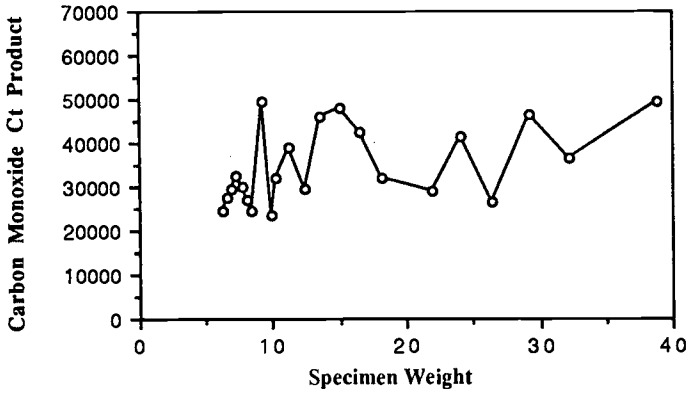

FIG. 11—*Southern pine.*

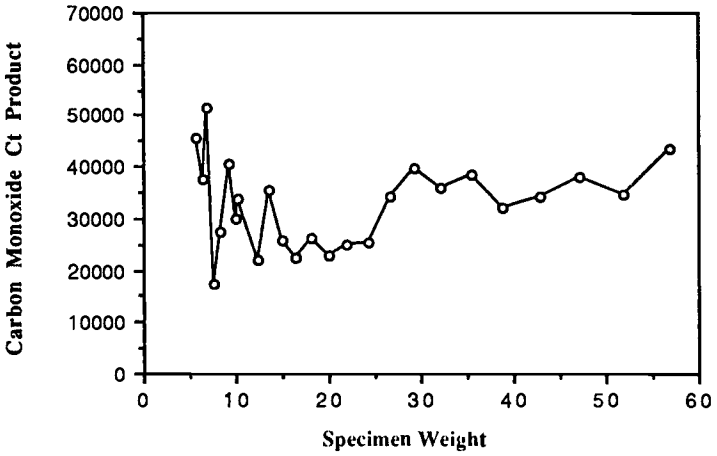

FIG. 12—*Douglas fir.*

There was a very good correlation with the three red oak LC_{50} values and the CO_2/CO ratios (Fig. 13). The other woods were not so dramatic in their correlation. The ratios did increase as the specimen weights increased, but without the plateaus associated with the LC_{50} values (Figs. 14 to 16). Douglas fir ratios did, however, fluctuate in the lower weight range, coinciding with the fluctuation of deaths in the same weight range.

From these data it appeared there were changes occurring as the specimen weight increased. The heavier the specimen the larger the amount of CO_2 released in relationship to the CO. These data then underscored the fact that the burning characteristics were changing as the specimen weight increased, but they did not answer why this was so.

One observation made was that the extent of flaming seemed to be different as the specimen weight increased. In order to determine if this were a factor in the changing CO_2/CO ratio and the multiple LC_{50} values, the extent of flaming was measured. Deviation from the programmed furnace temperature was used as the indication of flaming, i.e., the larger the deviation the larger the degree of flaming. The area of this deviation was labelled "maximum ∂ temperature area."

Copyright by ASTM Int'l (all rights reserved) Wed Feb 07 10:53:32 UTC 2024
Downloaded/printed by
The University of Delaware pursuant to License Agreement. No further reproductions authorized.

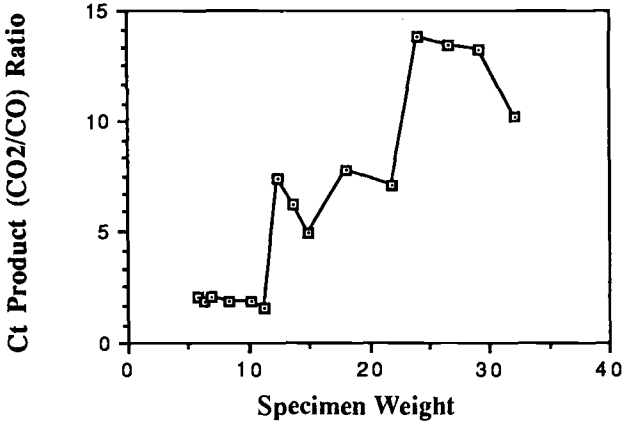

FIG. 13—*Red oak.*

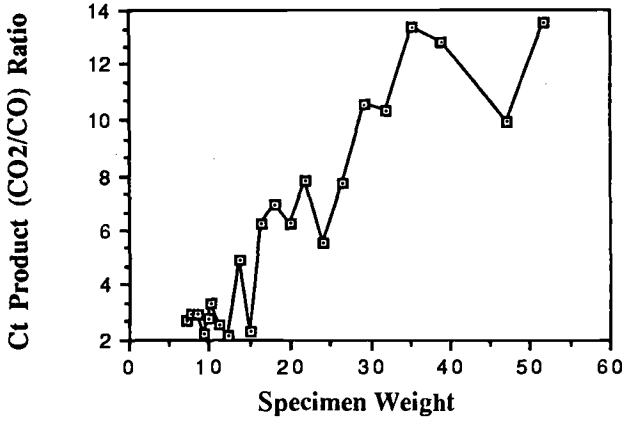

FIG. 14—*White oak.*

The "maximum ∂ temperature area" incorporated the area between the programmed and actual furnace temperature from the time at which the temperature began departing from the programmed temperature to the time at which it returned to the programmed temperature. Any deviation after that point was not incorporated into the area. The area after that point was considered a mixture of attempts by the computer to control the furnace temperature and specimen flaming, consequently not a true deviation of the furnace temperature due to the influence of the specimen.

Figures 17 to 20 illustrate the data from these analyses. These demonstrate that there was a continual change in the flaming as the specimen weight increased, but there was no correlation with the various LC_{50} values.

Conclusions

Results in Table 1 demonstrate that there were not just two but three LC_{50} values for red oak as well as for southern pine. Thus, the phenomenon of a dual LC_{50} value is not an anom-

Copyright by ASTM Int'l (all rights reserved) Wed Feb 07 10:53:32 UTC 2024
Downloaded/printed by
The University of Delaware pursuant to License Agreement. No further reproductions authorized.

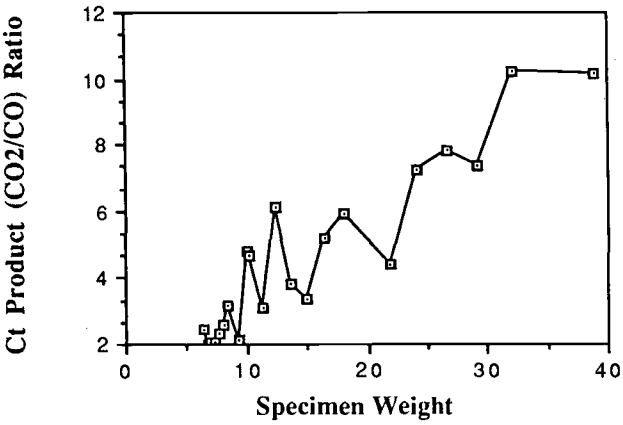

FIG. 15—*Southern pine.*

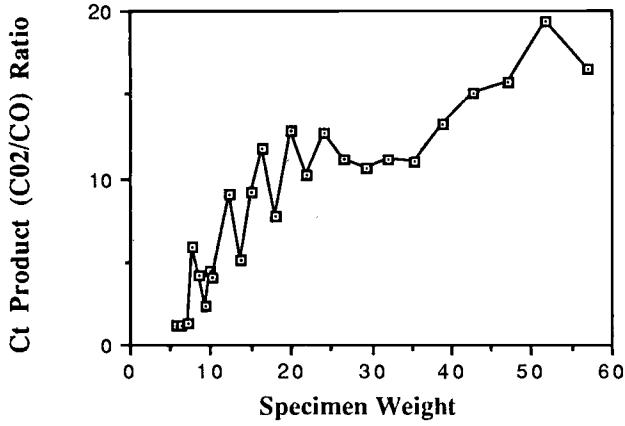

FIG. 16—*Douglas fir.*

aly restricted to red oak, nor is it restricted to only two LC_{50} values. White oak and Douglas fir were found to have one confirmed LC_{50} value. However, these woods (Table 2) had two other weight ranges in which only two or three consecutive specimen weights resulted in deaths. This could mean that two additional LC_{50} values might exist for white oak and Douglas fir.

These results demonstrate that the phenomenon of a dual LC_{50} value is more complex than previously thought. When there was only a dual LC_{50} anomaly for red oak, there was one theory that the mode of burning was producing the different values. This resulted from observations that the furnace temperature did not deviate from the programmed temperature with the smaller specimens but did with the larger ones. Deviation from the programmed temperature was assumed to be the result of the specimen flaming. Thus, the dual LC_{50} values were associated with an apparent nonflaming and flaming specimen. This would mean that, with the smaller specimen and nonflaming mode, more CO would be generated per unit mass of specimen. In the apparent flaming mode, the specimen would burn producing less CO per unit mass, requiring a larger weight to generate lethal CO concentrations.

Copyright by ASTM Int'l (all rights reserved) Wed Feb 07 10:53:32 UTC 2024
Downloaded/printed by
The University of Delaware pursuant to License Agreement. No further reproductions authorized.

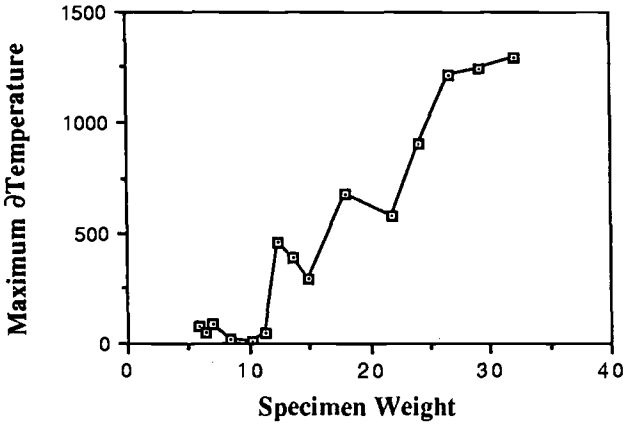

FIG. 17—*Red oak.*

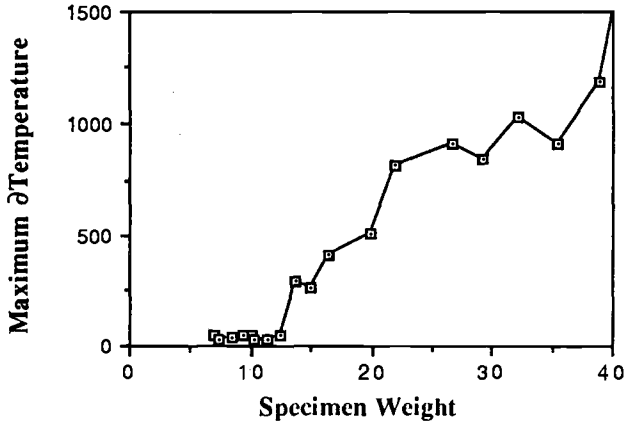

FIG. 18—*White oak.*

The nonflaming and flaming modes provided one hypothesis as long as there were only two LC_{50} values. Three LC_{50} values for red oak and southern pine and only one for Douglas fir and white oak prevented the acceptance of that theory, at least without some revision.

Refinement of that theory required more data concerning the burning characteristics of these woods. One parameter indicative of the burning characteristics was the CO_2/CO ratio. Values used in these calculations were the area under the curve so as to represent the total quantity of gases generated.

Plots of the CO_2/CO ratios revealed that the burning characteristics did change as the specimen weight increased. In fact, the red oak data displayed a very good correlation with its LC_{50} values. Correlations with the other woods were not so impressive, except that the ratio did continue to change as the specimen's weight increased.

One possible explanation for the continually changing CO_2/CO ratios was that different degrees of flaming were generated depending on the specimen's weight. If the flaming were more intensive at higher specimen's weights, resulting in different burning characteristics, then the three LC_{50} values for red oak and southern pine could be explained to be the result

Copyright by ASTM Int'l (all rights reserved) Wed Feb 07 10:53:32 UTC 2024
Downloaded/printed by
The University of Delaware pursuant to License Agreement. No further reproductions authorized.

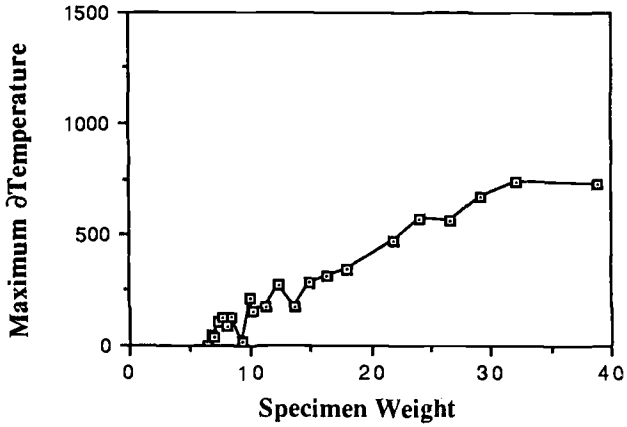

FIG. 19—*Southern pine.*

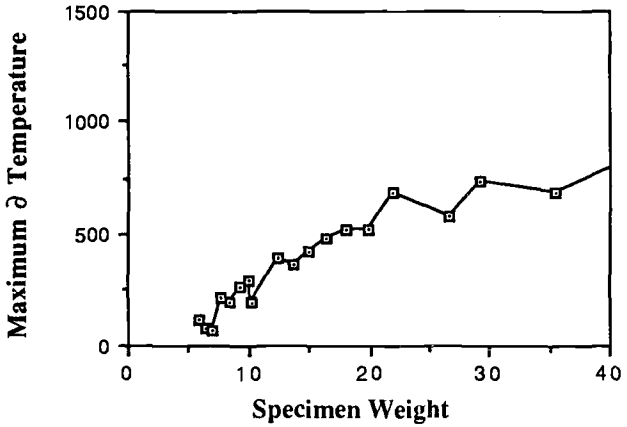

FIG. 20—*Douglas fir.*

of a nonflaming and two flaming modes. That, however, would not explain the singular LC_{50} values for Douglas fir and white oak.

The maximum ∂ temperature area was the parameter monitored for the degree of flaming. As before with red oak, there was some degree of correlation, albeit not as good as with the CO_2/CO ratio. The other woods displayed no correlation with their LC_{50} values. The maximum ∂ temperature area did, however, continue to increase with the increased specimen weight.

While there was no overriding correlation for all the woods between their LC_{50} values and CO_2/CO ratios or the maximum ∂ temperature areas, there were data supporting the premise that a change in the burning characteristics as the specimen weight increased was occurring. The changing maximum ∂ temperature area could explain why the CO_2/CO ratio increased along with the specimen weight.

The poor correlation of LC_{50} values between the above parameters could be explained, in part, by the presence of other toxicants. A general class of chemicals known to be present in wood smoke is aldehydes [*4*]. Acrolein is one specific aldehyde identified in wood smoke and

Copyright by ASTM Int'l (all rights reserved) Wed Feb 07 10:53:32 UTC 2024
Downloaded/printed by
The University of Delaware pursuant to License Agreement. No further reproductions authorized.

has been investigated for its toxicological properties [5]. However, acrolein and aldehydes are usually associated with postexposure deaths of 1 h to three days later. Since these post-exposure deaths would occur after the 10-min-observation period, their involvement with these results are unlikely.

Implication that this phenomenon was related to char formers results from red oak, a char former, having multiple LC_{50} values. That implication, however, was not substantiated. These data demonstrated that not all the woods tested had multiple LC_{50} values, even though all the woods were char formers.

The following list summarizes the conclusions that can be drawn from this study:

1. Red oak was not the only wood that has more than one LC_{50} value.
2. Red oak and southern pine had three LC_{50} values.
3. White oak and Douglas fir had one LC_{50} value, but may have had more than one.
4. No correlation between maximum carbon monoxide concentrations and the multiple LC_{50} values was found.
5. Maximum carbon monoxide concentrations did not suggest a change in burning characteristics as the specimen weight increased.
6. Correlations between CO Ct products and LC_{50} values and the ratio of Ct products of CO_2 and CO and LC_{50} values were better than the correlation between maximum carbon monoxide concentration and LC_{50} values.
7. The ratio of Ct products of CO_2 and CO indicated that there was a change in the burning characteristics as the specimen weight increased.
8. The maximum ∂ temperature area also indicated a change in the burning characteristics and could explain its occurrence.
9. These multiple LC_{50} values cannot be strictly related to nonflaming and flaming modes.

These data demonstrated that there was no correlation between the LC_{50} values and nonflaming or flaming modes and that not all the woods exhibited LC_{50} values. Therefore, the overall conclusion was that there is an increased probability of other products having multiple LC_{50} values.

Acknowledgment

Funding for this project was provided by the National Forest Products Association's Fire Research Program.

References

[1] Alarie, Y., "The Toxicity of Smoke from Polymeric Materials During Thermal Decomposition," *Annual Review of Pharmacology and Toxicology,* Vol. 25, 1985, pp. 325–347.
[2] Weil, C. S., "Tables for Convenient Calculation of Median-Effective Dose (LC_{50} or ED_{50}) And Instructions In Their Use," *Biometrics,* Vol. *8*, 1952, pp. 249–263.
[3] Article 15, Part 1120—New York State Fire Prevention and Building Code, New York Standards & Fire Information Network, Office of Fire Prevention and Control, Albany, NY.
[4] Ohlemiller, T. J., Kashiwagi, T., and Werner, K., "Products of Wood Gasification," NBSIR 85-3127, National Bureau of Standards, Washington, DC, April 1985.
[5] Kaplan, H. L., Grand, A. F., Switzer, W. G., Mitchell, D. S., Rogers, W. R., and Hartzell, G. E., "Effects of Combustion Gases on Escape Performance of the Baboon and the Rat," *Journal of Fire Sciences,* Vol. 3, 1985, pp. 228–244.

Copyright by ASTM Int'l (all rights reserved) Wed Feb 07 10:53:32 UTC 2024
Downloaded/printed by
The University of Delaware pursuant to License Agreement. No further reproductions authorized.

DISCUSSION

A. Tewarson[1] *(written discussion)*—When wood is heated, there are generally two regions of decomposition. We have reported two values for heat of gasification. The products there may be different, as the first stage is associated with noncharring and second with charring. Your results with variations in LC_{50} may be related to these differences.

J. C. Norris (author's closure)—There is evidence indicating the existence of different regions of thermal decomposition in woods. However, to link these regions with the multiple LC_{50} values will be difficult. That hypothesis stems from the generalization that all woods have these different regions of thermal decomposition; but of the woods reported, not all have the same number of LC_{50} values. That is not to say, however, that the different regions and their decomposition products do not contribute to the lethal environment in some way. Consequently, there is no simple correlation between the thermal regions and LC_{50} values.

[1] Factory Mutual Research Corp. 1151 Boston Providence Turnpike, Norwood, MA 02062.

Copyright by ASTM Int'l (all rights reserved) Wed Feb 07 10:53:32 UTC 2024
Copyright © 1990 by ASTM International www.astm.org
Downloaded/printed by
The University of Delaware pursuant to License Agreement. No further reproductions authorized.

Smoke Chemistry

Copyright by ASTM Int'l (all rights reserved) Wed Feb 07 10:53:32 UTC 2024
Downloaded/printed by
The University of Delaware pursuant to License Agreement. No further reproductions authorized.

John D. Ryan,[1] *Vytenis Babrauskas,*[2] *Thomas J. O'Neill,*[3] *and Marcelo M. Hirschler*[4]

Performance Testing for the Corrosivity of Smoke

REFERENCE: Ryan, J. D., Babrauskas, V., O'Neill, T. J., and Hirschler, M. M., **"Performance Testing for the Corrosivity of Smoke,"** *Characterization and Toxicity of Smoke, ASTM STP 1082,* H. K. Hasegawa, Ed., American Society for Testing and Materials, Philadelphia, 1990, pp. 75–88.

ABSTRACT: The corrosivity of combustion products has arisen as an issue for both product manufacturers and standards bodies. While many industries can have concerns in this area, electronic communications and control equipment are especially vulnerable to the problem. The best way to manage the smoke corrosivity issue is to avoid a fire. In the event a fire does occur, a number of actions must be taken. An important consideration is that the materials and products used should have been chosen with due consideration of their corrosion-causing potential. To do this requires a suitable corrosivity test.

It has traditionally been assumed that smoke corrosivity is directly correlated to the emission of acid gases. The results of recent experiments have shown that materials which do not release acid gases can, nevertheless, cause corrosion of metal surfaces, as determined by metal loss. In addition, for electrical equipment there are two other types of related nonthermal damage from combustion products which must be considered, viz., ohmic bridging and degradation of contacts.

Laboratory tests proposed to date to measure the corrosive effects of combustion products all have significant deficiencies: some methods are not performance-based at all and are merely tests for pH. In others, unrealistic specimen heating or unrealistic exposure targets are used. To facilitate the development of a better test, a series of criteria have been developed. A specific test method was evolved from these criteria. The method is performance-based and incorporates realistic fire heating conditions.

KEY WORDS: Smoke corrosivity, fire testing, corrosion of electronic equipment, smoke, cone corrosimeter, fire effects, acid gases, corrosion, testing

Concern about corrosion-related effects is becoming pronounced in mission-critical areas, especially those dependent on communications and control equipment. The concern has arisen since fire incidents have been reported where corrosion damage significantly exceeded thermal fire damage. This paper addresses the emergence of the corrosion issue and attempts to formulate an appropriate response. The present study documents some of the initial steps being taken; thus, it should be seen as exploratory in nature, with considerable use of anecdotal evidence. In addition to defining the overall problem and the possible strategies for attack, an outline will be given of a proposed test developed by an interorganizational working group that appears to meet a series of acceptability criteria.

[1] E. I. Du Pont de Nemours, Wilmington, DE 19898.
[2] National Institute of Standards and Technology, Gaithersburg, MD 20899.
[3] E. I. Du Pont de Nemours, Hemel Hempstead, United Kingdom.
[4] B. F. Goodrich, Avon Lake, OH 44012.

Copyright by ASTM Int'l (all rights reserved) Wed Feb 07 10:53:32 UTC 2024
Copyright © 1990 by ASTM International www.astm.org
Downloaded/printed by
The University of Delaware pursuant to License Agreement. No further reproductions authorized.

An international conference sponsored by the American Society for Testing and Materials (ASTM), the British Standards Institution (BSI), the International Electrotechnical Commission (IEC), and the International Organization for Standardization (ISO) on "Corrosive Effects of Combustion Products" was held in London (UK) in October 1987 to investigate the issue of smoke corrosivity in all its aspects [*1*]. That conference signified a landmark in the understanding of smoke corrosivity, particularly since the issue had not been addressed by an international forum since a much earlier (1969) Stockholm conference [*2*]. A few of the presentations will be discussed here. Some concerns developed in that conference serve as a suitable starting point. One statement from that conference is worth highlighting: "Fire is destructive and dangerous!!" (A. Morris, Fire Research Station, UK [*3*]). This simple truth emphasizes the context of our concerns—danger to life (primarily from toxic effects) and destruction to property (primarily from thermal effects) must always be anticipated from fires. Corrosion damage will generally be a secondary concern *if* proper precautions have been taken to avoid unanticipated corrosion losses.

Recently Di Nenno [*4*] surveyed the literature to determine the scope of both the problem and its available solutions. His study suggests there is still no clear understanding of the magnitude of smoke corrosivity problems, at least in the United States. There is some evidence of problems caused by postfire corrosion following the decomposition of highly halogenated products. Although laboratory studies show that halogenated acids can cause corrosion, the economic evidence of such effects is as yet largely anecdotal and qualitative.

The interest in Europe in proposing solutions to the smoke corrosivity problem has been, to date, more crystallized than in the United States. The issue seems to have been raised early by an article published in a German insurance magazine in April 1968 [*5*]. This was followed, much later, by misinformation resulting from the well-publicized ship fires in the Falklands campaign in 1982 [*6*]. It is interesting to recount an example of the misinformation following the Falklands campaign. The smoke seen coming from the burning HMS Sheffield was originally attributed to halogenated cables. It was discovered later, however, that <4% of the cables present on board were PVC-based, and that the smoke was mainly due to the burning of the unspent rocket fuel, diesel fuel, and even cooking oil, since the missile had made impact near the galley [*7,8*].

The question of corrosive damage provoked by chemical attack on structures and equipment in contact with fire effluents is one at the center of many developments and much discussion. This issue was also addressed at the London conference by P. Eulenburg (Chief, Essen Fire Brigade, West Germany [*9*]): "Measures to increase efficiency of fire fighting will not be completely successful in minimizing damage caused by corrosive products. The optimal approach involves better measures of fire prevention!" He added: "The volume of corrosive combustion products generated is dependent on chemical structure, as well as the quantity and surface geometry of the used or stored plastic materials." Thus, "If the quantity of generated corrosive combustion products is to be minimized, this can only be done by reducing stored or manufactured quantities."

Common sense prescriptions, such as by Chief Eulenburg, have a very valid role. More drastically, in some cases the short-term response to the corrosion issue has been to eliminate, or at least limit, the use of poly(vinyl chloride) and other halogenated materials on the assumption that halogenated products are the only ones responsible for the amount and corrosive nature of smoke. Alternatively, this has taken the form of test requirements on acidity of combustion products, which have been included in some specifications in a misguided effort to reduce the hazard to critical equipment. Such responses to the smoke corrosivity issue have been described as "quick and not necessarily wise" (H. L. Malhotra, UK, Chairman, International Organization for Standardization Advisory Committee on Fire Testing [*10*]). The problem is, of course, that such simple solutions are not founded on a compre-

Copyright by ASTM Int'l (all rights reserved) Wed Feb 07 10:53:32 UTC 2024
Downloaded/printed by
The University of Delaware pursuant to License Agreement. No further reproductions authorized.

hensive, economic problem analysis, nor do they offer any incentive for optimizing the performance of materials or products.

The objective of minimizing fire hazard to personnel and to equipment resulting from the involvement of combustibles in fire is universally supported. This is generally understood to be achieved with "low fire hazard products." It is the means of measuring or specifying the fire performance requirements for such products which is a source of controversy. To consider these means in their proper context, it is necessary to elaborate on the fire hazard assessment process. Corrosive smoke products will be seen to have an integral role in this analysis process.

Fire Hazard Assessment

The question that has to be answered is one of performance: What is the extent to which smoke from a material or product will cause corrosion in the event of a fire under appropriate conditions of use? The question is best answered by a systematic fire hazard assessment procedure.

The fire hazard assessment process has the following main steps:

1. Define the problem, the performance expected, and the acceptable limits.
2. Define the fire scenario(s).
3. Model the fire resulting from the chosen scenario.
4. Determine the contribution of the product being evaluated to fire.
5. Accept or reject the product.

Step 4 requires that performance data be available for the product; this, in turn, requires a valid test method.

The decision tree in Figure 1 illustrates this process. This decision tree takes into account the fire properties of the product of interest as well as the amount of smoke produced and

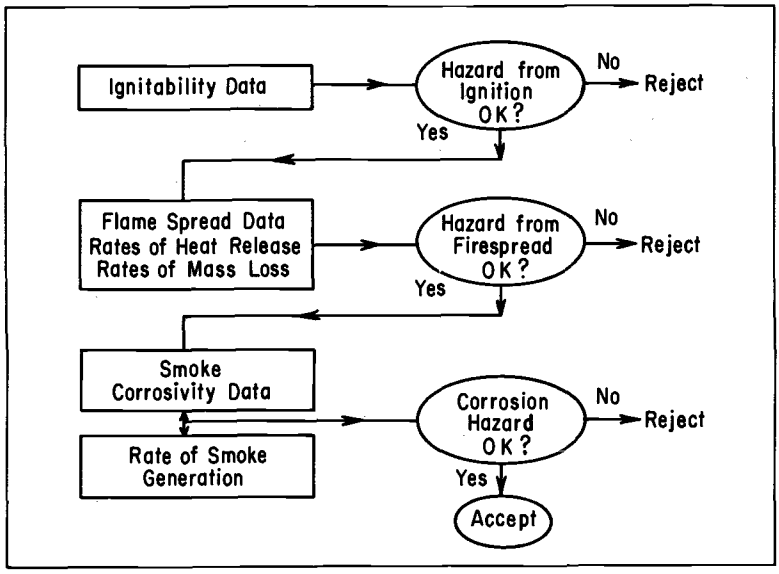

FIG. 1—*Decision tree approach to smoke corrosivity hazard assessment.*

Copyright by ASTM Int'l (all rights reserved) Wed Feb 07 10:53:32 UTC 2024
Downloaded/printed by
The University of Delaware pursuant to License Agreement. No further reproductions authorized.

its corrosive nature. Judgments must be made based on the scenario(s) of use for the acceptance criteria in each case.

Our major concern in this paper is with the necessary test methods. The hazard due to corrosion cannot be taken out of context, however. Corrosivity and fire size are, perforce, related. It has now become clear that the single property which most clearly defines the magnitude of a fire is the maximum rate of heat release [*11,12*]. This property governs not only the burning rate (and mass loss rate) of the product being evaluated but also the amount of surrounding items which will be burnt. The rate of heat release will also therefore govern the overall amount of smoke and combustion products being generated in the fire, since other products will be ignited only if sufficient heat reaches them rapidly. Similarly, ignitability and other properties shown in Fig. 1 must also be correctly tested before the assessment can be completed.

A more generalized smoke corrosivity decision tree has also been developed by the ASTM Task Group on Smoke Corrosivity, E5.21 TG70, under the chairmanship of H. J. Roux [*13*] (Figure 2). It takes into account not only the production of corrosive smoke (CS) but also the management of the corrosive smoke generated. For instance, measures can be taken to stem, if not stop, the corrosion reactions after a fire [*14*]. This option of decontamination and restoring to service equipment which has been exposed to corrosive smoke is not yet widely appreciated. Costs for such restoring to service may range from 3 to 15% of the value of the equipment, which can make it attractive compared to systematic replacement. This paper will not dwell on details of this management process, but simply note that using such a decision tree will materially assist in comprehensive planning efforts.

Damage from Corrosion and Related Effects

Nonthermal damage from a fire can occur to both the structure of a building and to any commodity located within it. For some areas, however, the potential effects of such damage

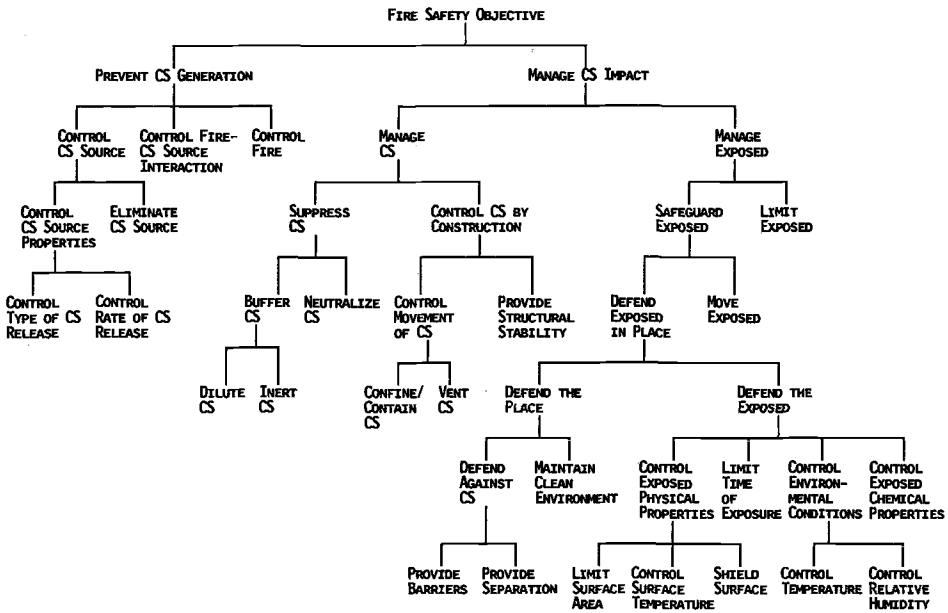

FIG. 2—*Draft smoke corrosivity tree.*

Copyright by ASTM Int'l (all rights reserved) Wed Feb 07 10:53:32 UTC 2024
Downloaded/printed by
The University of Delaware pursuant to License Agreement. No further reproductions authorized.

are likely to be especially significant. These include communications and control equipment, computers, and other electronic devices. For this reason, the scope of this paper will be restricted to considering damage to electrical and electronic equipment.

For electronic equipment, three types of nonthermal damage to a target from corrosion and related effects are identified: (*a*) increased circuit resistance due to a loss of metal (the process traditionally described as corrosion); (*b*) ohmic bridging between portions of a circuit not intended to have a conductive path; and (*c*) the degradation of electrical contacts. Ohmic bridging occurs when conductive aerosols are deposited on an electrical device and lower the resistance between different points of the circuit. Contacts degradation can occur through chemical action or mechanical intrusion, but, in either case, result in increased contacts resistance, failure to close entirely, or else erratic operation.

Traditionally it has been assumed that smoke corrosivity is due solely to the action of the acid gases emitted. The results of some recent corrosion studies [*15*], using the materials listed in Table 1, have clearly shown that materials which do not release acid gases can, nevertheless, cause corrosion of metal surfaces, as determined by loss of metal. These studies were carried out by exposing the samples in a 500-dm^3 chamber (NBS smoke chamber, lined with polytetrafluoroethylene (PTFE). The combustion device was an external quartz beaker, set to a temperature of 600°C. The combustor did not heat the atmosphere of the chamber to a significant extent. In these studies, steel and copper surfaces were exposed at very high temperature (600°C) and at freezing water temperature. The surfaces were thoroughly cleaned prior to exposure to eliminate any residual oil or dirt, and some were coated with a thin protective layer of oil. After exposure, all surfaces were kept for 28 days before analysis.

The three halogenated materials were the only ones that emitted combustion gases of any significant acidity (Fig. 3). In fact, the nitrogen-containing materials emitted an alkaline mixture of combustion products. This would suggest that, according to the acid gas emission tests proposed to measure corrosion, only the three chlorinated materials should yield corrosive combustion products and that the nitrogen materials might even be corrosion inhibitors.

The results of the experiments indicated, however, that each of the smokes caused metal loss for steel and for copper. At room temperature, there was somewhat more corrosion of steel (Fig. 4) due to the chlorinated materials than due to the others, but there was no correlation between this effect and the hydrogen chloride (HCl) concentration. Indeed, the results show that a ten-fold increase in maximum HCl concentration produced no significant difference in metal loss for the steel coupons exposed.

Corrosion was minimized if the steel surfaces were treated one day after exposure to clean

TABLE 1—*Materials used in the study.*

Designation	Description
NPR	Commercial polychloroprene (Neoprene W)
PVC WR	Standard (noncommercial) poly(vinyl chloride) wire and cable formulation
PVC LH	Low-halogen (noncommercial) poly(vinyl chloride) wire and cable compound
DFIR	Douglas fir wood
PE	Polyethylene wire and cable nonhalogen flame retardant commercial compound (Union Carbide DEQD-1388, black)
PS	Commercial polystyrene pellets (Dow Styron 6069)
WOOL	Unbleached unwoven wool fibers (sample used previously for smoke toxicity testing)
NYLON	Commercial nylon pellets (Du Pont Zytel 103 HSL)
NONE	No combustible material

Copyright by ASTM Int'l (all rights reserved) Wed Feb 07 10:53:32 UTC 2024
Downloaded/printed by
The University of Delaware pursuant to License Agreement. No further reproductions authorized.

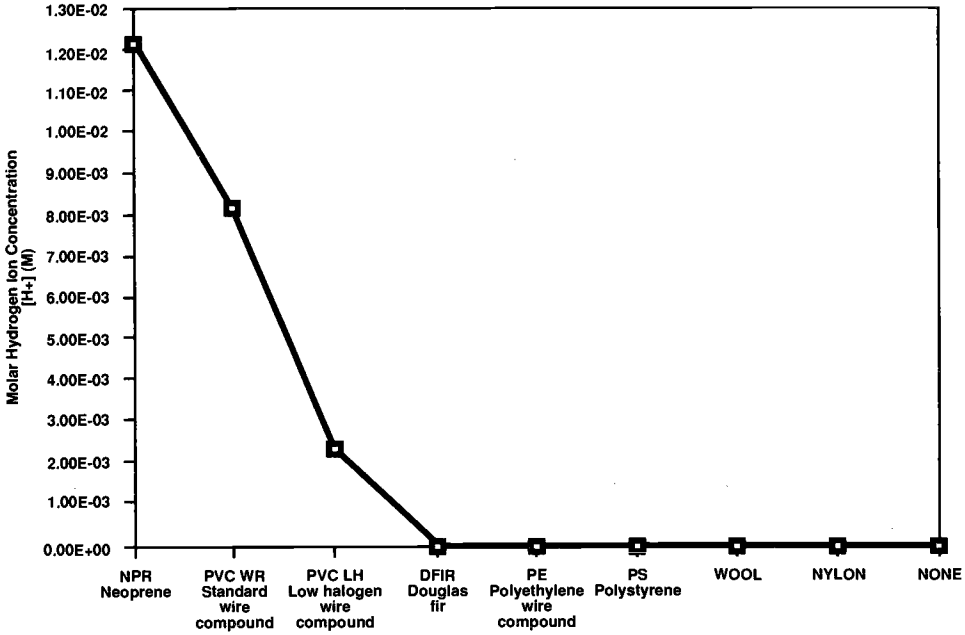

FIG. 3—*Results of acid gas emission testing.*

off the combustion debris. Similarly, having a preoiled surface considerably decreased the corrosion due to acid gases.

Some steel surfaces were also exposed at very high temperatures (600°C). Under this condition all the smokes caused about the same amount of corrosion, within experimental error, and the level was essentially no different from that caused by exposures to a hot humid atmosphere containing no combustion products at all (Fig. 5).

The copper surfaces exposed to smoke were copper mirrors. The electrical resistance of the copper mirror was measured before and after exposure. All smokes caused the resistance of the copper surfaces to increase to almost infinity, indicating sufficient corrosive removal of the metal to break the circuit continuity. Since it was impossible to differentiate among the various smokes in this way, the amount of copper lost from the surface was then determined. The results indicate that the copper surfaces, in the warm environment, were most sensitive to the nitrogen-containing compounds; smoke from burning nylon caused nearly twice as much metal loss as the other products as measured by weight loss (Table 2).

The metal-loss corrosion issue is somewhat complicated, as is obvious from Fig. 6, which shows different ways of looking at corrosion from the smoke of materials: (*A*) acid gas emission; (*B*) corrosion of copper mirrors; (*C*) average corrosion of steel coupons; and (*D*) corrosion of steel coupons in warm experiments. Clearly, both halogenated products and those not containing halogen are causing corrosion of steel and of copper, and the levels of corrosion are not significantly different, depending on the fire scenario. The most important conclusions of these studies was that all the fire smokes were corrosive.

The corrosivity of water-soluble acid gases is particularly enhanced by the forced condensation of smoke when the target surfaces are exposed at a temperature well below that of the rest of the room. This was shown by the experiments in which samples were cooled to freezing water temperatures.

Copyright by ASTM Int'l (all rights reserved) Wed Feb 07 10:53:32 UTC 2024
Downloaded/printed by
The University of Delaware pursuant to License Agreement. No further reproductions authorized.

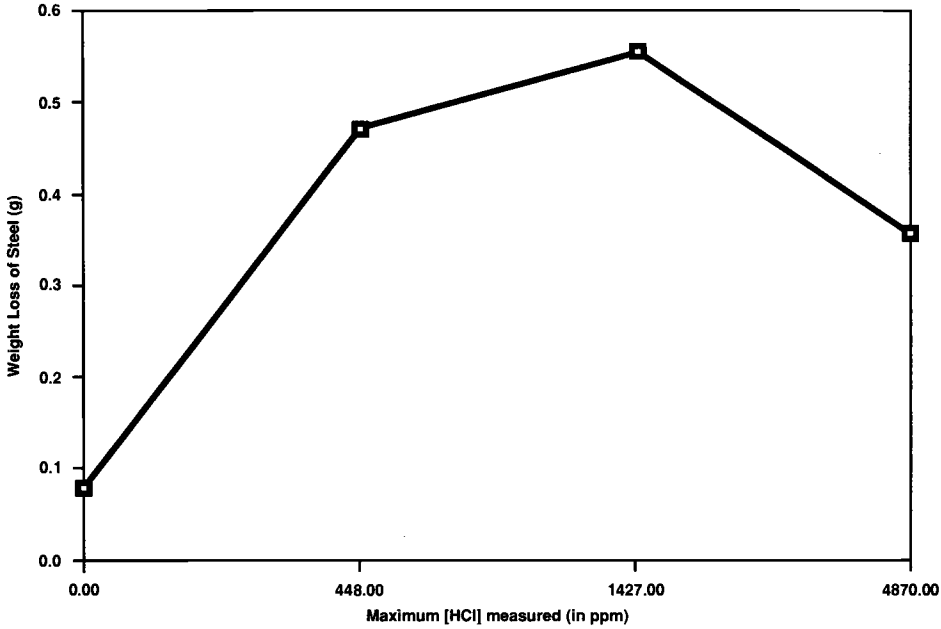

FIG. 4—*Corrosion of steel coupons (room temperature).*

In summary, these exploratory studies served to indicate that, under the conditions of high temperature and high humidity which prevail in fires, many combustion products can be corrosive, regardless of whether they do or do not contain halogens, nitrogen, phosphorus, or other specific atoms.

Test Development

The studies above showed that corrosion damage will depend on many factors which cannot be assessed simply by using a laboratory test for halogen content or effluent acidity.

In order to determine the hazard associated with corrosion damage and to place the risk in proper engineering perspective, there is a need for the development of test procedures and assessment scenarios which take into account the factors, including cost, which determine the optimum preventive measures or posttreatment measures in any given situation.

It is being recognized by many authorities, including the ISO and the IEC, that a problem of this complexity can be resolved only if test procedures are evolved which reflect the expected end-use conditions of the materials or systems involved.

The Association of Plastics Manufacturers (APME) in Europe has issued a statement in support of the adoption of standards and test methods that seek to secure optimal safety and functional performance of plastics in defined fire hazard situations. The position of APME can be summarized as follows:

1. Standards should be based on performance and not on the chemical composition of materials.
2. Performance should be assessed with appropriate test methods which relate to the hazard and which are pertinent to the intended use of the material.

Copyright by ASTM Int'l (all rights reserved) Wed Feb 07 10:53:32 UTC 2024
Downloaded/printed by
The University of Delaware pursuant to License Agreement. No further reproductions authorized.

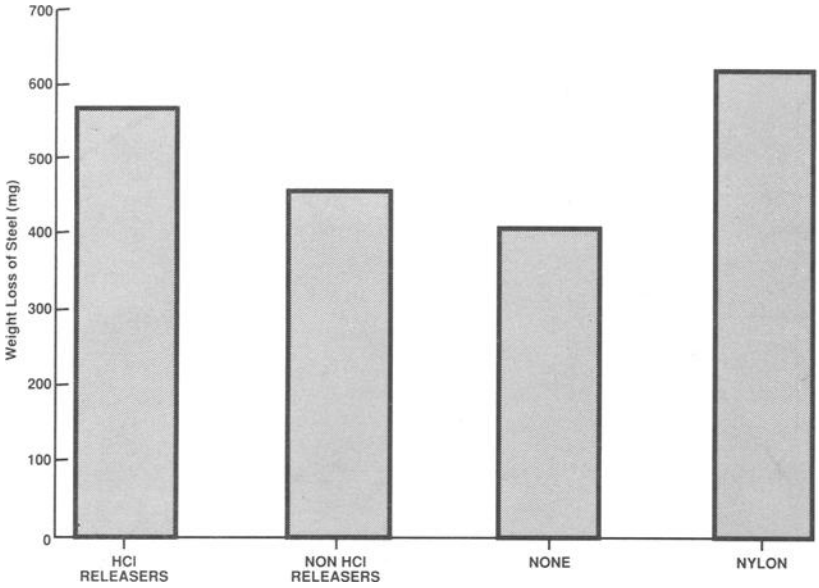

FIG. 5—*Results of exposure of steel to combustion products (600°C).*

TABLE 2—*Corrosivity of smoke towards copper mirrors (micrograms weight loss) (in warm environment).*

Nylon	19
Wool	15
PVC standard wire compound	12
Douglas fir	12
Polyethylene wire compound	12
PVC low-halogen wire compound	10
Neoprene	10
Polystyrene	7

3. Performance assessments should take into account all functional requirements relevant to the intended use of the material.

The required criteria for an acceptable test for corrosion and related damage have been fleshed out in more detail by the ASTM E 5.21 TG70 Task Group [*13*]. These ten criteria, listed in Table 3, have been presented at the International Conference on "Corrosive Effects of Combustion Products" and have also been adopted in the United States by the Society of the Plastics Industry.

In practice, however, most laboratory tests for corrosivity advanced to date fall far short of meeting these ten criteria. Specifically, most such tests, e.g., ones from IEC, CEGB, and DIN [*16–18*], have been designed to measure acid gas evolution and not actual corrosion damage. These tests, which monitor only conductivity or pH as a measure or corrosivity, do not, of course, measure fire performance. Such indirect, or derived, tests, which do not rely on direct corrosion or function impairment-criteria, may have utility for quality control monitoring applications, but are clearly not suited for primary product testing and qualification.

Copyright by ASTM Int'l (all rights reserved) Wed Feb 07 10:53:32 UTC 2024
Downloaded/printed by
The University of Delaware pursuant to License Agreement. No further reproductions authorized.

The ASTM Task Group did find an example of an improved test, one which is performance-based. Following a fire in one of its facilities, in which considerable postfire corrosion was observed, the National Telecommunications Laboratory of France (CNET) developed a test procedure to assess the corrosivity of combustion products of materials [*19*]. A diagram of the CNET test is shown as Fig. 7. The method consists of burning a sample of the material of interest (600 mg, accompanied by 100 mg of polyethylene) in a thermostatted chamber (of volume 20 dm^3) at a high relative humidity and causing condensation of the combustion gases onto a printed circuit board (cooled to a temperature below that of the chamber). The resistance of the circuit board is measured, and the resulting increase in resistance is assigned to the corrosivity of the corresponding smoke. A complex product-rating scheme has been proposed for this test. The rating includes not only the circuit-board corrosion results, but also factors derived from the limiting oxygen index (LOI) test for flammability (ASTM Method for Measuring the Minimum Oxygen Concentration to Support Candle-like Combustion of Plastics (Oxygen Index) D 2863) and an autoignition temperature test. A material

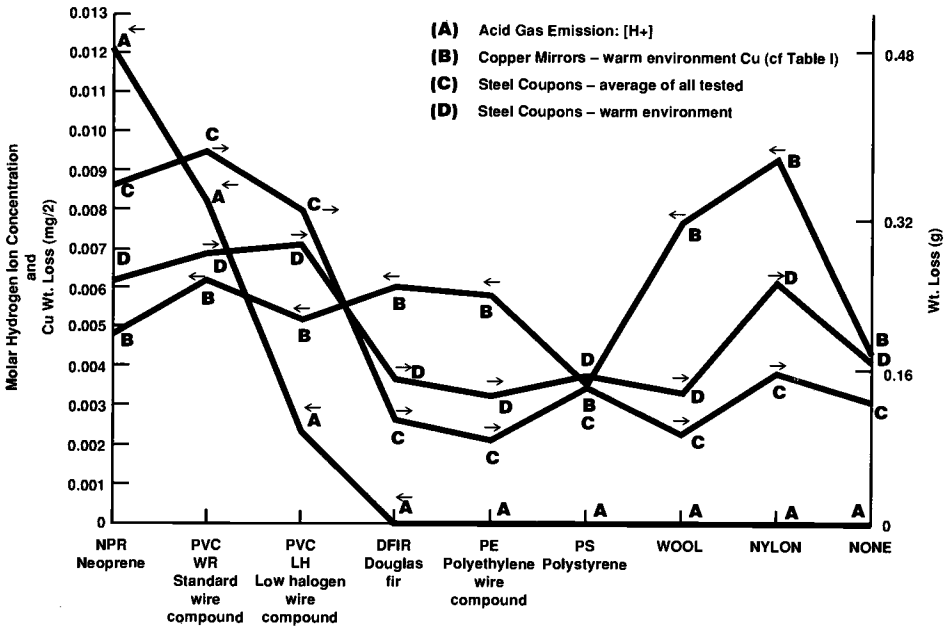

FIG. 6—*Results of exposure of steel and copper to combustion products.*

TABLE 3—*Criteria for a smoke corrosivity test (ASTM E 5.21.70).*

1. Test should measure performance.
2. Combustion module should simulate real fire energies and growth rates.
3. All products should be treated in the same manner.
4. Combustion conditions should be capable of being varied.
5. The exposure module should reflect real life conditions.
6. The exposure target should be capable of being varied.
7. Protocol should allow a reasonable time between exposure and measurement.
8. Protocol should consider transport of the combustion products and their deposition on the target surface.
9. Test protocol should not require excessively long use of equipment or operator time.
10. Test equipment should be relatively low priced.

Copyright by ASTM Int'l (all rights reserved) Wed Feb 07 10:53:32 UTC 2024
Downloaded/printed by
The University of Delaware pursuant to License Agreement. No further reproductions authorized.

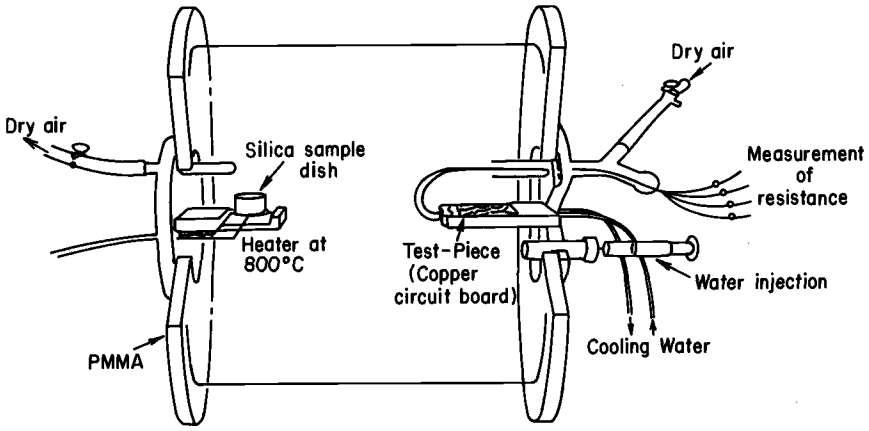

FIG. 7—*CNET corrosivity chamber.*

which has a higher autoignition temperature or requires a higher oxygen concentration for sustained combustion (higher LOI) is permitted a higher degree of corrosivity.

The CNET test method was the first test advanced that conformed to Requirement 1 of Table 3 in that it actually measured performance. It fails, however, to meet some of the other important requirements of Table 3. The combustion module does not simulate real fires in that the sample is combusted by heating it to about 800°C in just a few seconds. This results, in many cases, in specimen behavior which is very different from what happens under actual radiative heating in a fire. The specimen is also required to be crushed and powdered, which does not allow for a realistic exposure to composite products. Other difficulties include the forced condensation of water-soluble gases onto the target and the unrealistically brief time for corrosion after exposure. Even with this latter shortcoming, the CNET test has been judged by many laboratories to fail Criterion 9, namely, that technician testing time per test should not be excessive.

An issue which is not addressed and which cannot be addressed by simple test procedure changes is postexposure cleaning. This can only be done in a real fire after a considerable time lag because of the need of fire fighters to complete their work and for a variety of bureaucratic or commercial considerations. It is essential, therefore, when attempting to model corrosion from a real fire scenario in a test, to allow for an adequate period of time between exposure and measurement (Criterion 7). The 1 h allowed by the CNET test does not adequately represent the time between the occurrence of a fire and the time restorative measures can get started. Since restoration specialists consider that, at a minimum, one day tends to elapse before their work can be started, it is considered more appropriate to allow at least one day for the corrosion period.

The International Organization for Standardization Technical Subcommittee on Plastics Combustibility (ISO/TC61/SC4/WG2) is currently investigating means of adapting the CNET test method for use with other combustion modules. It is also investigating the use of the CNET combustion module with a top temperature of 400°C. Work within ISO will concentrate initially on combustion systems such as are used in the German annular furnace (DIN 53436), a modified NBS smoke chamber [ASTM Test Method for Specific Optical Density of Smoke Generated by Solid Materials (E 662)] equipped with a radiant conical heat source, and the Cone Calorimeter (ASTM P 190 [*20–21*]). Other potential changes in the CNET protocol include the investigation of a long postexposure period and the elimination of the cooling of the target.

Copyright by ASTM Int'l (all rights reserved) Wed Feb 07 10:53:32 UTC 2024
Downloaded/printed by
The University of Delaware pursuant to License Agreement. No further reproductions authorized.

A New Proposed Test

Since the CNET test was judged to be the best currently available and yet was still seen to have serious deficiencies, the ASTM Task Group, with some informal participation by members of the ISO Subcommittee, undertook to develop a new test. The objectives for the new test were:

1. To meet, as well as possible, all the desired criteria of Table 3.
2. To develop a test for corrosivity using standard samples of electronic components and circuits to be corroded (targets). The inverse problem—corrosive susceptibility of various components to standard corrosive atmospheres—is not addressed at the present time.
3. To include corrosion due to metal loss, ohmic bridging, and degradation of electric contacts.

Single or dual chamber. The preliminary question to be asked is whether the apparatus should be, like the CNET test, of a single-chamber design or whether there should be separate chambers for specimen combustion and for target exposure. The limitation, as learned by operating the CNET test with the single-chamber design, is that the entire apparatus must be devoted to waiting for the corrosion to take place. As described above, it is considered that a period of approximately 24 h must be allowed for this. Thus Criterion 9 is violated. With a dual-chamber design, by contrast, it is possible to make detachable exposure modules. Thus, the main test apparatus needs to be occupied only for the duration of the combustion (which may be on the order of 30 min); after this time period, the exposure chamber can be closed, detached, and stored awaiting further measurements.

Flow-through or closed. Once a choice of a dual-chamber design is made, there are still four geometric choices to be made. The apparatus can have any combination of closed or flow-through combustion chamber and closed or flow-through exposure chamber. Experience shows that reasonable-thickness specimens of actual combustibles burn for 30 min or less under typical fire-heating conditions. Thus, a system where both chambers are flow-through is not viable if 24 h of exposure time is required and only 30 min of combustion time available. For the same reason, a system where the combustion chamber is closed while the exposure chamber is flow-through is no better. A system where both chambers are closed is possible, but makes for a difficult oxygen-management situation in the combustion chamber (since flaming may cease as oxygen levels drop). The last alternative is a flow-through combustion chamber coupled to a closed exposure chamber. This combination was judged to be the most promising.

The combustion chamber. In view of Criterion 2, a combustion module more realistic than the one associated with the CNET test (or with the earlier tests) was sought, specifically, a flow-through module. Experience has been good with the conical heating system, as used in the Cone Calorimeter [*20–21*]. This combustion system allows composite samples of up to 50 mm thickness to be tested in a realistic manner without crushing or powdering. Both heating fluxes and oxygen levels can readily be controlled with such a combustion system. Figure 8 shows the proposed chamber. In addition to selecting a suitable combustor, the combustion conditions themselves have to be appropriately prescribed. This has to be done by careful consideration of the full-scale scenario(s) to be represented. It should start with exploratory small- and large-scale experiments. These have yet to be designed.

The exposure chamber. The existing methods for closed chamber testing for corrosivity were not deemed suitable for use. Instead, a rather simple system involving syringe sampling was developed. The targets are located at the base on a large, 5-L syringe. This syringe is closed at the start of the test. During the test an electric stepper motor progressively pulls the syringe open, drawing in the combustion products. The stepper motor receives its electric

Copyright by ASTM Int'l (all rights reserved) Wed Feb 07 10:53:32 UTC 2024
Downloaded/printed by
The University of Delaware pursuant to License Agreement. No further reproductions authorized.

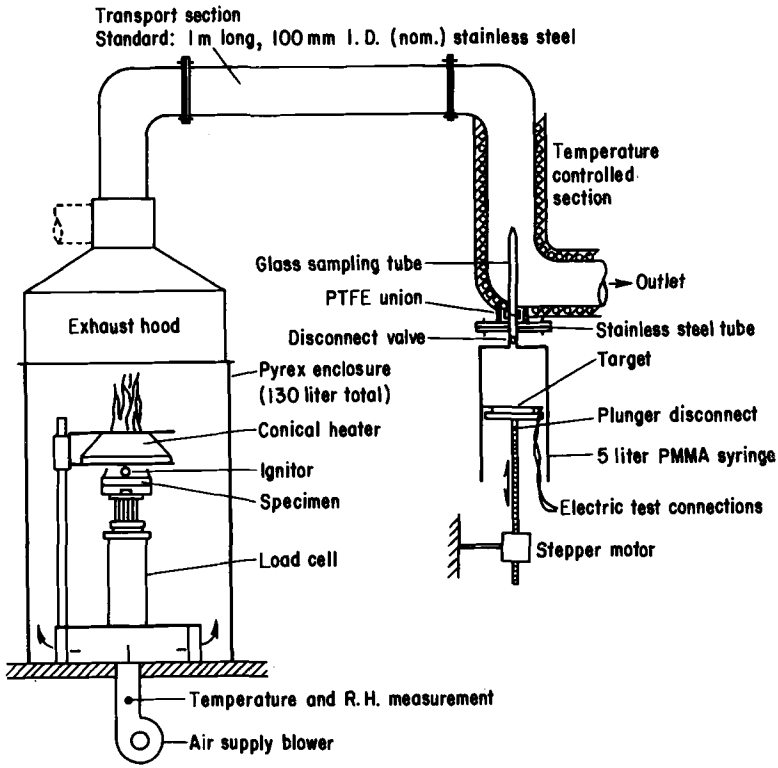

FIG. 8—*Cone corrosimeter.*

control signal from the specimen load cell. At the end of the exposure period, a valve is closed, allowing the syringe to be removed from the apparatus and stored in a controlled-temperature environment while corrosion is taking place. The exposure module does not employ forced condensation of combustion gases but allows condensation to occur at room conditions, simulating a room remote from the fire.

The targets. The three forms of corrosion and nonthermal damage being considered are in no sense redundant or subsumed one by another. Thus, three different targets were seen to be needed. For determining metal (copper) loss, a continuous serpentine printed-circuit trace is used, containing two halves. One half of the trace is exposed to the test atmosphere and the other one is coated with an impermeable coating and serves as the reference. The gain in resistance is measured by comparing the two halves of an alternating-current Wheatstone bridge circuit. This is a realistic target, as demanded by Criterion 5. Targets for determining ohmic bridging typically involve discontinuous circuit traces, although a standard pattern suited to present purposes still has to be finalized. Similarly, for determining contacts degradation, multiple electric relay-type contacts are utilized, with a geometry, again, yet to be finalized.

The heating flux. The conical heater assembly can provide heat fluxes up to 100 kW/m^2 on the specimen face. For routine testing, the Task Group has been considering the use of 50 kW/m^2 since that represents both the upper reaches of localized heating attained during preflashover fire stages and a plausible value found to occur after flashover. Specimen ignition is accomplished by means of an electric spark, but the specimen, once ignited, is also

Copyright by ASTM Int'l (all rights reserved) Wed Feb 07 10:53:32 UTC 2024
Downloaded/printed by
The University of Delaware pursuant to License Agreement. No further reproductions authorized.

heated by its own flame. The design is not restricted to a single heating flux value, and, in line with Criterion 4, the conditions can be varied to simulate a wide range of fire conditions.

General arrangements. The proposed test uses a 130-L combustion chamber, a controlled air inflow obtained from an air supply blower mounted beneath the sample. The value of the airflow rate is an important variable characterizing the combustion conditions; a rate of about 10 L/s is being considered by the Task Group, but the exact value remains to be determined. Sample exposed face is 100 by 100 mm, with a thickness of up to 50 mm. The sample is placed horizontally on a load cell, continuously monitoring the sample mass. All samples are treated identically, as set out in Criterion 3.

The test procedure. A pretest is first conducted to determine the amount of sample mass loss during a 30 -min test period. This information is used to set the controls on the stepper motor. These controls are set so that the syringe is empty at the start, full at $t = 30$ min, and that the rate of syringe filling is proportional to the rate of specimen mass loss for points in between. To start the actual test, a new syringe, bearing the test targets, is attached to the sampling port. The test is conducted for 30 min. If the pretest burn was, in fact, identical to the test burn, then at the end of that time the syringe is exactly full. The disconnect valve is closed, and the syringe is removed and stored in a temperature-controlled environment for 24 h. Electric measurement on the targets are made before exposure and after the postexposure period only.

Future extensions of the method. One issue potentially capable of being addressed by this test is the transport and decay of smoke (Criterion 8). This can be done by altering the exhaust duct wall material or the length of a transfer section of the duct.

At the time of this symposium, various portions of the test method had been developed and checked out by laboratories cooperating with the effort of TG70 of ASTM E5.21. Several are now in the process of building units as described, and data from these should be available in the near future.

Conclusions

Postfire corrosion is an important issue and especially so in mission-critical areas such as electronic communication, computers, naval ships, and nuclear power plants. Because of its importance, the issue has to be addressed in a systematic, inclusive way. To date, the issue has been addressed mostly by developing not-too-successful test methods. These test methods have often consisted of assays for conductivity or pH alone and did not include any measures of actual corrosivity performance. As a first step in the present attack on the problem, organized by ASTM Task Group E5.21 TG70, a detailed decision tree has been developed. This decision tree establishes the framework for making informed decisions.

The problem was also seen to require the development of test methods which are well-founded on the principles of fire hazard assessment. An initial task was formulated: to develop an acceptable test for determining the effects of corrosion and related nonthermal damage on electrical and electronic equipment. To guide the work and to gauge the success, a list was developed of ten criteria a successful corrosivity test should meet. The present work was restricted to examining the relative corrosion damage-causing potential of combustibles involved in fire. The inverse problem of examining the relative susceptibility of electric components to corrosion damage (for a fixed corrosive atmosphere) has been deferred for future work.

Based on experience with existing tests on special ad hoc experiments and on knowledge gained in the process of developing related flammability tests, a new test method is proposed. The method avoids the known limitations of existing tests. Since the test is still under development, a detailed characterization of performance cannot be given. However, it is felt that the design will meet the ten requisite criteria far better than existing apparatuses.

Copyright by ASTM Int'l (all rights reserved) Wed Feb 07 10:53:32 UTC 2024
Downloaded/printed by
The University of Delaware pursuant to License Agreement. No further reproductions authorized.

References

[1] *Corrosive Effects of Combustion Products,* international conference sponsored by ASTM, IEC, and ISO, London, October 1987. OMC, Fire and Materials Ltd., London.
[2] *SKYDD 69 (Protection 69): Plastics—Fire—Corrosion,* proceedings of the international symposium and 15th Nordic fire protection day, Stockholm, 23 April 1969, Swedish Fire Protection Association, Stockholm, October 1969.
[3] Morris, A., in *Corrosive Effects of Combustion Products,* international conference sponsored by ASTM, IEC, and ISO, London, October 1987. OMC, Fire and Materials Ltd., London.
[4] Di Nenno, P. J., *Corrosive Effects of Combustion Products,* international conference sponsored by ASTM, IEC, and ISO, London, October 1987. OMC, Fire and Materials Ltd., London.
[5] "The Burning of Plastics and Its Consequences," *Schaden Spiegel,* April 1968.
[6] *Transactions of the Institute of Marine Engineers (Conference),* Vol. 98, London, UK, Conference 1 (1986).
[7] Cawte, M., "Fires in Ships—Experience from the Falklands Campaign," *Proceedings Interflam '85,* Vol. 12, Interflam, Ltd., Guildford, England, March 1985, pp. 211–216.
[8] Wettern, D., "Lessons Learned from the Falklands Conflict," *Jane's Defence Weekly,* 1 Aug. 1987, pp. 194–196.
[9] Eulenburg, P., in *Corrosive Effects of Combustion Products,* international conference sponsored by ASTM, IEC, and ISO, London, October 1987. OMC, Fire and Materials Ltd., London.
[10] Malhotra, H. L., in *Corrosive Effects of Combustion Products,* international conference sponsored by ASTM, IEC, and ISO, London, October 1987. OMC, Fire and Materials Ltd., London.
[11] P. H. Thomas, "How Heat Release Influences Fire Hazard," *Fire: Control the Heat . . . Reduce the Hazard,* QMC Fire & Materials Centre, London, 1988, pp. 1–1 to 1–6.
[12] Babrauskas, V., "Effective Measurement Techniques for Heat, Smoke, and Toxic Gases," *Fire: Control the Heat . . . Reduce the Hazard,* QMC Fire & Materials Centre, London, 1988, pp. 4.1 to 4.10.
[13] Roux, H. J., in *Corrosive Effects of Combustion Products,* international conference sponsored by ASTM, IEC, and ISO, London, October 1987. OMC, Fire and Materials Ltd., London.
[14] K. Ashley, in *Corrosive Effects of Combustion Products,* international conference sponsored by ASTM, IEC, and ISO, London, October 1987. OMC, Fire and Materials Ltd., London.
[15] Hirschler, M. M. and Smith, G. F., *Fire Safety Journal* Vol. 15, No. 1, 1989, pp. 57–93.
[16] Test on Gases Evolved During Combustion of Electric Cables, Part 1: Determination of the Amount of Halogen Acid Gas Evolved During the Combustion Polymeric Materials Taken from Cables, International Electrotechnical Commission (CEI), IEC Standard 7541, 1982.
[17] Test for Type Approval of Cables, E/TSS/EX5/8056, Pt. 3, Central Electricity Generating Board, Leatherhead, England, 1984.
[18] Prufung an Kabeln und isolierten Leitungen. Korrosivitat von Brandgasen. (DIN 57 472-Pt. 813). Deutsche Elecktrotechnische Kommission, Federal Republic of Germany (1983).
[19] "Fire Performance: Determination of the Corrosiveness of Effluents," 158 CNET/LAB/SER/ENV, National Centre for Telecommunications Studies (CNET), France, 1983.
[20] Babrauskas, V., "Development of the Cone Calorimeter, A Bench Scale Heat Release Rate Apparatus Based on Oxygen Consumption," *Fire and Materials,* Vol. 8, 1984, pp. 81–95.
[21] Proposed Test Method for Heat and Visible Smoke Release Rates for Materials and Products using an Oxygen Consumption Calorimeter (E-5 Proposal P 190), *Annual Book of ASTM Standards,* Vol. 04.07, American Society for Testing and Materials, Philadelphia, 1986.

Copyright by ASTM Int'l (all rights reserved) Wed Feb 07 10:53:32 UTC 2024
Downloaded/printed by
The University of Delaware pursuant to License Agreement. No further reproductions authorized.

Arthur F. Grand[1]

Steady State Combustion of Polymeric Materials

REFERENCE: Grand, A. F., **"Steady State Combustion of Polymeric Materials,"** *Characterization and Toxicity of Smoke, ASTM STP 1082,* H. K. Hasegawa, Ed., American Society for Testing and Materials, Philadelphia, 1990, pp. 89–99.

ABSTRACT: A laboratory method has been developed for the combustion of polyvinyl chloride (PVC) and other polymeric materials in such a way as to produce a constantly flowing, steady-state atmosphere for animal toxicity studies. The method is based on the principles of the German Standard DIN 53 436. However, the present method has a much larger combustion tube and specimen, more versatility in specimen size and air dilution rates, utilizes radiant heating, and has achieved continuous flaming combustion as well as nonflaming. Steady-state atmospheres in a large animal exposure chamber were maintained for up to 60 min under nonflaming conditions and up to 25 min under flaming conditions. A broad range of smoke concentrations have been achieved (e.g., smokes from PVC containing between 400 and 8000 ppm HCl have been produced). The apparatus has the capability for application to research studies on the chemical or toxicological nature of smokes from materials or products and may be applicable to computer modeling of toxic fire hazards.

KEY WORDS: combustion, polymers, polyvinyl chloride, hydrogen chloride, fire tests

Toxicological studies performed at Southwest Research Institute (SwRI) on the effects of hydrogen chloride (HCl) in smoke on juvenile baboons [*1*] and on rodents required a means for the generation of a steady-state atmosphere from the combustion of polyvinyl chloride (PVC). The experimental design called for animals to be exposed to a series of "square-wave" (constant-concentration) atmospheres of HCl.

Hydrogen chloride gas has a tendency to "decay" from smoke atmospheres, depending on the amount of moisture present and on the surfaces and configuration of the apparatus [*2*]. Therefore, in order to create a constant level of HCl in PVC smoke for between 15 and 30 min, a flow-through combustion system was developed in which fresh sample was continuously exposed to fixed heating conditions for the duration of the experiment. Thus, a constant rate of generation of HCl was achieved without appreciable decay. It was important, also, that most of the specimen be consumed during the period of combustion so that the products evolved would not be only "early" combustion products.

The apparatus described in this paper was based on the principles of the DIN 53 436 test apparatus [*3,4*] and on the modification of that design used by Purser [*5*]. The method will be described herein, along with experiments on PVC and three other polymeric materials, in order to demonstrate its potential utility.

[1] Staff scientist, Southwest Research Institute, San Antonio, TX 78228.

Copyright by ASTM Int'l (all rights reserved) Wed Feb 07 10:53:32 UTC 2024
Copyright © 1990 by ASTM International www.astm.org
Downloaded/printed by
The University of Delaware pursuant to License Agreement. No further reproductions authorized.

TABLE 1—*Comparison of three laboratory combustion tube devices.*

	DIN 53 436 [3]	Purser [5]	This Device
Length of tube, cm	130	32	153
Diameter of tube, cm	3.9 (O.D.)	3.8 (I.D.)	7.6 (O.D.)
Airflow, L/min	1.7	1.5	20
Specimen size, g	5	1.3	10–100
Specimen (or oven) travel rate, cm/min	0.1	0.3	0.8–12.9
Method of heating	Tube furnace	Tube furnace	Radiant heating
Moving part	Furnace	Tube	Specimen boat

Description of Apparatus

Background

This apparatus was developed to meet the needs of the toxicology programs referenced above. No toxicity test apparatus presently in existence was (or is) capable of satisfying the demands for a steady-state combustion device producing the large quantity of smoke required. The differences among this apparatus, the DIN 53 436, and Purser's modification are illustrated in Table 1.

The most significant differences between this apparatus and the others shown in the table are the size of the combustion tube (this device has more than twice the diameter of the others) and the achievable travel rates (up to nearly 13 cm/min for this apparatus, compared to 0.1 and 0.3 cm/min). This permits a much larger specimen to be used in this apparatus (we have used up to 100 g, compared to 5 g or less for the others), which results in a larger volume of smoke produced. Radiant heating was selected for this apparatus for several reasons: (1) to try to approximate the nature of heating associated with real fires; (2) to permit greater visibility of the specimen within the combustion tube; and (3) to limit the horizontal extent of the heated zone. The sample is pulled past the furnace in this device (rather than the furnace moving along the combustion tube) in order to simplify the process of continually exposing fresh specimen and to permit greater flexibility in the rate of travel of the specimen.

The DIN combustion method is conducted at a fixed temperature, generally under nonflaming conditions. Einbrodt et al. [6] reported the problems in attempting to conduct flaming combustion. This was also reported more recently by Prager [7]. These results will be discussed later in comparison to the results obtained in this study.

Apparatus

The combustion device and animal exposure chamber are shown schematically in Fig. 1. The combustion tube used for these experiments was a quartz tube 153 cm long and 7.6 cm in diameter. A stainless steel combustion boat (one of several, ranging 50 to 110 cm long) was situated inside the tube. The boat was lined with aluminum foil, and the specimen was evenly distributed along the length of the boat. Two different types of radiant heat furnaces were located outside the tube in order to provide the heat flux conditions necessary for both flaming and nonflaming combustion. The combustion boat, containing a preweighed quantity of sample, was pulled at a constant rate under the preset radiant heat flux. The heat flux, sample loading, and rate of travel of the combustion boat necessary to achieve the proper concentration of smoke was determined for each new material. A constant flow of dry air

Copyright by ASTM Int'l (all rights reserved) Wed Feb 07 10:53:32 UTC 2024
Downloaded/printed by
The University of Delaware pursuant to License Agreement. No further reproductions authorized.

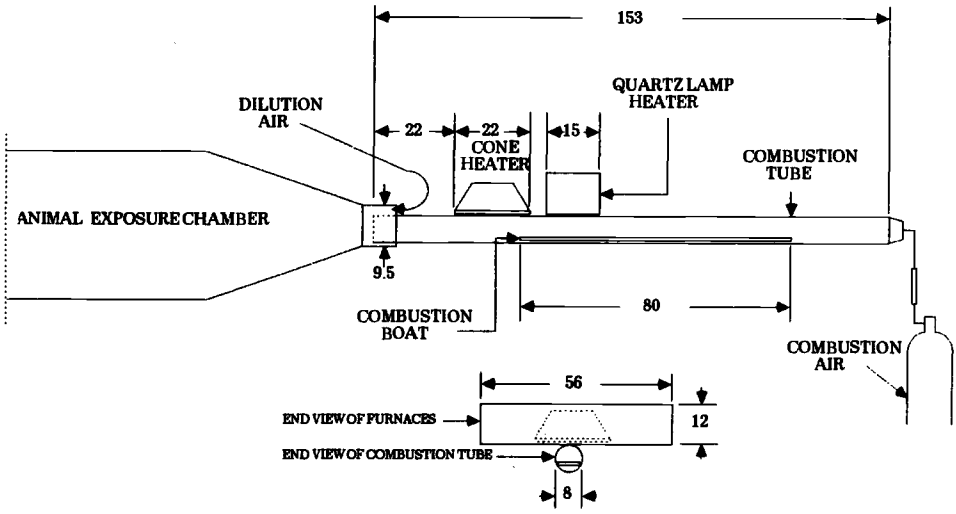

FIG. 1—*Schematic drawing of the continuous combustion apparatus, including dimensions.*

(20 L/min) was metered into the combustion tube; unconditioned laboratory air was added for dilution (see Fig. 1) in order to make up the total flow rate. Flow rates of from 50 L/min to over 200 L/min were used. Control of the airflow was provided by an exhaust blower and variable speed controller. The flow rate was monitored by the pressure drop across an orifice plate in the exhaust line.

The system was designed for either flaming or nonflaming combustion. A "cone" heater, the same design used in the cone calorimeter [*8*], was used for the moderate heat fluxes (2 to 3 W/cm^2) needed for nonflaming combustion of PVC and flaming and nonflaming combustion of the other materials. A heating unit made up of two tungsten-quartz radiant heat lamps was used for the higher heat fluxes (up to 6 W/cm^2) required for sustained flaming of PVC. Under the present test configuration, the cone heater was unable to produce this higher heat flux. A hot wire ignition coil was used to initiate flaming combustion.

The main indicator that the system was working properly was continuous monitoring of some product of combustion in the animal exposure chamber. For PVC, HCl was measured by a newly developed continuous tritration analyzer (CTA), which has been described previously [*9*]. For other materials, concentrations of carbon monoxide (CO) and carbon dioxide (CO_2) were used as the primary indicators of rate of burning and of achievement of "steady state" combustion. The concentration of "smoke" [which, as defined in ASTM Terminology Relating to Fire Standards (E 176) would include the total of all the mass lost by the specimen, whether it be solid, liquid, or gas, and may be expressed in milligrams/liter] in the exposure chamber may be calculated, if desired, from the following: (1) the total loading of the specimen in the combustion boat minus the weight of residue after the test; (2) the rate of travel of the boat; and (3) the total air dilution through the test apparatus. Although this calculation requires some assumptions (i.e., that the sample was distributed evenly over the entire length of the boat and that the residue was also constant over the entire length), it gives an indication of the concentration of smoke for comparison with other combustion devices (this would be important in comparison of smoke toxicity information, for example).

Copyright by ASTM Int'l (all rights reserved) Wed Feb 07 10:53:32 UTC 2024
Downloaded/printed by
The University of Delaware pursuant to License Agreement. No further reproductions authorized.

The orifice plate was "calibrated" for these experiments by flowing a known quantity of pure CO_2 into the flow-through system and measuring the resultant concentration of CO_2 inside the animal exposure chamber.

Experimental Procedure

Selection of Materials

The PVC material used in all the studies reported was supplied by the BF Goodrich Co. It was described as standard rigid "PVC compound" and contained 2 parts lubricant and 2 parts stabilizer for each 100 parts of PVC resin. This material was supplied in small pellet-like chunks, which were laid side by side in the combustion boat in order to achieve the loading required.

The Douglas fir used in these studies was cut from lumber yard stock typically used for fire research studies at SwRI. The 3.8-cm (1½-in.) width of a nominal "2 × 4" was a convenient size for our combustion boat. The board was cut to the desired thicknesses, 0.3, 0.6, and 1.3 cm (⅛, ¼, and ½ in.), respectively, for testing.

The flexible polyurethane foam material was donated by The National Institute of Standards and Technology (formerly National Bureau of Standards). This material is a typical non-fire-retarded flexible polyurethane foam, density approximately 25 kg/m^3. It was cut to specimens 2.5 cm (1 in.) high and 3.2 cm (1¼ in.) wide for testing.

Two rigid polyurethane/polyisocyanurate foams (30 to 35 kg/m^3 density) were supplied by the Dow Chemical Co. These foams were cut to 2.5 cm (1 in.) high and 3.2 cm (1¼ in.) wide. For one series of experiments, 2.5-cm cubes were cut.

Determination of Required Heat Flux Levels

Heat flux was measured by a small heat flux transducer, temporarily located inside the quartz tube, as a function of power to the particular heater used (cone heater or tungsten-quartz lamps). The desired flux level was established prior to the experimentation and checked periodically thereafter. Also, heat flux maps, both horizontally (lengthwise along the specimen boat) and vertically (from the bottom of the boat up to the 1-in. height of the foam specimens), were determined.

Determination of the heat flux setting and the rate of travel of the specimen had to be done empirically. With knowledge of the flammability properties of the specimen and the desired smoke concentration, a target heat flux and rate of sample travel were selected. For flaming combustion, it was relatively easy to observe whether or not sustained flaming was achieved at any given heat flux setting and, if so, whether the flames were proceeding along the specimen at a rate similar to the rate of travel of the combustion boat. Then, by trial and error, the *minimum* heat flux required to sustain flaming combustion was selected. The optimum rate of travel of the specimen was determined to be that at which most of the specimen was consumed while still maintaining continuous burning.

Selecting the test parameters for nonflaming combustion was somewhat more subjective. The *maximum* heat flux which did not allow spontaneous ignition to occur was selected for each material. The rate of travel was then chosen so that nonflaming combustion proceeded at a sufficiently rapid rate to generate a steady-state smoke concentration while still consuming as much of the specimen as possible (for certain char-forming materials, it was difficult to achieve a large percentage mass loss in this apparatus).

Copyright by ASTM Int'l (all rights reserved) Wed Feb 07 10:53:32 UTC 2024
Downloaded/printed by
The University of Delaware pursuant to License Agreement. No further reproductions authorized.

Results

Combustion of PVC

In order to achieve continuous flaming combustion of PVC, a heat flux of approximately 6 W/cm^2 was required, along with an ignition coil. Once ignition was obtained and the rate of travel of the combustion boat controlled to approximately 3.3 cm/min, the PVC burned at a steady rate to the end of the specimen.

Data on HCl and CO concentrations for one of the test runs under flaming conditions are plotted in Fig. 2. The somewhat erratic nature of the HCl curve for this relatively long time period may be due to the response of the continuous titration analyzer [*9*], although the presence of moisture in the combustion atmosphere could contribute to changes in the concentration of HCl over time. Nevertheless, the approximately constant concentration of HCl for the duration of the experiment is apparent from the figure. The smooth CO concentration curve confirms the steadiness of the combustion process. A steady-state combustion period of between 20 and 30 min is illustrated by the data in the figure.

Nonflaming combustion of PVC pellets in this apparatus was accomplished at a heat flux of 3 W/cm^2, with a rate of travel of the combustion boat of 0.86 cm/min. Different loadings of PVC could be accommodated under these conditions, along with adjustment of the air dilution rate, in order to achieve a broad range of HCl concentrations. The entire process was much more easily controlled under nonflaming conditions than under flaming. First of all, the slow rate of travel of the specimen permitted a longer time for measuring and then establishing the desired concentration of HCl. Also, the lack of moisture under nonflaming conditions probably enhanced the stability of the HCL concentration.

The repeatability of HCl evolution from the combustion of PVC for a series of runs under both flaming and nonflaming conditions is shown in Table 2. The quantity of PVC (g/min) was estimated from the loading of PVC pellets and the rate of travel of the combustion boat, assuming an even distribution over the length of the boat. The quantity of HCl produced

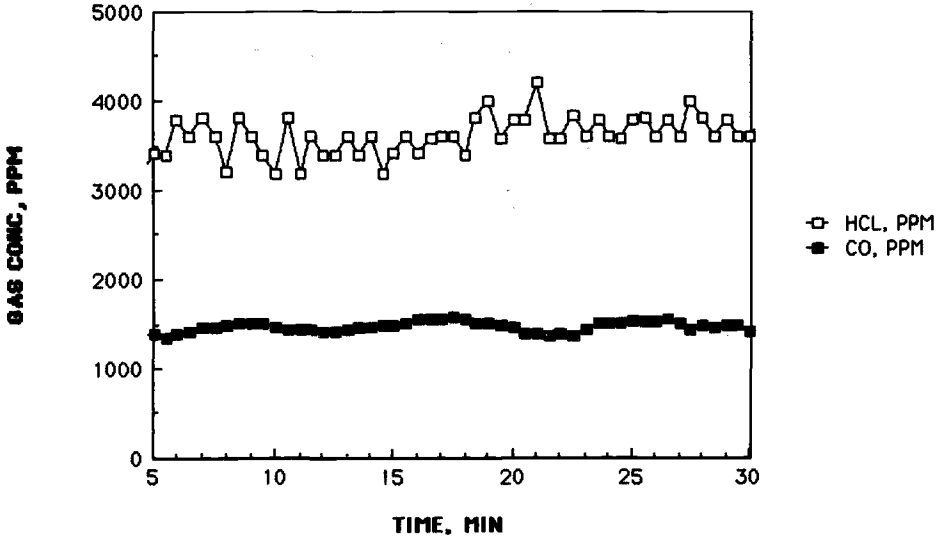

FIG. 2—*Plot of hydrogen chloride (HCl) and carbon monoxide (CO) concentrations in the animal exposure chamber from flaming combustion of PVC.*

Copyright by ASTM Int'l (all rights reserved) Wed Feb 07 10:53:32 UTC 2024
Downloaded/printed by
The University of Delaware pursuant to License Agreement. No further reproductions authorized.

was then estimated from the average concentration of HCl over some time period and the average rate of airflow over that same period (conversion of liters of HCl to grams of HCl was done by assuming that the HCl was behaving as an ideal gas). The mass loss of the specimens for the runs shown in the table (although not factored into these calculations) was around 95% for flaming and between 75 and 85% for nonflaming.

The theoretical yield of HCl that could be produced from this PVC compound is 0.56 g HCl/g PVC. Thus, the data in Table 2 represent apparent recovery factors from 70 to over 100 percent. The uncertainties in the equilibrium concentration of HCl for any given quantity of PVC in the boat may be due to a combination of several experimental factors, including the following: (1) the steadiness of forward motion of the specimen; (2) the evenness of distribution of the specimen over the length of the boat; (3) the rate of combustion of the specimen; (4) the air dilution factor; and (5) the humidity of the laboratory air. In actual practice, a certain "target" concentration of HCl was sought (for animal toxicity studies), and the air dilution rate was changed during the course of the experiment in order to achieve this concentration.

The usual range of HCl concentrations sought during these studies is illustrated in Table 2 (i.e., approximately 2000 to 6000 ppm). During the course of development of the apparatus, concentrations as low as 400 and as high as 8000 ppm HCl were achieved.

Combustion of Other Materials

Three additional test materials have been examined in a preliminary fashion in this apparatus. These are: (1) Douglas fir, (2) flexible polyurethane foam, and (3) rigid polyurethane/polyisocyanurate foam. As was determined for the PVC, the critical heat flux and burning rates were determined for each of these materials under both flaming and nonflaming conditions. These values are summarized in Table 3, along with the data for PVC.

The wood specimens appeared to burn steadily and reproducibly; however, a major product of the combustion of wood, carbon monoxide (CO), showed an unusual pattern of concentration over time during the flaming combustion experiments. Upon evaluation of the CO and CO_2 data, it appeared that CO from the residual char (i.e., from that part of the specimen past the heated zone) was slowly building up in the animal exposure chamber as the test proceeded, with the result being a non-steady-state condition in the atmosphere. The

TABLE 2—*Steady-state HCl data from combustion of PVC.*

Test[a] ID	PVC,[b] g/min	Avg HCl, ppm	HCl g/min	g HCl / g PVC
F-1	1.8	3600	0.86	0.48
F-2	1.8	4300	1.1	0.61
F-3	3.0	5500	1.2	0.40
F-5	0.90	1900	0.47	0.52
F-6	1.5	2300	0.73	0.49
NF-1	1.0	3700	0.55	0.55
NF-2	1.0	4500	0.40	0.40
NF-3	0.85	2600	0.43	0.51
NF-4	1.3	5700	0.60	0.46
NF-5	0.51	1800	0.22	0.43

[a] F = Flaming; NF = Nonflaming; F-4 is missing due to incomplete data.
[b] Conditions: *Flaming*—6 W/cm^2, 110 cm boat, 3.3 cm/min specimen travel rate; *Nonflaming*—3 W/cm^2, 50 cm boat, 0.86 cm/min specimen travel rate.

Copyright by ASTM Int'l (all rights reserved) Wed Feb 07 10:53:32 UTC 2024
Downloaded/printed by
The University of Delaware pursuant to License Agreement. No further reproductions authorized.

TABLE 3—*Heat flux and rate of burning for four polymeric materials.*

	Flaming		Nonflaming	
	Heat Flux,[a] W/cm^2	Specimen Travel Rate,[b] cm/min	Heat Flux,[a] W/cm^2	Specimen Travel Rate,[b] cm/min
Polyvinyl chloride	6	3.3	3	0.86
Douglas fir	3	3.2–6.5	2	0.8
Flexible polyurethane foam	<2	>12.9	2	6.5
Rigid polyurethane foam	3	>12.9	3	1.6

[a] Heat flux listed is a "nominal" value, measured directly under the heater and at the bottom of the sample tray (a heat flux distribution map was prepared for more detailed analyses). "<2" means that the sample continued to burn into an area of substantially lower heat flux.

[b] Travel rate >12.9 means that the rate of burning exceeded the maximum rate of travel of the specimen in this apparatus.

CO_2 data, on the other hand, which represents a gas more directly related to the flaming portion of the experiment, was quite steady for the duration of the test. Under nonflaming combustion conditions, the CO concentration was much more steady. A plot of CO versus time for Douglas fir (1.3 mm thickness) under nonflaming conditions is shown in Fig. 3. The figure illustrates the effect of two different airflow rates (the step change in concentration) during the course of the test run. The test conditions under which these data were obtained were 2 W/cm^2 heat flux and 0.8 cm/min specimen travel rate.

The flexible polyurethane foam specimens burned so readily that even the maximum rate of travel (12.9 cm/min) was insufficient to keep up with the flame travel (see Table 3). As a result, the maximum duration of flaming for the longest specimens possible in the current

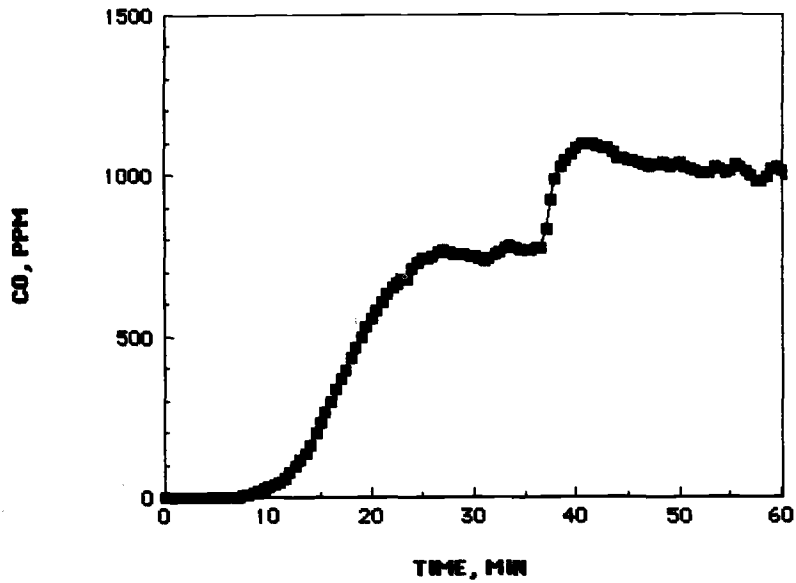

FIG. 3—*Plot of carbon monoxide concentration in the animal exposure chamber from nonflaming combustion of a Douglas fir specimen (at two different dilution airflows).*

Copyright by ASTM Int'l (all rights reserved) Wed Feb 07 10:53:32 UTC 2024
Downloaded/printed by
The University of Delaware pursuant to License Agreement. No further reproductions authorized.

test apparatus was less than 10 min. A "steady state" atmosphere, as evaluated by the gas concentration curves, existed for only a few minutes. Under nonflaming conditions, however, the combustion process was more controlled. Figure 4 is an example of the concentrations of CO and unburned hydrocarbons from flexible polyurethane foam under nonflaming conditions (two different airflow rates are illustrated by the step change in concentration). These data were obtained at 2 W/cm^2 and a specimen travel rate of 6.5 cm/min. The flexible foams melted and decomposed readily upon application of heat with up to 80% weight loss under nonflaming combustion.

The rigid polyurethane/polyisocyanurate foams did not melt (as did the flexible foams). They each produced a char upon the application of heat or flame and maintained their approximate size and shape. As a result, only 30 to 50% of the mass of the rigid foams was consumed, even under flaming conditions. However, in a manner similar to the flexible foam specimens, flames spread rapidly across the surface of the rigid foams, with the result that even the maximum specimen travel rate (12.9 cm/min) could not keep up with the flame spread rate (Table 3). A plot of CO versus time for the rigid foam specimen under flaming conditions is illustrated in Fig. 5. The equilibrium portion of this experiment (at 3 W/cm^2 and 1.6 cm/min) appeared to be about 5 min in duration. As for the flexible foam specimens, the decomposition process for the rigid foams was much more controlled under nonflaming conditions.

An interesting and important variation of the procedure was tested with the rigid foams. A "specimen" comprising a series of 1-in. cubes, separated by 1 in. of noncombustible material, was successfully burned. The rate of burning was thus able to be slowed down from greater than 12.9 cm/min to approximately 6.5 cm/min. Decreasing the diluent airflow produced an essentially "steady" combustion atmosphere for nearly 10 min (Fig. 6).

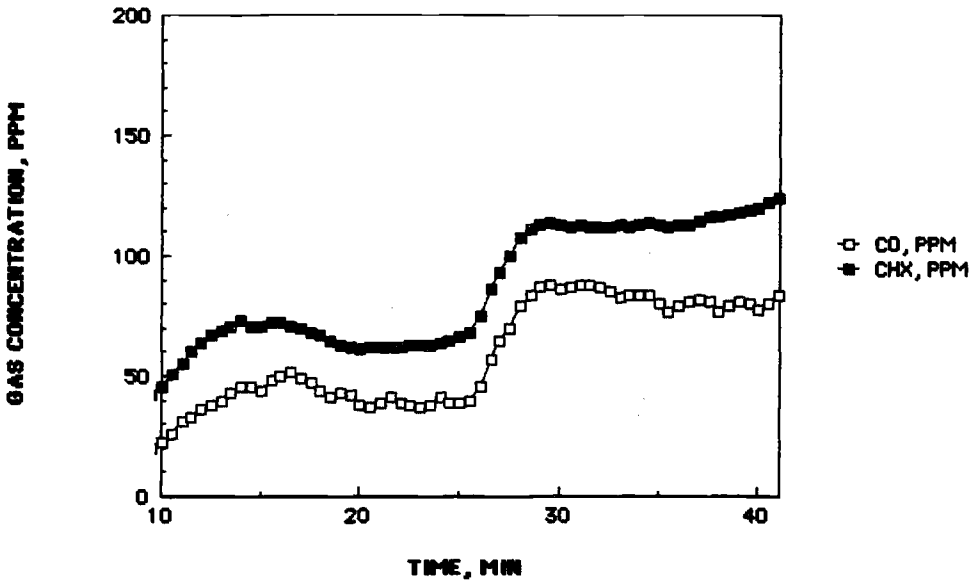

FIG. 4—*Plot of carbon monoxide and "unburned hydrocarbons" (CHx) concentrations in the animal exposure chamber from nonflaming combustion of a flexible polyurethane foam (at two different dilution airflows).*

Copyright by ASTM Int'l (all rights reserved) Wed Feb 07 10:53:32 UTC 2024
Downloaded/printed by
The University of Delaware pursuant to License Agreement. No further reproductions authorized.

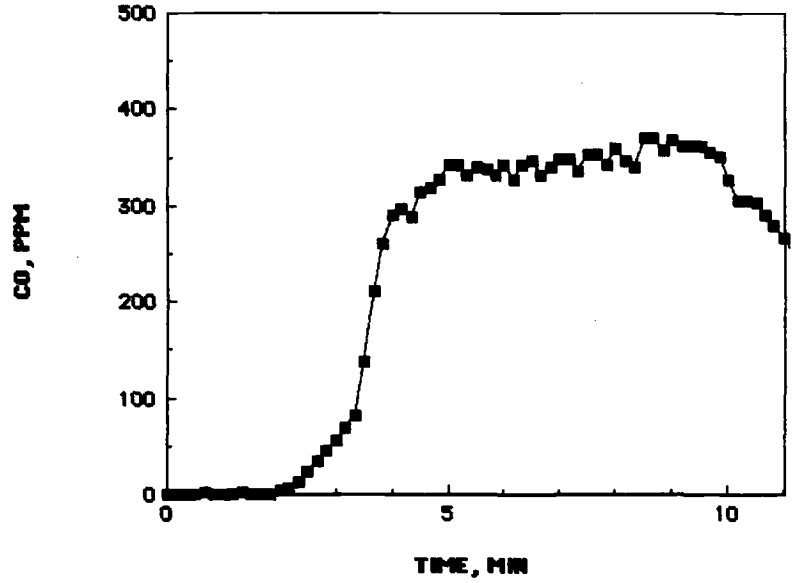

FIG. 5—*Plot of carbon monoxide concentration in the animal exposure chamber from flaming combustion of a rigid polyurethane foam.*

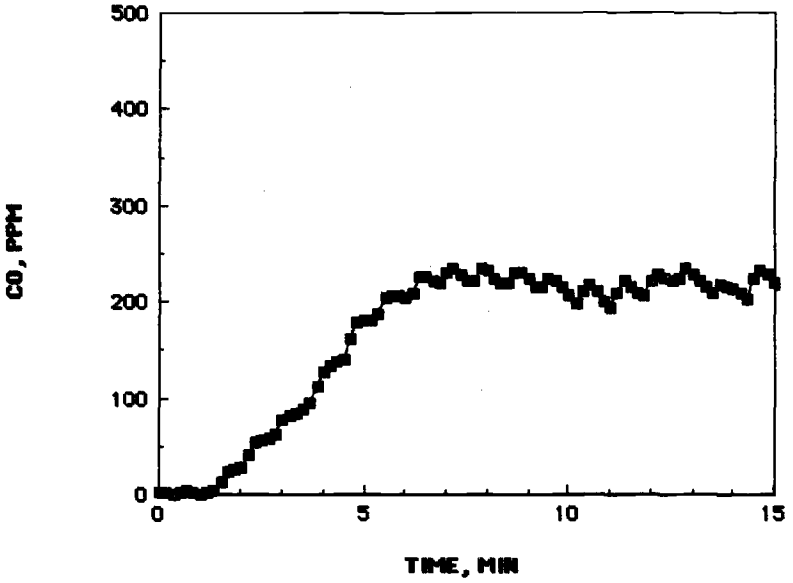

FIG. 6—*Plot of carbon monoxide concentration in the animal exposure chamber from flaming combustion of a series of individual cubes of a rigid polyurethane foam.*

Copyright by ASTM Int'l (all rights reserved) Wed Feb 07 10:53:32 UTC 2024
Downloaded/printed by
The University of Delaware pursuant to License Agreement. No further reproductions authorized.

Conclusions

The apparatus was designed for combustion of PVC, and it performed very well for that application. Although a limited amount of data has been reported in this paper, over 70 experimental runs have been conducted with PVC using this experimental setup. The data from many of these other experiments are not conducive to the type of analysis shown in Table 2 because the air dilution rates are not accurately known (any error in the air dilution rate directly affects the measured quantity of HCl).

Extension of the applicability of this apparatus and methodology to three other materials was performed to test the system. The three materials were intentionally selected to be difficult ones to adapt to this protocol. It appears, from the experiments conducted so far, that this device is more suited to materials that burn relatively slowly.

Steady-state conditions for combustion of PVC were able to be maintained for approximately 20 to 25 min under flaming conditions and for approximately 60 min under nonflaming conditions. The nonflaming experiments were conducted using the 50-cm combustion boat; using the longer (110-cm) boat, the time could have been extended to over 2 h. The range of HCl concentrations produced in laboratory experiments was from 400 to 8000 ppm; however, there is almost no limit to the range of smoke concentrations for this type of material (i.e., dense particles with a controllable rate of burning). Larger quantities of material could be used to achieve higher smoke concentrations, or increased airflow rates could be used for further dilution in order to achieve lower smoke concentrations.

For the three other materials (Douglas fir, flexible polyurethane foam, and rigid polyurethane/polyisocyanurate foam), a limited time period of steady-state combustion (ranging from only a few minutes for certain flaming experiments to 20 min or more for nonflaming) was generally achieved. These conditions may be adequate for short-term toxicity studies; however, certain modifications to the apparatus (e.g., provision for an even longer combustion boat) or to the test procedure (e.g., lower dilution air flows) would be necessary to achieve a longer "steady-state" time period and/or higher concentration.

Nonflaming combustion conditions were easier to control than flaming combustion because the flames often proceeded faster than the maximum rate of travel of the specimen (except for the PVC). This is similar to the problem of conducting flaming combustion in the DIN 53 436 apparatus, as discussed by Einbrodt et al. [*6*] and Prager et al. [*7*]. One of their suggestions for slowing down the rate of burning was to separate pieces of specimen by either an air space or a noncombustible barrier. This is what we performed for one of the test runs reported herein (data shown in Fig. 6). With better control over the rate of travel of the specimen and the air streams, we were able to achieve a much steadier combustion gas profile than reported by these researchers in the DIN apparatus.

The apparatus and methodology continue to hold promise for several applications to combustion research. Two of these may be described as follows:

1. Analysis of acute toxic effects, other than lethality, are critical to our understanding of response of humans to fire. This device continues to have the potential for application to exposure of nonhuman primates or other animal species to combustion atmospheres. The particular advantages of this apparatus are that a steady-state (or "square-wave") concentration of combustion products can be produced for the duration of the exposure, that a sufficient concentration of smoke can be produced to cause acute effects, and that a large animal exposure chamber (e.g., 200 L) can be employed.

2. The composition of smokes from materials may be highly dependent on the way in which the material is burned (e.g., on the imposed heat flux, oxygen availability, etc.). For example, the quantities of CO produced under the conditions of these tests, relative to the

Copyright by ASTM Int'l (all rights reserved) Wed Feb 07 10:53:32 UTC 2024
Downloaded/printed by
The University of Delaware pursuant to License Agreement. No further reproductions authorized.

amount of specimen burned, may be different than those from other laboratory combustion devices. This apparatus may therefore have application to research on the nature of the smoke produced from materials under various test conditions. Furthermore, since computer simulations represent a series of incremental "step" changes, the concentrations of gases produced in this test apparatus may represent unique equilibrium conditions with application to fire modeling.

Acknowledgments

The author wishes to gratefully acknowledge the several sources of funding for this research: The Vinyl Institute initiated this program, funding the development of the apparatus and many of the toxicological studies referred to herein; The National Institute of Standards and Technology (formerly National Bureau of Standards) supported further toxicological studies involving PVC in which this apparatus was used; and Southwest Research Institute, under its internal research program, supported the studies involving materials other than PVC.

Acknowledgment is made of the donation of the materials used in this study, described previously, by The BF Goodrich Co., NIST (NBS), and The Dow Chemical Co.

The author further wishes to express appreciation for the excellent work by and valued discussions with Anthony J. Valys, Southwest Research Institute, in the continuing development of this apparatus.

References

[1] Kaplan, H. L., Anzueto, A., Switzer, W. G., and Hinderer, R. K., "Acute Respiratory Effects of Inhaled Polyvinyl Chloride (PVC) Smoke in Non-human Primates," *The Toxicologist,* Abstracts of Paper, Society of Toxicology, 26th Annual Meeting, Vol. 7, No. 1, February 1987, p. 202.

[2] Beitel, J. J., Bertelo, C. A., Carroll, Jr., W. F., Grand, A. F., Hirschler, M. M., and Smith, G. F., "Hydrogen Chloride Transport and Decay in a Large Apparatus: II. Variables Affecting Hydrogen Chloride Decay," *Journal of Fire Sciences,* Vol. 5, No. 2, March/April 1987, pp. 71–145.

[3] German Standard DIN 53 436, Part 1 (April 1981).

[4] Prager, F. H., "Assessment of Fire Model DIN 53 436," *Journal of Fire Sciences,* Vol. 6, No. 1, January/February 1988, pp. 1–79.

[5] Purser, D. A. and Woolley, W. D., "Biological Studies of Combustion Atmospheres," *Journal of Fire Sciences,* Vol. 1, No. 2, March/April 1983, pp. 118–144; supplemented by personal communication, November 1984.

[6] Einbrodt, H. J., Hupfeld, J., Prager, F. H., and Sand, H., "The Suitability of the DIN 53 436 Test Apparatus for the Simulation of a Fire Risk Situation with Flaming Combustion," *Journal of Fire Sciences,* Vol. 2, November/December 1984, pp. 427–438.

[7] Prager, F. H., Einbrodt, H. J., Hupfeld, J., Muller, B., and Sand, H., "Risk Oriented Evaluation of Fire Gas Toxicity Based on Laboratory Scale Experiments—The DIN 53 436 Method," *Journal of Fire Sciences,* Vol. 5, No. 5, September/October 1987, pp. 287–362.

[8] Babrauskas, V., "Development of the Cone Calorimeter—A Bench Scale Heat Release Rate Apparatus Based on Oxygen Consumption," *Fire and Materials,* Vol. 8, 1984, pp. 81–95; also, NBSIR-82-2611, National Institute of Standards and Technology, 1982.

[9] Grand, A. F., "Continuous Monitoring of Hydrogen Chloride in Combustion Atmospheres and in Air," *Journal of Fire Sciences,* Vol. 6, January/February 1988, pp. 61–79.

Copyright by ASTM Int'l (all rights reserved) Wed Feb 07 10:53:32 UTC 2024
Downloaded/printed by
The University of Delaware pursuant to License Agreement. No further reproductions authorized.

Archibald Tewarson[1] *and Mohammed M. Khan*[1]

Generation of Smoke from Electrical Cables

REFERENCE: Tewarson, A. and Khan, M. M., **"Generation of Smoke from Electrical Cables,"** *Characterization and Toxicity of Smoke, ASTM STP 1082,* H. K. Hasegawa, Ed., American Society for Testing and Materials, Philadelphia, 1990, pp. 100–117.

ABSTRACT: Results are presented in this paper for the generation of smoke in terms of smoke yield, mass optical density, and specific corrosion constant for electrical cables during fire propagation. The data were measured in our studies on cable fire propagation. From this study, cables have been classified into three groups based on the Fire Propagation Index.

For Group 3 cables, self-sustained fire propagation rate is expected to be very rapid, and both thermal (heat) and nonthermal (smoke) damages are expected. For Group 2 cables, self-sustained fire propagation is expected to be less rapid than for Group 3 cables. Thermal and nonthermal fire damages are expected from Group 2 cables, although the severity is expected to be less than for Group 3 cables. For Group 1 cables, self-sustained fire propagation is expected to be difficult. In the presence of external heat fluxes or cable overheating due to electrical faults, fire propagation is expected to be sustained. For Group 1 cables, thermal fire damage is not expected; however, depending on the cables, nonthermal fire damage is expected. For Group 1A cables, nonthermal fire damage is not expected, and for Group 1B cables, nonthermal damage is expected.

The data from the study suggest that nonthermal fire damage is not expected if the following conditions are satisfied: (1) Fire Propagation Index is less than 10; (2) smoke yield is less than 0.30 g/g; (3) mass optical density is less than 0.11 m^2/g; and (4) the specific corrosion constant of the cable is less than 0.92×10^{-6} μm/h ppm.

KEY WORDS: electrical cables, fire propagation, corrosion and smoke damage, nonthermal damage

Nomenclature

A	Total surface area of the material involved in fire (m^2)
c_p	Specific heat (kJ/g°K)
c_m	Concentration of material vapors (ppm)
c_s	Concentration of smoke (g/m^3)
c_{corr}	Concentration of condensate corrosive compounds on the surface of the metal (ppm)
d	Cable diameter (m)
D	Optical density
D_{Mass}	Mass optical density (m^2/g)
FPI	Fire Propagation Index (−)
$\dot{G}''$	Generation rate (g/m^2s)
ΔH_{Ch}	Chemical heat of combustion (kJ/g)
k	Thermal conductivity (kW/°K)
K_v	Effective visibility constant (m^2)
l	Optical pathlength (m)

[1] Manager, Flammability section, and research scientist, respectively, Factory Mutual Research Corp., Norwood, MA 02062.

Copyright by ASTM Int'l (all rights reserved) Wed Feb 07 10:53:32 UTC 2024
Copyright © 1990 by ASTM International www.astm.org
Downloaded/printed by
The University of Delaware pursuant to License Agreement. No further reproductions authorized.

l_v Distance over which an observer can clearly see an object or read a sign (m)
L Heat of gasification (kJ/g)
n Number of cables
p Power or exponent generally found to be close to unity for flaming fires but much less than unity for nonflaming fires
$\dot{q}''$ Heat flux (kW/m^2)
$\dot{Q}''_{Ch}$ Chemical heat release rate (kW/m^2)
ΔT Ignition temperature above ambient (°K)
$\dot{V}_T$ Total volumetric flow rate (m^3/s)
V_T Total volume (m^3)
w_{corr} Weight loss of metal due to corrosion resulting in change in metal thickness (μm)
W_T Total weight of material vapors (g)
Y Yield (g/g)
α Fraction of corrosive compounds deposited on the surface
β Fraction of the mixture of material vapors and air present as water
ξ Particle optical density or specific extinction coefficient (m^2/g)
ρ Density (g/m^3)
χ_R Radiative component of chemical heat release rate
η Specific corrosion constant (μm/h ppm)

Subscripts

corr Corrosive
e External
f Material vapors
fs Flame
HCl HCl solution
m Material vapors
Mass Mass optical
n Net
rr Reradiation
s Smoke
T Total
v Visibility

Superscripts

· Per unit of time (s^{-1})
″ Per unit surface area of the material (m^{-2})

Polymers

Cl Chlorine
ECTFE Copolymer of ethylene and chlorotrifluoroethylene
EPR Copolymer of ethylene and propylene
EPDM Copolymer of ethylene, propylene, and nonconjugated diene
PE Polyethylene
PE-Cl-s Chlorosulfonated polyethylene
PS Polystyrene
PP Polypropylene

Copyright by ASTM Int'l (all rights reserved) Wed Feb 07 10:53:32 UTC 2024
Downloaded/printed by
The University of Delaware pursuant to License Agreement. No further reproductions authorized.

PTFE	Polytetrafluoroethylene
PU	Polyurethane
PMMA	Polymethylmethacrylate
PVC	Polyvinylchloride
TFE	Copolymer of tetrafluoroethylene and ethylene
XLPO	Crosslinked polyolefin
XLPE	Crosslinked polyethylene

Introduction

Generation of heat and smoke during fire propagation and steady burning are responsible for creating hazardous environments in fires (smoke is defined as a mixture of solid, liquid, and gaseous compounds). Smoke generated in fires is responsible for creating toxic and corrosive environments with reduced visibility.

In general, environments created in fires can be divided into two categories: (1) *thermal environments:* these environments are created as a result of the generation of heat, and (2) *nonthermal environments:* these environments are created as a result of the generation of smoke. In flaming fires, hazards due to both thermal and nonthermal environments can be present, whereas in nonflaming fires, hazards are predominantly due to nonthermal environments.

The fire community has been concerned with hazards from thermal and nonthermal environments (toxicity and reduced visibility [*1–4*]) and protection requirements such as sprinklers [*5*]. Very little attention, however, has been given to nonthermal fire damage due to corrosion and smoke and their protection requirements [*6*]. Numerous studies have been performed to: (1) quantify various compounds generated in fires and their toxic effects on animals [*1–4*]; (2) understand and quantify solid particulates (soot) formation in flames [*7–14*]; (3) understand and quantify generation of smoke in fires [*15–25*]; (4) understand and quantify smoke movement [*26–28*]; and (5) develop engineering relationships for smoke control for fire safety design [*29–31*].

For the quantification of nonthermal fire damage and protection requirements, a long-range study has been undertaken at Factory Mutual Research Corporation [*6*]. This paper presents some preliminary results dealing with the formation of solid and liquid particulates and water-soluble corrosive compounds from electrical cables.

Background

Generation of Solid and Liquid Particulates in Fires

Generation of solid and liquid particulates (smoke)[2] in fires of various materials has been quantified [*20–22,24,25*]. Data have been reported for the smoke yield and optical density. Yield is defined as the ratio of the mass generation rate of smoke to the mass generation rate of material vapors during fire propagation [*24*]

$$Y_s = \dot{G}''_s/\dot{G}''_f \tag{1}$$

[2] In this paper, *smoke* is defined as the mixture of solid and liquid particulates, although the common definition of "smoke" also includes gaseous products.

Copyright by ASTM Int'l (all rights reserved) Wed Feb 07 10:53:32 UTC 2024
Downloaded/printed by
The University of Delaware pursuant to License Agreement. No further reproductions authorized.

where

Y_s = the yield of smoke (g/g),
$\dot{G}''_s$ = the mass generation rate of smoke (g/m^2s), and
$\dot{G}''_f$ = the mass generation rate of material vapors or mass loss rate (g/m^2s).

$\dot{G}_f$ can be expressed as [*24*]

$$\dot{G}''_f = \dot{q}''_n/L \tag{2}$$

where

$\dot{q}''_n$ = the net heat flux absorbed by the material and is equal to $\dot{q}''_e + \dot{q}''_{fs} - \dot{q}''_{r,r}$, where $\dot{q}''_e$ is the external heat flux (kW/m^2), $\dot{q}''_{fs}$ is the flame heat flux (kW/m^2) and $\dot{q}''_{r,r}$ is the surface reradiation loss (kW/m^2), and
L = the heat of gasification (kJ/g).

From Eqs 1 and 2

$$\dot{G}''_s = Y_s(\dot{q}''_n/L) \tag{3}$$

The light transmission characteristics of smoke are commonly expressed as optical density, D

$$D = \log_{10}(I_o/I) \tag{4}$$

where I/I_o is the fraction of light transmitted through smoke. Visibility through smoke depends on D and is expressed as

$$l_v = K_v(D/l) \tag{5}$$

where

l_v = the distance over which an observer can clearly see an object or read a sign,
K_v = the effective visibility constant, and
l = the optical pathlength.

In fires, D/l is the most common measurement for smoke.

D/l depends on the smoke concentration, c_s, in the environment as well as on the physical characteristics of particulates and the light source. The relationship between D/l and c_s can be expressed as [*24*]

$$D/l = \xi c_s \tag{6}$$

where c_s is in g/m^3 and ξ is the smoke optical density (specific extinction coefficient) (m^2/g). In fires, c_s can be defined as [*24*]

$$c_s = A\dot{G}''_s/\dot{V}_T \tag{7}$$

where

A = the total surface area of the material involved in the fire (m^2), and
$\dot{V}_T$ = the total volumetric flow rate of well-mixed mixture of smoke with air (m^3/s).

Copyright by ASTM Int'l (all rights reserved) Wed Feb 07 10:53:32 UTC 2024
Downloaded/printed by
The University of Delaware pursuant to License Agreement. No further reproductions authorized.

From Eqs 1, 6, and 7

$$D/l = D^{p}_{Mass}(A\dot{G}''_f/\dot{V}_T) \tag{8}$$

where D_{Mass} is the mass optical density expressed as

$$\xi Y_s = D^{p}_{Mass} \tag{9}$$

where D_{Mass} is in m^2/g and p is a power close to unity for flaming fires and significantly less than unity for nonflaming fires.

From Eqs 5 and 8

$$l_v = K_v D^{p}_{Mass}(A\dot{G}''_f/\dot{V}_T) \tag{10}$$

And from Eqs 2 and 10

$$l_v = K_v(D^{p}_{Mass}/L)(A/\dot{V}_T)\dot{q}''_n \tag{11}$$

Equation 11 suggests that visibility through smoke is expected to depend on: (1) K_f (physical characteristics of smoke and light source); (2) D_{Mass}/L (ratio of two basic material fire properties, independent of fire size if fires are turbulent but dependent on the light source, fire ventilation, and charring properties of materials); (3) A (geometry and fire size); (4) $\dot{V}_T$ (airflow and mixing); and (5) $\dot{q}''_n$ (fire environment heat fluxes). Data for the mass optical density for small- and large-scale fires for over 300 materials have been measured in the Factory Mutual small (50-kW), intermediate (500-kW), and large-scale (5000-kW) flammability apparatuses, shown in Fig. 1 [*32*]. The mass optical densities have also been measured at the National Bureau of Standards [*25*].

Corrosion

Corrosion is defined as unwanted chemical reactions on materials; there are eight types of corrosions which occur in the everyday world under the ambient environmental conditions enhanced by air pollution. Extensive literature is available on the subject of nonfire related corrosion [*33–37*].

In most cases, halogen ions (chloride, bromide, and fluoride) in combination with solid and liquid particulates have been responsible for the nonthermal fire damage. For most metals, corrosion is rapid if the relative humidity is in the range of 70 to 80%. Halogen ions are found to be absorbed on the solid smoke particulates. Also, the particulates can be electrically charged [*38*]. Smoke particulates thus can carry corrosive agents, as well as electrical charges, and enhance damage due to corrosion and electrical discharges when deposited on delicate electrical and electronic components and machines. A critical relative humidity value of 30% at 20°C is recommended for arresting corrosion damage. A chloride ion deposit of 10 mg/m^2 is suggested to be the lower limit for corrosion [*35*]. In the combustion/pyrolysis of 10 g of polymer sample in a 0.2-m^3 vessel, the following surface deposits were found in 3 h [*39*]: (1) 2300 mg/m^2 from PVC; 700 mg/m^2 from PTFE; and (3) 490 mg/m^2 from TFE polymer.

Corrosion damage associated with the deposition of solid and liquid particulates in smoke on surfaces is expected to depend on: (1) concentration of particulates in the environment; (2) flow velocity and direction of smoke relative to the surface; (3) size, configuration, and nature of the surface; (4) relative humidity and temperature; and (5) duration of exposure. The relationship between the weight loss of a metal due to corrosion resulting in thickness

Copyright by ASTM Int'l (all rights reserved) Wed Feb 07 10:53:32 UTC 2024
Downloaded/printed by
The University of Delaware pursuant to License Agreement. No further reproductions authorized.

change, w_{corr}, and total concentration of the material vapors, c_m, assuming a first order reaction, can be expressed as

$$\int_o^t dw_{corr}/dt = \eta c_m \tag{12}$$

$$w_{corr}/c_m = \eta t \tag{13}$$

where w_{corr} is in μm, t is in h, c_m is in ppm, and η is the specific corrosion constant (μm/h ppm).

From Eq 7, the concentration of condensate corrosion compounds on the surface of the metal, c_{corr}, can be expressed as

$$c_{corr} = \left(\int_o^t (\alpha A \dot{G}''_f \times 10^6) dt \Big/ \int_o^t (\beta \dot{V}_T) dt \right) \tag{14}$$

where c_{corr} is in ppm, α is the fraction of the corrosive compounds deposited on the surface, and β is the fraction of the mixture of material vapors and air present as water. From Eq 14

$$c_{corr} = (\alpha/\beta)(W_l/V_T) \times 10^6 \tag{15}$$

where

W_T = the total weight of material vapors generated in the fire (g), and
V_t = the total volume of smoke air mixture (m^3). W_l/V_t can be defined as the average concentration of material vapors in g/m^3.

Fire Propagation in Electrical Cables and Expected Nonthermal Damage

The nonthermal fire damage depends on the concentrations of solid, liquid, and gaseous compounds present in smoke. Smoke concentration, on the other hand, depends on the fire propagation rate, airflow rate, and mixing of smoke with air. It has been shown that cables can be classified on the basis of their self-sustained fire propagation characteristics using the Fire Propagation Index (FPI), as defined as [*40*]

$$\text{FPI} = 1000[\chi_R A \dot{Q}''_{Ch}/\Pi n d]^{1/3}/\Delta T(k\rho c_p)^{1/2} \tag{16}$$

$$\text{FPI} = 1000[(\chi_R \Delta H_{Ch}) A \dot{G}''_f/\Pi n d]^{1/3}/\Delta T(k\rho c_p)^{1/2} \tag{17}$$

where

χ_R = the radiative component of the chemical heat release rate, taken as 0.40,
$\dot{Q}''_{Ch}$ = the chemical heat release rate (kW/m^2),
n = the number of cables,
d = the cable diameter (m),
ΔT = the ignition temperature above ambient (°K),
k = the thermal conductivity (kW/mK),
ρ = the density (g/m^2),
c_p = the specific heat (kJ/g°K), and
ΔH_{Ch} = the chemical heat of combustion (kJ/g).

Copyright by ASTM Int'l (all rights reserved) Wed Feb 07 10:53:32 UTC 2024
Downloaded/printed by
The University of Delaware pursuant to License Agreement. No further reproductions authorized.

Chemical heat release rate is calculated from the generation rates of CO_2 and CO [*20*]. The cables are classified as follows [*40*]:

Group 1 Cables

Fire Propagation Index for cables in this group is less than 10. Fire propagation is not expected to be self-sustained. For cables in this group, fire propagation is possible only if internal and/or external heat sources are present.

Group 2 Cables

Fire Propagation Index for cables in this group is equal to or greater than 10, but is less than 20. Fire propagation is expected to be self-sustained, and the rate is expected to increase linearly with time.

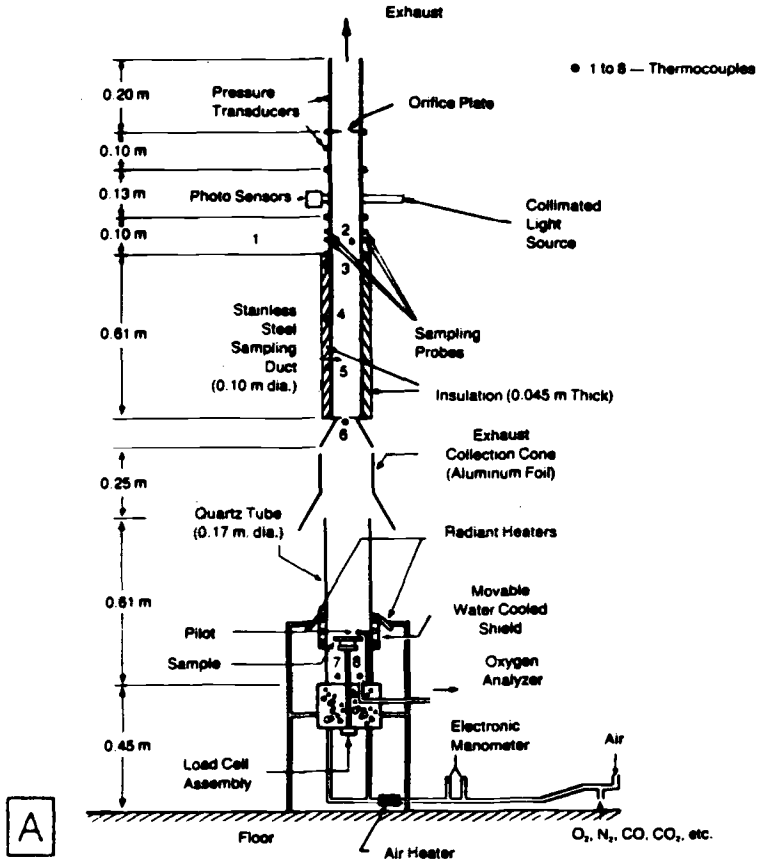

FIG. 1—*Flammability apparatus used in the experiments: (*A*) 50 kW-scale; (*B*) 500 kW-scale; and (*C*) 5000 kW-scale.*

Copyright by ASTM Int'l (all rights reserved) Wed Feb 07 10:53:32 UTC 2024
Downloaded/printed by
The University of Delaware pursuant to License Agreement. No further reproductions authorized.

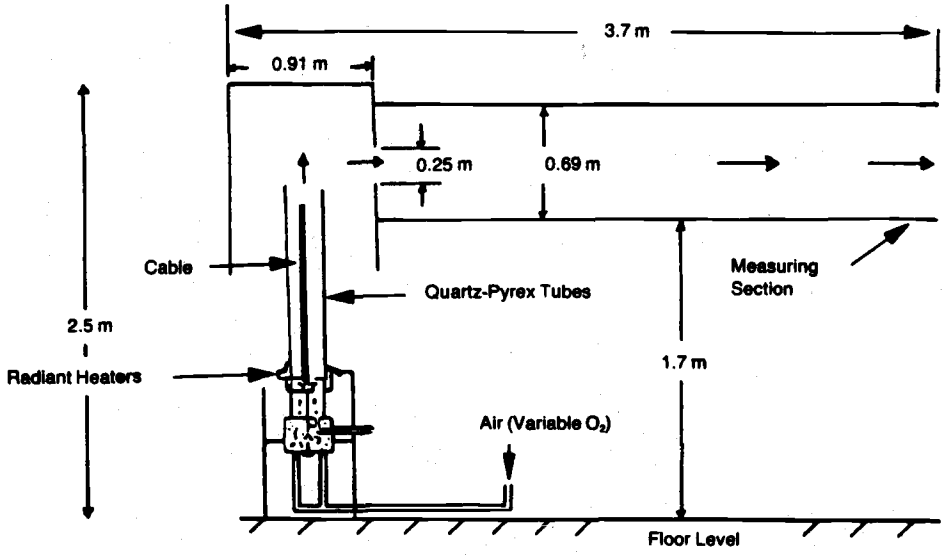

B

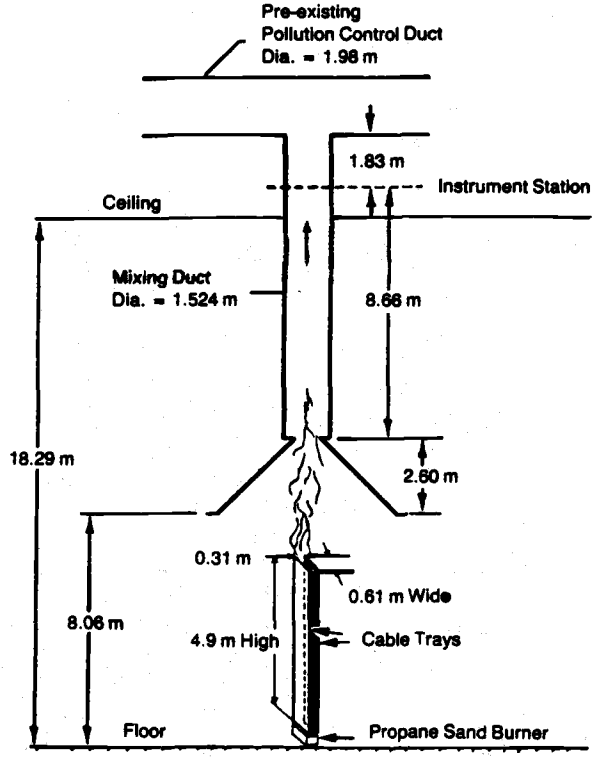

C

Copyright by ASTM Int'l (all rights reserved) Wed Feb 07 10:53:32 UTC 2024
Downloaded/printed by
The University of Delaware pursuant to License Agreement. No further reproductions authorized.

Group 3 Cables

Fire Propagation Index for cables in this group is equal to or greater than 20. Fire propagation is expected to be self-sustained, and the rate is expected to increase exponentially with time.

During fire propagation, heat and smoke are generated with different rates, depending on the cable group. For Group 3 cables, heat and smoke are expected to be generated very rapidly and in large amounts; thermal and nonthermal fire damages are expected. Thus it would be necessary to provide adequate fire protection. For Group 2 cables, thermal and nonthermal damages would be less severe than Group 3 cables; protection requirements would be less restrictive than for Group 3 cables.

For Group 1 cables, thermal damage is not expected; damage due to nonthermal damage as a result of internal or external heat sources is possible depending on the cable insulation and jacketing materials and the additives. Therefore, it is necessary to divide Group 1 cables into two subgroups: (1) Group 1A: nonthermal fire damage is not expected from cables in this group; and (2) Group 1B: nonthermal damage is expected from cables in this group.

Experiments

Small-scale cable fire propagation experiments were performed in the Factory Mutual small- (50 kW-) and intermediate- (500 kW-) scale flammability apparatuses, shown in Figs. 1A and 1B [*40–43*]. Large-scale cable fire propagation experiments were performed in the Factory Mutual large- (5000 kW-) scale flammability apparatus, shown in Fig. 1C [*40–42*].

In the experiments, measurements were made for the critical heat flux and thermal response of cables, fire propagation rate, generation rates of heat and smoke, light obscuration by smoke, and smoke corrosivity. Critical heat flux is the minimum heat flux at or below which there is no ignition, and thermal response is the property of the material related to its thermal conductivity, density, and specific heat and ignition temperature.

Ignition Experiments

Critical heat flux and thermal response were determined from ignition experiments, using 0.13-m-long horizontal samples with both ends tightly covered with heavy duty aluminum foil.

Fire Propagation Experiments

Fire propagation rate, generation rates of heat and smoke, and light obscuration by smoke were determined using 0.10, 0.25, 0.38, 0.61, and 1.25-m-long single vertical cables and a 0.61 m-long vertical bundle of three cables. In the experiments, cable samples were kept inside a 0.25-m-diameter and 0.61-m-long glass tube attached on the top to an aluminum tube of the same dimensions. The bottom 0.20 m of the cable was exposed to 50 kW/m^2 of external heat flux in the presence of a pilot flame. Air with a flow rate of 0.005 m^3/s with oxygen concentration in the range of 0 to 50% was introduced at the bottom of the glass tube. In the large-scale cable fire experiments, two 4.9-m-long and 0.61-m-wide vertical sheets of Marinite, separated by 0.30 m, were used. A single layer of cables touching each other was attached to both the Marinite sheets, with cables facing each other. A 61-kW propane air sand burner, placed at the bottom between the sheets, was used as an ignition source. Under this geometry, flame radiation is enhanced by about 50% [*42*].

Copyright by ASTM Int'l (all rights reserved) Wed Feb 07 10:53:32 UTC 2024
Downloaded/printed by
The University of Delaware pursuant to License Agreement. No further reproductions authorized.

Smoke Corrosivity Experiments

Experiments were performed with 0.13-m-long cable samples. The material vapors generated from the fire were bubbled through 100 mL of distilled water. After the experiment, the solution was stirred for several hours and was filtered to remove the solid particulates. A mild steel probe was then placed in the filtered solution, and cumulative corrosion was measured every 5 h. Cumulative value of the generation rate of material vapors was also determined. For calibration, 0.1 *M* HCl solution and research grade polymethyl-methacrylate (PMMA), polyvinylchloride (PVC), and natural gas burner were used. The cumulative value of the generation rate of material vapors/100 mL of distilled water used in the experiment was defined as the concentration of the material vapors.

Experimental Results

Generation Rate of Smoke

Figure 2 shows the data for the generation rate of smoke from various materials as a function of the ratio of the net heat flux absorbed by the material to heat of gasification. The data were measured in the Factory Mutual 50 kW-scale flammability apparatus. The data satisfy Eq 3 and show that the yield of smoke depends on the chemical structure of the material.

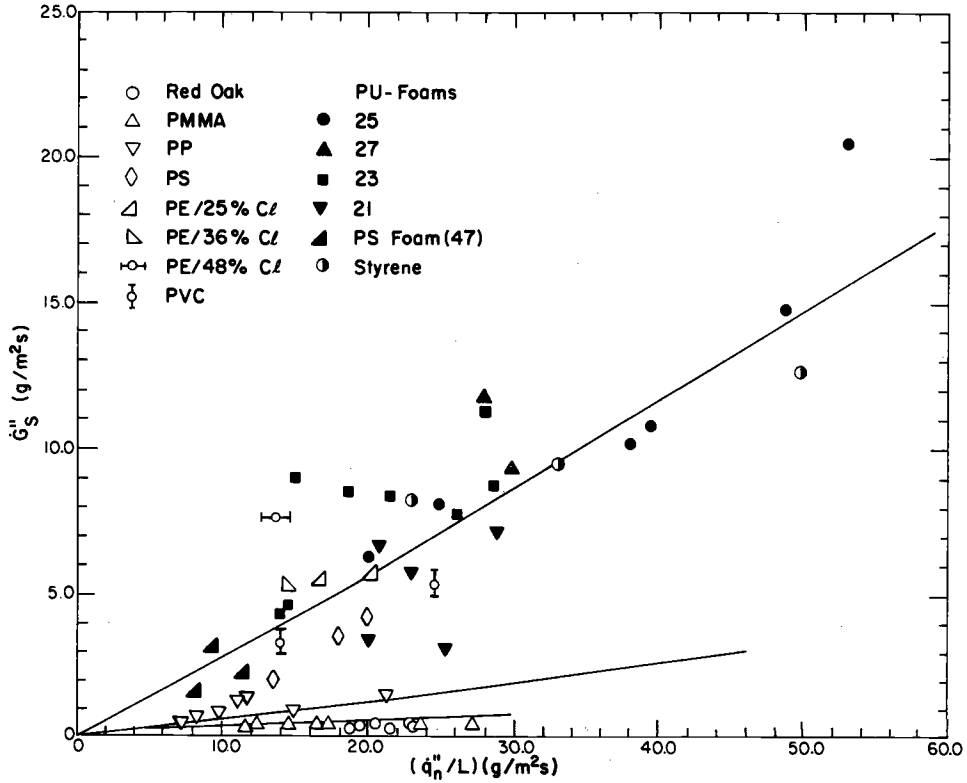

FIG. 2—*Relationship between mass generation rate of solid particulates in smoke and the ratio of net heat flux absorbed by the material and its heat of gasification.*

Copyright by ASTM Int'l (all rights reserved) Wed Feb 07 10:53:32 UTC 2024
Downloaded/printed by
The University of Delaware pursuant to License Agreement. No further reproductions authorized.

Smoke data measured at Factory Mutual Research Corp. suggest that it is possible to classify materials for their smoke-generating characteristics based on the nature of the chemical bonds between carbon, hydrogen, oxygen, nitrogen, sulfur, and halogens atoms [*32,44*]. It is possible to use such a classification for cables based on the generic nature of the insulation and jacketing materials and additives.

The generation rate of smoke from cables is expected to follow the fire propagation rate. Thus, Group 3 cables are expected to have higher smoke generation rates than Group 2 cables; Group 2 cables are expected to have higher smoke generation rates than Group 1 cables.

Three of the important fire properties associated with smoke-generating characteristics are smoke yield, mass optical density, and specific corrosion constant. The generation rate of smoke depends on the smoke yield (Eq 3), visibility depends on the mass optical density (Eq. 11), and smoke corrosivity depends on the specific corrosion constant (Eq 13).

Smoke Yield and Mass Optical Density for Electrical Cables

Figure 3 shows the relationship between the mass optical density and smoke yield for flaming fires of cables and polymers and nonflaming fires of polymers; data are taken from Ref *24*. The data suggest that the mass optical density is proportional to the yield of smoke with a power close to unity for flaming fires, but much less than unity for nonflaming fires.

The smoke data suggest that for Group 1A cables (nonthermal damage is not expected), smoke yield is less than 0.03 g/g and mass optical density is less than 0.11 m^2/g. Figure 4 shows the optical density per unit pathlength in large-scale cable fires for a Group 1A cable and a group 1B cable. Since the optical density per unit pathlength is proportional to smoke concentration (Eq 6), the data in Fig. 4 show that the concentration of smoke generated from Group 1A cable is significantly less than the concentration of smoke generated from Group 1B cable.

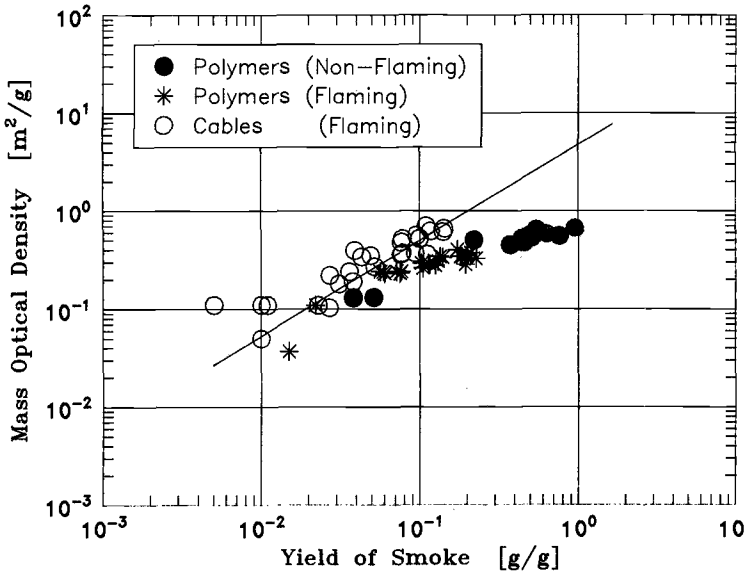

FIG. 3—*Relationship between mass optical density and yield of smoke for flaming and nonflaming fires.*

Copyright by ASTM Int'l (all rights reserved) Wed Feb 07 10:53:32 UTC 2024
Downloaded/printed by
The University of Delaware pursuant to License Agreement. No further reproductions authorized.

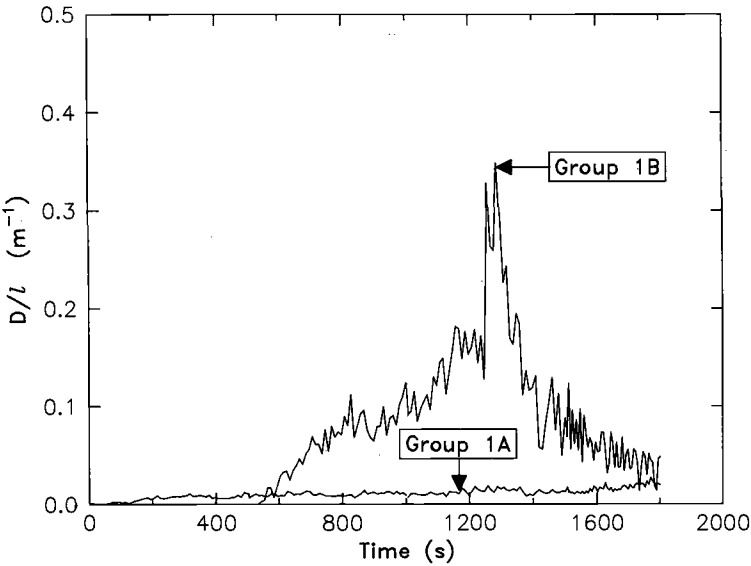

FIG. 4—*Optical density per unit pathlength in large-scale cable fires of a Group 1A and a Group 1B Cable.*

Smoke Corrosivity

In the experiments, ten cables and 0.1 *M* HCl solution and PMMA and PVC research grade polymers as calibration materials were used. Smoke corrosivity was measured in terms of weight loss of mild steel due to corrosion by the fire products.

The corrosion data for 0.1 *M* HCl solution and PVC and PMMA polymers are shown in Fig. 5, where weight loss due to corrosion is normalized by the concentration of HCl and PVC and PMMA vapors (original data are reported in Ref *43*). The corrosion data are linear functions of time, as expected from Eq 13, the slopes being equal to the specific corrosion constants. The corrosion data for PVC and HCl solution are very close to each other, whereas PMMA shows negligible corrosion as expected. The specific corrosion constants are listed in Table 1.

The corrosion data for cables are shown in Fig. 6. The weight loss due to corrosion normalized by the cable vapor concentration is a linear function of time, a relationship similar to the one found for the HCl solution, PVC, and PMMA. The specific corrosion constants for cables determined from the slopes are listed in Table 1. The data have been arranged in terms of halogenated and nonhalogenated materials and are plotted in Fig. 7; specific corrosion constants for 0.1-*M*-HCl solution and PMMA and PVC polymers are also included in the figure.

The specific corrosion constant is one of the fire properties determining the corrosivity of smoke. Under similar heat flux exposure conditions, the specific corrosion constants suggest that fire products from cables with fluorinated insulation and jacketing materials are expected to have the highest corrosivity, about four times the corrosivity expected from the PVC polymer and about 30 times the corrosivity expected from the PVC polymer and about 30 times the corrosivity expected from the nonhalogenated crosslinked polyethylene/crosslinked polyethylene cable. For the cables examined in this study, the data suggest that under similar heat flux exposure conditions, the corrosivity of the fire products of silicone/crosslinked polyolefin cable, crosslinked polyolefin/crosslinked polyolefin cables, and cables

Copyright by ASTM Int'l (all rights reserved) Wed Feb 07 10:53:32 UTC 2024
Downloaded/printed by
The University of Delaware pursuant to License Agreement. No further reproductions authorized.

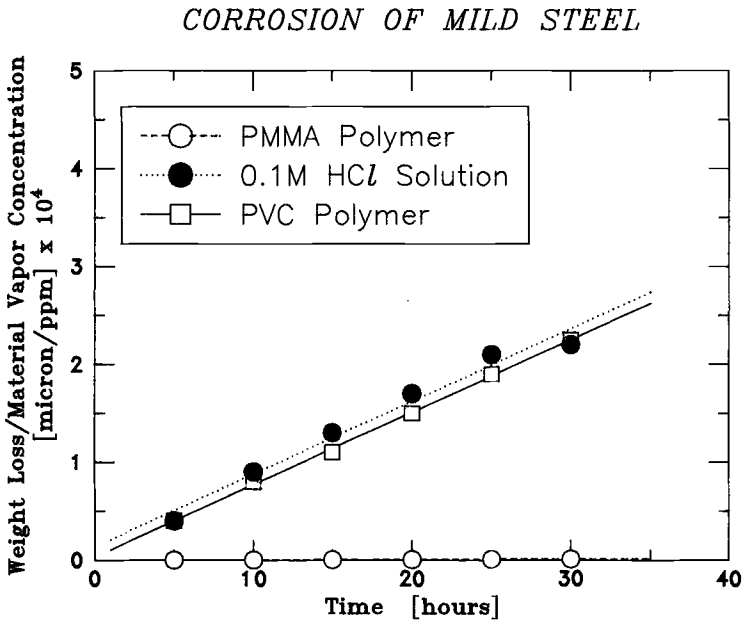

FIG. 5—*Weight loss of mild steel expressed as change in metal thickness per unit concentration of 0.1* M *HCl solution and material vapor concentration of PMMA and PVC polymers.*

TABLE 1—*Specific corrosion constant of material*[a].

Sample	Specific Corrosion Constant (μm/h ppm) $\times 10^4$
NONHALOGENATED POLYMER	
PMMA	0.00047
CABLE	
XLPE/XLPE[b]	0.0092
EPR/XLPO-1	0.039
EPR/XLPO-2	0.040
Si/XLPO	0.059
XLPO/XLPO-1	0.073
XLPO/XLPO-2	0.081
XLPO/XLPO-3	0.093
XLPO/XLPO-4	0.103
EPR	0.076
EPDM	0.085
HALOGENATED SOLUTION	
0.1 *M* HCl	0.074
POLYMER	
PVC	0.073
CABLE	
ECTFE	0.255
PTFE	0.293

[a] Based on corrosion of mild steel by the water-soluble compounds.
[b] No halogenated additives.

Copyright by ASTM Int'l (all rights reserved) Wed Feb 07 10:53:32 UTC 2024
Downloaded/printed by
The University of Delaware pursuant to License Agreement. No further reproductions authorized.

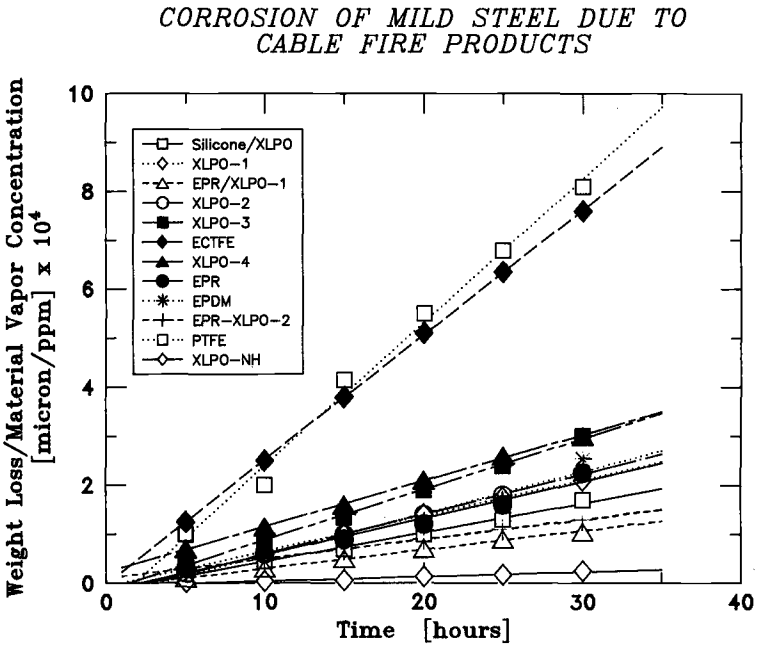

FIG. 6—*Weight loss of mild steel expressed as change in metal thickness per unit material vapor concentration due to corrosion by the water-soluble cable fire products.*

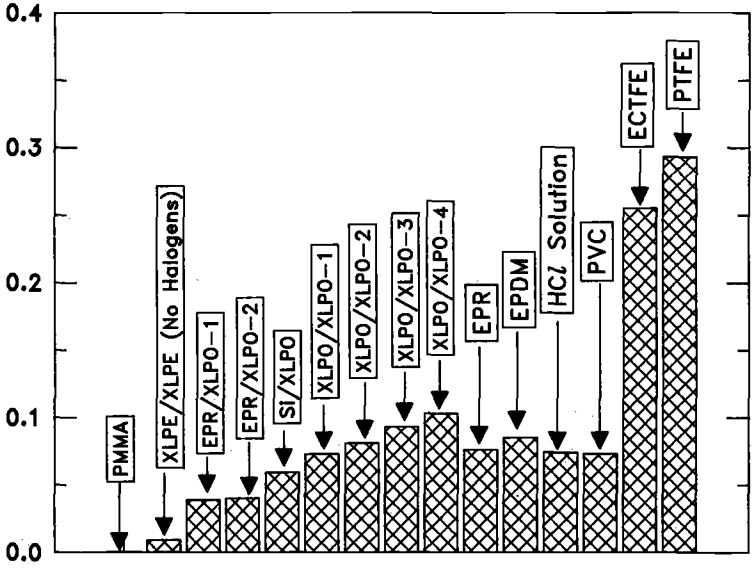

FIG. 7—*Specific corrosion constant (micron/ppm) × 10⁴ of cables, HCl solution, and PVC and PMMA.*

Copyright by ASTM Int'l (all rights reserved) Wed Feb 07 10:53:32 UTC 2024
Downloaded/printed by
The University of Delaware pursuant to License Agreement. No further reproductions authorized.

with copolymer of ethylene and propylene and ethylene, propylene, and nonconjugated diene are expected to be similar to the corrosivity expected from the PVC polymer; corrosivity of these cables is expected due to the additives in the cable insulation and jacketing materials.

The specific corrosion constants also suggest that within the cables with crosslinked polyolefin jackets, fire products of cables with ethylene and propylene copolymer insulation are expected to have lower corrosivity than the fire products from cables with silicone and crosslinked polyolefin insulations. A comparison of specific corrosion constants suggests that nonthermal fire damage is not expected from the cable fire products if the constants are less than 0.92×10^{-6} μm/h ppm.

Summary

During fire propagation, electrical cables are expected to generate heat and smoke. Smoke is defined as a mixture of solid, liquid, and gaseous compounds generated in the fire. Generation of heat and smoke follows the fire propagation rate, which is characterized by the Fire Propagation Index.

Cables have been classified into three groups:

1. Group 3: cables with rapid self-sustained fire propagation rate. The Fire Propagation Index is equal to or greater than 20. Both thermal (heat) and nonthermal (smoke) fire damages are expected.
2. Group 2: self-sustained fire propagation rate not as rapid as the rate for Group 3 cables. Both thermal and nonthermal fire damages are expected, although the severity is expected to be less than it is for Group 3 cables.
3. Group 1: cables are expected to have difficulty in sustaining fire propagation, unless external heat flux is present or cables are overheated due to electrical faults. The Fire Propagation Index is less than 10. Thermal fire damage is not expected. Also for Group 1A cables, nonthermal fire damage is not expected, but it is expected for Group 1B cables.

Tentatively, the data from the study suggest that nonthermal fire damage is not expected if the following conditions are satisfied: (1) Fire Propagation Index is less than 10; (2) yield of smoke is less than 0.03 g/g; (3) mass optical density is less than 0.11 m^2/g; and (4) the specific corrosion constant of the cable is less than 0.92×10^{-6} μm/h ppm. These conditions need to be examined in detail and validated through experiments.

References

[1] *Fire and Smoke: Understanding the Hazards,* Committee on Fire Toxicology, Board on Environmental Studies and Toxicology Commission on Life Sciences, National Research Council, National Academy Press, Washington, DC, 1986.

[2] Purser, D. A., "Toxicity Assessment of Combustion Products," Chap. 14, Sec. 1, p. I-200 in *The SFPE Handbook of Fire Protection Engineering,* P. J. DiNenno, Ed., National Fire Protection Association, Quincy, MA, 1988.

[3] Kaplan, H. L., Grand, A. F., and Hartzell, G. E., "A Critical Review of the State-of-the-Art of Combustion Toxicology," Final Report SWRI Project No. 01-6862, Southwest Research Institute, San Antonio, TX, June 1982.

[4] Anderson, R. C., Croce, P. A., Feeley, F. G., and Sakura, J. D., "Study to Assess the Feasibility of Incorporating Combustion Toxicity Requirements into Building Material and Furnishing Codes of New York State, Vols. 1, 2, and 3, Technical Reports Reference 88712, Arthur D. Little, Inc., Cambridge, MA, May 1983.

[5] Yao, C., "Early Suppression Fast Response Sprinkler Systems," *Chemical Engineering Progress,* September 1988, p. 38.

Copyright by ASTM Int'l (all rights reserved) Wed Feb 07 10:53:32 UTC 2024
Downloaded/printed by
The University of Delaware pursuant to License Agreement. No further reproductions authorized.

[6] "Where There's Smoke," Factory Mutual Research Corp. update, Vol. 1, No. 2, E. K. Casaccio, Ed., Factory Mutual Research Corp., Norwood, MA, May 1987.
[7] *Particulate Carbon Formation During Combustion,* D. C. Siegla, and G. W. Smith, Eds., Plenum Press, New York, NY, 1981.
[8] Goldberg, E. D., *Black Carbon in the Environment—Properties and Distribution,* John Wiley & Sons, New York, NY, 1985.
[9] Haynes, B. S. and Wagner, H. G., "Soot Formation," *Prog. Energy Combustion Science,* Vol. 7, 1981, p. 229.
[10] Calcote, H. F., "Mechanisms of Soot Formation in Flames—A Critical Review," *Combustion and Flame,* Vol. 42, 1981, p. 215.
[11] Smith, O. I., "Fundamentals of Soot Formulation in Flames with Application to Diesel Engine Particulate Emissions," *Prog. Energy Combustion Science,* Vol. 7, 1981, p. 275.
[12] Senkan, S. M., Robinson, J. M., and Gupta, A. K., "Sooting Limits of Chlorinated Hydrocarbon-Methane-Air Premixed Flames," *Combustion and Flame,* Vol. 49, 1983, p. 305.
[13] Mclintock, I. S., "The Effect of Various Diluents on Soot Production in Laminar Ethylene Diffusion Flames," *Combustion and Flame,* Vol. 12, 1968, p. 217.
[14] Muller-Dethlefs, K. and Schlader, A. F., "The Effect of Steam on Flame Temperature, Burning Velocity and Carbon Formation in Hydrocarbon Flames," *Combustion and Flame,* Vol. 27, 1976, p. 205.
[15] Saito, F., "Smoke Generation from Building Materials," *Fifteenth Symposium (International) on Combustion,* The Combustion Institute, Pittsburgh, PA, 1974, p. 269.
[16] Bankston, C. P., Zinn, B. T., Browner, R. F., and Powell, E. A., "Aspects of the Mechanism of Smoke Generation by Burning Materials," *Combustion and Flame,* Vol. 41, 1981, p. 273.
[17] Morikawa, T., "Evolution of Soot and Polycylic Aromatic Hydrocarbons from Combustion and Pyrolysis of Polymers and Low Molecular Weight Hydrocarbons," *Fire Science and Technology,* Vol. 4, 1984, p. 27.
[18] Pasternak, M., Zinn, B. T., and Browner, R. F., "Studies of the Chemical Mechanism of Smoke Particulates Formation During the Combustion of Chlorinated Polymers," *Combustion Science and Technology,* Vol. 28, 1982, p. 263.
[19] Boudene, C., Jouany, J. M., and Truhaut, R., "Protective Effect of Water Against Toxicity of Pyrolysis and Combustion Products of Wood and Poly (Vinyl Chloride)," *Journal of Macromol, Science-Chemistry,* Vol. AIII (8), 1977, p. 1529.
[20] Tewarson, A., "Experimental Evaluation of Flammability Parameters of Polymeric Materials," Chap. 3, p. 97 in *Flame Retardant Polymeric Materials,* Vol. 3, M. Lewin, S. M. Atlas, and E. M. Pearce, Eds., Plenum Press, New York, NY, 1982.
[21] Tewarson, A., "Particulate Formulation in Fires," Large-Scale Fire Phenomenology Conference, Washington, DC, Defense Nuclear Agency, September 1984.
[22] Tewarson, A., "Prediction of Fire Properties of Materials, Part I: Aliphatic and Aromatic Hydrocarbons and Related Polymers," Technical Report J. I. OK3R3.RC, Factory Mutual Research Corp., Norwood, MA, July 1986.
[23] Crutzen, P. J., Galbally, I. E., and Bruhl, C., "Atmospheric Effects from Post-Nuclear Fires," *Climatic Change,* Vol. 6, 1984, p. 324.
[24] Tewarson, A., "Generation of Heat and Chemical Compounds in Fires," Chap. 1–13, p. 1–179 in *The SFPE Handbook of Fire Protection Engineering,* P. J. DiNenno, Ed., National Fire Protection Association Press, Quincy, MA, 1988.
[25] Mulholland, G. W., "Smoke Production and Properties," Chap. 1–25, p. 1–368 in *SFPE Handbook of Fire Protection Engineering,* P. J. DiNenno, Ed., National Fire Protection Association Press, Quincy, MA, 1988.
[26] Heskestad, G., "Fire Plumes," Chap. 1–6, p. 1–107 in *SFPE Handbook of Fire Protection Engineering,* P. J. DiNenno, Ed., National Fire Protection Association Press, Quincy, MA, 1988.
[27] Jaluria, Y., "Natural Convection Wall Flows," Chap. 1–7, p. 1–116 in *SFPE Handbook of Fire Protection Engineering,* P. J. DiNenno, Ed., National Fire Protection Association Press, Quincy, MA, 1988.
[28] Emmons, H., "Vent Flows," Chap. 1–8, p. 1–130 in *SFPE Handbook of Fire Protection Engineering,* P. J. DiNenno, Ed., National Fire Protection Association Press, Quincy, MA, 1988.
[29] Cooper, L. Y., "Compartment Fire Generated Environment and Smoke Filling," Chap. 2–7, p. 2–116 in *SFPE Handbook of Fire Protection Engineering,* P. J. DiNenno, Ed., National Fire Protection Association Press, Quincy, MA, 1988.
[30] Hinkley, P. L., "Smoke and Heat Venting," Chap. 2–3, p. 2–33 in *SFPE Handbook of Fire Protection Engineering,* P. J. DiNenno, Ed., National Fire Protection Association Press, Quincy, MA, 1988.

Copyright by ASTM Int'l (all rights reserved) Wed Feb 07 10:53:32 UTC 2024
Downloaded/printed by
The University of Delaware pursuant to License Agreement. No further reproductions authorized.

[31] Klote, J. H., "Smoke Control," Chap. 3-9, p. 3-143 in *SFPE Handbook of Fire Protection Engineering,* P. J. DiNenno, Ed., National Fire Protection Association Press, Quincy, MA, 1988.
[32] Tewarson, A., "Mass Optical Density of Smoke in Small and Large-Scale Fires," Factory Mutual Research Corp., Norwood, MA (paper to be published).
[33] Fontana, M. G. and Greene, N. D., *Corrosion Engineering,* McGraw-Hill Book Company, New York, NY, 1978.
[34] Bellan, J. and Elghobashi, S., "Corrosive Effects of Burning Fuels," NASA Technical Brief Vol. 9, No. 2, Item 96, NASA Contract No. NAS 7-100, Jet Propulsion Laboratory, California Institute of Technology, Pasadena, CA, 1985.
[35] Comizzoli, R. B., Frankenthal, R. P., Milner, P. C., and Sinclair, J. D., "Corrosion of Electronic Materials and Devices," *Science,* Vol. 234, October 1986.
[36] *Corrosion and Deposits from Combustion Cases: Abstracts and Index,* J. E. Radway, Ed., Hemisphere Publishing Corp., Washington, DC, 1985.
[37] Reid, W. T., "Corrosion and Deposits in Combustion Systems," Chap. 11, p. 35, in *Combustion Technology, Some Modern Developments,* H. B. Palmer and J. M. Beer, Eds., Academic Press, New York, NY, 1974.
[38] Erlandsson, R. and Strand, G., "An Investigation of Physical Characteristics Indicating Primary or Secondary Electrical Damage," *Fire Safety Journal,* Vol. 8, 1984/85, p. 97.
[39] Sandmann, H. and Widmer, G., "The Corrosiveness of Fluoride-Containing Fire Gases on Selected Steel," *Fire and Materials,* Vol. 10, 1986, p. 4.
[40] Tewarson, A. and Khan, M. M., "Electrical Cables—Evaluation of Fire Propagation Behavior and Development of a Fire Test Protocol," Technical Report J.I. OM2E1.RC, Factory Mutual Research Corp., Norwood, MA, November 1988.
[41] Tewarson, A. and Khan, M. M., "Fire Propagation Behavior of Electrical Cables," *Second International Symposium on Fire Safety Science,* Tokyo, Japan, June 1988, Hemisphere Publishing Co., New York, NY, 1989, p. 791.
[42] Tewarson, A. and Khan, M. M., "Flame Propagation for Polymers in Cylindrical Configuration and Vertical Orientation," *22nd International Symposium on Combustion,* Seattle, WA, August 1988, The Combustion Institute, Pittsburgh, PA, 1988, p. 1231.
[43] Tewarson, A., Khan, M. M., and Steciak, J. S., "Combustibility of Electrical Wire and Cable for Rail Transit Systems, Vol. I, Flammability," Technical Report DOT-TSC-UMTA-83-4.1, U.S. Dept. of Transportation, National Technical Information Service, Springfield, VA, April 1982.
[44] Tewarson, A., "Smoke Point Height and Fire Properties of Materials," Technical Report J.I. OK3R3.RC, Factory Mutual Research Corp., Norwood, MA, May 1988.

DISCUSSION

V. Babrauskas[1] *(written discussion)*—Your data for the relationship between soot yield (g/g) and specific extinction area (m^2/g) show that

$$\text{specific extinction area} \propto (\text{soot yield})^{0.5}$$

The work of all the previous investigators[2-6], by contrast, showed a first-power rather than a square-root dependence. The prestigious Committee on the Atmospheric Effects of Nuclear

[1] NIST, Gaithersburg, MD 20899.
[2] King, T. Y., "Smoke and Carbon Monoxide Formation from Materials Tested in the Smoke Density Chamber, NBSIR 75-901, National Bureau of Standards, Gaithersburg, MD, 1975.
[3] Seader, J. D. and Ou, S. S., "Correlation of the Smoking Tendency of Materials," *Fire Research,* Vol. 1, 1977, pp. 3-9.
[4] Crutzen, P. J., Galbally, I. E., and Bruhl, C., "Atmospheric Effects from Post-Nuclear Fires," *Climatic Change,* Vol. 6, 1984, pp. 323-364.
[5] Wolff, G. T., et al., "Particulate Carbon at Various Locations in the United States," *Particulate Carbon Atmospheric Life Cycle,* G. T. Wolff, R. L. Klimisch, Eds., Plenum, New York, 1982, pp. 297-315.
[6] Gerber, H. and Hindman, E., "Data Collation, *Light Absorption by Aerosol Particles,* H. E. Gerber and E. E. Hindman, Eds., Spectrum Press, Hampton, VA, 1982, pp. 387-393.

Copyright by ASTM Int'l (all rights reserved) Wed Feb 07 10:53:32 UTC 2024
Downloaded/printed by
The University of Delaware pursuant to License Agreement. No further reproductions authorized.

Explosions also adopted a linear relationship[7]. A linear relationship, of course, assumes that combustion conditions are kept constant, *i.e.,* pyrolyzing and flaming data are not intermixed.

Could you (1) explain what is different about your experimental conditions compared to the earlier work and (2) offer an explanation based on aerosol optics theory that might suggest why such a square-root dependence could come about?

A. Tewarson (author's closure)—We have extensive data on smoke (Refs *20* and *24* of this paper) which have been used by many researchers (some of your references) for various applications such as the atmospheric effects of nuclear explosions.

As indicated in our paper under Concepts, and in Fig. 3 of our paper,

$$\text{MOD} \propto Y_s^p$$

where $p \approx 1.0$ for flaming fires and $p \ll 1.0$ for nonflaming fires. Our data in Fig. 3 pertain to flaming and nonflaming fires and well-ventilated and underventilated conditions.

As conditions change from flaming to nonflaming and from well-ventilated to underventilated, the ratio of the amounts of solid particulates (predominantly solid carbon) to liquid particulates (no solid carbon) decreases. The aerosol optics theory used for fire smoke assumes particulates to be pure solid carbon; thus it is difficult to use the theory to explain our experimental correlations.

[7] Committee on the Atmospheric Effects of Nuclear Explosions, *The Effects on the Atmosphere of a Major Nuclear Exchange,* National Research Council, Washington, 1985.

Copyright by ASTM Int'l (all rights reserved) Wed Feb 07 10:53:32 UTC 2024
Downloaded/printed by
The University of Delaware pursuant to License Agreement. No further reproductions authorized.

Smoke Characterization

Copyright by ASTM Int'l (all rights reserved) Wed Feb 07 10:53:32 UTC 2024
Downloaded/printed by
The University of Delaware pursuant to License Agreement. No further reproductions authorized.

Jeffrey S. Newman[1]

Smoke Characterization in Enclosure Environments

REFERENCE: Newman, J. S., **"Smoke Characterization in Enclosure Environments,"** *Characterization and Toxicity of Smoke, ASTM STP 1082,* H. K. Hasegawa, Ed., American Society for Testing and Materials, Philadelphia, 1990, pp. 121–134.

ABSTRACT: Experimental results from fire tests conducted with well-defined fire sources in large enclosures are presented which demonstrate the applicability of previously derived relationships to heat/smoke transport and smoke characterization within enclosure environments. Smoke concentrations are found to be conserved quantities which are readily predicted from fire source quantification. While the impact of forced ventilation needs to be further addressed, ventilation is shown to have a significant effect on fuel combustion chemistry.

KEY WORDS: smoke, fire modeling, heat/smoke transport, enclosure-environments

Nomenclature

A	$g/c_pT_o\rho_o$
$Ah^{1/2}/\dot{m}_f$	Ventilation parameter ($m^{5/2}$ s/kg)
$\bar{c}$	Average coefficient of particulate extinction
$C^*_{i,p}$	Nondimensional concentration of i with exponent p
c_p	Specific heat of air (kJ/g K)
C_i	Concentration of product i (g/m^3)
f_s	Generation efficiency (g particulates/g fuel)
f_v	Particulate volume/gas volume
g	Acceleration of gravity (m/s^2)
H	Characteristic ceiling height (m)
H_c	Convective heat of combustion (kJ/g)
I	Light intensity
k_s	Maximum theoretical yield (g carbon/g fuel)
l	Optical path length (m)
p	Fire-growth exponent
$\dot{Q}_c$	Convective heat release rate (kW)
r	Radius from fire axis (m)
r_m	Most probable particle radius (m)
T	Gas temperature (K)
ΔT	Gas temperature rise above ambient (K)
ΔT^*_p	Nondimensional temperature rise with exponent p
t	Time (s)

[1] Research specialist, Factory Mutual Research Corp., Norwood, MA 02062.

Copyright by ASTM Int'l (all rights reserved) Wed Feb 07 10:53:32 UTC 2024
Copyright © 1990 by ASTM International www.astm.org
Downloaded/printed by
The University of Delaware pursuant to License Agreement. No further reproductions authorized.

t_o Reference or transit time (s)
t_o^* Nondimensional transit time with exponent p
t_p^* Nondimensional time with exponent p
x Vectorial location of observation point
Y_i Yield of product i (g_i/g fuel)
Y_p Yield of particles (#/g fuel)

Greek

α_c Fire intensity parameter (kW/s^p)
β_i Yield of i per unit energy release (g/kJ)
λ Wavelength (m)
ρ Density (g/m^3)
τ_λ Turbidity or extinction coefficient (1/m)

Subscripts

CO_2 Carbon dioxide
i Product i
o Initial or reference
g Gaseous mixture of smoke diluted with air
s Solid aerosol or particulate

Introduction

The characterization of "smoke" requires increasingly more specific information concerning instantaneous particulate properties, particularly when assessing fire environments in enclosures. Optical techniques to characterize smoke particulates are especially attractive since they provide continuous measurements without disturbing the environment. Previous work [*1*,*2*] has detailed the application of a multiple wavelength optical technique which, when coupled with theoretical considerations, provides a simple reliable method of quantifying characteristics of smoke particulates from diffusion fires. In addition, it has been recently demonstrated [*3*] that yields of chemical compounds and smoke particulate characteristics can change dramatically with a change in ventilation conditions, such as in an enclosure environment where the supply of air may be restricted. For example, quantifying changes in particulate properties is shown to be useful in addressing the impact of ventilation on fire chemistry, which in turn relates to the smoke toxicity of a given fire scenario.

This paper deals with our current experimental study on smoke transport and characterization in large enclosure fires to complement detailed laboratory results for smoke particulate properties (e.g., volume fraction, mass concentration, generation efficiency, particulate size, and particulate yield).

Smoke Characterization

When a monochromatic beam of light passes through smoke, the fraction of light transmitted can be expressed as

$$I/I_o = e^{(-\tau\lambda l)} \tag{1}$$

Copyright by ASTM Int'l (all rights reserved) Wed Feb 07 10:53:32 UTC 2024
Downloaded/printed by
The University of Delaware pursuant to License Agreement. No further reproductions authorized.

where

I = the transmitted intensity,
I_o = the initial intensity,
τ_λ = the turbidity or extinction coefficient of the smoke (1/m), and
l = the optical path length (m).

The turbidity (often referred to as the optical density) is a complex function of the particle radius, the particle size distribution, the particle extinction efficiency, the incident wavelength, and the complex refractive index of the smoke. It is useful to extend the measurement of τ_λ to fundamental smoke properties. The following discussion summarizes previous work [*1*,*2*] which results in simplified expressions for several smoke characteristics based upon extinction measurements.

Using Mie scattering theory to calculate the extinction efficiency for homogeneous spherical particles, values of the most probable particle size (i.e., the mode of the particle size distribution), r_m, were calculated and tabulated as a function of a nondimensional extinction coefficient. For a variety of materials studied, r_m varied over the range from 0.04 to 0.09 μm (typically 0.065 to 0.085 μm). Within the typical particle size range encountered, an average coefficient of particle extinction, $\bar{c}$, was found such that

$$f_v = \frac{\tau_\lambda \lambda}{\bar{c}} \tag{2}$$

where

f_v = the particulate volume fraction,
λ = the incident wavelength, and
$\bar{c} \simeq 7.0$.

In addition, it was shown that the following simple expression for particulate mass concentration, C_s (g/m^3), could be written for the various materials investigated in overventilated flaming conditions

$$C_s = \rho_s f_v = \frac{\rho_s \tau_\lambda \lambda}{\bar{c}} \tag{3}$$

where $\rho_s \simeq 1.1 \times 10^6$ g/m^3.

The generation efficiency of particulates is therefore

$$f_s = \frac{\rho_s}{\rho_g k_s} f_v \tag{4}$$

where

ρ_g = the density of mixture of smoke diluted with air (g/m^3), and
k_s = the maximum theoretical yield of particulates expected on complete conversion of fuel carbon to particulates.

Finally, the yield of particulates, Y_p, can be defined by the following expression

$$Y_p = \frac{f_v}{18.62 \rho_g r_m^3} \tag{5}$$

Copyright by ASTM Int'l (all rights reserved) Wed Feb 07 10:53:32 UTC 2024
Downloaded/printed by
The University of Delaware pursuant to License Agreement. No further reproductions authorized.

TABLE 1—*Particulate properties for various fuels.*[a]

Fuel	k_s	r_m (μm)	Y_p (10^{12}/g)	f_s
Coal	0.99	0.078	6.8	0.068
Polystyrene	0.92	0.078	13.2	0.140
Kerosene	0.87	0.073	8.4	0.077
Polypropylene	0.86	0.079	5.4	0.063
Polyethylene	0.86	0.077	4.5	0.049
Propylene	0.86	0.076	7.0	0.073
Ethylene	0.86	0.072	1.9	0.017
Heptane	0.84	0.077	2.7	0.030
Propane	0.82	0.068	2.7	0.021
Nylon	0.64	0.075	7.5	0.100
PMMA	0.60	0.068	2.2	0.023
Douglas fir	0.53	0.062	0.34	0.003
	CHLORINATED COMPOUNDS			
Polyethylene/Cl	0.56	0.090	8.6	0.240
Polychloroprene	0.55	0.090	6.6	0.180
PVC	0.39	0.083	7.7	0.230
Styrene Butadiene Rubber/Cl	0.29	0.073	15.2	0.420

[a] Taken from Ref *2*.

where the numerical constant is derived explicitly from integration of the particle size distribution. Table 1 summarizes k_s, r_m, Y_p, and f_s for the fuels studied.

Scaling Theory for Fire Product Transport

Scaling relationships have been developed [*4*] for the transport of fire products generated by "power-law" fires. By definition, the convective heat release rate of a power-law fire, $\dot{Q}_c$, varies as some power of time

$$\dot{Q}_c = \alpha_c t^p \tag{6}$$

where

α_c = the fire intensity parameter, kW/s^p,
t = the time, s, and
p = the order of the fire.

The scaling theory is based on maintaining constant Froude number and predicts the following functional relationships for geometrically similar enclosures

$$\Delta T_p^* = fn(t_p^*, x/H) \tag{7}$$

$$C_{i,p}^* = fn(t_p^*, x/H) \tag{8}$$

where

ΔT_p^* = the nondimensional temperature rise (with the subscript p signifying a dependence on the exponent p),
t_p^* = the nondimensional time,
x/H = the nondimensional vectorial coordinate with H a characteristic ceiling height, m, and
$C_{i,p}^*$ = the nondimensional concentration of product i.

Copyright by ASTM Int'l (all rights reserved) Wed Feb 07 10:53:32 UTC 2024
Downloaded/printed by
The University of Delaware pursuant to License Agreement. No further reproductions authorized.

The nondimensional variables are related to corresponding physical quantities by the following expressions

$$\Delta T_p^* = [A^{-2/(3+p)} T_o^{-1} g] \alpha_c^{-2/(3+p)} H^{(5-p)/(3+p)} \Delta T \tag{9}$$

$$C_{i,p}^* = A^{-(1+p)/(3+p)} \alpha_c^{2/(3+p)} H^{-(5-p)/(3+p)} \beta_i \tag{10}$$

$$t_p^* = A^{1/(3+p)} \alpha_c^{1/(3+p)} H^{-4/(3+p)} (t - t_o) \tag{11}$$

where

ΔT = the gas temperature rise relative to ambient, K,
β_i = Y_i/H_c, with Y_i the yield of product i per unit mass of fuel consumed (g/g) and H_c the convective heat of combustion (kJ/g),
t_o = a reference time selected for convenience, s, and
A = $g/(c_p T_o \rho_o)$, with g = acceleration of gravity (m/s^2), c_p = specific heat of air (kJ/g K), T_o = ambient temperature (K), ρ_o = ambient air density (g/m^3).

Experiments

Experiments were performed in a large heavily instrumented enclosure with dimensions of 18.29 by 12.19 by 6.10 m high (60 by 40 by 20 ft high). A number of fire sources were investigated including heptane, methanol, propylene, PMMA, and various electrical cable types and configurations with variable forced ventilation conditions from 1 to 10 room changes per hour. Simultaneous gas temperature and multiwavelength smoke extinction measurements were made as well as multiplexed gas concentration measurements (i.e., carbon dioxide, carbon monoxide, oxygen, and hydrocarbons).

Results

Test data from three fire tests have been selected for initial analysis in order to develop baseline relationships for the transport of fire products in enclosures, e.g., heat and smoke particulates. The selected fire tests had well-defined fire sources—a steady heat release rate propylene gas fire, a growing propylene fire, and a heptane pan fire. Forced ventilation conditions were all fixed at one change per hour, i.e., essentially quiescent ambient preignition conditions.

Heat Release Rates

Figure 1 plots the convective heat release rate, $\dot{Q}_c$, versus time for each of the three selected fires. Each fire is identified by the appropriate α_c and p as determined by Eq 6. The two propylene fires were obtained using a 0.91-m-dia, 0.58-m-high calibrated sand burner described in Ref 5. The order zero fire ($p = 0$) was a step change fire with a value of α_c of 304 kW. (It should be noted that for steady fires α_c is equivalent to $\dot{Q}_c$.) The second order fire ($p = 2$) was a programmed fire designed to precisely follow Eq 6 with a value for α_c of 0.00523 kW/s^2. The third fire was a heptane pan fire, which was represented well by $p = ½$ with a corresponding value of 24.6 kW/s$^{1/2}$ for α_c. Even though there is considerable scatter in this representation (as indicated by comparison between the solid line and symbols in the figure), subsequent analysis will demonstrate this discrepancy is not significant.

Copyright by ASTM Int'l (all rights reserved) Wed Feb 07 10:53:32 UTC 2024
Downloaded/printed by
The University of Delaware pursuant to License Agreement. No further reproductions authorized.

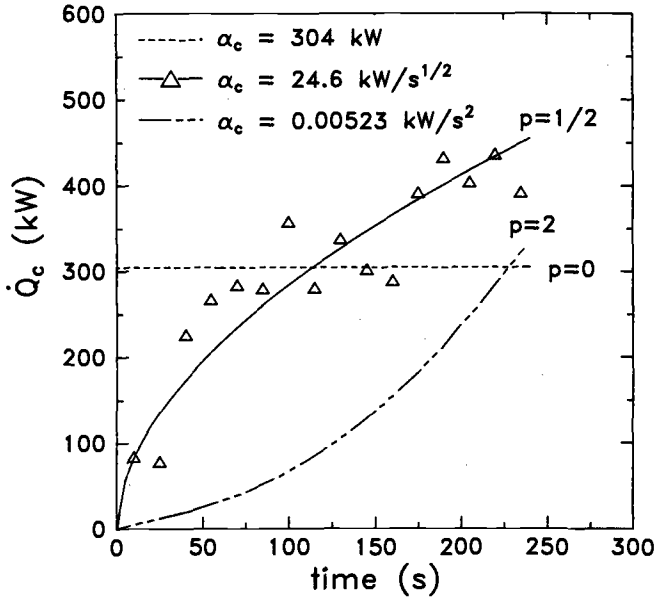

FIG. 1—*Convective heat release rate versus time for a step change propylene sand burner fire (*p = *0), growing propylene sand burner fire (*p = *2), and heptane pan fire (*p = ½*).*

Transit Times

The determination of the correct functionality of the scaled temperature, ΔT_p^*, and scaled concentrations, $C_{i,p}^*$, on scaled time, t_p^*, as represented by Eqs 7 and 8, require the selection of an appropriate reference time, t_o, in order to evaluate t_p^* in Eq 11. It was determined that the total (vertical plus horizontal) transit time of the fire product front from the fire source surface to any location of interest served as a useful time reference. Figure 2 gives the scaled transit time, t_o^*, versus nondimensional radial distance r/H (where r = radial distance from the fire axis, m), for the three different p fires. The data indicate similar dependence of the scaled transit times on r/H, irrespective of the order p of the fires, and are fairly well fit by the polynomial equation shown and represented by the line in the figure.

Temperature Distribution

Figure 3 gives an example of the time dependent gas temperature rise (ΔT) measured in the layer of the flow underneath the ceiling extending to depths of ~0.05 H, where excess temperatures and velocities are fairly constant at their local maximum values [*6–8*]. The data from Fig. 3 for each of the three p fires are replotted in Fig. 4 in the forms defined by Eqs 9 and 11 for the scaled gas temperature rise, ΔT_p^*, and time, t_p^*, respectively. In the formulation of t_p^*, the reference time is the transit time as given in Fig. 2. While each set of data is well fit by a straight line on the log-log plot in Fig. 4, both the slope and coefficient of each line are observed to be a separate function of p.

Similar plots to Fig. 4 can be made for each r/H value, which, for brevity, have not been included. The general trend is for the scaled temperature profile to steepen and the magnitude to reduce with increasing r/H, presumably due to ceiling heat losses. The following

Copyright by ASTM Int'l (all rights reserved) Wed Feb 07 10:53:32 UTC 2024
Downloaded/printed by
The University of Delaware pursuant to License Agreement. No further reproductions authorized.

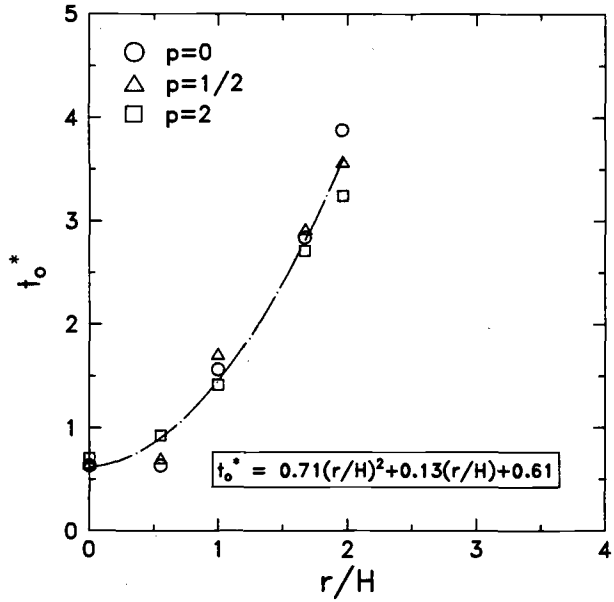

FIG. 2—*Scaled transit times versus nondimensional radial distance.*

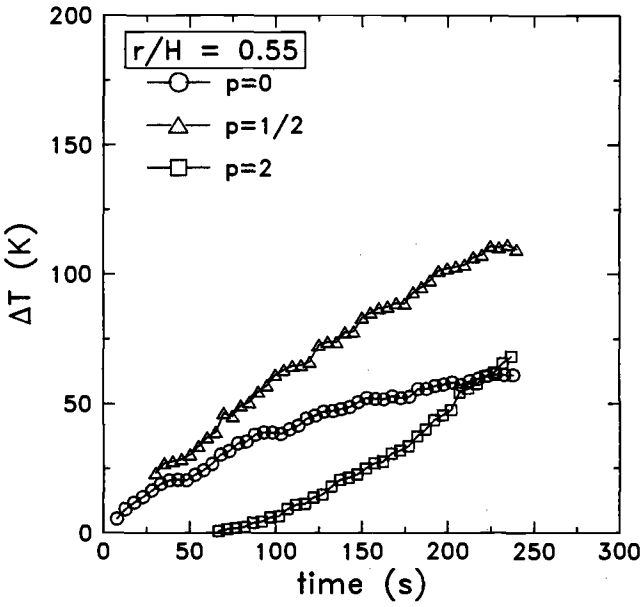

FIG. 3—*Near maximum gas temperature rise versus time for* r/H = *0.55.*

Copyright by ASTM Int'l (all rights reserved) Wed Feb 07 10:53:32 UTC 2024
Downloaded/printed by
The University of Delaware pursuant to License Agreement. No further reproductions authorized.

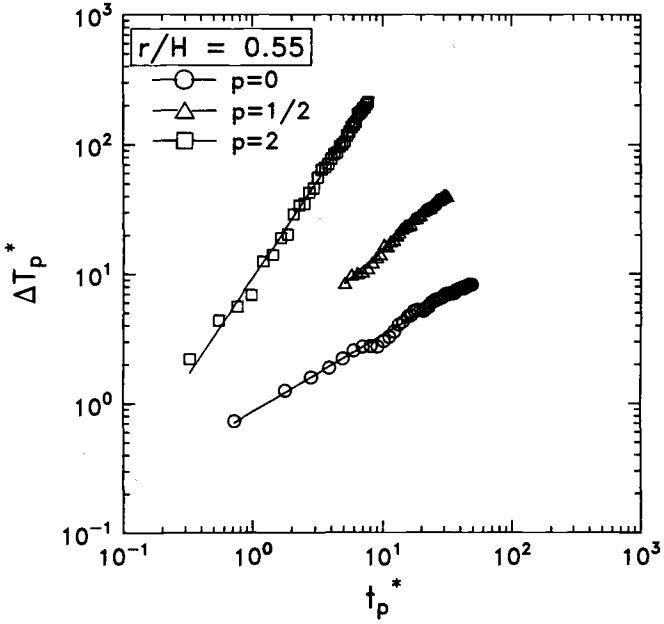

FIG. 4—*Scaled temperature rise versus scaled time at* r/H = *0.55.*

expression has been developed from the simultaneous solution for each measured p profile at several r/H positions

$$\Delta T_p^* = 0.45(3p + 1)\{(r/H)^{-1} t_p^{*(r/H)^{0.25}}\}^{(0.5p+0.75)} \tag{12}$$

It should be noted in Eq 12 that the p and r/H dependence occur both in the exponent as well as the coefficient. Figure 5 is a replot of the data previously given in Fig. 4 using the form of Eq 12. The line of slope and coefficient one in the figure is for comparison purposes, representing an idealized perfect fit. Figures 6 and 7 give similar results for r/H of 1.0 and 1.67, respectively. As indicated by the data in Figs. 5–7, Eq 12 gives a good representation to within ±20% of the general functional relationship from modeling theory (i.e., Eq 8).

Carbon Dioxide Concentration Distribution

The scaled carbon dioxide concentration rise, $C_{CO_2,p}^*$ is plotted in Fig. 8 versus t_p^* for r/H = 0.55 and 1.67. $C_{CO_2,p}^*$ was calculated from Eq 10 using experimentally measured values for β_{CO_2} of 0.0918 and 0.106 g/kJ for propylene and heptane, respectively. It is significant to note that the data from the two radial locations nearly coincide for the same value of p. This reveals that for a conserved quantity like CO_2 (and unlike temperature), there is little dependence of the scaled values with r/H. (It should be noted that if the transit time to each radial position was not considered, the data would not coincide.)

Since at a given r/H the $C_{CO_2,p}^*$ profiles do not match the corresponding ΔT_p^* profiles, it is useful to develop a basis of comparison other than that given by Eq 12. Heat losses should be minimized nearer the fire axis and thus more closely represent the conserved concentra-

Copyright by ASTM Int'l (all rights reserved) Wed Feb 07 10:53:32 UTC 2024
Downloaded/printed by
The University of Delaware pursuant to License Agreement. No further reproductions authorized.

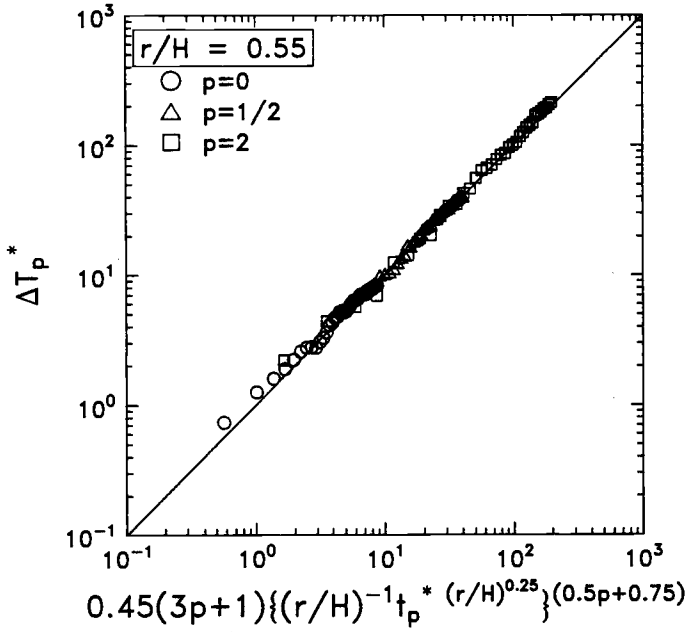

FIG. 5—*Scaled temperature/time correlation for* r/H = *0.55.*

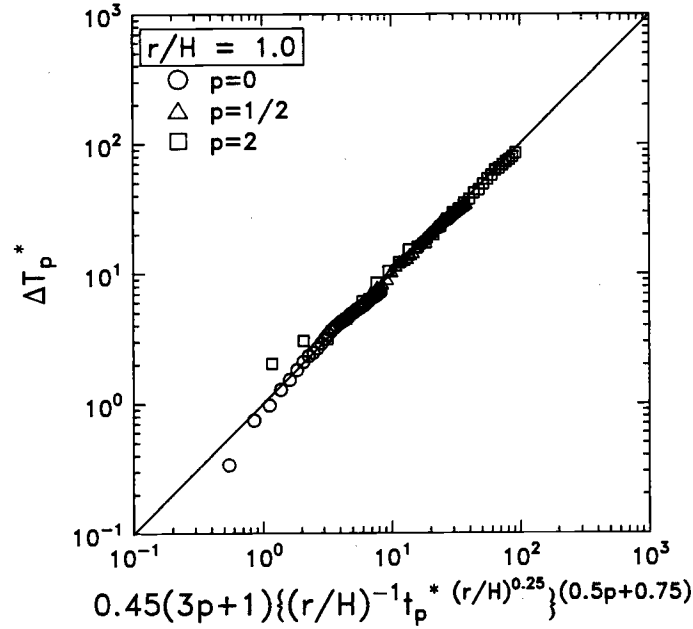

FIG. 6—*Scaled temperature/time correlation for* r/H = *1.0.*

Copyright by ASTM Int'l (all rights reserved) Wed Feb 07 10:53:32 UTC 2024
Downloaded/printed by
The University of Delaware pursuant to License Agreement. No further reproductions authorized.

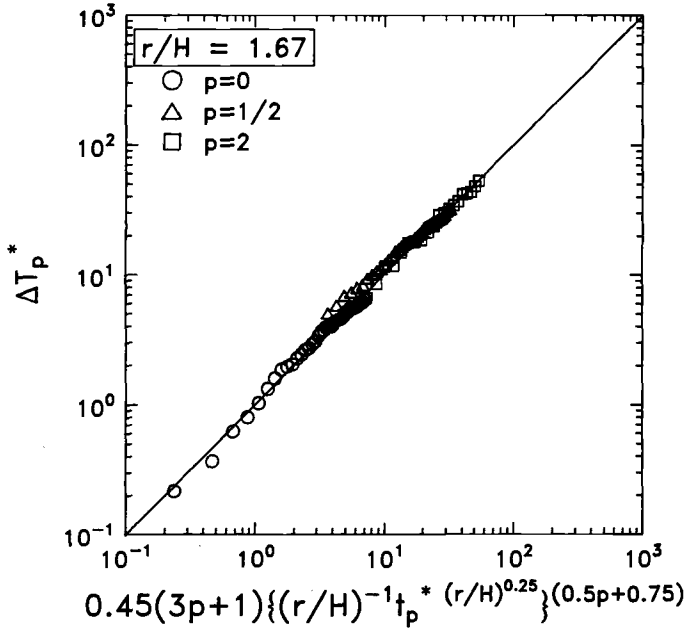

FIG. 7—*Scaled temperature/time correlation for* r/H = *1.67.*

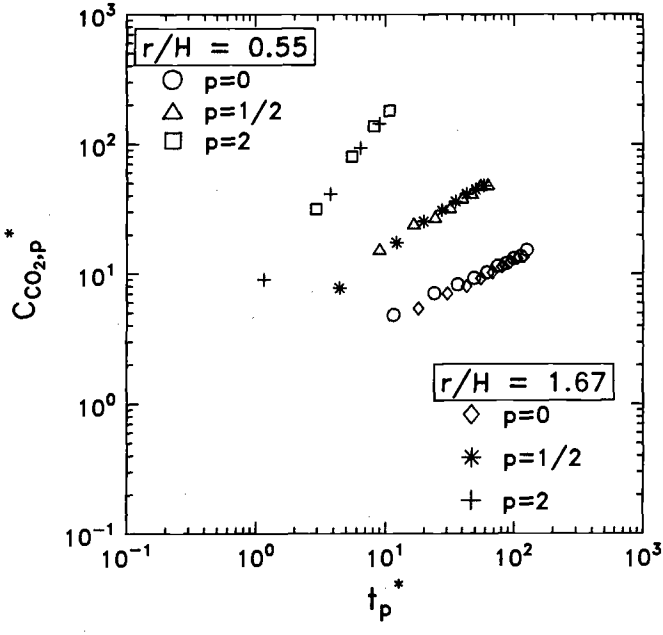

FIG. 8—*Scaled carbon dioxide concentration rise versus scaled time for* r/H = *0.55 and 1.67.*

Copyright by ASTM Int'l (all rights reserved) Wed Feb 07 10:53:32 UTC 2024
Downloaded/printed by
The University of Delaware pursuant to License Agreement. No further reproductions authorized.

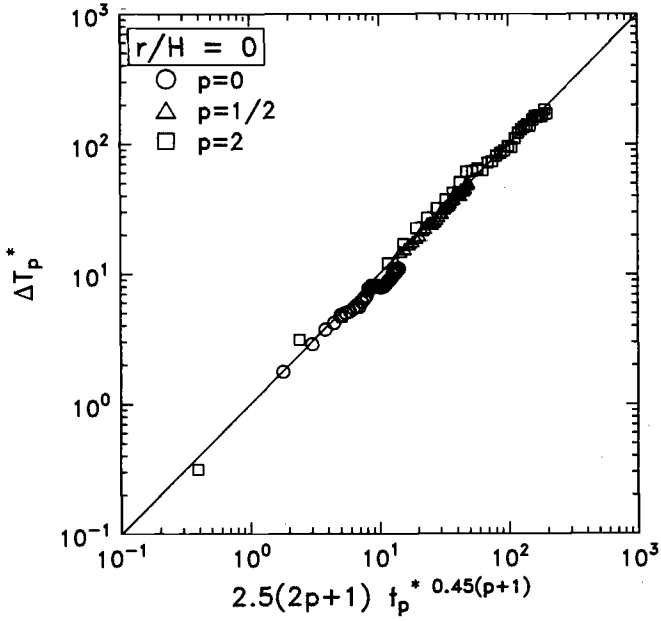

FIG. 9—*Scaled temperature/time correlation for* r/H = *0.*

tion profiles. Figure 9 gives the centerline ($r/H = 0$) scaled temperature as correlated by the following equation

$$\Delta T_p^* = 2.5(2p + 1)t_p^{*0.45(p+1)} \tag{13}$$

Figure 10 plots $C_{CO_2,p}^*$ versus the right hand side of Eq 13 for the data in Fig. 8 with the solid line as an idealized reference. The data for the different p fires collapse nicely with a slope essentially identical to the centerline scaled temperature profile but 38% offset. It is unclear whether this offset is due to concentration losses outside the region where the fire plume impinges on the ceiling or temperature measurement errors. Gas concentration measurement errors are discounted due to data consistency in results from different fire sources (type and growth rate) and different radial positions. However, from a practical standpoint, regardless of the exact explanation, Eq 13 can be rewritten for $C_{CO_2,p}^*$ by multiplying the right hand side by 0.62

$$C_{CO_2,p}^* = 1.6(2p + 1)t_p^{*0.45(p+1)} \tag{14}$$

Smoke Particulate Concentration Distribution

Smoke concentration data were next selected for analysis. Extinction measurements of the form given by Eq 1 were translated into particulate concentration data using Eq 3. $C_{s,p}^*$ was calculated from Eq 10 using experimentally measured values for β_s of 0.00233 and 0.000933 g/KJ for propylene and heptane, respectively. Figure 11 plots $C_{s,p}^*$ versus the correlation parameter containing p and t_p^*, previously given in Figs. 9 and 10. While there is considerably more scatter in the particulate concentration data compared to the CO_2 data, the correlation is again very good, with the data collapsing for both variable p and r/H. It also appears that

Copyright by ASTM Int'l (all rights reserved) Wed Feb 07 10:53:32 UTC 2024
Downloaded/printed by
The University of Delaware pursuant to License Agreement. No further reproductions authorized.

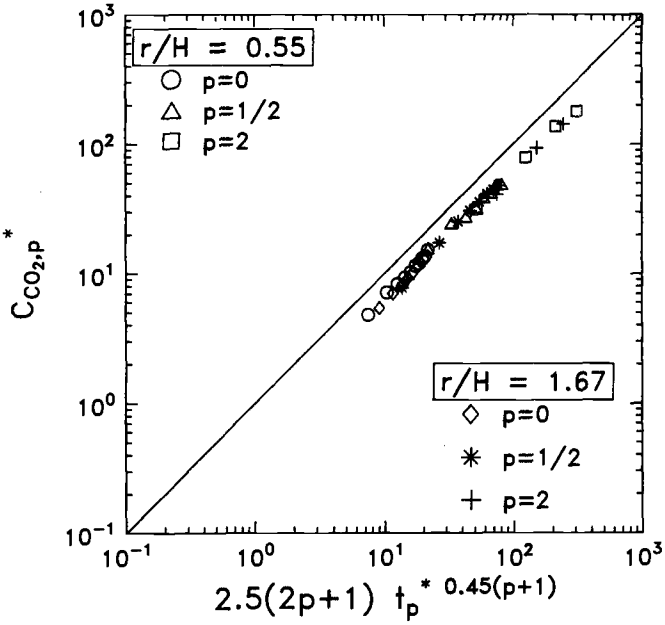

FIG. 10—*Scaled carbon dioxide concentration/time correlation for* r/H = *0.55 and 1.67.*

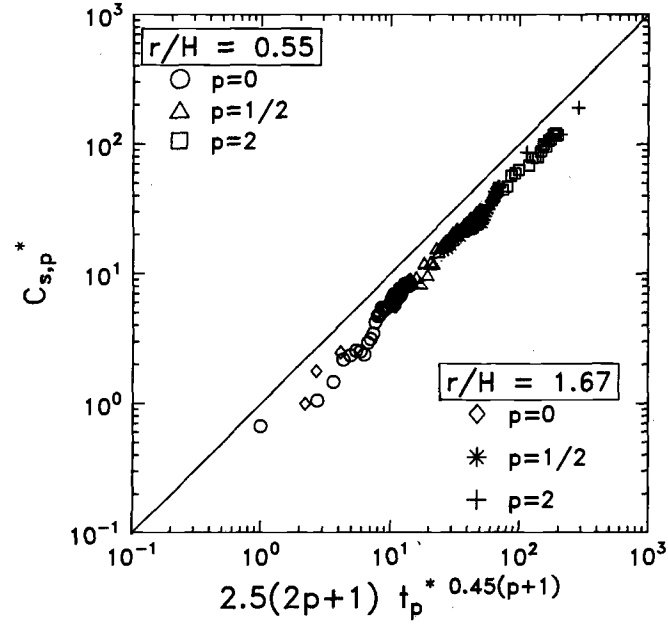

FIG. 11—*Scaled particulate concentration/time correlation for* r/H = *0.55 and 1.67.*

Copyright by ASTM Int'l (all rights reserved) Wed Feb 07 10:53:32 UTC 2024
Downloaded/printed by
The University of Delaware pursuant to License Agreement. No further reproductions authorized.

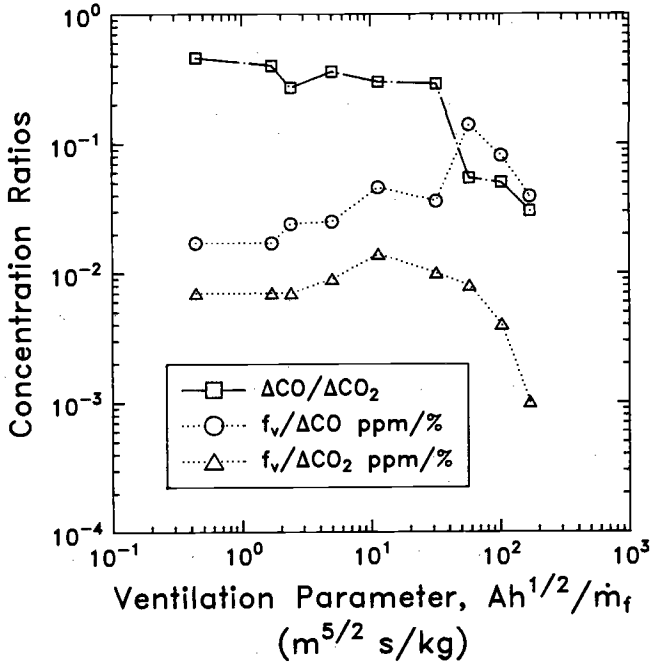

FIG. 12—*Concentration ratios verus ventilation parameter* [2].

the particulate data map onto the CO_2 data, indicating both that particulates are essentially conserved and that Eq 14 is equally applicable to particulates. (It should be noted that particle concentrations may also be assessed using values for Y_p given in Table 1.) Therefore, it appears that Eq 14 can be a useful tool in assessing smoke transport in enclosures.

Ventilation Effects

While the current data have yet to be analyzed for a complete description of the impact of forced ventilation on the enclosure smoke environment, vented enclosure data using wood crib fires from Ref *9* have been previously analyzed [*2*] to demonstrate the dependence of relative gas and particulate concentrations on various ventilation conditions. Figure 12 plots three concentration ratios, $\Delta CO/\Delta CO_2$, $f_v/\Delta CO$ and $f_v/\Delta CO_2$ versus a ventilation parameter. f_v is the particulate volume fraction as defined in Eq 2. The ventilation parameter is given in Ref *9* as $Ah^{1/2}/\dot{m}_f$, where A = vent area (m^2), h = vent height (m), and $\dot{m}_f$ = fuel free (without enclosure) burning rate (kg/s). The data in the figure illustrate a strong effect of ventilation on chemistry, i.e., as ventilation is reduced, fuel carbon is preferentially converted to CO and particulates instead of CO_2. Since the form of Eq 10 assumes constant fuel chemistry, the impact of certain ventilation conditions may need to be considered for general smoke transport correlations in enclosures.

Summary

1. Results have been presented which demonstrate the applicability of previously derived scaling relationships [*4*] to heat and smoke transport in enclosures.

Copyright by ASTM Int'l (all rights reserved) Wed Feb 07 10:53:32 UTC 2024
Downloaded/printed by
The University of Delaware pursuant to License Agreement. No further reproductions authorized.

2. Scaled temperatures are shown to be well-defined time-dependent functions of the fire intensity, fire growth rate, enclosure geometry (i.e., ceiling height), and nondimensional radial distance from the fire axis.

3. Scaled carbon dioxide and smoke concentrations are found to be conserved quantities which are readily predicted from fire source characterization.

4. Forced ventilation effects, although not yet fully characterized, can impact both on smoke transport as well as fuel combustion chemistry.

References

[1] Newman, J. S. and Steciak, J., "Characterization of Particulates from Diffusion Flames," *Combustion and Flame,* Vol. 67, 1987, p. 55.

[2] Newman, J. S. and Steciak, J., "Particulate Generation from Diffusion Flames," *Proceedings,* 1987 ASME/JSME Thermal Engineering Conference Honolulu, Hawaii, 22–27 March, 1987, ASME, New York.

[3] Newman, J. S. and Tewarson, A., "Stoichiometry and Flame Heights in Diffusion Flames," presented at the poster session of the Twenty-Second International Symposium on Combustion, University of Washington, Seattle, WA, 14–19 Aug., 1988, to be published.

[4] Heskestad, G., "Similarity Relations for the Initial Convective Flow Generated by Fire," Paper No. 72-WA/HT-17, American Society of Mechanical Engineers, New York, November 1972.

[5] Heskestad, G. and Hill, J. P., "Experimental Fires in Multiroom/Corridor Enclosures," FMRC J.I. 0J2N8.RU, Factory Mutual Research Corp., Norwood, MA, 1985.

[6] Thomas, P. H., "The Distribution of Temperature and Velocity Due to Fire Beneath Ceilings," Note 141, Fire Research Station, Boreham Wood, Herts, Fire Research, 1955.

[7] Alpert, R. L., "Fire Induced Turbulent Ceiling Jet," Report 19722-2, Factory Mutual Research Corp., Norwood, MA, 1971.

[8] Heskestad, G. and Delichatsios, M. A., "The Initial Convective Flow in Fire," Seventeenth Symposium (International) on Combustion, The Combustion Institute, Pittsburgh, 1979, p. 1113.

[9] Croce, P. A., "Modeling of Vented Enclosure Fires: Part I, Quasi-Steady Wood-Crib Source Fire," FMRC J.I. 7A0R5.GU, Factory Mutual Research Corp., Norwood, MA, July 1978.

Copyright by ASTM Int'l (all rights reserved) Wed Feb 07 10:53:32 UTC 2024
Downloaded/printed by
The University of Delaware pursuant to License Agreement. No further reproductions authorized.

Hao C. Tran[1]

Correlation of Wood Smoke Produced from NBS Smoke Chamber and OSU Heat Release Apparatus

REFERENCE: Tran, H. C., **"Correlation of Wood Smoke Produced from NBS Smoke Chamber and OSU Heat Release Apparatus,"** *Characterization and Toxicity of Smoke, ASTM STP 1082,* H. K. Hasegawa, Ed., American Society for Testing and Materials, Philadelphia, 1990, pp. 135–146.

ABSTRACT: In this study, we examined smoke generation from red oak and Douglas-fir plywood using the National Bureau of Standards (NBS) smoke density chamber in the smoldering mode at 2.0, 2.5, and 3.0 W/cm^2 of heating flux. The data included optical density and particulate (soot) mass concentration, both as a function of time and heating flux. Data from the NBS chamber were compared to data from a dynamic smoke measurement apparatus, the Ohio State University (OSU) calorimeter. Because of basic differences between the NBS chamber and the OSU apparatus and between the units of measurement used in these methods, the results were reduced to a common unit, particulate mass per unit area of exposed specimen surface. Comparison of the data at 2.5 W/cm^2 of heating flux showed reasonable agreement.

KEY WORDS: wood smoke, smoke optical density, particulate concentration

Nomenclature

A	Exposed area of specimen, m^2
C/A	Smoke particulate mass per unit exposed area of specimen, g/m^2
C_s	Particulate concentration of smoke, g/m^3
D	Optical density
D_s	Specific optical density
i	Heating flux, W/cm^2
I	Transmitted light intensity
I_0	Incident light intensity
L	Light path, m
SR	Cumulative (total) smoke release, SMOKE/m^2
SRR	Smoke release rate, SMOKE/min · m^2
t	Time, min
T	Absolute temperature, K
T%	Transmittance, percent
T_i	Absolute temperature of air entering the chamber
T_o	Absolute temperature of air leaving the chamber
V	Chamber volume, m^3
V_i/t	Flow rate of air entering the chamber, m^3/min
V_o/t	Flow rate of air leaving the chamber, m^3/min

[1] Wood scientist, USDA Forest Service, Forest Products Laboratory, Madison, WI 53705-2398.

Copyright by ASTM Int'l (all rights reserved) Wed Feb 07 10:53:32 UTC 2024
Copyright © 1990 by ASTM International www.astm.org
Downloaded/printed by
The University of Delaware pursuant to License Agreement. No further reproductions authorized.

Introduction

Smoke is a general term that describes all products of pyrolysis and combustion. It includes gaseous products, liquid droplets, and solid particles called soot or particulate. Traditionally, smoke is characterized by its ability to block light transmittance, resulting in poor visibility. Thus, test apparatuses such as the National Bureau of Standards (NBS) smoke density chamber, used in ASTM Test Method for Specific Optical Density of Smoke Generated by Solid Materials (E 662-83), have been developed.

The smoke chamber is a sealed box, and smoke is therefore allowed to accumulate. During the process of accumulation, smoke may decay, agglomerate, settle, or recycle through the radiant heater and the flames (if present). Transmittance of a light beam through a fixed light path is continuously monitored. There is a need to compare smoke data produced from the smoke chamber to data from a flow-through apparatus, where smoke is measured continuously as it is produced. In this paper, I will present some smoke data from an Ohio State University (OSU) calorimeter, ASTM Test Method for Heat and Visible Smoke Release Rates for Materials and Products (E 906-83). The OSU data will be compared to data from the NBS smoke chamber by an analogy analysis.

Background

A few definitions are needed in the reduction of test data. Transmittance (T%) is obtained from the ratio of incident light intensity I_0 to transmitted light intensity I

$$T\% = 100(I/I_0) \tag{1}$$

Optical density D is proportional to the concentration of the light-absorbing species according to Lambert-Beer's law and is defined as

$$D = \text{Log}(I_0/I) = \text{Log}(100/T\%) \tag{2}$$

ASTM Method E 662-83 (the NBS smoke chamber) defines specific optical density D_s as

$$D_s = DV/AL \tag{3}$$

where

V = the volume of the chamber,
A = the exposed surface of the specimen, and
L = light path.

D and D_s are dimensionless. For the standard smoke chamber volume and specified specimen size

$V = 0.51\ m^3$,
$A = 0.004\ m^2$,
$L = 0.914$ m, and
$D_s = 132\ D$.

Seader et al. [*1–5*] derived predictive parameters based on particulate mass concentration and specimen mass loss. Parameters such as mass optical density (MOD) and particulate optical density (POD) were suggested. However, the importance of particulate mass concentration in quantifying smoke was recognized. The analysis showed that for a particular

Copyright by ASTM Int'l (all rights reserved) Wed Feb 07 10:53:32 UTC 2024
Downloaded/printed by
The University of Delaware pursuant to License Agreement. No further reproductions authorized.

smoke, with a fixed particle size and density, optical density should be proportional to particulate concentration.

Indeed, King [6] showed that there is a linear relationship between optical density and particulate mass concentration of smoke for some wood and plastic materials. The proportionality constants depend on the type of materials and on whether or not the materials are involved in flaming combustion. Tran [7] showed that the proportionality holds for red oak and Douglas-fir plywood within a range of 2.0 to 3.0 W/cm^2 of heating flux in the smoldering mode in the NBS smoke chamber.

A flow-through apparatus is needed for measuring the smoke release rate (SRR). For this purpose, we used an OSU heat release apparatus. Air is forced through the chamber at a constant rate (0.04 m^3/s). The combustion products flow out of the chamber through a stack, and optical density across the stack is monitored. Smoke data reduction uses Eqs 1 and 2 and the formula for SRR

$$\text{SRR} = \frac{D}{kLA}(V_o/t) \tag{4}$$

$$V_o/t = (V_i/t)(T_o/T_i) \tag{5}$$

where

V_o/t and V_i/t = the flow rates of air leaving and entering the chamber, respectively, and
T_o and T_i = the absolute temperature of air leaving and entering the chamber, respectively.

V_o/t is calculated based on the known flow rate of air entering the chamber and the temperature of the air entering and leaving the chamber. ASTM Method E 906-83 defines the arbitrary unit of SRR as SMOKE/min · m^2. The conversion factor k is therefore 1 m^2/SMOKE. For our chamber, L = 0.134 m, A = 0.0196 m^2, and V_i/t = 2.4 m^3/min.

Experimental

Materials

Two wood products were used in the experiments in both the NBS smoke chamber and the OSU apparatus: red oak and three-ply Douglas-fir plywood. The specimens were conditioned in a 25°C, 50% relative humidity environment prior to tests. All specimens were 9.5 mm thick and cut to the specified dimensions. For the NBS smoke chamber, the specimens were 76.2 by 76.2 mm, and for the OSU apparatus, 152.4 by 152.4 mm.

The average moisture contents of the red oak and Douglas-fir plywood specimens were 6.8 and 7.4%, respectively. Coefficients of variation in specimen mass were 3.92% for red oak and 8.54% for Douglas-fir plywood. Specific gravities of red oak and Douglas-fir plywood specimens on an ovendry basis were about 0.70 and 0.49, respectively.

For both test apparatuses, the specimens were wrapped in two layers of aluminum foil, backed by 12.5-mm ceramic wool. The foil and ceramic wool insulated the back side and reduced heat loss from the unexposed surface. The specimens and the backing were held in place with the holders described in the ASTM standards.

Test Procedure

NBS Smoke Chamber—The tests have been described by Tran [7]; they are summarized here. The tests were designed to obtain optical density, specimen mass loss, and particulate

Copyright by ASTM Int'l (all rights reserved) Wed Feb 07 10:53:32 UTC 2024
Downloaded/printed by
The University of Delaware pursuant to License Agreement. No further reproductions authorized.

concentration. Because we had no means of obtaining particulate concentration and specimen mass loss continuously, runs of different durations were conducted for each species in triplicate. The durations were arbitrarily selected as 4, 8, 10, 12, and 14 min. Transmittance was monitored continuously throughout each run. At the end of each run, two vacuum flasks of known volumes (nominally 2 L) were used to draw smoke samples through fiberglass filters of known dry weights. The fiberglass filters were dried overnight under vacuum and over phosphorus pentoxide and weighed again. The smoke sample volumes were calculated based on flask volume, chamber temperature, and flask temperature. The particulate concentration (g/m^3) was obtained by dividing the dry weight gain by the sample volume. The specimens and holders were weighed before and after each test to determine weight loss.

For each material, three heating flux levels were used: 2.0, 2.5, and 3.0 W/cm^2, without pilot ignition. A total of 90 tests were conducted (two materials, three flux levels, five durations, and three replicates).

OSU Apparatus—For comparison with the NBS smoke chamber data, the smoke release rates (SRR) from red oak and Douglas-fir plywood were obtained at 2.5 W/cm^2 of heating flux without pilot ignition. Transmittance was monitored with a collimated white light beam, similar to that of the NBS chamber. Particulate concentration and specimen mass loss were not measured. Douglas-fir plywood specimens were tested in triplicate, and red oak specimens were tested in duplicate.

Results

NBS Smoke Chamber

Specimen weight loss was calculated as the percentage of original specimen weight, shown in Fig. 1 for red oak and Douglas-fir plywood, respectively. Each data point represents the average of three replicate runs. The maximum and minimum limits are included to show variability between runs. Evidently, weight loss is a function of time and flux.

For each run, the smoke particulate concentration was based on an average for two filters. Smoke particulate concentrations of red oak and Douglas-fir plywood are shown in Fig. 2.

Optical density, which is a logarithmic function of inverse transmittance, is suspect when

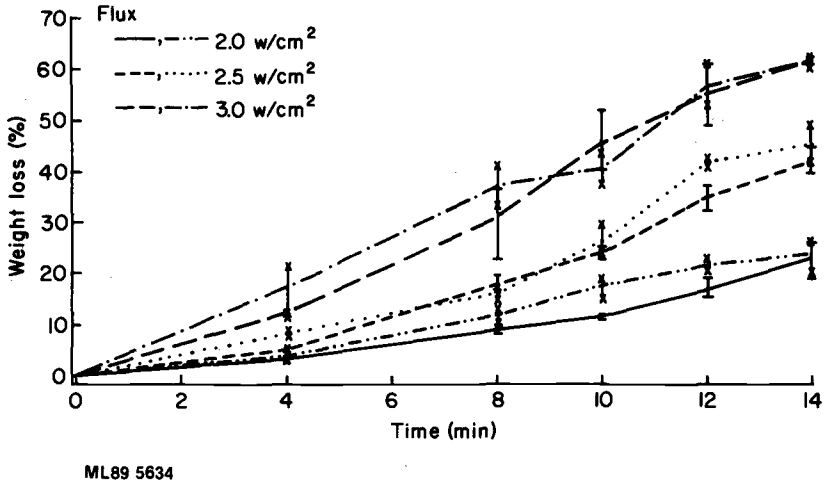

FIG. 1—*Weight loss of red oak and Douglas-fir specimens tested in NBS smoke chamber. Each data point represents the average of three replicate runs. Ranges are maximum and minimum values. – –, ---, and ——— indicate red oak. The other three lines indicate Douglas-fir.*

Copyright by ASTM Int'l (all rights reserved) Wed Feb 07 10:53:32 UTC 2024
Downloaded/printed by
The University of Delaware pursuant to License Agreement. No further reproductions authorized.

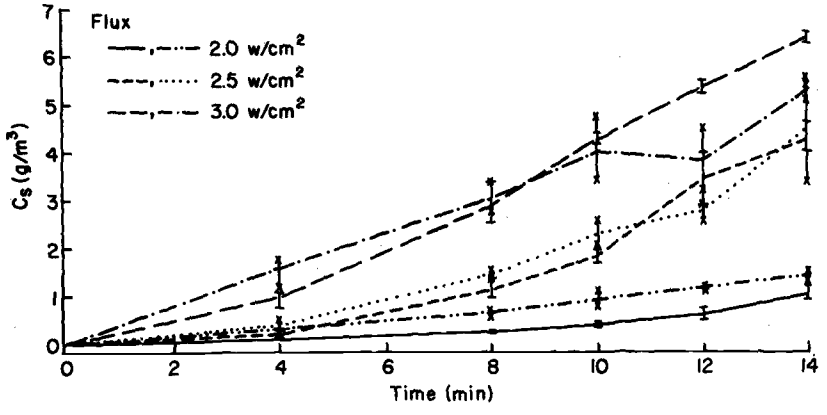

FIG. 2—*Smoke particulate concentration (C_s) of red oak and Douglas-fir specimens tested in NBS smoke chamber. Each data point represents the average of three replicate runs. Ranges are maximum and minimum values. – –, ---, and ——— indicate red oak. The other three lines indicate Douglas-fir.*

specific optical density exceeds 300 ($T < 1\%$). Therefore, we discarded all specific optical density data above 300. The optical density values below 300 were correlated with smoke particulate concentrations of corresponding runs and are shown in Fig. 3 for red oak and Douglas-fir plywood. There is a fairly linear relationship between particulate concentration and specific optical density.

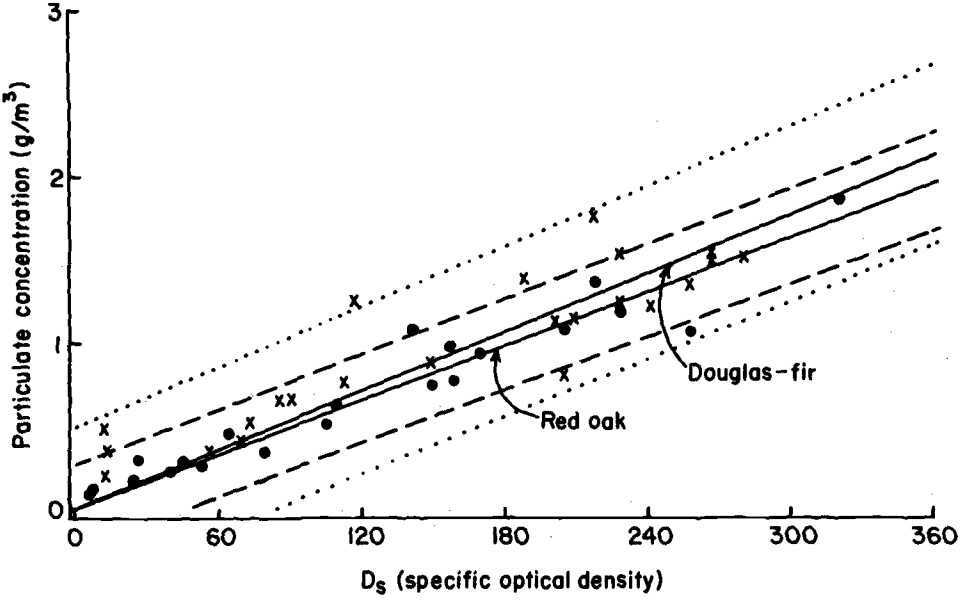

FIG. 3—*Optical density by particulate concentration for red oak (•) and Douglas-fir (x) specimens tested in NBS smoke chamber. Broken lines represent 95% confidence limits: dashed lines, red oak; dotted lines, Douglas-fir.*

Copyright by ASTM Int'l (all rights reserved) Wed Feb 07 10:53:32 UTC 2024
Downloaded/printed by
The University of Delaware pursuant to License Agreement. No further reproductions authorized.

OSU Apparatus

Two runs were made with red oak and three with Douglas-fir plywood at 2.5 W/cm^2 of heating flux without pilot ignition. The conditions were analogous to those runs in the NBS smoke chamber at the same heating flux, except that in the OSU apparatus, the smoke was swept out continuously. Smoke data were reduced as described in Eqs 1, 2, 4, and 5. The SRR was calculated in units of SMOKE/min · m^2. The SRR was integrated over time to give cumulative smoke release (SR) in units of SMOKE/m^2. To show the variability between tests, the SRR of red oak and Douglas-fir plywood are shown in Figs. 4 and 5, respectively. For both red oak and Douglas-fir plywood the SRR were low for the first 8 min of the test. The SRR then rose quickly, resulting in a large peak at about 10 min. The large peak at the end of the test is associated with the active pyrolysis of the back side of the specimen. Since this side of the specimen is almost adiabatic because of the insulation, heat builds up toward the end of the test. The association of the large peak with the back side of the specimen explains the large variability in the magnitude and time of occurrence of the peak. In most cases, the specimens did not ignite, except for Replicate 3 with Douglas-fir plywood. The SRR decreased significantly when the specimen ignited.

The cumulative (total) SR was obtained by integrating the SRR curves; it is expressed in units of SMOKE/m^2. Total SR from red oak and Douglas-fir plywood is shown in Fig. 6. Again, variability between runs was high toward the end of the tests, especially with Douglas-fir plywood.

Discussion

Although the two apparatuses used in this experiment have different configurations, they have one common basis: optical density measurement. Therefore, with proper analysis, their data may be reconciled.

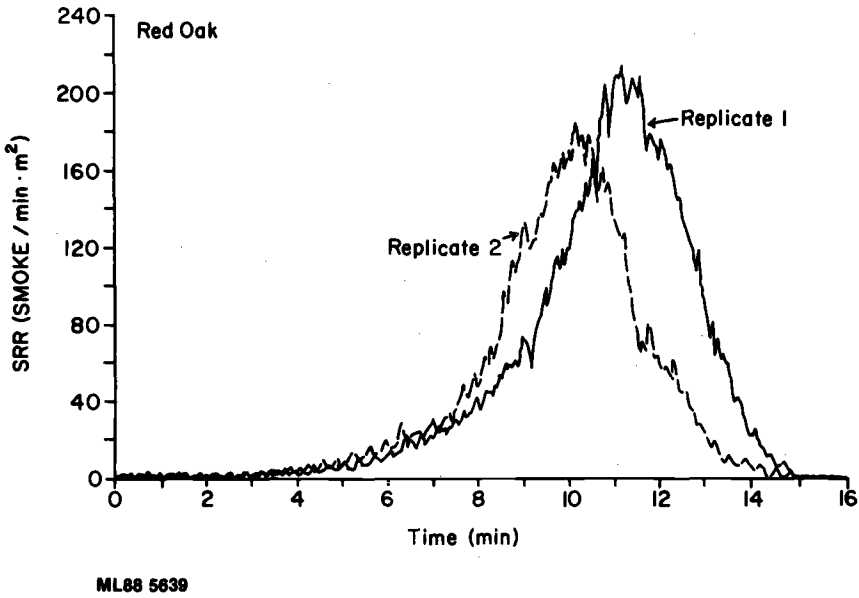

FIG. 4—*Smoke release rate (SRR) of red oak specimens tested in OSU apparatus. Replicate 1, solid line; Replicate 2, dashed line.*

Copyright by ASTM Int'l (all rights reserved) Wed Feb 07 10:53:32 UTC 2024
Downloaded/printed by
The University of Delaware pursuant to License Agreement. No further reproductions authorized.

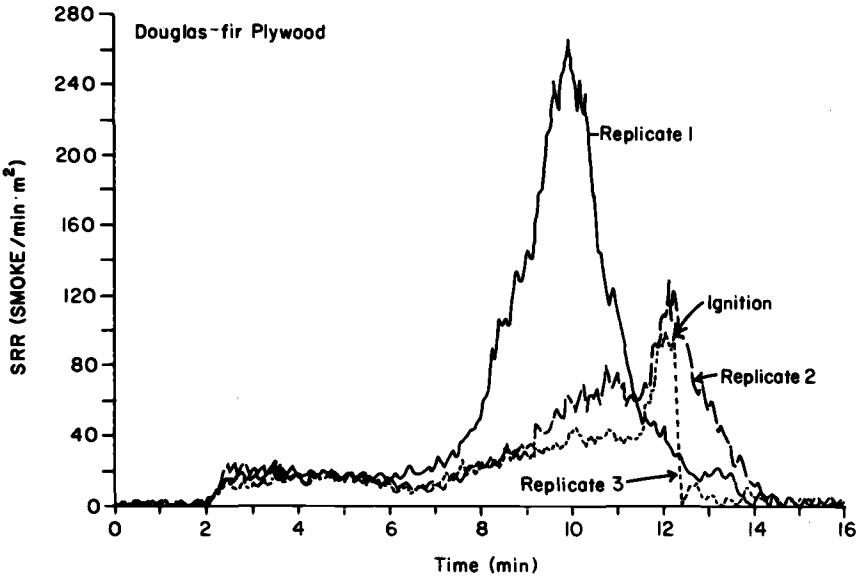

ML88 5640

FIG. 5—*Smoke release rate (SRR) of Douglas-fir plywood specimens tested in OSU apparatus. Replicate 1, solid line; Replicate 2, dashed line; Replicate 3, dotted line.*

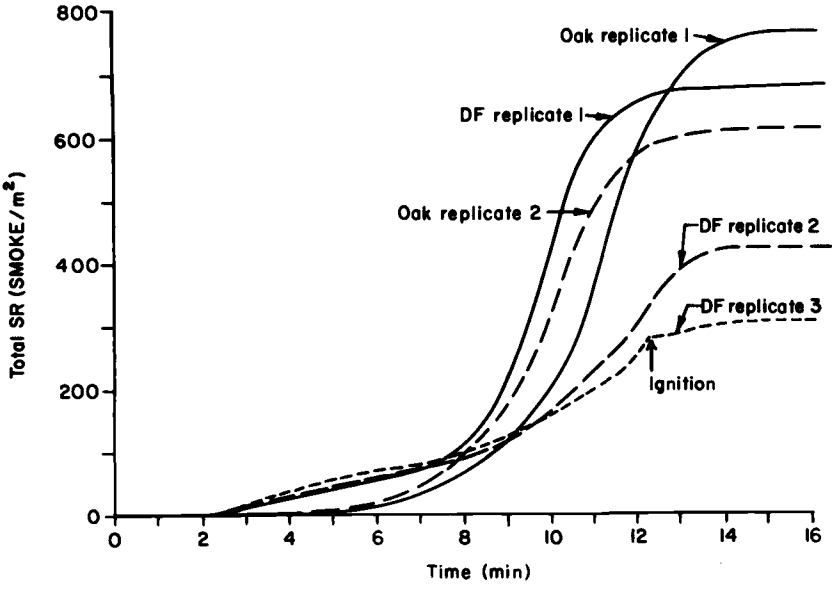

ML89 5632

FIG. 6—*Total smoke release (SR) of red oak and Douglas-fir (DF) specimens tested in OSU apparatus.*

Copyright by ASTM Int'l (all rights reserved) Wed Feb 07 10:53:32 UTC 2024
Downloaded/printed by
The University of Delaware pursuant to License Agreement. No further reproductions authorized.

To compare the data, the two methods must have a common unit of smoke measurement. Optical density is not a universal measurement because it is specific to each test configuration. A more general measure would be optical density over a unit length of smoke path (D/L), in the unit of m^{-1}. However, we could not compare D/L between the two test apparatuses because of their different configurations. Therefore, we chose to use a measurement of particulate mass per unit exposed area of specimen (C/A) in grams per square metre as the common basis for comparison. This selection was based on the assumption that if a material is exposed to a particular heating condition, it will release a repeatable amount of particulate per unit area exposed.

The smoke particulate concentration (C_s), in grams per cubic metre, obtained in the NBS smoke chamber can be simply described by a family of equations for each flux level of the form

$$C_s = 10^a t^b \tag{6}$$

where

t = time in minutes, and
a and b = constants.

Regression constants were found using a least squares regression analysis (Table 1). Total particulate mass per unit exposed area of specimen is calculated as follows

$$C/A = C_s(V/A) \tag{7}$$

For the NBS smoke chamber, $V = 0.51\ m^3$ and $A = 0.004\ m^2$. The C/A for red oak and Douglas-fir plywood at 2.5 W/cm^2 heating flux in the NBS chamber can be calculated from Eq 7 and the curve of C_s as a function of time (Table 1).

For red oak

$$\begin{aligned} C/A &= 10^{-2.254} t^{2.541} (0.51/0.004) \\ &= 0.710 t^{2.541}\ g/m^2 \end{aligned} \tag{8}$$

For Douglas-fir plywood

$$\begin{aligned} C/A &= 10^{-1.486} t^{1.837} (0.51/0.004) \\ &= 4.164 t^{1.837}\ g/m^2 \end{aligned} \tag{9}$$

TABLE 1—*Regression constants for NBS smoke chamber data.*[1]

Material	Flux, W/cm^2	a		b		R^2
		Coefficient	Standard Error	Coefficient	Standard Error	
Red oak	2.0	−2.257	0.144	1.909	0.146	0.934
	2.5	−2.254	0.108	2.541	0.112	0.975
	3.0	−0.979	0.071	1.581	0.072	0.976
Douglas-fir plywood	2.0	−1.228	0.111	1.205	0.116	0.893
	2.5	−1.486	0.084	1.837	0.087	0.972
	3.0	−0.351	0.086	0.922	0.089	0.892

NOTE: R = coefficient of determination.
[1] See Eq 6.

Copyright by ASTM Int'l (all rights reserved) Wed Feb 07 10:53:32 UTC 2024
Downloaded/printed by
The University of Delaware pursuant to License Agreement. No further reproductions authorized.

TABLE 2—*Proportionality constants for NBS smoke chamber data.*[a]

Material	n		
	Coefficient	Standard Error	R^2
Red oak	178.9	5.955	0.976
Douglas-fir plywood	161.2	7.507	0.954
Overall	167.4	5.056	0.961

[a] See Eq 10.

The linear relationship between specific optical density and smoke particulate concentration obtained in the NBS smoke chamber is shown in Fig. 3 and can be described in the form

$$D_s = nC_s \tag{10}$$

There is a nearly linear relationship between D_s and C_s as shown in the 95% confidence interval (dotted lines) in Fig. 3. The proportionality constants (n) for red oak and Douglas-fir plywood were obtained by linear regression analysis (Table 2).

To use the values in Table 2 for the OSU chamber, we have to convert them to the common unit D/L. D/L is proportional to C_s as shown below

$$D/L = \frac{D_s}{132L} \tag{11}$$

where

$L = 0.914$ m.

For red oak

$$D/L = \frac{178.9C_s}{(132)(0.914)} = 1.483C_s \tag{12}$$

For Douglas-fir plywood

$$D/L = \frac{161.2C_s}{(132)(0.914)} = 1.336C_s \tag{13}$$

Because no relationship between smoke optical density and particulate concentration was obtained with the OSU chamber, we assumed that the linearity obtained in the NBS chamber would hold for the OSU apparatus for the same materials. Assuming the proportionality constants between D/L and C_s for red oak and Douglas-fir plywood (Eqs 12 and 13), we proceeded to calculate C/A. By substituting Eqs 12 and 13 into Eq 5, we obtained relationships between D/L and SRR.

For red oak

$$(C_s/A)(V_o/t) = \text{SRR}/1.483 \tag{14}$$

Copyright by ASTM Int'l (all rights reserved) Wed Feb 07 10:53:32 UTC 2024
Downloaded/printed by
The University of Delaware pursuant to License Agreement. No further reproductions authorized.

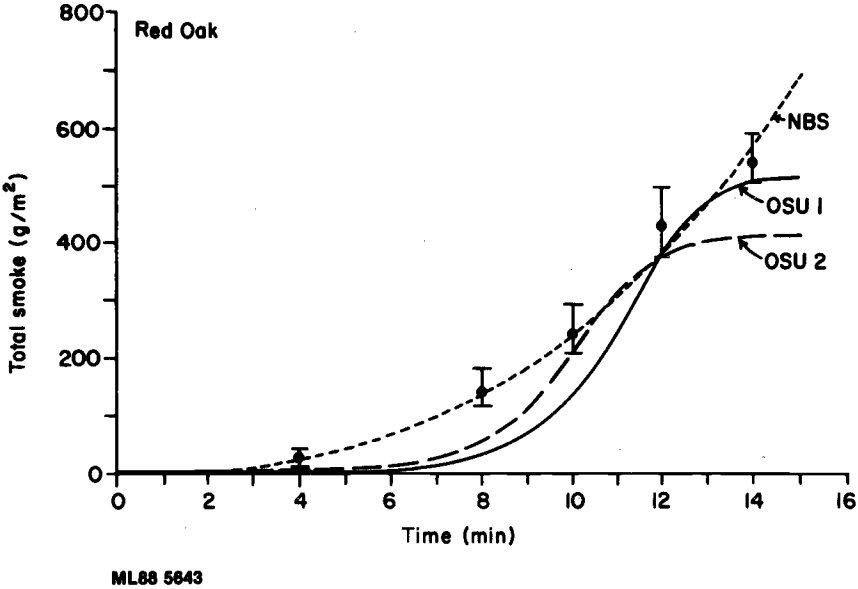

FIG. 7—*Smoke particulate mass per unit area of red oak specimens tested in OSU apparatus. Mean values of specimens tested in NBS smoke chamber and their maximum and minimum values shown for comparison.*

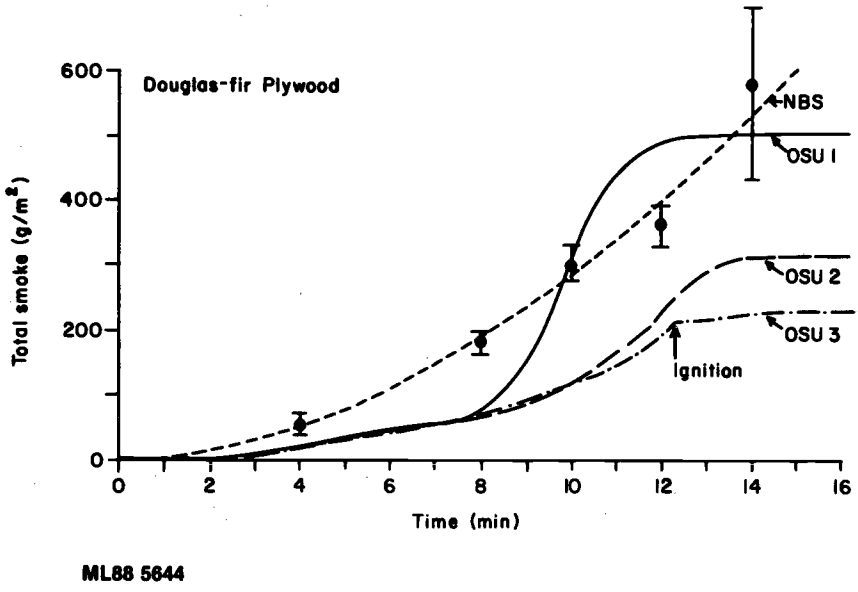

FIG. 8—*Smoke particulate mass per unit area of Douglas-fir plywood specimens tested in OSU apparatus. Mean values of specimens tested in NBS smoke chamber and their maximum and minimum values shown for comparison.*

Copyright by ASTM Int'l (all rights reserved) Wed Feb 07 10:53:32 UTC 2024
Downloaded/printed by
The University of Delaware pursuant to License Agreement. No further reproductions authorized.

For Douglas-fir plywood

$$(C_s/A)(V_o/t) = \text{SRR}/1.336 \tag{15}$$

Both equations are in units of $g/m^2 \cdot$ min. The integrals of Eqs 14 and 15 over time give C/A in the following forms:

For red oak

$$C/A = \text{Total SR}/1.483 \tag{16}$$

For Douglas-fir plywood:

$$C/A = \text{Total SR}/1.336 \tag{17}$$

The value for C/A is in grams per square metre, and it is derived from the total SR curves (Fig. 6) and Eqs 16 and 17. The resulting C/A values are compared with C/A values derived from the NBS smoke chamber (Eqs 8, 9) and are shown in Figs. 7 and 8. The mean C/A values of specimens tested in the NBS chamber and their maximum and minimum values are shown for comparison.

By using the same unit of C/A in grams of smoke particulate per unit area of specimen as a function of time, the data from the two apparatuses are in the same order of magnitude. The agreement between the two apparatuses is better for red oak than for Douglas-fir plywood (Figs. 7, 8). However, the curves have different shapes. Data from the NBS chamber more closely resemble an exponential curve, up to 14 min. The OSU data follow an original exponential growth period, followed by a stagnant period. The OSU SRR curves (Figs. 4, 5) also show that SRR peaks at about 10 to 13 min. The data from the NBS chamber do not show any sign of peak smoke release because measurements were made at discrete intervals. It is also possible that the smoke accumulated in the NBS chamber may have decayed or settled so that a peak is not detected.

Up to 10 min, the OSU data are consistently lower than those of the NBS smoke chamber. This difference between the two apparatuses can be explained by two possibilities. The first possibility is that the smoke meter in the OSU apparatus is not accurate in the low range of smoke concentration. An SRR of 20 SMOKE/min $\cdot$ m^2 corresponds to an optical density of 0.013. Calibrations of the smoke system of our OSU apparatus with optical density filters of 0 (no filter), 0.04, 0.1, and 0.3 showed good response, indicating that the system can detect smoke in this low range. In our equipment setup and data acquisition system, optical density is proportional to the voltage recorded with voltage = 1.547 D. For an optical density of 0.013, the voltage = 0.020 V or 20 mV. The resolution of our 12-bit data acquisition system is 2.44 mV. Thus, the noise-to-signal ratio is more than 10% in this low range. Despite the noise, the signal should be accurate.

The second possibility is the fact that the C/A of the NBS chamber was calculated directly based on measured particulate concentration. In the OSU apparatus, the proportionality between particulate concentration and optical density is assumed. In the low range of D_s, corresponding to the early stages of exposures, particulate concentration is underestimated using the linear regression lines (Fig. 3). Thus, C/A for the OSU apparatus could be underestimated. Beyond 10 min of run time, the data are in better agreement.

Concluding Remarks

In this study, we obtained particulate mass concentrations in the NBS smoke chamber and established the proportionality between optical density and particulate concentration for

Copyright by ASTM Int'l (all rights reserved) Wed Feb 07 10:53:32 UTC 2024
Downloaded/printed by
The University of Delaware pursuant to License Agreement. No further reproductions authorized.

red oak and Douglas-fir plywood. Using the proportionality established, we reduced optical density data of red oak and Douglas-fir plywood in the OSU chamber to particulate concentration. We found the unit of particulate mass produced per unit area (C/A) to be the appropriate basis to compare data from the two apparatuses. We tried to reconcile the data from the two apparatuses for red oak and Douglas-fir plywood under similar conditions (2.5 W/cm^2 without pilot flame). Although the reduced data from the two apparatuses have the same order of magnitude, we have not been able to reconcile them exactly.

The major difference between a flow-through apparatus such as the OSU calorimeter and the smoke box is the kind of data obtained. With a flow-through system, the rate of smoke release can be measured. Cumulative data can be easily obtained from the rate data by integration. Cumulative smoke quantities are measured with the sealed box. As shown with the NBS smoke data, it is difficult to derive the smoke release rate.

Rate data are preferred for fire growth modeling because of the transient nature of fire growth. Because the material area involved in smoke production and its exposure history change with time, a model needs to be able to keep track of these variables and to calculate smoke production of the involved objects. The current state of the art in smoke production measurement is based on the relationship between SRR using optical measurement (extinction coefficient or optical density) and burning rate such as mass loss rate. This relationship can be obtained with both types of apparatuses. However, the flow-through apparatuses have many advantages over the sealed box because of their ability to measure both SRR and burning rate.

References

[1] Chien, W. P., Seader, J. D., and Birky, M. M., "Monitoring Weight Loss in an NBS Smoke Density Chamber," *Fire Technology,* Vol. 9, No. 4, 1973, pp. 285–298.

[2] Seader, J. D. and Chien, W. P., "Mass Optical Density as a Correlating Parameter for the NBS Smoke Density Chamber," *Journal of Fire and Flammability,* Vol. 5, 1974, pp. 151–163.

[3] Chien, W. P. and Seader, J. D., "Prediction of Specific Optical Density for Smoke Obscuration in an NBS Smoke Density Chamber," *Fire Technology,* Vol. 11, No. 3, 1985, pp. 206–218.

[4] Seader, J. D. and Chien, W. P., "Physical Aspects of Smoke Development in the NBS Smoke Density Chamber," *Journal of Fire and Flammability,* Vol. 6, 1974, pp. 294–310.

[5] Seader, J. D. and Ou, S. S., "Correlation of Smoking Tendency of Materials," *Fire Research,* Vol. 1, 1977, pp. 3–9.

[6] King, T. Y., "Empirical Relationships between Optical Density and Mass Density of Smoke," *Journal of Fire and Flammability,* Vol. 6, 1975, pp. 222–227.

[7] Tran, H. C., "Quantification of Smoke Generated from Woods in the NBS Smoke Chamber," *Journal of Fire Sciences,* Vol. 6, 1988, pp. 163–180.

Copyright by ASTM Int'l (all rights reserved) Wed Feb 07 10:53:32 UTC 2024
Downloaded/printed by
The University of Delaware pursuant to License Agreement. No further reproductions authorized.

Charles M. Fleischmann,[1] *Raymond L. Dod,*[1] *Nancy J. Brown,*[1] *Tihomiv Novakov,*[1] *Frederick W. Mowrer,*[2] *and Robert B. Williamson*[1]

The Use of Medium-Scale Experiments to Determine Smoke Characteristics

REFERENCE: Fleischmann, C. M., Dod, R. L., Brown, N. J., Novakov, T., Mowrer, F. W., and Williamson, R. B., **"The Use of Medium-Scale Experiments to Determine Smoke Characteristics,"** *Characterization and Toxicity of Smoke, ASTM STP 1082,* H. K. Hasegawa, Ed., American Society for Testing and Materials, Philadelphia, 1990, pp. 147–164.

ABSTRACT: A series of medium-scale smoke experiments were conducted at the University of California, Berkeley. Representative fuels, such as wood, asphalt roofing shingles, and liquid hydrocarbons, were burned as medium-scale fuel packages in the open, with no restriction on the ventilation. For some of the fuels, the experiments were also conducted in a burn room under limited ventilation conditions. The effects of different combustion conditions resulting from differences in fuel composition, geometry, and ventilation were determined.

Smoke emission factors measured for burning wood under well-ventilated conditions were in the range of 0.1 to 0.3%, but under limited ventilation conditions they increased an order of magnitude to the 2 to 3% range. Under well-ventilated conditions, the smoke emission factors measured for asphalt were in the 12% range and those for No. 2 fuel oil were in the 11% range. Burning in the compartment also affected the emission factors and smoke characteristics of fuel oil.

The results of the medium-scale experiments presented in this paper show that the smoke emission factors are not only dependent on the properties of a given fuel, but also on the environmental conditions under which the fuel was burned. Specifically, the influence of ventilation rate, fuel mass loss rate, temperature, and residence time are important. Although more research is required before a standardized medium-scale fire test to measure smoke production can be developed, the need for such a test standard is clearly demonstrated by these results.

KEY WORDS: compartment fires, smoke emission factors, rate of heat release, wood, hydrocarbons, asphalt, ventilation, medium scale tests

Smoke from fires accounts for at least 50% of all fire deaths and billions of dollars in damage each year. In the last two decades significant advances have been made to improve our understanding of smoke movement and smoke characteristics, but we still lack the ability to predict the amount and the characteristics, both physical and chemical, of the smoke produced by fires. A better understanding of the physical and chemical properties of smoke particles is important for many reasons. The toxicity of the particles depends on their chemical composition, while their ability to penetrate into the human lung depends on the particle size distribution, a physical property. The atmospheric effects of smoke particles such as radiative transfer, atmospheric residence times, and chemical reactivity are also determined by both physical and chemical properties. A new interest in the amount and characteristics of

[1] Lawrence Berkeley Laboratory, University of California, Berkeley, CA 94720.
[2] Department of Fire Protection Engineering, University of Maryland, College Park, MD 20740.

Copyright by ASTM Int'l (all rights reserved) Wed Feb 07 10:53:32 UTC 2024
Copyright © 1990 by ASTM International www.astm.org
Downloaded/printed by
The University of Delaware pursuant to License Agreement. No further reproductions authorized.

smoke produced by fires is stimulated by the recent concerns with the global environmental effects of postnuclear fires.

The concept of "nuclear winter" has been postulated with a number of assumptions regarding the smoke produced by postnuclear exchange fires [*1,2*]. The general premise is that following the use of nuclear weapons, sufficient smoke would be generated from fires and deposited in the atmosphere to cause a decrease in the incident solar energy reaching the Earth's surface. Such a change in the net radiative balance could cause global cooling. Whether nuclear winter would occur in the aftermath of a nuclear exchange depends largely on the quantity and nature of the smoke generated, its distribution in the atmosphere, and its optical characteristics.

Smoke is defined by ASTM E 176 as "the airborne solid and liquid particulates and gases evolved when a material undergoes pyrolysis or combustion" [*3*]. Using this definition, smoke can be separated into two prime components: (1) particulates and (2) gases. Particulates are the primary cause of reduced visibility, and they may also have a physiological effect, such as increased heart rate of occupants exiting from a burning structure [*4*]. Airborne particulates are the component of smoke which are responsible for activating smoke detection devices. Carbon monoxide, the principal gas for causing injury and death among occupants and fire service personnel, is one of many toxic gases contained in smoke.

Most of our current understanding of smoke has been derived from small-scale experiments where the sample is either ignited by a pilot flame and allowed to burn freely or exposed to a radiant energy source and undergoes smoldering combustion in a chamber of fixed volume. Typically, more smoke is produced under smoldering conditions; however, smoldering combustion is generally only a threat to the occupants in the room of origin and has little effect on other areas of the building. The piloted ignition tests use small samples which typically burn with a laminar flame lacking the turbulence, radiation, and ventilation characteristics present in actual fires.

This paper reports on experiments performed at the Fire Research Laboratory of the University of California at Berkeley aimed at characterizing the smoke produced from medium- to full-scale experiments and relates them to smoke measurements from bench-scale experiments. The term "medium scale" is used to characterize the 200 to 1000-KW fire experiments that produce flames a few metres in height. The term "full scale" infers the use of a full-scale room for the limited ventilation experiments. Though considered full scale by the fire research community, these experiments are also used by the nuclear winter research community, and therefore the term "medium scale" is also being used throughout this paper. Both terms are in contrast to "bench-scale" experiments in which the flames are generally laminar and the rates of heat release are less than 20 KW.

Sixteen experiments were conducted on representative urban fuels including plywood, whole wood, asphalt roofing shingles, and No. 2 fuel oil. Smoke was characterized by the mass of airborne particulates, the size distribution of the particulates, and the carbon characteristics of the particulates, i.e., "graphitic," or "black," carbon and organic carbon. Mass loss and rate of heat release (RHR) were recorded during each experiment to characterize the combustion.

Experimental Facility

The experimental facility used to conduct the fire experiments is shown in Fig. 1. It consists of 1100 m^3 (38 000 ft^3) "high-bay" room, a forced ventilation system, data acquisition facilities, and auxiliary sample preparation and storage area.

The ventilation system begins with a 3.0 by 3.0-m (10 by 10-ft) canopy hood designed to capture the products of combustion generated during a fire experiment. The ventilation sys-

Copyright by ASTM Int'l (all rights reserved) Wed Feb 07 10:53:32 UTC 2024
Downloaded/printed by
The University of Delaware pursuant to License Agreement. No further reproductions authorized.

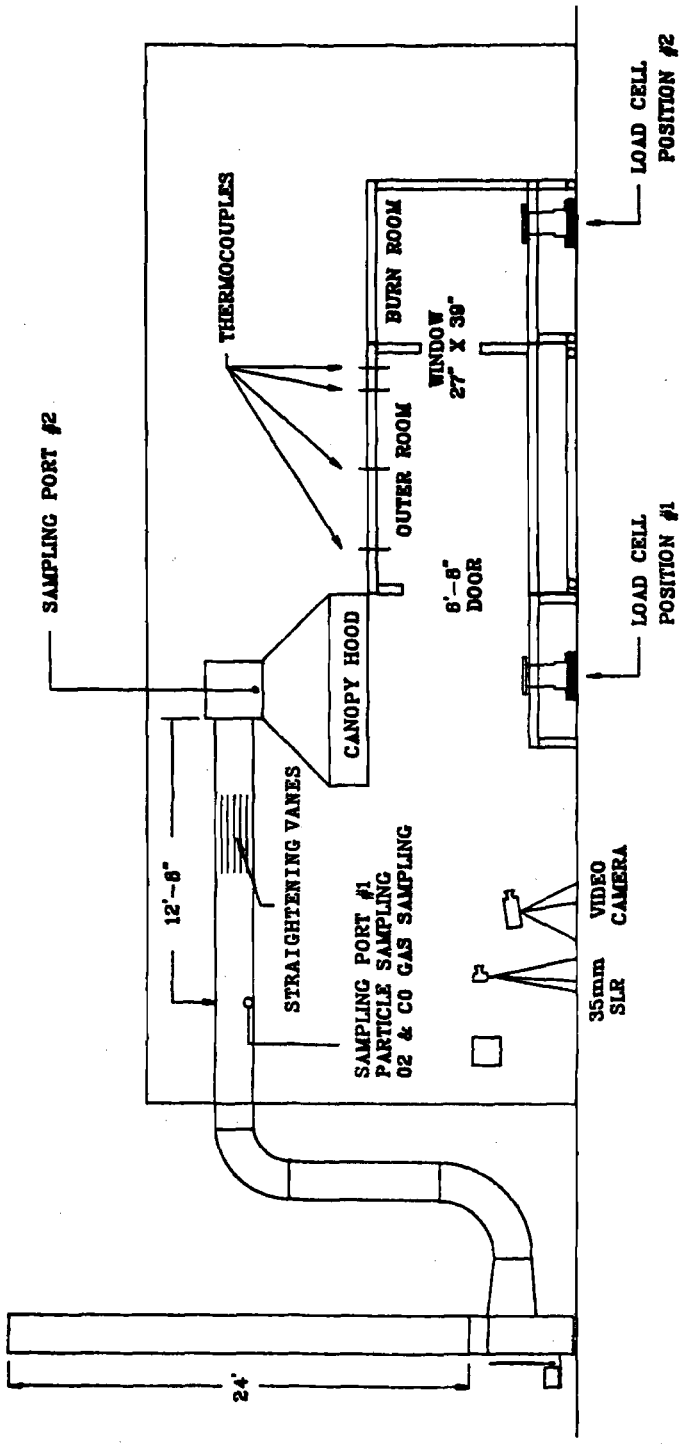

FIG. 1—*Schematic diagram of the experimental facility used in this work.*

tem is capable of transporting combustion products at a maximum rate of approximately 4 Sm^3/s (8000 Sft^3/min). (Note that this flow is given in "standard" (S) units, i.e., corrected for temperature.) The canopy hood is connected to the exhaust fan by 0.61-m (2-ft)-diameter stainless steel ducting. The 0.92-m (3-ft)-diameter exhaust fan is driven by a 1.5-kW (2-hp) power a-c motor, and the flow rate of the exhaust system is controlled by a solid state, a-c motor controller.

The experiments reported here were either conducted on a 2.4 by 2.4-m (8 by 8-ft) platform directly under the hood or in a 2.4 by 2.4 by 2.4-m (8 by 8 by 8-ft) "burn room" which is connected by an opening to another room 2.4 by 3.7 by 2.4 m (8 by 12 by 8 ft), which has a doorway under the hood. The burn room, which is constructed of a steel frame with steel stud walls, rests on a fire-resistant floor elevated above the floor of the laboratory to permit instrumentation to be located below the burn room. The walls and ceiling of the room can be built to simulate different types of construction. During these experiments, the small burn room was lined with ceramic fiber insulation blankets, while the outer larger room was lined with gypsum wallboard. The location of the platform and the burn room are shown in Fig. 1. The burn room and ventilation system are capable of sustaining postflashover fires of several megawatts for up to ½-h duration.

Experimental Procedure

During these 16 experiments, the fire and smoke were characterized by measuring the rate of heat release, the fuel mass loss rate, and the smoke emission factors. The rate of heat release was determined using oxygen depletion calorimetry [*5*]. This method for determining the heat release rate is based on the assumption that all carbonaceous fuels release approximately the same amount of heat per unit mass of oxygen consumed (13.1 MJ/kg). The oxygen concentration was measured using a Beckman paramagnetic oxygen analyzer. Carbon monoxide concentration was also measured for all the experiments and in later experiments, such as the No. 2 fuel oil and the second asphalt experiments, carbon dioxide concentration was also measured. The gas concentration measurements were performed by extracting gas samples from the exhaust stream for analysis. Values of gas concentrations and duct flow conditions were recorded every 5 s by a laboratory minicomputer. Flow rates in the exhaust stream were determined using a bidirectional low-velocity probe, as described by McCaffrey and Heskestad [*6*], which is accurate to within 10%.

The fuel mass loss during burning was measured using a Toledo scale Model 8132 which was, depending on the experiment, placed under the platform or the burn room. The output from the scale was recorded in real time using the computer-controlled data acquisition system.

Aerosol particulate sampling for this series of experiments was conducted primarily from the exhaust duct at a point approximately 2 m (6 ft) downstream of the straightening vanes. Sampling probes were inserted at this point to accommodate the stacked-filter pair. Further sampling was conducted in Experiments (Exps.) 3 to 16 by placing a sampling probe in the plenum directly above the hood. Another stacked-filter pair was used to collect the plenum samples. The plenum samples were then used to provide qualitative information regarding changes in the particulate carbon content and morphology which could potentially occur during the 0.3 to 0.5-s transit of the duct to the primary sampling ports. All the filters used were 47-mm-diameter quartz fiber. The mass of the sample was determined for each filter by using a Cahn Model 4700 electrobalance.

The carbon content for each filter was determined by combustion of the sample in oxygen and then measuring the resulting CO_2 with a CO_2 Coulometer (Coulometrics, Inc., Model 5010 [*7*]). Further characterization of the carbon content in the filter was obtained using

Copyright by ASTM Int'l (all rights reserved) Wed Feb 07 10:53:32 UTC 2024
Downloaded/printed by
The University of Delaware pursuant to License Agreement. No further reproductions authorized.

thermal-evolved gas analysis (EGA) for carbon. This technique has been used to characterize collected aerosol carbon particles by type, i.e., "organic," "black," or "carbonate" carbon [*8,9*]. All the samples analyzed in this study showed a dominant black carbon peak and no carbonate, allowing for a clear differentiation between black and organic carbon. The sampling procedure and reliability of the method used in this study is discussed in greater detail by Dod et al. [*10*].

Experiments

Sixteen experiments were conducted on representative urban fuels. In six of the experiments, Douglas fir plywood was burned in a parallel plate geometry, as shown schematically in Fig. 2. The fuel geometry, one of the two idealized cases presented by Babrauskas and Williamson [*11*], represents the condition in which the fuel specimens create their own environment independent of the greater surroundings. The nominal separation distance between the plywood sheets was 0.15 m (0.5 ft) for all the plywood experiments, except for Exp. 2

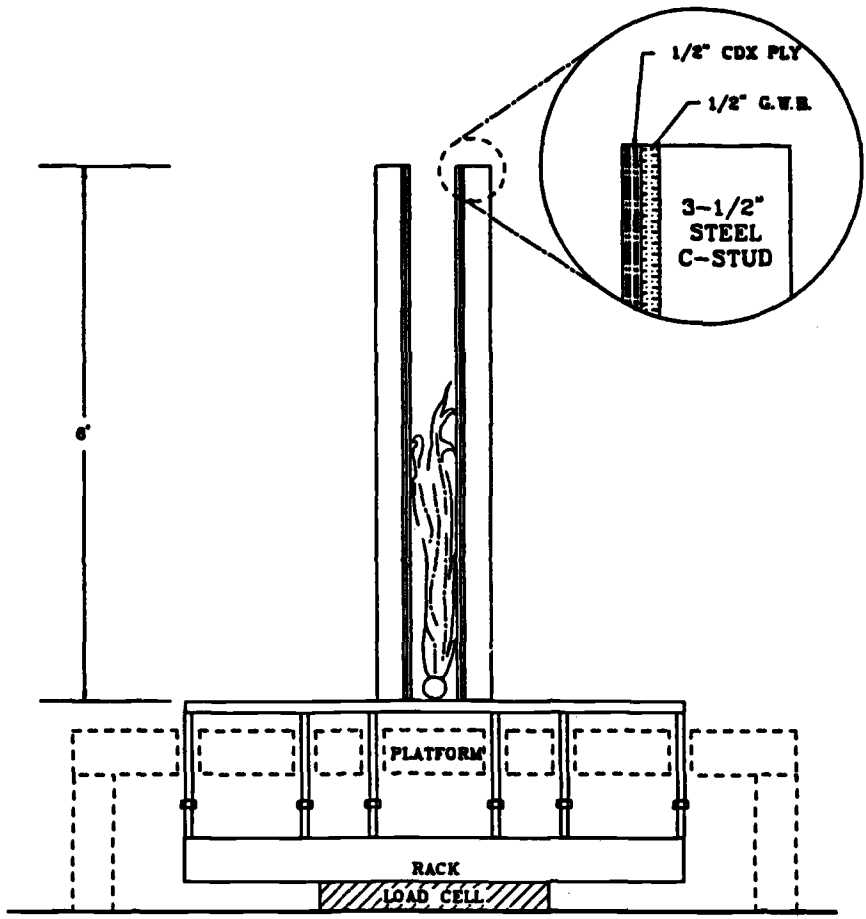

FIG. 2—*Schematic diagram of the parallel plate apparatus used for the plywood experiments.*

Copyright by ASTM Int'l (all rights reserved) Wed Feb 07 10:53:32 UTC 2024
Downloaded/printed by
The University of Delaware pursuant to License Agreement. No further reproductions authorized.

where the separation distance was reduced to 0.10 m (0.33 ft). A catch pan was not provided in Exps. 1 and 2, thus allowing the burning mass that fell away to be included in the fuel mass loss. This was corrected in the remaining experiments by using a wire mesh catch basket. A propane-fired gas flame was used to ignite the plywood faces and was extinguished after the fuel specimen reached a self sustaining stage of burning. For Exps. 1–5, 5-ply CDX grade Douglas fir plywood 1.3 cm (0.5 in.) thick was used. For Exp. 6, 3-ply Douglas fir plywood which was also 1.3 cm (0.5 in.) thick, but had a thicker veneer, was burned. Experiment 6 could be thought of as being an intermediate step between Exps. 1–5 where plywood samples were used and the whole wood experiments described below.

For the whole wood experiments, the specimens were burned in a wood crib geometry. Wood cribs have been used for a long time as a fuel for fire research because of their good reproducibility. Heat confinement within the wood cribs and radiation between the burning surfaces allow sticks of substantial cross section to burn efficiently. Each crib weighed 28 kg and was made of kiln-dried Douglas fir whole wood sticks 3.6 by 3.6 by 45.0 cm (1.4 by 1.4 by 18.0 in.) arranged in 15 layers of six sticks. The spacing between the sticks was 4.8 cm (1.9 in.) to yield a lattice work box with rectangular faces of the dimensions given in Table 1. The ignition of each crib was accomplished by burning heptane in a 0.3-m (1.0-ft)-diameter pan located on the platform beneath the crib. Smoke emission measurements were not started until the heptane had been completely consumed. In Exp. 7, a single wood crib was burned in the open with unrestricted ventilation. For Exp. 7, the mass loss rate of the crib was governed by the crib porosity, as defined by Thomas [*12*].

In Exps. 8 and 9, three wood cribs were burned in the burn room in order to investigate the effects of the compartment on the smoke production. The compartment had a single opening (window) 0.76 by 1.0 m (2.5 by 3.3 ft) centered horizontally on the wall leading to the outer room with the top of the opening located 2.0 m (6.7 ft) above the floor (see Fig. 1). This opening was small enough to force the fire to burn under limited ventilation conditions, i.e., the fuel mass loss rate was controlled by the window opening.

In two experiments, asphalt roofing shingles were burned in an angular geometry, as shown in Fig. 3. This configuration represents the burning of a roof with the impingement

TABLE 1—*Summary of variables in all the experiments.*

Experiment Number	Material	Ventilation	Specimen	
			Height, m	Width, m
1	plywood	open	1.83	1.22
2	plywood	open	1.83	1.22
3	plywood	open	1.83	1.22
4	plywood	open	1.83	1.22
5	plywood	open	1.22	1.83
6	plywood	open	1.83	1.22
7	wood crib	open	0.62	0.47
8	3 wood cribs	room	0.62	0.47
9	3 wood cribs	room	0.62	0.47
10	asphalt	open	1.86	1.22
11	asphalt	open	1.86	1.22
12	1 pan #2 fuel oil	open	0.56 dia	
13	1 pan #2 fuel oil	open	0.56 dia	
14	2 pan #2 fuel oil	open	2 × 0.56 dia	
15	2 pan #2 fuel oil	open	2 × 0.56 dia	
16	1 pan #2 fuel oil	room	0.56 dia	

Copyright by ASTM Int'l (all rights reserved) Wed Feb 07 10:53:32 UTC 2024
Downloaded/printed by
The University of Delaware pursuant to License Agreement. No further reproductions authorized.

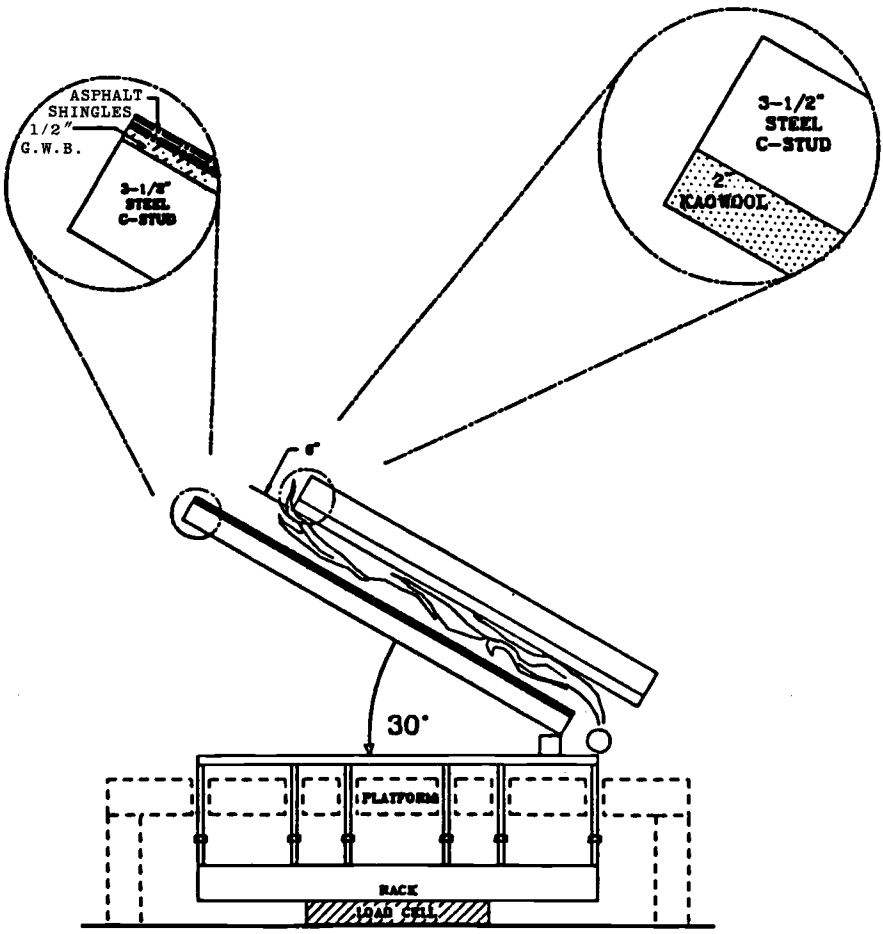

FIG. 3—*Schematic diagram of the angled parallel plate apparatus used for the asphalt roofing shingle experiments.*

of an external flame. A parallel surface of noncombustible Kaowool material was used to increase the radiation feedback to the fuel surface, which helped to sustain the burning of the roofing material after the propane flame had been extinguished.

For the liquid hydrocarbon fuel experiments, No. 2 fuel oil was burned. The fuel oil was burned in a circular pan 56 cm (22 in.) in diameter and 28 cm (11 in.) high. A pool fire is a typical geometry for both liquid and solid hydrocarbon fuels in a horizontal configuration. In each experiment, except for Exp. 13, 8.9 cm (3.5 in.) of fuel was floated on top of 19.1 cm (7.5 in.) of water. The water was used as a "filler" to reduce the total amount of fuel required. In Exp. 13, 2.5 cm (1.0 in.) of fuel was floated on 25.4 cm (10 in.) of water. Because of the high ignition temperature of fuel oil, 250 mL (8.5 oz) of heptane was floated on the surface of the fuel to augment ignition. Smoke emission measurements were performed after the heptane had burned. For Exps. 12 and 13, a single pan was burned on the platform in the open. As a simple method for scaling the fire, two pans were burned in the open in Exps. 14 and 15. The two pans were placed tangent to one another. For Exp. 16, a single pan was placed in the burn room as described above. The burn room was again used to investigate

Copyright by ASTM Int'l (all rights reserved) Wed Feb 07 10:53:32 UTC 2024
Downloaded/printed by
The University of Delaware pursuant to License Agreement. No further reproductions authorized.

the effects of the compartment on the hydrocarbon fires. In this experiment the fire was not ventilation limited. A summary of the 16 experiments is given in Table 1.

Experimental Results

Parallel Plywood Sheets

In Exps. 1 through 6, plywood sheets were burned in a parallel plate geometry of the dimensions given in Table 1. The plies of wood were attached to each other by a layer of adhesive that burned differently from the wood. In these experiments, a decrease in the heat release rate could frequently be observed in the period during which a second ply was being ignited from the backside of the most recently burning layer of veneer. A typical heat release rate curve for this geometry is shown in Fig. 4, where the RHR curve for Exp. 3 is shown. Note the decrease in heat release rate at 11 min, which occurred when the second ply was being ignited.

The emission factors for all the experiments are given in Table 2 and are compared graphically in Fig. 5. With the exception of Exp. 2, the emission factors for the first five experiments were remarkably similar and seemed quite independent of minute-to-minute variations in the heat release rates. The measured particulate carbon emission factors for these experiments were nearly identical (0.17 ± 0.01%), indicating the degree of reproducibility which can be achieved for specimens burning under similar conditions (Fig. 6). In Exp. 2 identical plywood sheets were used, but they were configured with a 10-cm (4-in.) gap between them, causing the fire to have more restricted ventilation than during the other five 5-ply plywood experiments. This reduction in ventilation explains the large value for the measured emission factors in Exp. 2. The results of the 3-ply and the 5-ply experiments are

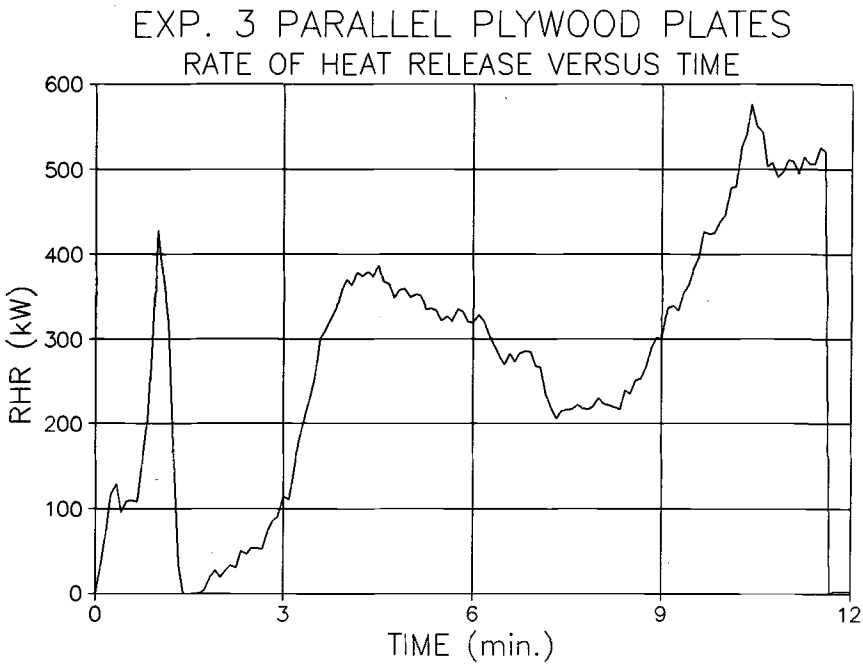

FIG. 4—*Rate of heat release curve for Exp. 3.*

Copyright by ASTM Int'l (all rights reserved) Wed Feb 07 10:53:32 UTC 2024
Downloaded/printed by
The University of Delaware pursuant to License Agreement. No further reproductions authorized.

TABLE 2—*Emission factors from duct total filters for all the experiments.*

Experiment No.	Fuel	Emission Factors: Total Mass	Noncarbon Mass	Total Carbon	Black Carbon	Organic Carbon	Sampling Time
1	plywood		0.00%	0.16%	0.13%	0.03%	1:20 to 7:15
2	plywood	0.24%	0.00%	0.23%	0.17%	0.06%	3:22 to 10:22
3	plywood	0.17%	0.02%	0.15%	0.12%	0.04%	1:20 to 11:32
4	plywood	0.19%	0.03%	0.16%	0.13%	0.04%	1:20 to 10:35
5	plywood	0.20%	0.01%	0.18%	0.13%	0.05%	1:30 to 11:30
6	plywood	0.14%	0.04%	0.10%	0.09%	0.01%	4:30 to 11:30
7	1 crib	0.09%	0.01%	0.08%	0.05%	0.02%	4:20 to 13:50
8	3 cribs room	1.96%	0.55%	1.41%	1.12%	0.29%	3:30 to 14:25
9	3 cribs room	3.60%	0.49%	3.11%	2.57%	0.54%	4:00 to 14:30
10	C roofing	13.94%	2.05%	11.89%	10.03%	1.85%	1:15 to 13:25
11	C roofing	10.22%	1.86%	8.35%	6.23%	2.12%	2:00 to 9:00
12	1 pan oil	11.65%	2.08%	9.57%	8.78%	0.78%	2:00 to 9:00
13	1 pan oil	10.95%	1.48%	9.47%	8.86%	0.61%	5:00 to 13:00
14	2 pans oil	8.42%	0.56%	7.86%	7.27%	0.59%	3:30 to 8:30
15	2 pans oil	7.61%	0.58%	7.02%	6.50%	0.53%	4:30 to 9:00
16	1 oil—room	5.06%	2.43%	2.63%	1.97%	0.66%	7:00 to 17:00

NOTE: sampling times are from time of ignition.

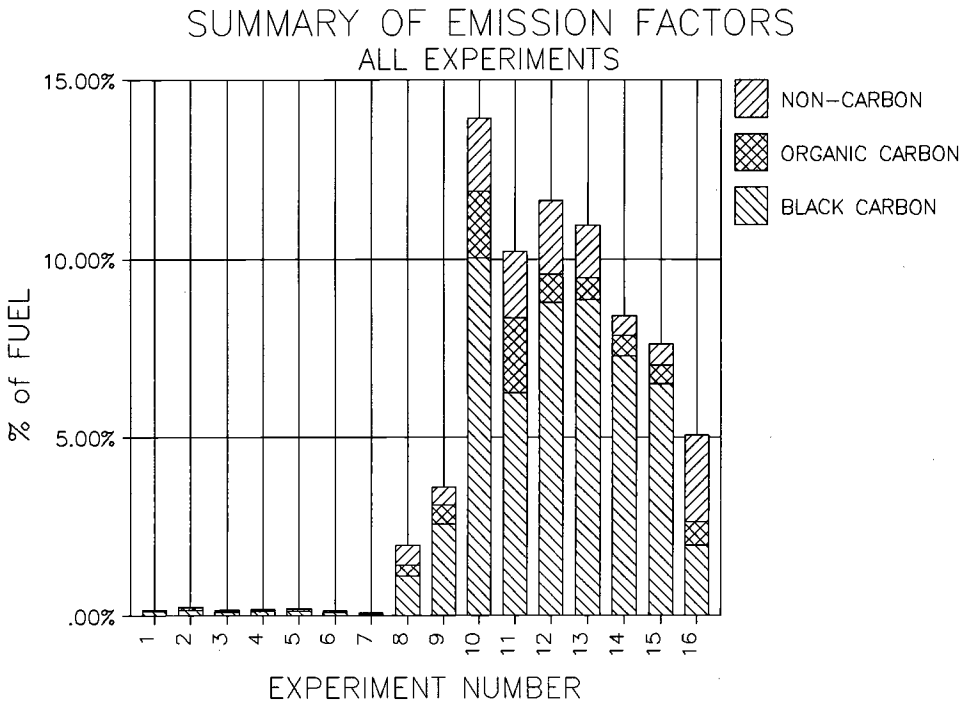

FIG. 5—*Emission factors for all the experiments.*

Copyright by ASTM Int'l (all rights reserved) Wed Feb 07 10:53:32 UTC 2024
Downloaded/printed by
The University of Delaware pursuant to License Agreement. No further reproductions authorized.

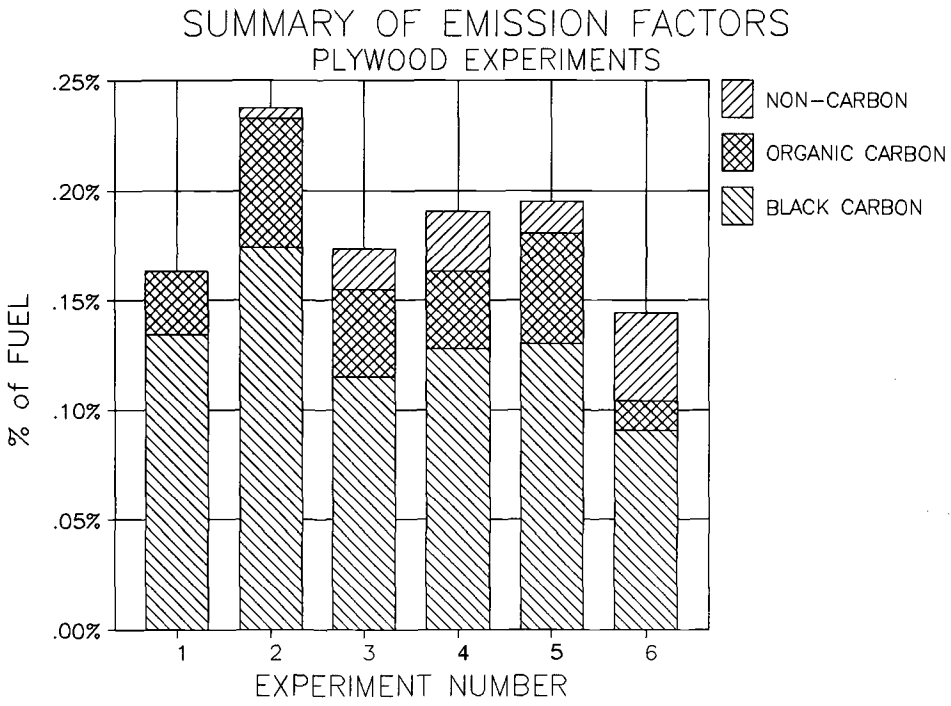

FIG. 6—*Emission factors for the plywood experiments.*

not expected to be identical since the 3-ply fuel has thicker veneer layers and contains less adhesive. This may be the reason that the fuel in Exp. 6 burned in a manner between the 5-ply plywood and whole wood.

Wood Cribs

Experiment 7 involved burning a single wood crib in the open under well-ventilated conditions. Figure 7 is a plot of the rate of heat release versus time. Ignition of the crib is accomplished in approximately 3 min. Sampling for smoke particles occurred between 4.3 and 13.8 min, and for most of this period burning is nearly steady-state with an average heat release rate of 230 KW.

The next two experiments, Exps. 8 and 9, involved burning three wood cribs in an interior room ventilated only by a window. This type of combustion is characteristic of a postflashover fire. Reproducibility of the combustion characteristics in the two experiments is extremely good. Measurements of mass loss of the fuel during both of these experiments indicate that the burning was steady state. Mass loss during the 25-min period following ignition was 73 kg including the mass of the cribs and the heptane ignition fluid. Figure 8 shows the RHR curve for Exps. 8 and 9. Following the combustion of the heptane, the rate of heat release increased from 600 to 1000 KW. The spike in each of the rate of heat release curves, shown in Fig. 8, corresponds to the burning of paper from the gypsum wall board in the outer room.

The emission factors for the wood crib experiments are compared graphically in Fig. 9. Ventilation-limited conditions caused an order of magnitude difference in the smoke pro-

Copyright by ASTM Int'l (all rights reserved) Wed Feb 07 10:53:32 UTC 2024
Downloaded/printed by
The University of Delaware pursuant to License Agreement. No further reproductions authorized.

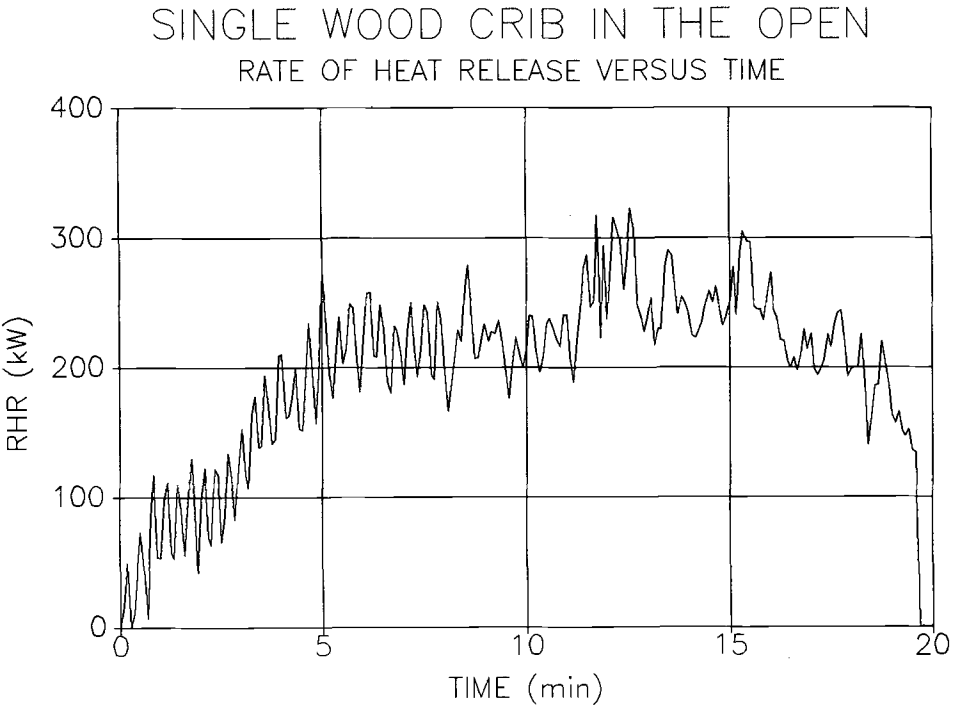

FIG. 7—*Rate of heat release curve for Exp. 7.*

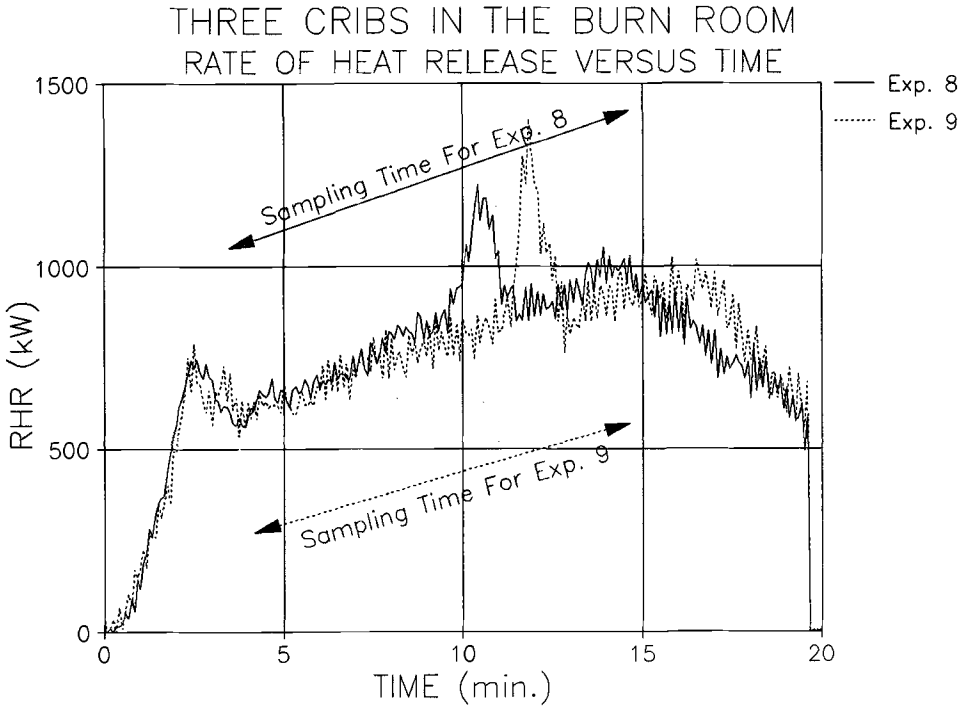

FIG. 8—*Rate of heat release curve for Exps. 8 and 9.*

Copyright by ASTM Int'l (all rights reserved) Wed Feb 07 10:53:32 UTC 2024
Downloaded/printed by
The University of Delaware pursuant to License Agreement. No further reproductions authorized.

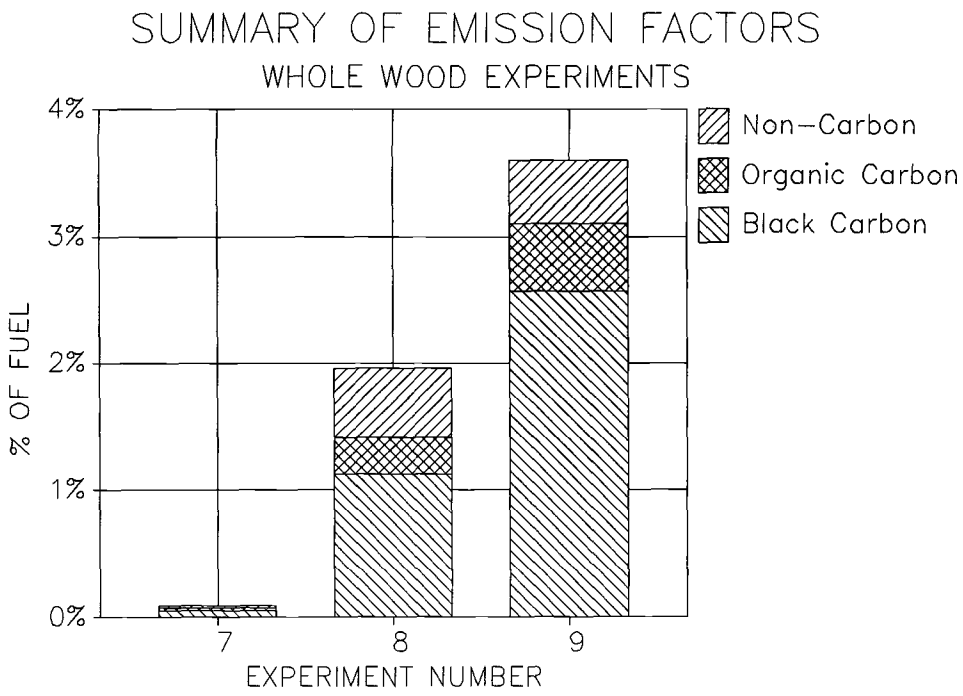

FIG. 9—*Emission factors for the whole wood experiments.*

duction. There was a difference in the sampling times, relative to the rate of heat release, between Exps. 8 and 9. Experiment 8 included the last 2 to 3 min of its maximum heat release rate, while in Exp. 9 the sampling was terminated just after the spike in the heat release rate. The sampling times are shown in Fig. 8 and are given in Table 2. The difference in the sampling time resulted in an increase in the emission factors, which indicates an increase in the smoke production.

Asphalt Shingles

Experiments 10 and 11 involved burning asphalt shingles in a configuration designed to simulate roof burning as a result of direct impingement of an external flame. During the asphalt shingle experiments, pieces of the specimen often melted, dripped, and burned in the catch pan underneath. Both samples ignited in 3 min, and each specimen underwent steady-state burning as evidenced by the nearly constant slopes of the individual mass loss curves. The two experiments did have different burning rates: 0.36 kg/min for Exp. 10, and 0.45 kg/min for Exp. 11. The rate of heat release for Exp. 10, shown in Fig. 10, decreased during the experiment. A similar behavior was also seen in Exp. 11. This decrease may be due, in part, to the burning of the cellulosic material used for lining the shingles.

In Fig. 11 the emission factors for the asphalt experiments are shown graphically. Burning of asphalt roofing shingles produced the largest emission factors observed in this series of experiments. The smoke particulates were in excess of 10% of the consumed fuel mass, nearly two orders of magnitude greater than those observed for the wood fires burning under similar ventilation conditions. Particle collection for Exp. 10 was initiated earlier and was continued for a period 50% longer than for Exp. 11. It is interesting to note that the increased

Copyright by ASTM Int'l (all rights reserved) Wed Feb 07 10:53:32 UTC 2024
Downloaded/printed by
The University of Delaware pursuant to License Agreement. No further reproductions authorized.

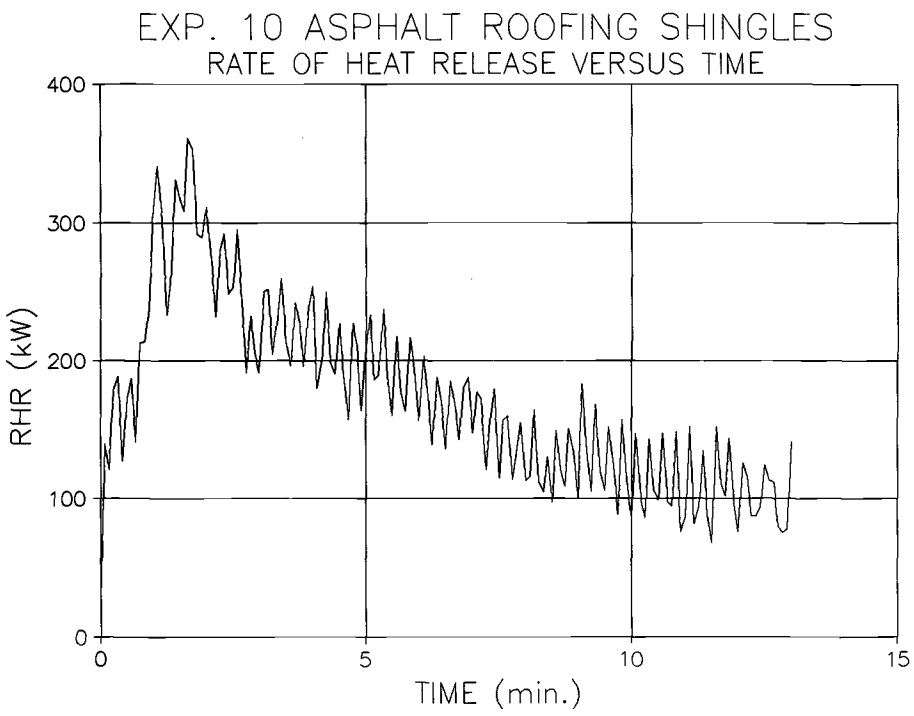

FIG. 10—*Rate of heat release curve for Exp. 10.*

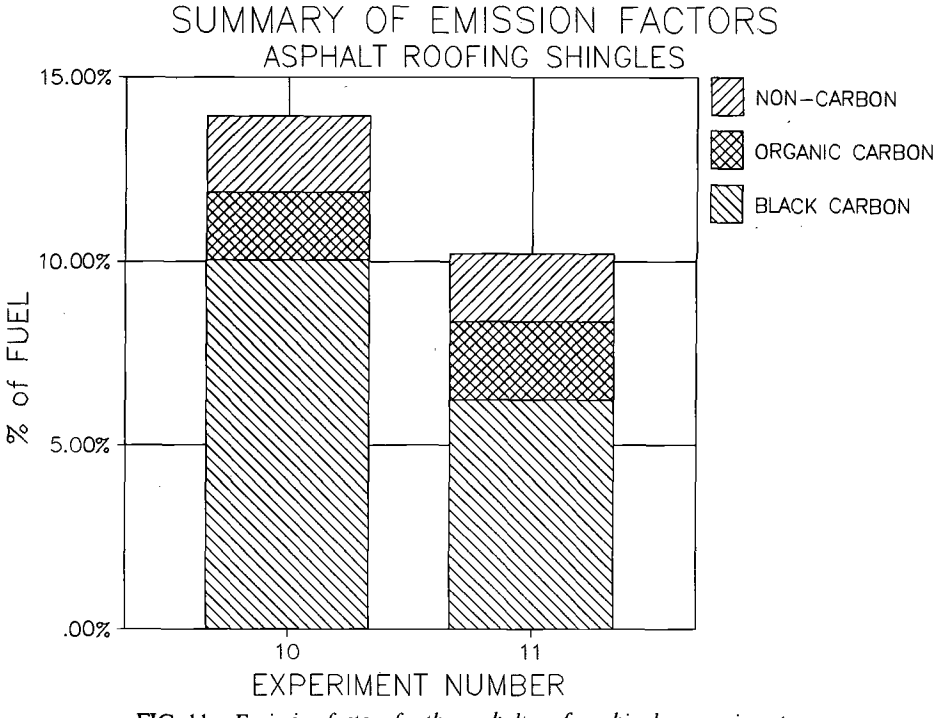

FIG. 11—*Emission factors for the asphalt roofing shingles experiments.*

Copyright by ASTM Int'l (all rights reserved) Wed Feb 07 10:53:32 UTC 2024
Downloaded/printed by
The University of Delaware pursuant to License Agreement. No further reproductions authorized.

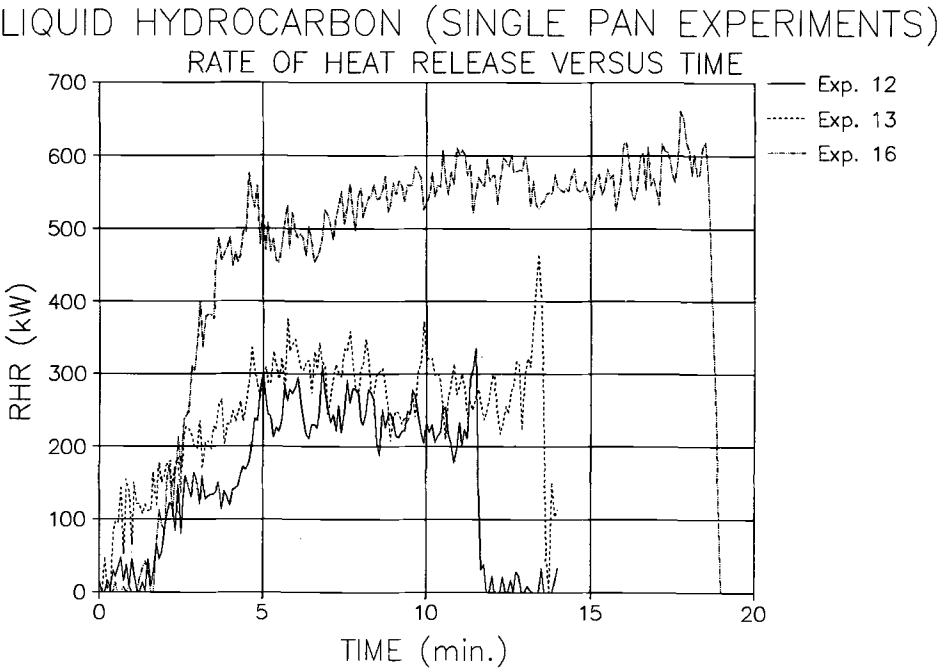

FIG. 12—*Rate of heat release curve for Exps. 12, 13, and 16.*

sampling time for Exp. 10 caused an increase in the emission factors of less than 10% in the organic carbon and noncarbon; yet the black carbon emission factor increased more than 30%.

Liquid Hydrocarbons

In Exps. 12 and 13, a pan of No. 2 fuel oil was burned in the open with no restriction on the ventilation. The RHR curves for Exps. 12 and 13 are shown in Fig. 12. The combustion characteristics for all the fuel oil experiments are summarized in Table 3. The values in Table 3 are averaged over the steady-state burning period. The mass loss rate recorded for Exps. 12 and 13 is lower than the reported mass loss rate per unit area ($\dot{m}''$) for large tank fires 0.039 kg/m^{2}s ($\pm$0.003) [*13*]. However, the mass loss rate for this pan size is governed by the radiation feedback from the flame. The flames were considered optically thin, and optically

TABLE 3—*Summary of combustion characteristics for No. 2 fuel oil experiments.*

Experiment Number	$\dot{m}''$, kg/(m·m·s)	RHR, KW	h_c, MJ/kg
12	0.027	240	36
13	0.032	290	37
14	0.040	710	37
15	0.037	680	37
16	0.054	570	43

NOTE: Values are averaged over steady-state burning period.

Copyright by ASTM Int'l (all rights reserved) Wed Feb 07 10:53:32 UTC 2024
Downloaded/printed by
The University of Delaware pursuant to License Agreement. No further reproductions authorized.

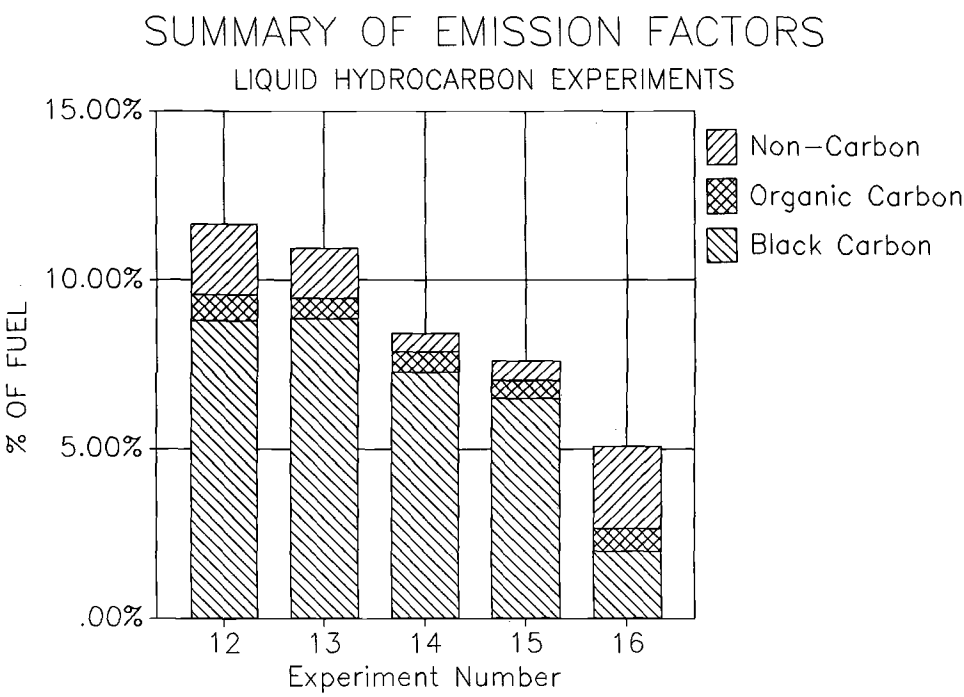

FIG. 13—*Emission factors for the fuel oil experiments.*

thin pool fires typically have lower mass loss rates. The emission factors for all the No. 2 fuel oil experiments can be compared graphically by examining Fig. 13. For Exps. 12 and 13, the total emission factor is over 10%, with the black carbon emission factor accounting for over 70% of the total particulate.

In Exps. 14 and 15 two pans were burned in the open with no restriction on the ventilation. The RHR curves for Exps. 14 and 15 are shown in Fig. 14, and an increase in the mass loss rate occurs (Table 3) which is most likely due to the increased radiation to the fuel surface from the adjacent pan. The most interesting result of the two-pan experiments is the reduction in the emission factors as compared with those of the single-pan experiments burning in the open. Reproducibility of the emission factors and the combustion characteristics for both the one- and two-pan experiments is quite good, as seen in Fig. 13 and Table 3.

Experiment 16 was conducted with one pan in the burn room with a single window. During this experiment, the fire reached flashover conditions within the room of origin, and this increased the radiation feedback to the fuel surface. The increased radiation contributed substantially to the increase in mass loss rate noted for oil burning in the compartment. In addition to the higher mass loss rate, the net heat of combustion (h_c) was also found to be slightly higher than that of the single-pan experiments in the open. The net heat of combustion was obtained by dividing the average rate of heat release, over the steady-state burning period, by the average mass over the same steady-state time period. This apparent increase in the calculated heat of combustion is believed to be a result from the increased residence time and more complete burning of the pyrolizates at the elevated temperature within the room. This elevated temperature allows many of the unburned pyrolyzates to burn within the room before being quenched in the plume. The increase in the rate of heat release is larger than the increase in the mass loss rate because more of the volatilized fuel burns in the compart-

Copyright by ASTM Int'l (all rights reserved) Wed Feb 07 10:53:32 UTC 2024
Downloaded/printed by
The University of Delaware pursuant to License Agreement. No further reproductions authorized.

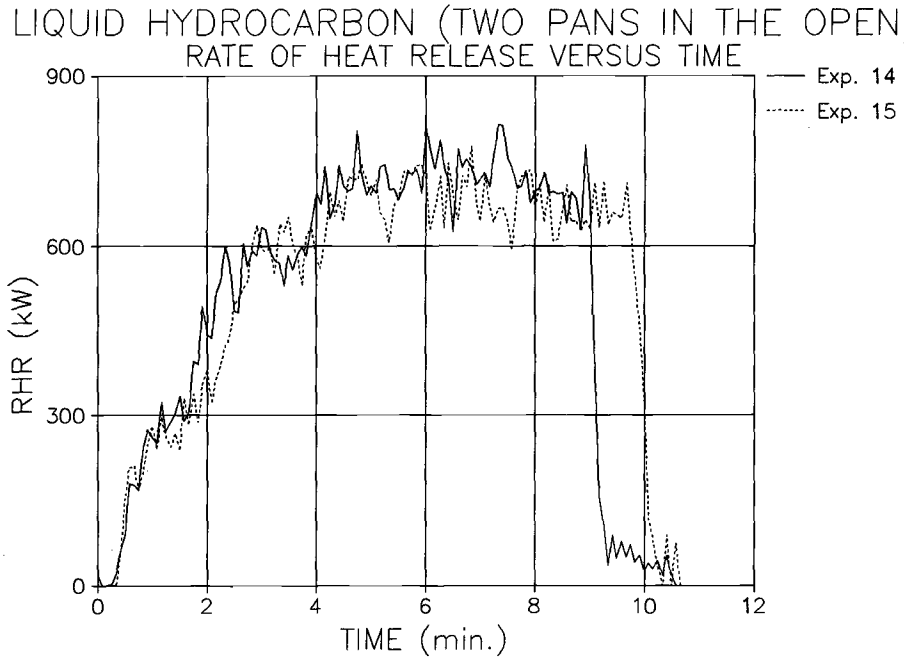

FIG. 14—*Rate of heat release curve for Exps. 14 and 15.*

ment. The rate of heat release curve for Exp. 16 is shown in Fig. 12 for comparison with the single-pan experiments in the open.

The compartment had a significant effect on the smoke emission factors. Emission factors are reduced by more than a factor of two in the compartment. The most pronounced effect was on the black carbon emission factor, which was decreased by nearly a factor of four when compared to the single-pan experiments in the open. The changes in emission factors are clearly shown in Fig. 13.

Discussion and Conclusion

The most important result of the experiments described above is the considerable influence of the compartment on the production of smoke. As shown in Fig. 9, the smoke emission factors measured for wood cribs burning in the compartment were more than an order of magnitude higher than those burning in the open. In addition, the smoke from the compartment fire was thick and black, similar in appearance to the smoke produced by burning plastic or oil. For the fuel oil experiment, the compartment had the opposite effect. In the experiment conducted in the compartment, the smoke production was significantly reduced from those conducted in the open, as seen in Fig. 13. It is, therefore, important to analyze the combustion and ventilation characteristics of the compartment-burning experiments to account for the seemingly different results. In the compartment, the mass flow rate of air into the compartment ($\dot{m}_a$) can be approximated by [14]

$$\dot{m}_a = 0.52wH^{3/2} \quad (1)$$

Copyright by ASTM Int'l (all rights reserved) Wed Feb 07 10:53:32 UTC 2024
Downloaded/printed by
The University of Delaware pursuant to License Agreement. No further reproductions authorized.

where

w = the width of the compartment opening, and
H = the height of the compartment opening.

The mass stoichiometric ratio for wood burning is 5.7. The fire is ventilation limited for wood if the mass burning rate of wood $\dot{m}_b$ is equal to

$$\dot{m}_b = (0.52/5.7)wH^{3/2} \tag{2}$$

For our compartment, $wH^{3/2}$ is 0.76 $m^{5/2}$, yielding an $\dot{m}$ = 0.068 kg/s which is identical to the value measured for Exp. 9 and very close to the value measured for Exp. 8 (0.071 kg/s). Thus the wood cribs burning in the compartment were ventilation limited. In contrast, the oil fires in the compartment were not. Assuming a stoichiometric ratio of 14.7, the measured fuel mass loss rate of 0.054 $kg/m^2 \cdot s$ is approximately one half the value computed for ventilation-limited conditions. For wood crib burning in the compartment, the emission factors were larger because of the incomplete combustion characteristics of the environment. In contrast, the emission factors for the oil decreased in the compartment because of the higher temperature and increased residence time of the pyrolyzates within the compartment, which resulted in more complete combustion and substantial soot burnout.

These results are not only important to building fire safety but also to the study of the nuclear winter hypothesis. Wood is one of the major building materials used in the United States. It is reasonable to assume that large quantities of wood would burn, under both restricted and unrestricted ventilation conditions, in postnuclear fires. The results of the asphalt roofing shingles demonstrate the significant impact a single material might have on the urban smoke production in the postnuclear environment. The smoke emission factors found for asphalt roofing shingles, averaged for the two experiments, was over 12% with more than 60% being black carbon.

Further research is necessary in order to more accurately quantify the amount of air required to reduce the smoke production within a compartment. The next series of experiments should include: (1) wood cribs in the burn room where the mass loss rate is not limited by the size of the window, (2) hydrocarbon pool fires in the compartment where the window is small enough to control the fuel mass loss rate.

Acknowledgments

The authors are greatly indebted to William MacCracken, Rene LaFever, and Nicholas A. Dembsey for their assistance in performing the experiments. Cecile Grant's expert editorial assistance and constant support are warmly acknowledged. Financial support was provided in part from the Defense Nuclear Agency and the University of California Institute on Global Conflict and Cooperation. The Lawrence Berkeley Laboratory is operated by the University of California for the Department of Energy under contract DE-AC03-76SF00098.

References

[1] Turco, R. P., Toon, O. B., Ackerman, T. P., Pollack, J. B., and Sagan, C., *Science*, Vol. 222, 1983, p. 1283.
[2] Turco, R. P., Toon, O. B., Ackerman, T. P., Pollack, J. B., and Sagan, C., *Scientific American*, Vol. 251, 1984, p. 33.
[3] "E 176-86: Standard Terminology Relating to Fire Standards," in *ASTM Fire Test Standards*, 2nd ed., American Society for Testing and Materials, Philadelphia, 1988, pp. 116–120.

Copyright by ASTM Int'l (all rights reserved) Wed Feb 07 10:53:32 UTC 2024
Downloaded/printed by
The University of Delaware pursuant to License Agreement. No further reproductions authorized.

[4] Jin, T., *Proceedings of the 4th Joint Panel Meeting of the UJNR Panel on Fire Research and Safety,* Building Research Institute, Ministry of Construction, Tokyo, 1979.
[5] Parker, W. J., "Calculations of the Heat Release Rate by Oxygen Consumption for Various Applications," NBSIR 81-2427-1, National Bureau of Standards, Center for Fire Research, Gaithersburg, MD, 1982.
[6] McCaffrey, B. J. and Heskestad, G., *Combustion and Flame,* Vol. 26, 1976, p. 125.
[7] Huffman, E. W. D., "Performance of a New Carbon Dioxide Coulometer," *Microchemical Journal,* Vol. 22, 1977, pp. 567–573.
[8] Dod, R. L. and Novakov, T., "Application of Thermal Analysis and Photoelectron Spectroscopy for the Characterization of Particulate Matter," in *Industrial Applications of Surface Analysis,* L. A. Casper and C. J. Powell, Eds., American Chemical Society, Washington, 1982, pp. 397–404.
[9] Novakov, T., "Microchemical Characterization of Aerosols," in *Nature, Aim and Methods of Microchemistry,* Springer Verlag, Vienna, Austria, 1981, pp. 141–165.
[10] Dod, R. L., Brown, N. J., Mowrer, F. W., Novakov, T., and Williamson, R. B., "Smoke Emission Factors from Medium Scale Fires: Part 2," *Aerosol Science and Technology,* Vol. 10, No. 2, 1989. pp. 20–27.
[11] Babrauskas, V. and Williamson, R. B., "Post-Flashover Compartment Fires: Basis of a Theoretical Model," *Fire and Materials,* Vol. 2, No. 2, 1978, pp. 39–53.
[12] Thomas, P. H., "Fire in Enclosures," Building Research Establishment Current Paper, CP 30/74, Fire Research Station, Borehamwood, U.K., 1974.
[13] Babrauskas, V., "Estimating Large Pool Fire Burning Rate," *Fire Technology,* Vol. 19, 1983, pp. 251–261.
[14] Drysdale, D., *An Introduction to Fire Dynamics,* John Wiley and Sons, 1985, pp. 310–311.

Copyright by ASTM Int'l (all rights reserved) Wed Feb 07 10:53:32 UTC 2024
Downloaded/printed by
The University of Delaware pursuant to License Agreement. No further reproductions authorized.

George T. Tamura[1] *and John H. Klote*[2]

Experimental Fire Tower Studies on Controlling Smoke Movement Caused by Stack and Wind Action

REFERENCE: Tamura, G. T. and Klote, J. H., **"Experimental Fire Tower Studies on Controlling Smoke Movement Caused by Stack and Wind Action,"** *Characterization and Toxicity of Smoke, ASTM STP 1082,* H. K. Hasegawa, Ed., American Society for Testing and Materials, Philadelphia, 1990, pp. 165–177.

ABSTRACT: Studies have been undertaken to develop a fire-safe elevator for evacuating handicapped people and for aiding firefighters. Methods were developed for predicting adverse pressure differences across the walls of the elevator shaft and lobbies caused by wind and building stack action and in combination with those caused by a fire. The predictions were verified by tests conducted in a ten-story experimental fire tower. The level of mechanical pressurization required to prevent smoke contamination of elevators could be determined by summing the pressure differences caused by these forces. The tests demonstrated that mechanical pressurization of the elevator shaft or lobbies can be effective in preventing smoke contamination of these shafts and lobbies.

KEY WORDS: elevator, pressure, smoke control, testing, fire safety, weather, high rise

Although a fire may be confined within a fire-resistant compartment, smoke can readily spread beyond it to adjacent areas through leakage paths in the enclosure, such as crack openings in the wall, floor, and ceiling, and around pipes, ducts, and doors. These openings can permit a substantial flow of toxic gases whenever the pressures in a smoke-contaminated space are greater than those in adjacent spaces.

For the purpose of this paper, smoke is considered to consist of the airborne solid and liquid particulates and gases evolved when a material undergoes pyrolysis or combustion, together with the quantity of air that is entrained or otherwise mixed into the mass. The following equation can be used to determine the rate of smoke flow

$$F = C(\delta P)^n \tag{1}$$

where

F = air or smoke flow rate,
C = flow coefficient,
δP = pressure difference, and
n = flow exponent.

[1] Senior research officer, Institute for Research in Construction, National Research Council of Canada, Ottawa, Ontario, Canada.
[2] Leader of smoke management research, Center for Fire Research, National Institute of Standards and Technology, Gaithersburg, MD.

Copyright by ASTM Int'l (all rights reserved) Wed Feb 07 10:53:32 UTC 2024
Copyright © 1990 by ASTM International www.astm.org
Downloaded/printed by
The University of Delaware pursuant to License Agreement. No further reproductions authorized.

Equation 1 shows that the flow rate depends on the flow characteristics of the leakage opening in a building element (C and n) and on the pressure difference (δP) across it. This paper deals with the determination of the pressure differences caused by wind and stack action associated with normal building heating in combination with that caused by a fire. The pressure difference caused by fire because of thermal expansion and buoyancy and the pressure difference caused by the piston effect of a moving elevator car have been reported by Tamura and Klote [*1,2*]. Mechanical ventilation systems, when shut down during a fire emergency, provide additional passageways for smoke to leave the fire compartment but do not contribute to adverse pressure differences. If they are operating, however, imbalances in their rates of supply and exhaust can impose adverse pressure differences across the enclosure of a fire compartment.

Information on adverse pressure differences is required in designing smoke control systems to prevent smoke flow into escape routes such as stairs and elevators. The work described in this paper is part of a joint project being conducted by the National Research Council of Canada (NRCC) and the National Institute of Standards and Technology (NIST) on developing a fire-safe elevator for evacuating handicapped people and for aiding firefighters. Methods for calculating pressure differences caused by wind and stack action and the results of tests conducted in the ten-story experimental fire tower of the NRCC National Fire Laboratory are presented.

Theory

Whereas stack action due to the temperature effect of fire acts over just the fire floor height, stack action due to the temperature difference between the inside and outside air during cold weather acts over the whole building height. It causes air to flow into a building from outdoors at low levels, upward through openings in the floors and vertical shafts, and out at upper levels. A reverse flow pattern occurs during warm weather when a building is cooled. The level at which there is no air inflow or outflow is called the neutral pressure level; at this level the pressures inside and outside the building are equal. The location of the neutral pressure level for tall buildings, which depends on the size and distribution of leakage openings in the outside walls and interior separations, can vary from 0.3 to 0.7 of the total building height [*3*].

The pressure differences due to stack action can be calculated by

$$\delta P_s = hg(\rho_o - \rho_i) = hg\rho_i(T_i - T_o)/T_o \tag{2}$$

where

δP_s = pressure difference caused by stack action, Pa,
h = distance from the neutral pressure level, m,
g = gravitational constant, m/s^2,
ρ = air density, kg/m^3,
T = absolute temperature, K,
o = outdoor, and
i = indoor.

If the building interior is completely open, the pressure differences caused by stack action as calculated by Eq 2 are taken entirely across the outside walls. Equation 2 is for naturally occurring stack effect in the absence of other driving forces such as wind, a ventilation system, or buoyancy of fire gases. This relation is for constant densities, and it has been validated extensively. If the interior is divided by partitions, this pressure difference is distributed

Copyright by ASTM Int'l (all rights reserved) Wed Feb 07 10:53:32 UTC 2024
Downloaded/printed by
The University of Delaware pursuant to License Agreement. No further reproductions authorized.

across the outside walls, interior walls, and the walls of vertical shafts. In this analysis, pressure losses due to vertical airflow inside the shafts are assumed to be negligible. The ratio of the pressure difference across the outside walls divided by the pressure difference as calculated by Eq 2 is called the thermal draft coefficient (γ) and is an indicator of the tightness of the outside walls relative to the interior separations. It can be expressed as

$$\gamma = \delta P_w / \delta P_s \tag{3}$$

where

w = outside walls.

The value of γ can vary from zero for a building with loose outside walls to 1.0 for a building with very tight outside walls. Values of γ measured by Tamura and Wilson [*4*] for three tall open floor plan office buildings under normal operating conditions varied from 0.6 to 0.8, which indicated that the construction of the interior separations was relatively loose compared to that of the exterior wall. The value of γ can approach 1.0 when the central air handling systems are shut down during a fire because the air distribution ducts interconnect all floor spaces.

Considering series flow in the horizontal direction from outdoors to inside the vertical shafts, the value of γ can be calculated for a building with an open floor plan by

$$\gamma = \frac{1}{1 + (A_w/A_v)^2} \tag{4}$$

where

A = leakage area per floor, and
v = walls of all vertical shafts.

The pressure difference across the outside wall is

$$\delta P_w = \gamma \delta P_s \tag{5}$$

and for the wall of the vertical shaft is

$$\delta P_v = (1 - \gamma)\delta P_s \tag{6}$$

The pressure difference across an elevator lobby wall from series flow is given by

$$\delta P_l = \frac{1}{1 + (A_l/A_e)^2} \delta P_v \tag{7}$$

where

l = wall of elevator lobby, and
e = wall of elevator shaft on the lobby side.

Substituting Eq 6 for δP_v

$$\delta P_l = \frac{(1 - \gamma)}{1 + (A_l/A_e)^2} \delta P_s \tag{8}$$

Copyright by ASTM Int'l (all rights reserved) Wed Feb 07 10:53:32 UTC 2024
Downloaded/printed by
The University of Delaware pursuant to License Agreement. No further reproductions authorized.

From Eq. 8 one can calculate a pressure difference caused by stack action that would transport smoke into an elevator lobby on the fire floor.

Wind is another mechanism which can cause pressure differences across the exterior and interior separations of a building. The static pressure on a building surface due to wind is

$$P_s = C_p \frac{\rho V^2}{2} \tag{9}$$

where

p_s = static pressure on building surface, Pa,
C_p = wind pressure coefficient, dimensionless,
ρ = air density, kg/m^3, and
V = wind speed, m/s.

The value of C_p is usually referenced to the wind velocity at the roof level of a building. For a variety of rectangular buildings in the absence of local obstructions, the average values of C_p with wind at 90° to one of the wall surfaces are +0.8 for the windward wall and −0.4 for leeward and side walls. With wind at 45° they are +0.5 for the windward walls and −0.5 for the leeward walls [5].

The building internal pressure depends on the building surface pressures, leakage areas of the windward and leeward walls, and leakage areas of the interior partitions; for an open plan building it depends only on the leakage areas of the windward and leeward walls. The internal pressure adjusts between the windward and leeward pressures to maintain a balance of mass air inflow and outflow across the building envelope. If a large opening is created in the windward wall of a floor by a broken window due to fire, the pressure on that floor will approach the windward pressure, resulting in pressures higher than those on other floors. This causes smoke to enter vertical shafts and adjacent floors. Conversely, if a window breaks on the leeward wall, the pressure on the fire floor approaches that of the leeward wall, resulting in pressures lower than those on other floors. This causes air from the other floors to flow into the fire floor and smoke to flow through the opening to outdoors. Window breakage on both the windward and leeward walls can cause smoke to flow into the vertical shafts, but its main direction of movement will be from the windward to the leeward walls. However, fire gases will be generally driven out of the tops of broken windows by buoyancy even for windows on windward walls.

Test Procedure

Tests were conducted in the experimental fire tower, which is part of the experimental facilities of the National Fire Laboratory of the National Research Council of Canada, located near Ottawa, Ontario. The tower is 28 m high; the first and second floors are 3.6 m high and the other floors, 2.6 m. The plan view of a typical floor is shown in Fig. 1. The tower contains all the shafts and other features necessary to simulate air and smoke movement patterns in a typical multistory building, including elevator, stair, smoke exhaust, service, supply, and return air shafts. Two propane gas burner sets, each capable of producing heat at an output of 2.5 MW, are located in the second floor burn area. The exterior walls and the walls of vertical shafts have rectangular shutters that can be set to provide leakage areas of typical buildings. The leakage areas of the experimental fire tower given in Table 1 are set for a building with average airtightness and a floor area of 900 m^2, or seven times that of the experimental tower. They are based on measurements on several multistory buildings by Tamura and Shaw [6,7]. The leakage openings in the outside walls are located only in the

Copyright by ASTM Int'l (all rights reserved) Wed Feb 07 10:53:32 UTC 2024
Downloaded/printed by
The University of Delaware pursuant to License Agreement. No further reproductions authorized.

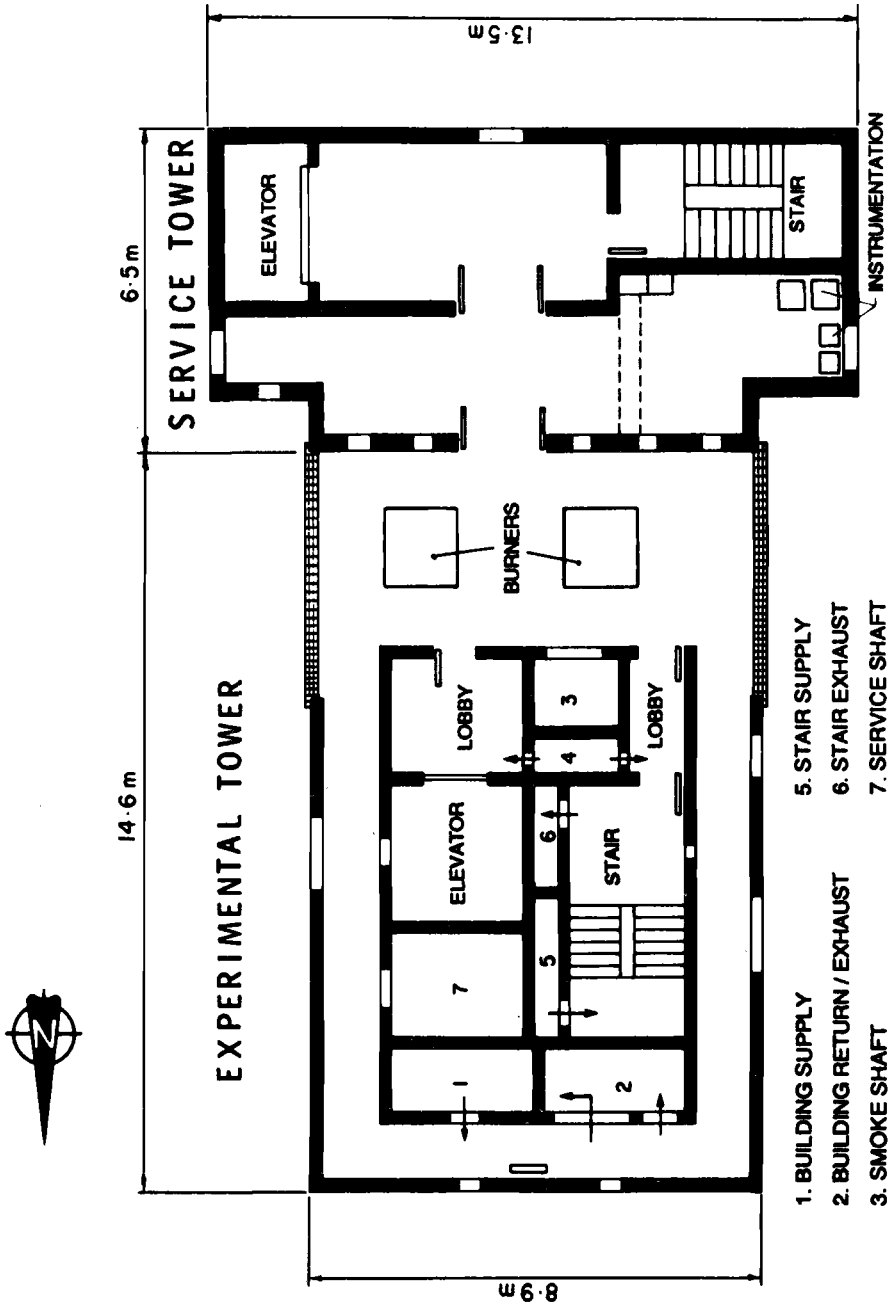

FIG. 1—*Plan of the experimental fire tower.*

TABLE 1—*Leakage flow areas per floor of the experimental fire tower (based on measurements in real buildings and simulating the air leakage characteristics of a building with a floor area of 1000 m²).*

Location	Area
	m^2
Outside walls	
East wall for each floor	0.037
West wall for each floor	0.037
2nd floor east wall vent open	0.464
2nd floor west wall vent open	0.464
Elevator	
Floor space to elevator shaft	0.006
Floor space to elevator lobby (lobby door closed)	0.028
Floor space to elevator lobby (lobby door open)	1.951
Elevator lobby to elevator shaft (elevator doors closed)	0.070
Elevator lobby to elevator shaft (elevator doors open)	0.557
Stairs	
Floor space to stairshaft	0.004
Floor space to stair lobby (lobby door closed)	0.023
Floor space to stair lobby (lobby door open)	1.951
Stair lobby to stairshaft (stair door closed)	0.023
Stair lobby to stairshaft (stair door open)	1.951
Vertical Shafts	
Floor space to service shaft	0.102
Floor space to supply air shaft[a]	0.186
Floor space to return air shaft[a]	0.186
Ceiling	0.052

[a] Shutters for supply and return air openings closed on the second floor.

east and west walls. To obtain the average wind pressure differences across the east and west wall of each floor, three outside static pressure taps that are manifolded are mounted on the outside surface, one at the center and the others 5 m on either side of the center.

Pressure differences across the outside walls and walls of all vertical shafts and associated lobbies on each floor are measured using static pressure taps mounted flush to the walls 0.3 m below the ceiling of each floor. All pressure lines are connected to a 24-port pressure switch equipped with a diaphragm-type magnetic reluctance pressure transducer and located on the same floor in the observation area. Carbon dioxide concentrations are measured on each floor in all vertical shafts, lobbies, corridors, and burn area by copper sampling tubes connected to a 12-port sampling switch unit with a nondispersive infrared gas analyzer. Temperatures are measured on each floor using chrome-alumel thermocouples at the same locations as for the carbon dioxide concentrations; in addition, three thermocouple trees are placed in the burn area. All devices of the three systems are controlled and monitored by a computer-based data acquisition and control system.

The tests to investigate pressure differences caused by stack action were conducted during winter at times when wind speeds were less than 16 km/h. These tests were conducted under different combinations of temperature, leakage area, and pressurization.

1. With a thermal draft coefficient of 0.98 and with leakage areas as given in Table 1, pressure differences across the exterior walls and the walls of vertical shafts were measured when outside temperatures were −11, −3, and 7°C, with an inside temperature of 22°C. At an outdoor temperature of −3°C, the east and west exterior wall vents on the second floor were opened to simulate windows broken during a fire.

Copyright by ASTM Int'l (all rights reserved) Wed Feb 07 10:53:32 UTC 2024
Downloaded/printed by
The University of Delaware pursuant to License Agreement. No further reproductions authorized.

2. At an outdoor temperature of −3°C, pressure differences were measured with thermal draft coefficients of 0.98, 0.85, and 0.74, obtained by adjusting the leakage openings of the supply air, exhaust air, and service shaft.
3. At an outdoor temperature of −10°C, with a thermal draft coefficient of 0.98, and with the outside wall vents on the second floor open, the elevator lobbies were pressurized to 25 Pa with outside air supplied to the elevator shaft. The pressure differences were then measured to determine the combined effect of stack action and mechanical pressurization.
4. Under the same conditions as for Situation 3, a fire test was conducted on the second floor to determine the combined effect of stack action, mechanical pressurization, and fire. By adjusting the propane gas flow rate, the fire temperature measured directly above the gas burners and just below the ceiling was maintained at 750°C with burner output of about 270 kW.

The wind tests were conducted with wind speeds of 25 to 40 km/h, with temperature differences between inside and outside of less than 6°C, and the leakage areas set for a thermal draft coefficient of 0.98. The wind tests were conducted to determine the effect of wind on the elevator/lobby wall pressure differences under several different conditions:

1. With both outside wall vents on the second floor closed.
2. With only the windward wall vent open, 0.464 m^2.
3. With only the leeward wall vent open, 0.464 m^2.
4. With both wall vents open.

These tests were followed by fire tests on the second floor with the fire temperature held at 550°C, again measured directly above the gas burners and just below the ceiling and with gas burner output of about 155 kW. The elevator lobby was pressurized through the elevator shaft to 11 Pa and tests were conducted with both outside wall vents on the fire floor closed, with both outside wall vents open, and with only the windward wall vent open.

Results and Discussions

The pressure differences across the outside walls caused by stack action for γ of 0.98 and outside temperatures of −11, −3, and 7°C are plotted in Fig. 2. As shown in this graph, the neutral pressure level was located at 53% of the tower height. The calculated values using Eqs 2 and 5 are shown as dashed lines in Fig. 2; they agreed well with the measured values.

Figure 3 shows the pressure differences measured across the elevator lobby wall at an outside temperature of −3°C and inside temperature of 22°C for γ of 0.74, 0.85, and 0.98. With the floor space as the reference pressure, a negative value indicates a flow of air from the floor space into the elevator lobby and a positive value indicates a flow in the opposite direction. In case of fire, therefore, a negative value would indicate a flow of smoke into the elevator lobby. The values calculated using Eq 8 for the same conditions agreed within 10% of the measured values. The good agreement between measurement and theory shown in Figs. 2 and 3 revalidates Eq 2 and validates Eq 8 over a wide range of leakage conditions representative of many commercial buildings.

For γ = 0.98, the pressure difference across the elevator lobby wall on the second floor was −0.5 Pa; when the outside wall vents on the second floor were opened, it increased to −5.4 Pa. This was accompanied by the lowering of the neutral pressure level from 53 to 41% of the building height; if it had remained at the same level, the pressure difference would have been −7.5 Pa across the elevator lobby wall at the second floor level. Assuming a pressure difference across the elevator lobby wall equal to that using Eq 2 and with the neutral

Copyright by ASTM Int'l (all rights reserved) Wed Feb 07 10:53:32 UTC 2024
Downloaded/printed by
The University of Delaware pursuant to License Agreement. No further reproductions authorized.

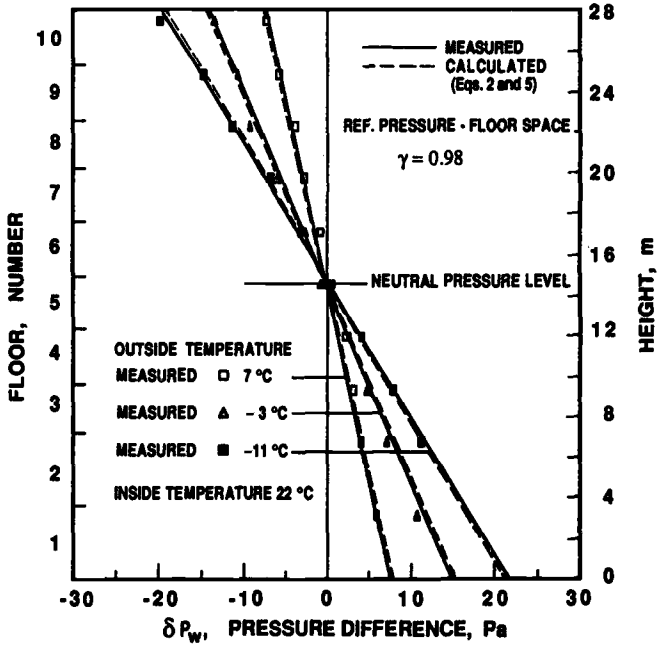

FIG. 2—*Pressure differences across outside wall versus outside air temperature.*

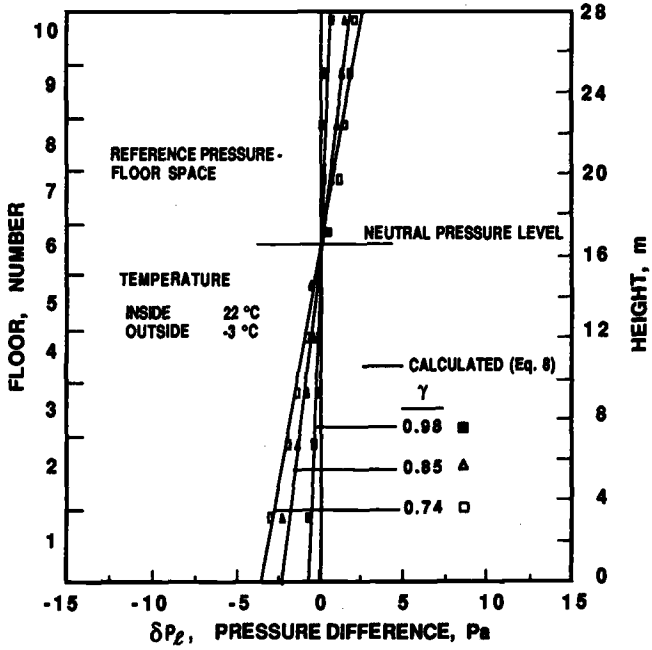

FIG. 3—*Pressure differences across elevator lobby wall versus thermal draft coefficient (γ).*

Copyright by ASTM Int'l (all rights reserved) Wed Feb 07 10:53:32 UTC 2024
Downloaded/printed by
The University of Delaware pursuant to License Agreement. No further reproductions authorized.

pressure level unchanged would give a conservative estimate for the situation where windows were broken.

In the field of air infiltration in buildings, it is generally accepted that adding the pressure differences caused by stack action and wind action is a good approximation to the pressure difference resulting from the two in combination. Experiments were conducted to see to what extent this approximation is appropriate to smoke control. The results of tests conducted to check the effect of pressurizing the elevator shaft with unheated outside air at −10°C and with the outside wall vents open on the second floor are shown in Fig. 4. The adverse pressure difference across the elevator lobby wall of the second floor without pressurization was −7.0 Pa. The elevator shaft was then pressurized, creating a pressure difference across the lobby wall on the second floor of 24 Pa. The supply air rate required for pressurization was 1400 L/s as compared to 1300 L/s with little or no stack action [*8*]. The calculated supply air rate based on the sum of the pressure difference caused by stack action and the NFPA 92A [*9*] recommended design pressurization of 25 Pa to deal with fire-induced pressure was 1470 L/s, which agreed well with the measured value. Figure 4 also shows the effect of fire at 750°C on the pressure difference across the wall of the pressurized elevator lobby. The pressure difference across the elevator lobby wall under fire conditions decreased from 24 to 15 Pa, a decrease of 9 Pa, which compares with the adverse pressure difference of −7 Pa caused by the fire of 750°C [*1*]. Thus the sum of the adverse pressure differences caused by stack action and fire should give a good estimate of the amount of pressurization required to prevent smoke migration into the elevator lobby for the test conditions. For these experiments, the smoke control system was balanced with a large opening from the fire floor to outside, which represented an open or broken window. For a system balanced without such an opening, a

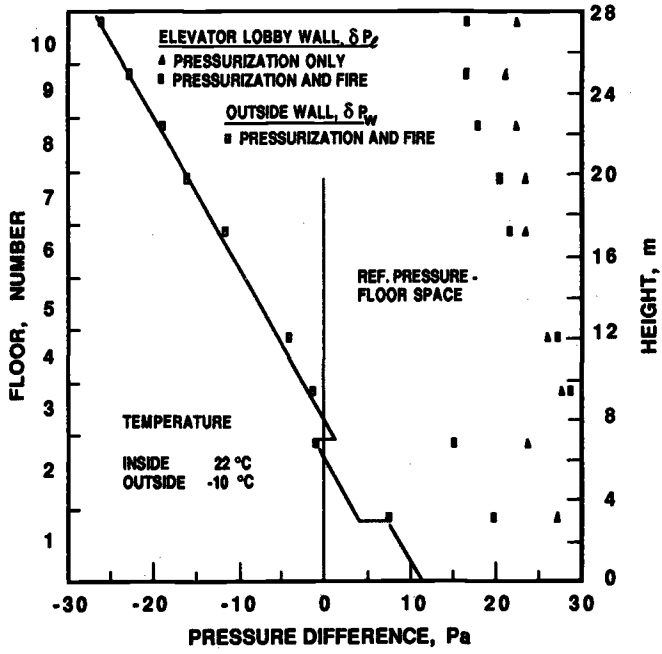

FIG. 4—*Pressure differences across outside wall and elevator lobby wall with elevator shaft pressurization (untempered outside supply air) and fire (750°C).*

Copyright by ASTM Int'l (all rights reserved) Wed Feb 07 10:53:32 UTC 2024
Downloaded/printed by
The University of Delaware pursuant to License Agreement. No further reproductions authorized.

broken window would result in a pressure jump across the elevator lobby, and the approach of adding wind effect and stack effect pressures would need to incorporate this jump as well.

During the burn tests, concentrations of carbon dioxide (one of the products of combustion) measured throughout the tower were regarded as surrogate smoke, and detailed information about these tests are provided by Tamura and Klote [*1*]. With the elevator shaft pressurized, the concentration of carbon dioxide relative to that in the burn area in the elevator shaft and lobbies was zero, except in the elevator lobby on the second floor, where it was 2.5%; concentrations less than 1% are assumed to be reasonably safe from a consideration of smoke obscuration [*10*]. Combustion products may have infiltrated the lobby due to thermal expansion of gases during the startup of the gas burners. With the elevator lobbies pressurized, the concentrations were zero in the lobbies and elevator shaft. This indicates that the lobby pressurization provides a higher level of protection, but a detailed hazard analysis would be required to determine the extent to which lobby pressurization is better.

Five wind tests with wind speeds ranging from 25 to 40 km/h with normal fluctuation and steady wind directions from W, WNW, and NW were conducted without a fire. They were intended to determine the effect of wind on the pressure differences across the elevator lobby wall for various settings of outside wall vents on the second floor. Table 2 gives the pressure differences across the west wall, east wall, and elevator lobby wall for the ten floors, for an average wind speed of 30 km/h from WNW. This was measured with an anemometer mounted on a pole on top of the tower, 36 m above ground level; the long axis of the tower is oriented in the north-south direction (Fig. 1). The corresponding wind speed measured with an anemometer 10 m above ground and 60 m west of the tower in an open field was about 25 km/h. The pressure differences across the windward wall (west) were about 40 Pa, about twice those of the leeward wall. Tests with wind from the west of 20 to 25 km/h gave similar results. From mass flow balance and with no leakage openings in the north and south walls, pressure differences across the west and east walls with equal openings should have been about the same. The effective area of the vent opening in the windward wall was less than that in the leeward wall by a factor of about 0.7. This could have been caused by some flow phenomenon such as stationary vortices resulting from fluctuations in wind speed or direction. Whether this reduction in effective area would occur when the vent area is distributed as cracks and not as a rectangular opening needs to be investigated.

TABLE 2—*Pressure differences across outside walls and elevator lobby walls for wind of 30 km/h, WNW, Pa (reference pressure—floor space).*

	Both Wall Vents Closed, 2nd Floor			West Wall Vents Open, 2nd Floor			East Wall Vent Open, 2nd Floor			Both Wall Vents Open, 2nd Floor		
Floor	West Wall	East Wall	Elev. Lobby Wall	West Wall	East Wall	Elev. Lobby Wall	West Wall	East Wall	Elev. Lobby Wall	West Wall	East Wall	Elev. Lobby Wall
10	20	−37	1.2	8	−33	1.7	30	−33	1.0	−3	−30	1.4
9	37	−25	0.9	19	−26	1.3	41	−32	0.5	6	−28	0.9
8	40	−23	0.8	20	−26	1.1	46	−33	−0.8	10	−27	0.8
7	40	−22	0.5	26	−23	0.9	50	−32	−0.0	18	−25	0.5
6	40	−20	0.3	19	−21	0.7	52	−30	−0.2	22	−25	0.3
5	41	−19	0.0	26	...	...	...	...	...	...	...	...
4	42	−18	−0.1	16	−19	0.3	54	−25	−0.6	26	−21	−0.1
3	44	−17	−0.3	20	−16	−0.1	54	−27	−0.7	27	−19	−0.5
2	33	−15	−0.5	10	−20	−9.6	65	− 7	6.0	25	−14	−1.8
1	42	−14	0.2	22	−13	0.2	54	−19	0.0	28	−10	0.1

Copyright by ASTM Int'l (all rights reserved) Wed Feb 07 10:53:32 UTC 2024
Downloaded/printed by
The University of Delaware pursuant to License Agreement. No further reproductions authorized.

For the five wind tests, the pressure differences across the elevator lobby wall on the second floor with both the windward and leeward wall vents closed varied from −0.1 to −0.5 Pa; when the windward wall vent on the second floor was opened, they varied from −1.5 to −9.6 Pa; when only the leeward vent was opened, they varied from 0.0 to 6.0 Pa; and when both vents were opened, they varied from −0.1 to −1.8 Pa.

The serious case is when only the windward wall vent is open. The value of −9.6 Pa for the elevator lobby wall represents a factor of 0.2 of the velocity head of 25 km/h measured at 10-m height in the open field. The corresponding value for the elevator shaft wall was −18 Pa or 0.37 of the velocity head. A factor of 0.5 of the velocity head may be appropriate to use for the adverse pressure due to wind in designing a pressurization system for buildings whose windows may break during a fire. Wind velocity for a given building height and surrounding terrain can be obtained from information given in Ref *5*.

To evaluate the performance of the smoke control system, wind tests were also conducted with a fire of 550°C on the second floor. Figure 5 shows the pressure differences measured across the elevator lobby wall at the 3.08-m level of the second floor. They are for an average wind speed of 25 km/h from the northwest measured on top of the tower. Before the fire test, when both vents on the second floor were closed, the pressure difference across the elevator lobby wall was −0.5 Pa. When only the windward outside wall vent was opened, it was −4.0 Pa; when only the leeward outside wall vent was opened, it was 1.2 Pa; and when both vents were opened, it was back to −0.5 Pa, the same as when both vents were closed. The elevator lobby was pressurized to 11 Pa with outside air supplied to the elevator shaft. This pressure difference was reduced to about 5 Pa when the burner was ignited and the fire temperature was controlled at 540°C; this is a reduction of 6 Pa, which compares with the adverse pressure caused by fire alone of −5 Pa [*1*]. When both leeward and windward wall vents were opened, the pressure difference was 6 Pa, but when only the windward wall vent was opened it fluctuated between ±6 Pa.

During the burn period with pressurization of the elevator shaft/lobby and with both vents closed (Step 6 of Fig. 5) and with them open (Step 7 of Fig. 5), the carbon dioxide concentrations were less than 1% of that in the burn area for both the elevator shaft and the lobbies on all floors, except for the lobby on the second floor, which had a concentration of 1.5%, probably caused by thermal expansion of gases at the time of ignition of the burner. The concentrations in the unpressurized stairshaft, stair lobby, and all floor spaces were well above the 1% level. When only the windward wall vent was opened, the concentrations in the elevator shaft and lobbies were less than 1%, except for the second floor lobby, where the concentration was 1.7%. In comparison, the concentration on the second floor in the unpressurized stairshaft was 28% and in the stairshaft lobby, 48%.

Mechanical pressurization of the elevator shaft with outdoor air greatly reduces the possibility of smoke contamination of the elevator shaft and lobbies. However, under high wind some smoke contamination can be expected with window breakages only in the windward wall. Venting also the leeward wall would greatly decrease this possibility as smoke would move horizontally from the windward to the leeward walls. Further study of wind effects is needed.

Summary

1. The good agreement between measurements and stack effect theory shown in Figs. 2 and 3 revalidates Eq 2 and validates Eq 8 over a wide range of leakage conditions representative of many commercial buildings.

2. For the conditions of these experiments, the adverse pressure differences of stack action and fire can be added to provide a good approximation of the pressure difference resulting

Copyright by ASTM Int'l (all rights reserved) Wed Feb 07 10:53:32 UTC 2024
Downloaded/printed by
The University of Delaware pursuant to License Agreement. No further reproductions authorized.

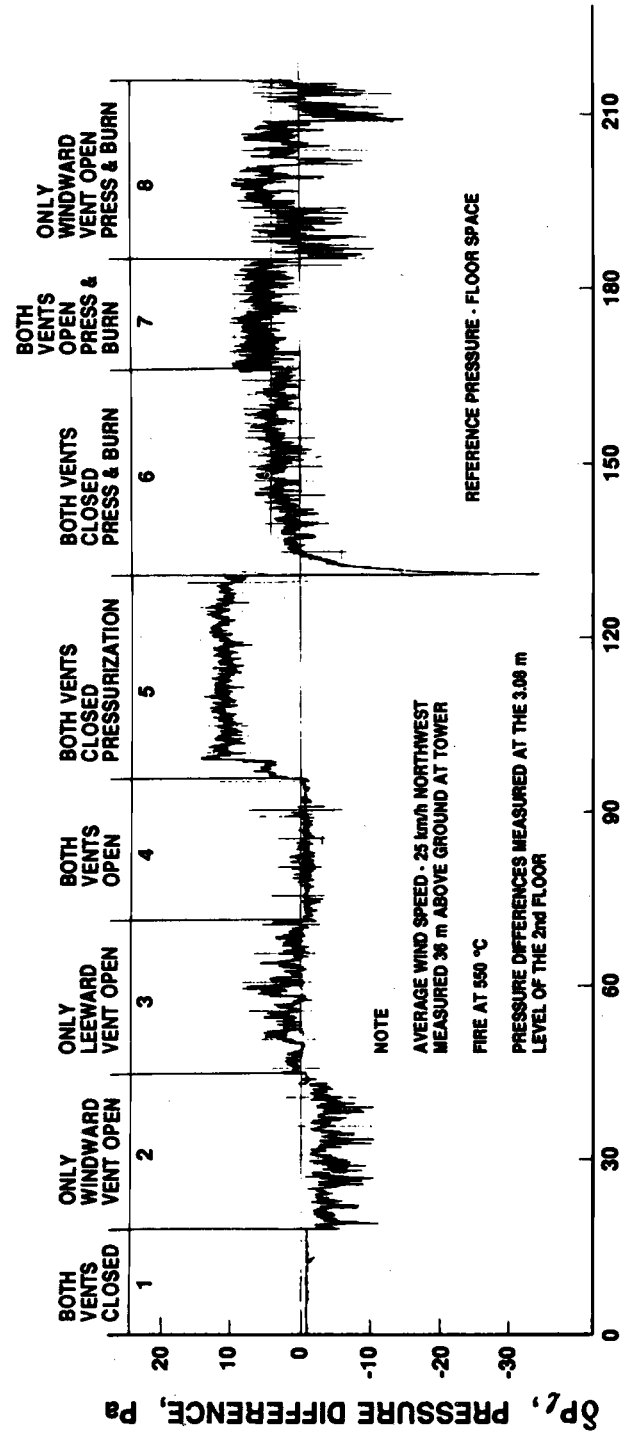

FIG. 5—*Pressure difference across elevator lobby wall on the 2nd floor caused by wind action, pressurization, and fire.*

from the two acting in combination and, hence, the amount of pressurization required to prevent smoke migration into the elevator lobbies under these conditions. A broken window can result in a jump in pressure difference across the elevator lobby, which is an important factor for designing these systems in most buildings.

3. Mechanical pressurization of the elevator shaft or of elevator lobbies greatly reduces the possibility of smoke contamination of the elevator shaft and lobbies due to stack action.

4. Mechanical pressurization of the elevator shaft greatly reduces the possibility of smoke contamination of the elevator shaft and lobbies due to wind action. However, further studies of wind effects are needed.

5. This study has provided methods for predicting adverse pressure differences across the walls of the elevator shaft and lobbies caused by wind and building stack action and in combination with those caused by a fire. Such design information is needed to determine the level of mechanical pressurization required to prevent smoke from entering the elevator shaft and lobbies.

Acknowledgment

The authors greatly acknowledge the contribution of R. A. MacDonald in setting up and conducting the tests in the experimental fire tower and processing the test results, of J. E. Berndt for assisting in running the data acquisition and control system and the gas burner system, and of other staff members of the National Fire Laboratory in assisting during the preparation and conduct of the tests.

References

[*1*] Tamura, G. T. and Klote, J. H., "Experimental Fire Tower Studies on Mechanical Pressurization to Control Smoke Movement Caused by Fire Pressures," *Proceedings,* 2nd International Symposium on Fire Safety Science, Tokyo, Japan, 1988.

[*2*] Klote, J. H. and Tamura, G. T., "Experiments of Piston Effect on Elevator Smoke Control," *ASHRAE Transactions,* Vol. 93, Pt. 2, 1987, pp. 2217–2228.

[*3*] "Handbook of Fundamentals, Chapter 22, Ventilation and Infiltration," American Society of Heating, Refrigerating, and Air-Conditioning Engineers, Inc., Atlanta, 1985, p. 22.3.

[*4*] Tamura, G. T. and Wilson, A. G., "Pressure Differences Caused by Chimney Effect in Three High Buildings," *ASHRAE Transactions,* Vol. 73, Part II, 1967, p. II.1.1–II.1.10.

[*5*] "Handbook of Fundamentals, Chapter 14, Air Flow Around Buildings," American Society of Heating, Refrigerating, and Air-Conditioning Engineers, Inc., Atlanta, 1985, p. 14.3.

[*6*] Tamura, G. T. and Shaw, C. Y., "Air Leakage Data for the Design of Elevator and Stair Shaft Pressurization Systems," *ASHRAE Transactions,* Vol. 82, Part 2, 1976, pp. 179–180.

[*7*] Tamura, G. T. and Shaw, C. Y., "Experimental Studies of Mechanical Venting for Smoke Control in Tall Office Buildings," *ASHRAE Transactions,* Vol. 84, Part 1, 1978, pp. 54–71.

[*8*] Tamura, G. T. and Klote, J. H., "Experimental Fire Tower Studies of Elevator Pressurization Systems for Smoke Control," *ASHRAE Transactions,* Vol. 93, Pt. 2, 1987, pp. 2235–2256.

[*9*] NFPA 92A, "Recommended Practice for Smoke Control Systems," National Fire Protection Association, Quincy, MA, Section 2-2.1, 1988.

[*10*] McGuire, J. H., Tamura, G. T., and Wilson A. G., "Factors in Controlling Smoke in High Buildings," *Proceedings,* ASHRAE Symposium on Fire Hazards in Buildings, San Francisco, CA, ASHRAE, Atlanta, GA, 1970, pp. 8–13.

Copyright by ASTM Int'l (all rights reserved) Wed Feb 07 10:53:32 UTC 2024
Downloaded/printed by
The University of Delaware pursuant to License Agreement. No further reproductions authorized.

Author Index

Copyright by ASTM Int'l (all rights reserved) Wed Feb 07 10:53:32 UTC 2024
Downloaded/printed by
Copyright © 1990 by ASTM International www.astm.org
The University of Delaware pursuant to License Agreement. No further reproductions authorized.

Subject Index

Copyright by ASTM Int'l (all rights reserved) Wed Feb 07 10:53:32 UTC 2024
Downloaded/printed by
The University of Delaware pursuant to License Agreement. No further reproductions authorized.

Copyright by ASTM Int'l (all rights reserved) Wed Feb 07 10:53:32 UTC 2024
Downloaded/printed by
The University of Delaware pursuant to License Agreement. No further reproductions authorized.

Copyright by ASTM Int'l (all rights reserved) Wed Feb 07 10:53:32 UTC 2024
Downloaded/printed by
The University of Delaware pursuant to License Agreement. No further reproductions authorized.

ISBN 0-8031-1386-2

Copyright by ASTM Int'l (all rights reserved) Wed Feb 07 10:53:32 UTC 2024
Downloaded/printed by
The University of Delaware pursuant to License Agreement. No further reproductions authorized.